Poznań University of Life Sciences
Faculty of Food Science and Nutrition

Uniwersytet Przyrodniczy w Poznaniu
Wydział Nauk o Żywności i Żywieniu

mgr Mahbuba Islam
139140

The application of Differential Scanning Calorimetry (DSC) for the quality assessment of selected edible oils

Rozprawa doktorska

wykonana pod kierunkiem

Prof. UPP dr hab. Jolanta Tomaszewska-Gras

Promotor pomocniczy

Dr. inż. Anna Kaczmarek

Katedra Zarządzania Jakością i Bezpieczeństwem Żywności

Wydział Nauk o Żywności i Żywieniu

Poznań, 2023

Dedication

Firstly, I would like to dedicate my dissertation work to my family and friends for its worth. Special gratitude to my loving parents, A.K.M. Nazrul Islam and Mrs. Shaheen Islam, whose continuous words of encouragement kept me going to face a new day and a new challenge. I am deeply thankful for my spouse, Dr. Sajjad Maruf, who stood by my side during all my challenges. His unwavering support, thoughtful discussions, and motivation illuminated my path, guiding me towards a positive resolution. Also, to my sister, Marzia Islam Ananna, whose warm jokes, and consistent adoration gave me the necessary energy in between my hectic work days. And of course, you two, Loki and Gaia, my sweet, cuddly felines, for running over my laptop, sleeping on top of notes and books and for reminding me to take a break when I was working for too long, you read me the best.

Even a prodigy like Harry Potter needed guidance and directions from Dumbledore. And here, I would like to thank my Dumbledore, my mentor and advisor, UPP dr hab. Jolanta Tomaszewska-Gras, for her unwavering support, expertise, and love of research, which allowed me to pursue this journey and become who I am today. A special thanks to my co-supervisor Dr. inż. Anna Kaczmarek, the enthusiasm, and high standard you had for the research encouraged me to embrace possibilities with innovative approaches. I would like to express my gratitude to my colleagues and co-authors for their valuable contributions, which helped me get the research works get published in prestigious journals. And lastly, I would also like to thank my colleagues and labmates from the “Department of Food Quality and Safety Management” for their generous support, patience and precious time.

Acknowledgement

This research was funded by the NATIONAL SCIENCE CENTRE, POLAND, grant number: 2018/31/B/NZ9/02762.

Summary

Traditional methods of assessing oil quality, including oxidative stability and authenticity, often involve time-consuming and environmentally unfriendly chemical analyses. Therefore, the aim of the study was to investigate the possibility of using the instrumental technique of differential scanning calorimetry (DSC) for the comprehensive characterization of cold-pressed edible oils, i.e. flaxseed, camelina and hempseed oil, obtained from different cultivars, in terms of assessing oxidative stability and its changes during storage as well as the possibility of assessing authenticity of oils and detecting adulteration with refined oils. In order to assess the oxidative stability of oils, the DSC oxidation test was used under isothermal (oxidation induction time, OIT) and non-isothermal conditions (oxidation onset temperature, Ton), which were additionally supported by kinetic calculations. Oxidation tests performed using different analysis conditions, i.e. at temperatures of 120, 140, 160 °C (isothermal test) and heating rates at 1, 2, 5, 10, 15 °C/min (non-isothermal test), showed different resistance to oxidation of two cold-pressed oils (flaxseed and camelina oils), due to different varieties and different fatty acid composition. For a broader characterization of the oxidation process, new parameters from the oxidation curves were determined, such as OET (oxidation completion time), oxidation rate, oxidation length (Δt) and oxidation end temperature (Tend), as well as calculations of the kinetics of the oxidation process by determining the activation energy parameters (E_a), oxidation rate constant (k) and half-time coefficient ($t_{1/2}$), which allowed for a more in-depth presentation of differences in oxidative stability due to different varieties of flaxseed oil and camelina oil. The study also allowed for the demonstration of strong negative correlations between DSC parameters and conventional chemical indicators of oxidative stability, such as the peroxide value (PV) or the TOTOX index. Significant negative linear correlations were also found between the content of α-linolenic acid and DSC parameters (OIT, Ton) for various varieties of flaxseed and camelina oils. In order to investigate the possibility of using DSC oxidation parameters (OIT, Ton) to distinguish fresh oils from stored ones, the research was extended to monitor changes during 6-month storage of three oils (flaxseed, camelina, hemp) using the DSC oxidation test (isothermal and non-isothermal), as well as chemical oxidation indicators. Significant negative linear correlations of DSC parameters were obtained for all oils with chemical indicators i.e. PV, p-anisidine value (pAV) and TOTOX. It was also found that the isothermal test (OIT) at a temperature of 120 °C allowed for the most effective monitoring of oxidative changes in oils, as for these conditions the highest correlation coefficients with

chemical indicators (PV, pAV, TOTOX) were obtained, compared to the non-isothermal test. The obtained results indicated the potential of the DSC technique for assessing the freshness and changes in oil stability during storage.

The second part of the research concerned the use of melting or crystallization phase transition profiles to assess the quality of oils. The first stage focused on examining the factors influencing the phase transition profile of oils, i.e., different scanning rates and the influence of oil storage on the phase transition curves. It has been shown that the heating rate significantly affects the shape of the curve, the number of peaks, their height and position as well as the enthalpy of the transition. The heating rate of 5 °C/min was considered the most suitable for use as a fingerprint because at this rate the profiles for different varieties of the same type of oil were most similar. Using the melting profile of flaxseed oil, the influence of storage time was also examined using the statistical process control method, i.e., X-bar and R control charts, to monitor thermodynamic changes caused by 6-month storage of the oil. As a result of these studies, 16 thermodynamic parameters were identified from the phase transition curves (peak temperature, intensity and enthalpy of transition peaks), showing an increasing or decreasing tendency during oil storage, which were considered as markers of oxidative changes in the oil. Additionally, 12 stable thermodynamic parameters were determined that can be used as markers of the authenticity of flaxseed oil.

In the next stage of the research, the possibility of using entire melting profiles in the context of untargeted analysis, using 7471 variables of the normalized heat flux, was tested to distinguish cold-pressed oils (flaxseed, camelina, hemp) from refined oils (rapeseed, soybean, sunflower) with the support of chemometric methods, mainly of the Orthogonal Partial Least Squares - Discriminant Analysis (OPLS-DA). Using this method, oils were successfully classified into six distinct classes, representing each oil type, obtaining high coefficients $R^2X(cum)= 0.971$ and $Q^2X(cum)= 0.887$, which confirmed the reliability and predictive accuracy of the model.

In the last stage of the research, the possibility of using the DSC melting profiles of flaxseed oil mixed with refined rapeseed oil in various concentrations was examined to detect adulteration by comparing various classification and regression chemometric models. Regression models, in particular the artificial neural networks (ANN) model, were the most effective in predicting the adulterant concentrations in flaxseed oil samples, already at the level of 5% refined rapeseed oil addition. Equally high accuracy coefficients for detecting the level of adulteration were obtained

for the Partial Least Squares (PLS) method. Among the analyzed classification models (LDA, MARS, SVM, and ANNs), the Linear Discriminant Analysis (LDA) method showed exceptional accuracy (99.5%) in the classification of oil samples based on the level of adulteration.

To sum up, the multi-aspect series of tests conducted allowed to demonstrate the versatility and potential of the DSC technique combined with chemometric tools for assessing the quality of cold-pressed oils, both fresh and stored. The use of this analytical technique to assess the stability and authenticity of cold-pressed oils offers more sustainable alternative to traditional chemical analyses, adapting to the changing needs of the food industry according to the principles of Green Chemistry. The conducted research presents the possibilities of using differential scanning calorimetry (DSC) as a reliable analytical instrument for the characterization and authentication of cold-pressed edible oils.

Streszczenie

Tradycyjne metody oceny jakości oleju w tym stabilności oksydacyjnej czy autentyczności obejmują często czasochłonne i nieprzyjazne dla środowiska analizy chemiczne. Stąd celem pracy było zbadanie możliwości wykorzystania instrumentalnej techniki różnicowej kalorymetrii skaningowej (DSC) do kompleksowej charakterystyki olejów jadalnych tłoczonych na zimno, tj. oleju lnianego, z nasion lnianki i konopnego, otrzymanych z różnych odmian, pod kątem oceny stabilności oksydacyjnej i jej zmian w trakcie przechowywania jak również możliwości oceny autentyczności olejów i wykrywania ich zafałszowań olejami rafinowanymi. W celu oceny stabilności oksydacyjnej olejów wykorzystano test oksydacji DSC w warunkach izotermicznych (czas indukcji utleniania, OIT) i nieizotermicznych (temperatura początku utleniania, Ton), które zostały dodatkowo wsparte obliczeniami kinetycznymi. Wykonane badania oksydacji, przy zastosowaniu różnych warunków analizy tj. w temperaturze 120, 140, 160 °C (test izotermiczny) i szybkości ogrzewania przy 1, 2, 5, 10, 15 °C/min (test nieizotermicznym), wykazały różną odporność na utlenianie dwóch olejów tłoczonych na zimno (oleju lnianego i oleju z lnianki), ze względu na różne odmiany i różny skład kwasów tłuszczowych. Dla szerszej charakterystyki procesu utleniania wyznaczono ponadto nowe parametry z krzywych oksydacji, takie jak OET (czas zakończenia utleniania), szybkość utleniania, długość utleniania (Δt) i temperatura końca utleniania (Tend), jak również wykonano obliczenia kinetyki procesu oksydacji wyznaczając parametry energii aktywacji (E_a), stałej szybkości reakcji (k) i połówkowego czasu reakcji ($t_{1/2}$), stałej oksydacji i czasu połówkowego, co pozwoliło na bardziej dogłębne przedstawienie różnic w stabilności oksydacyjnej ze względu na różne odmiany oleju lnianego i z nasion lnianki. Badaniu pozwoliły także na wykazanie silnych ujemnych korelacji pomiędzy parametrami DSC a konwencjonalnymi chemicznymi wskaźnikami stabilności oksydacyjnej, takimi jak liczba nadtlenkowa (PV) czy wskaźnik TOTOX. Stwierdzono również istotne ujemne korelacje liniowe pomiędzy zawartością kwasu α-linolenowego a parametrami DSC (OIT, Ton) dla różnych odmian olejów lnianych i z nasion lnianki. W celu zbadania możliwości wykorzystania parametrów utleniania DSC (OIT, Ton) do odróżnienia olejów świeżych od przechowywanych, badania rozszerzono o monitorowanie zmian podczas 6-miesięcznego przechowywania trzech olejów (lniany, lniankowy, konopny) za pomocą testu oksydacji DSC (izotermicznego i nieizotermicznego), jak i chemicznych wskaźników utleniania. Uzyskano istotne ujemne liniowe korelacje parametrów DSC dla wszystkich olejów ze wskaźnikami chemicznymi tj. PV, liczba

anizydynowa (pAV), wskaźnik TOTOX. Uznano także, że test izotermiczny (OIT) w temperaturze 120 °C pozwolił najskuteczniej śledzić zmiany oksydacyjne w olejach, jako że, dla tych warunków uzyskano najwyższe współczynniki korelacji ze wskaźnikami chemicznymi (PV, pAV, TOTOX), w porównaniu z testem nieizotermicznym. Uzyskane wyniki wskazały na potencjał techniki DSC do oceny świeżości i zmian stabilności oleju w trakcie przechowywania.

Druga część badań dotyczyła wykorzystania profili przejścia fazowego topnienia czy krystalizacji do oceny jakości olejów. W pierwszym etapie skupiono się na badaniu czynników wpływających na profil przemiany fazowej olejów, tj. różnych szybkości skanowania oraz wpływu przechowywania olejów na krzywe przemian fazowych. Wykazano, że prędkość ogrzewania wpływa istotnie na kształt krzywej, liczbę pików, ich wysokość i położenie jak również entalpię przemiany. Prędkość ogrzewania, wynoszącą 5 °C/min uznano za najbardziej przydatną w celu użycia jako „odcisku palca", gdyż dla tej prędkości profile dla różnych odmian tego samego rodzaju oleju charakteryzowały się największym podobieństwem. Wykorzystując profil topnienia oleju lnianego zbadano także wpływ czasu przechowywania, stosując metodę statystycznej kontroli procesu tj. karty kontrolne x-R, do monitorowania zmian termodynamicznych wywołanych 6-miesięcznym przechowywaniem oleju. W wyniku tych badań zidentyfikowano z krzywych przejścia fazowego, 16 parametrów termodynamicznych (temperatury piku, intensywności i entalpii pików przemiany), wykazujących w trakcie przechowywania olejów tendencję wzrostową lub malejąca, które uznano jako markery zmian oksydacyjnych oleju. Ponadto wyznaczono 12 stabilnych parametrów termodynamicznych, które mogą być użyte jako markery autentyczności oleju lnianego.

W kolejnym etapie badań sprawdzono możliwość wykorzystania całych profili topnienia w kontekście analizy niecelowanej, używając 7471 zmiennych znormalizowanego strumienia cieplnego, do odróżnienia olejów tłoczonych na zimno (lniany, z lnianki, konopny) od olejów rafinowanych (rzepakowy, sojowy, słonecznikowy) przy wsparciu metod chemometrycznych, głównie analizy dyskryminacyjnej zmiennych ortogonalnych metodą cząstkowych najmniejszych kwadratów, (OPLS-DA). Za pomocą tej metody skutecznie sklasyfikowano oleje w sześciu odrębnych klasach, reprezentujących każdy typ oleju, uzyskując wysokie współczynniki $R^2X(cum)= 0,971$ i $Q^2X(cum)= 0,887$, które potwierdziła niezawodność i dokładność predykcyjną modelu.

W ostatnim etapie badań zbadano możliwość wykorzystania profilu topnienia oleju lnianego zmieszanego z rafinowanym olejem rzepakowym w różnych stężeniach do wykrywania zafałszowań poprzez porównanie różnych klasyfikacyjnych i regresyjnych modeli chemometrycznych. Modele regresji, w szczególności model sztucznych sieci neuronowych (ANN), był najskuteczniejszy w przewidywaniu stężeń substancji fałszującej w próbkach oleju lnianego, już na poziomie 5% dodatku rafinowanego oleju rzepakowego. Równie wysokie wskaźniki dobroci dopasowania modelu do wykrywania poziomu zafałszowania uzyskano dla metody Cząstkowych Najmniejszych Kwadratów (PLS). Spośród analizowanych modeli klasyfikacyjnych (LDA, MARS, SVM, and ANNs), dla metody Liniowej Analizy Dyskryminacyjnej (LDA) wykazano wyjątkową dokładność (99,5%) w klasyfikacji próbek oleju na podstawie poziomu zafałszowań.

Podsumowując, przeprowadzony wieloaspektowy cykl badań pozwolił wykazać wszechstronność i potencjał techniki DSC w połączeniu z narzędziami chemometrycznymi do oceny jakości olejów tłoczonych na zimno zarówno świeżych jak i przechowywanych. Wykorzystanie tej techniki analitycznej do oceny stabilności i autentyczności olejów tłoczonych za zimno oferuje bardziej zrównoważoną alternatywę dla tradycyjnych analiz chemicznych, dostosowując się do zmieniających się potrzeb przemysłu spożywczego zgodnie z zasadami Zielonej Chemii. W przeprowadzonych badaniach przedstawiono możliwości wykorzystania różnicowej kalorymetrii skaningowej (DSC) jako wiarygodnego instrumentu analitycznego do charakteryzowania i uwierzytelniania olejów jadalnych tłoczonych na zimno.

Table of Contents

List of publications

A1. Tomaszewska-Gras, J.; Islam, M.; Grzeca, L.; Kaczmarek, A.; Fornal, E. Comprehensive Thermal Characteristics of Different Cultivars of Flaxseed Oil (Linum usittatissimum L.). Molecules 2021, 26, 1958. https://doi.org/10.3390/molecules26071958 (Will be referred as A1)

A2. Islam, M., Muzolf-Panek, M., Fornal, E. et al. DSC isothermal and non-isothermal assessment of thermo-oxidative stability of different cultivars of Camelina sativa L. seed oils. J Therm Anal Calorim 147, 10013–10026 (2022). https://doi.org/10.1007/s10973-022-11367-8 (Will be referred as A2)

A3. Islam, M.; Kaczmarek, A.; Grygier, A.; Tomaszewska-Gras, J. DSC Phase Transition Profiles Analyzed by Control Charts to Determine Markers for the Authenticity and Deterioration of Flaxseed Oil during Storage. Foods 2023, 12, 2954. https://doi.org/ 10.3390/foods12152954 (Will be referred as A3)

A4. Islam, M., Montowska, M., Fornal, E., Tomaszewska-Gras, J. (2023). Discrimination of Selected Cold-Pressed and Refined Oils by Untargeted Profiling of Phase Transition Curves of Differential Scanning Calorimetry. Polish Journal of Food and Nutrition Sciences, 224-232. https://doi.org/10.31883/pjfns/169425 (Will be referred as A4)

A5. Islam, M.; Kaczmarek, A.; Montowska, M.; Tomaszewska-Gras, J. Comparing Different Chemometric Approaches to Detect Adulteration of Cold-Pressed Flaxseed Oil with Refined Rapeseed Oil Using Differential Scanning Calorimetry. Foods 2023, 12, 3352. https://doi.org/10.3390/foods12183352 (Will be referred as A5)

A6. Islam, M., Kaczmarek, A. Tomaszewska-Gras, J. Differential scanning calorimetry as a tool to assess the oxidation state of cold-pressed oils during shelf-life. Journal of Food Measurement and Characterization (2023). https://doi.org/10.1007/s11694-023-02152-8 (Will be referred as A6)

Summary:

Total Impact Factor: 26.1

Total MEiN: 700

1. Introduction

The food industry's unwavering focus on food authenticity is a matter of paramount importance, ensuring products comply with their stated composition, absence of foreign substances, production processes, geographical and botanical origins, production timelines, and genetic makeup. Edible oils, serving as essential components of daily diet, furnish a significant portion of essential fatty acids and other lipids that play a pivotal role in human health. The quality and composition of these oils exert a direct influence on their nutritional value, sensory attributes, stability and shelf life. Thus, the comprehensive characterization of edible oils is essential for ensuring food safety and maintaining quality control standards in the food industry. The past years have witnessed the ascendancy of cold-pressed oils like flaxseed oils, camelina oils and hempseed oils, attributed to their exceptional nutritional content and versatile applications across industries (Durazzo et al., 2022; Ligěza et al., 2016; Ramadan, 2020). In 2021, the global cold-pressed oils market was valued at USD 27.05 billion, and it is expected to witness a 5.7% compound annual growth rate (CAGR) from 2022 to 2028 (Grand View Reasearch, 2021). Notably, the cold-pressing method has emerged as the preferred choice for crafting edible oil. This process preserves a remarkable combination of triacylglycerols (TAGs) and acylglycerols (mono- and diacylglycerol) (Kozub et al., 2023), along with an array of other bioactive compounds such as phenols, sterols, tocopherols, phospholipids, carotenoids and pigments. These oils are mainly renowned for their high content of essential fatty acids, particularly α-linolenic acid (ALA), which is a crucial component for human health. Flaxseed oil, derived from the seeds of the flax plant (*Linum usitatissimum* L.), stands out for its exceptionally high ALA content (Teh & Birch, 2013). ALA can be converted within the human body into beneficial compounds like eicosapentaenoic acid (EPA) and docosahexaenoic acid (DHA), both of which are vital for cardiovascular and overall health (Visentainer et al., 2005). Camelina oil, obtained from the seeds of *Camelina Sativa* L. plant, also boasts a notable nutritional profile. It is rich in unsaturated fatty acids, including *n*-3 fatty acids (Piravi-vanak et al., 2022), which contribute to its potential health benefits. Additionally, hempseed oil, extracted from the seeds of the hemp plant (*Cannabis Sativa* L.), is recognized for its unique combination of polyunsaturated fatty acids (PUFAs), particularly a well-balanced ratio of *n*-6 to *n*-3 fatty acids (3:1) (Simopoulos, 2008). Consumers are increasingly interested in incorporating cold-pressed oils from plant sources into their diets for essential nutrition. However, this trend sometimes prioritizes marketing strategies over product quality. Given the significance of cold-

pressed oil production, maintaining product quality during its shelf life in supermarkets is crucial. One major challenge about these oils is their high unsaturated fatty acid content makes them vulnerable to oxidative degradation due to the presence of unsaturated carbon bonds (C=C). This oxidation occurs during storage and processing and is driven by two distinct chemical mechanisms: autoxidation and photosensitized oxidation, depending on the type of oxygen involved ($^3O_2$ - atmospheric triplet oxygen, or $^1O_2$ - singlet oxygen). Autoxidation occurs when $^3O_2$ reacts with lipid free radicals, while photosensitized oxidation is triggered by exposure to light, sensitizers, and atmospheric oxygens, resulting in the production of $^1O_2$ (Choe & Min, 2006). To assess the degree of oxidation in these oils, an oxidation test is conducted, measuring the extent of oxidation that can lead to the development of off-flavors, odors, and potentially harmful compounds (Gordon, 2001).

Various analytical and chemical methods are available to assess oxidative stability (Saldana & Martinez-Monteagudo, 2013; Shahidi & Wanasundara, 2002), and the choice of method depends on the specific application and the type of oil under analysis. When studying the shelf life of oils and seeds over time, it is crucial to employ fast and practical methods for detecting deterioration stages accurately. Common chemical methods used in the food industry for measuring oxidative stability include peroxide value determination (PV), p-Anisidine value (p-AV), TOTOX value, and acid value (AV). These methods typically provide quantitative data regarding the chemical changes resulting from oxidation (Abramovič & Abram, 2005; Momot et al., 2023). However, they rely on the precision of the technician, the quality of chemicals and equipment, and can be labor-intensive, expensive, and involve the use of significant amounts of potentially harmful chemicals. In line with the green chemistry movement, there is a growing need to develop and implement instrumental methods for assessing oil quality. On that note, thermal analysis is a vital aspect of innovative food formulation research because temperature plays a crucial role in food production. DSC has proven to be a valuable tool for this purpose, which has become indispensable in addressing the challenges posed by the susceptibility of oils, especially cold-pressed oils, to oxidative degradation (Rajagukguk et al., 2023). The methodology hinges on the quantification of heat absorbed or liberated by a sample subjected to controlled temperature changes, in comparison to a reference material. These methodologies encompass both isothermal and non-isothermal approaches, each tailored for distinct objectives. Isothermal DSC experiments entail the maintenance of a constant temperature over a stipulated period, facilitating the observation of heat flow changes. This method

technique has proven particularly invaluable in assessing for evaluating oxidative stability-a pivotal parameter of impacting the quality longevity and category of edible oils. By subjecting oils to elevated temperatures within an oxygen rich environment, isothermal DSC captures the initiation and propagation of oxidation, thereby revealing the oil's susceptibility to rancidity and its overall oxidative stability (Saldana & Martinez-Monteagudo, 2013). Conversely, non-isothermal DSC oxidation test involves heating controlled temperature variations at the defined heating rate (Kozłowska & Gruczyńska, 2018). Furthermore, DSC, as a potent analytical tool, has progressively gained prominence in the characterization of fats and oils, notably within the domains of authenticity assessment and quality control. The thermal profiles of phase transition collected by DSC technique essentially can serve as distinctive "fingerprints" for each oil, enabling the authentication of fats and oils (Tomaszewska-Gras, 2016). This method elucidates an array of thermal properties, encompassing crystallization and melting phase transition curves, pivotal for both authenticity assessment and adulteration detection as well as polymorphism investigation (Sato et al., 2013). Extensive testing using DSC has been conducted on extra virgin olive oil (EVOO) to determine its origin and detect any adulteration with other oils. DSC has also been applied to analyze other fats and oils, including palm oil (Tan & Che Man, 2002), cocoa butter (Kerti, 2001), and various plant oils (Marina et al., 2009; Rudakov et al., 2021; Upadhyay et al., 2017). In the dairy industry, DSC has been employed to identify adulteration of butter with other fats, such as vegetable oils or animal fats (Tomaszewska-Gras, 2016). Additionally, it can assess the quality and traceability of milk and milk products (Coni et al., 1994; Nina Naquiah et al., 2017; Tomaszewska-Gras, 2013). It has also been utilized to determine quantitively adulteration of butter with water (Tomaszewska-Gras, 2012).

Considering the authentication of cold-pressed oils, the analysis of refined oils, such as rapeseed, soybean, and sunflower oils, also holds significance in the food industry. These refined oils are often cheaper and can be used to adulterate cold-pressed oils, compromising their authenticity and nutritional value. Therefore, it becomes essential to characterize these refined oils by various instrumental methods. The distinct melting or crystallization profiles, characterized by endothermic and exothermic peaks, differ across oils due to their unique fatty acid compositions (Yanty et al., 2011), thus can be used as fingerprints of edible oils and fats. By analyzing the melting and crystallization phase transitions using DSC, substantial progress has been made in identifying adulterants in oils and determining their origins (Barba et al., 2013; Rajagukguk et al.,

2022). Consequently, ensuring the authenticity and quality of these oils throughout their shelf life has become paramount, given their increasing popularity and economic significance.

Innovative study approaches were taken by supporting DSC analysis with chemometric tools, where researchers have developed authentication models that amplify DSC's efficiency in oil characterization (Maggio et al., 2012). This burgeoning demand for authenticity control has spurred the adoption of DSC techniques alongside chemometric analysis, culminating in a dependable methodology for profiling edible oils. Chemometric analysis encompasses the application of mathematical and statistical methods to unearth pertinent information from extensive datasets, thereby unveiling concealed patterns. Researchers have found success in combining analytical techniques with both linear and non-linear chemometric tools (Rocha et al., 2020) to create classification and regression models for analyzing oil samples. This highlights the significance of employing chemometric techniques such as linear discriminant analysis (LDA) (Zhang et al., 2019), multiple linear regression (MLR) (Sim et al., 2018), multivariate adaptive regression splines (MARS) (Rocha et al., 2012), support vector machine (SVM) (Peng et al., 2023), artificial neural networks (ANNs) (Giese et al., 2019), principle component analysis (PCA) (Bao et al., 2023), orthogonal partial least squares discriminant analysis (OPLS-DA) (Yuan et al., 2020), and partial least squares regression (PLS) (Hao et al., 2019). For example, to detect adulteration in extra virgin olive oils, researchers have used techniques like ultraviolet ion mobility spectrometry (UV-IMS) in combination with chemometrics such as principal component analysis (PCA) and LDA (Garrido-Delgado et al., 2018), as well as near-infrared spectroscopy with chemometric methods (Vanstone et al., 2018). Similar efforts have been made in assessing the authenticity of flaxseed oil using various analytical methods combined with statistical approaches, including mid-infrared spectroscopy (MIR) with partial least squares (PLS) (De Souza et al., 2015), gas chromatography–mass spectrometry (GC-MS) coupled with PCA and recursive support vector machine (R-SVM) (Sun et al., 2015), and other techniques like dielectric spectroscopy and Fourier transform infrared spectroscopy (FTIR) along with chemometrics (Elzey et al., 2016; Zhang et al., 2019).

The ascent in popularity of novel cold-pressed oils accentuates the need for standardized methods to detect adulteration and rancidity in the market. The persistent problem of adulterating expensive edible oils remains a significant concern for both the edible oil industry and consumer health. This deceptive practice, which has been recognized by experts for centuries (Carter, 1885), primarily stems from individuals seeking to increase their profits by diluting the product (FDA,

2009). This is facilitated by the lack of reliable tools for assessing the quality of food products, as noted by the Food and Agricultural Organization (FAO) (FAO, 2021). Despite considerable attention from researchers, food adulteration continues to occur frequently in affluent countries worldwide (Gelpí et al., 2002). The effort to combat this fraudulent activity places a substantial financial burden on the global food industry, with estimates suggesting an annual cost of around EUR 30 billion (European Commission, 2018). This underscores the economic impact of tackling fraudulent practices within the food sector. Researchers have explored the applicability of Differential Scanning Calorimetry (DSC) in detecting adulteration in different fats and oils, such as olive oils, vegetable oils, and animal fats (Islam et al., 2022). DSC, as an analytical method, offers the advantage of detecting changes related to variations in the composition of triacylglycerols, making it a valuable tool for oil authentication. DSC measures the thermodynamic parameters of temperature and enthalpy of phase transition without the need for chemical reagents, distinguishing it from liquid chromatography. This approach markedly enhances DSC's efficiency in characterizing edible oils by furnishing an inclusive and comprehensive interpretation of data. It facilitates concurrent assessment of multiple parameters and streamlines the classification of diverse oil samples based on their resemblances and disparities. Moreover, chemometric models can prognosticate the quality parameters e.g., during storage of oils (Cichocki et al., 2023).

In the light of this perspective, this study aims to exploit the potential of DSC in characterizing of edible oils, supported by the chemometric analysis in order to assess their authenticity as well as oxidative stability. The aim of this research was threefold, as presented in Figure 1. The primary objective was to establish a reliable and efficient approach for the comprehensive evaluation of oxidative stability for fresh and stored oils. Secondly, the research aimed to develop and evaluate a novel discrimination method to verify the authenticity of selected oils during shelf life by combining DSC profiling and advanced chemometric methods. Thirdly, a significant aspect of the research goal was to identify and quantify the presence of adulterants, particularly refined rapeseed oil in cold-pressed flaxseed oil. By combining DSC profiling with advanced chemometric tools, such as artificial neural networks, the research sought to provide a comprehensive application for the feasible detection of adulterants in cold-pressed oils. The research hypotheses to be tested include the suitability of DSC for authenticity assessment of cold-pressed oils and the quantitative detection of adulteration with refined oils, as well as the ability of DSC to assess deterioration of oils during storage.

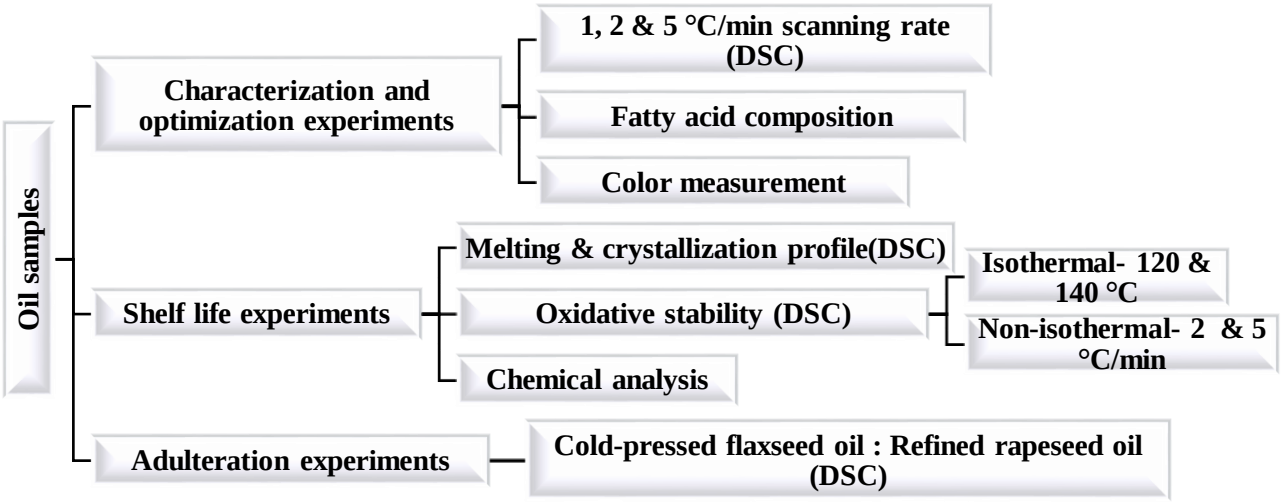

Figure 1. Diagram of the research plan.

2. Materials and methods

2.1 Materials

Figure 2 shows the process of the procuring and storing of the oil samples. Initially, 15 kg of seeds for each cultivar or batch of flax, camelina, and hemp were obtained from various sources and cold-pressed to extract oils.

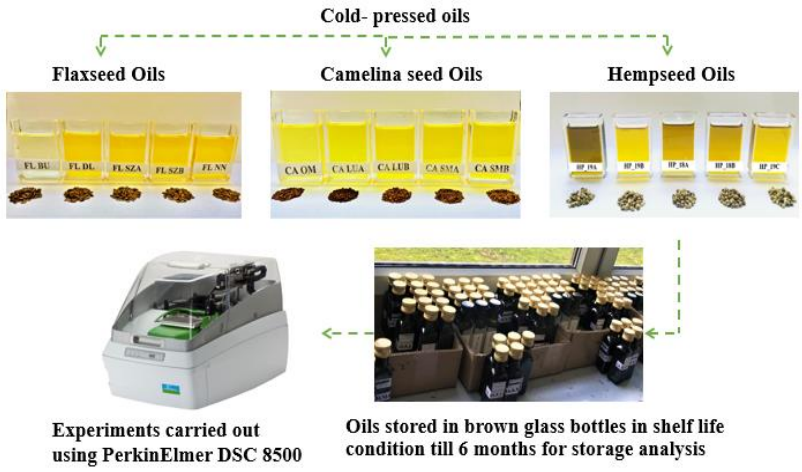

Figure 2. Oils procured for the experiment: three types of cold-pressed oils of different cultivars and from different sources (flaxseed, camelina and hempseed).

Specifically, for flax (*Linum usitatissimum* L.), seeds of the *Bukoz* cultivar from the Polish Institute of Natural Fibers and Medicinal Plants (Poznań, Poland), the *Dolguniec* cultivar from SEMCO manufactory (Śmiłowo, Poland), the *Szafir* cultivar from both SEMCO manufactory and Hodowla Roślin Strzelce Sp. z o.o. (Strzelce, Poland), and seeds of an unknown variety from VitaCorn company (Poznań, Poland) were collected. All hemp (*Cannabis sativa* L.) seeds of the Henola cultivar originated from five different suppliers and were collected from the Polish Institute of Natural Fibers and Medicinal Plants. Additionally, three cultivars of camelina (*Camelina sativa*) seeds were obtained from five suppliers. The spring *Omega* cultivar seeds were purchased from the Poznań University of Life Sciences (Agriculture Research Station Dłoń, Miejska Górka), while the *Luna* and *Śmiłowska* cultivar seeds were collected from SEMCO manufactory, which acquired seeds from various suppliers. All seeds were cold-pressed at the SEMCO manufactory under consistent conditions, ensuring the temperature remained below 50 °C. The pressed oils were left for 24 hours for decantation and then stored in brown glass bottles. These bottles were chosen for storage due to their excellent protection against light exposure, particularly harmful UV rays, and to replicate conditions similar to those available in the market. Until the characterization of the fresh oils, samples were kept in brown glass bottles at freezing temperature (-80 °C). Later, storage analysis was performed from the fresh condition until the sixth month of shelf life (Figure 2). For each storage period (0, 2nd, 4th, and 6th month), freshly opened bottles of each oil samples were used for all analyses. Throughout the shelf life, the samples were kept air-tight at room temperature (23–25 °C) near a window to expose them to ambient natural sunlight. This approach aimed to simulate real-life conditions that the oils might encounter during transportation, distribution, or in consumer households. On the other hand, nine refined oils (three for each type: rapeseed, sunflower, and soybean) were acquired from local Polish markets.

2.2 Methods

2.2.1 Fatty acid composition

Fatty acid composition was determined using Gas Chromatography-Flame Ionization Detector (GC-FID). For analysis, 15 mg of oil was dissolved in 1 mL of hexane from HPLC, Sigma Aldrich, St. Louis, MO, USA, followed by the addition of 1 mL of 0.4 N sodium methoxide. After stirring and leaving the samples for 15 minutes, 5 mL of distilled water was added, and the top layer was collected. The analysis of fatty acid methyl esters was carried out using a Trace 1300

chromatograph (Thermo Fisher Scientific, Waltham, MA, USA) following the AOCS official method (AOCS, 1997). Separation was performed on a Supelcowax 10 capillary column (30 m × 0.2 mm × 0.2 µm), with an injection in the splitless mode and a sample volume of 1 µL. Hydrogen was used as the carrier gas. The initial oven temperature was set at 160 °C and then increased to 220 °C at a rate of 12 °C per minute. The temperature was maintained at 220 °C for 20 minutes. Fatty acids were quantified using the percentage of the area method, where their retention times were compared to the standard 37-Component FAME Mix (Supelco, Sigma Aldrich). The analysis was performed on all samples in two replications.

2.2.2 Color measurement

The color measurements of oils were conducted following the steps from (Choo et al., 2007) using the Konica Minolta CM-5 spectrophotometer (Konica Minolta, Inc., Tokyo, Japan) along with SpectraMagicNx software (Konica Minolta, Inc., Tokyo, Japan). Before initiating the analysis, the instrument was calibrated using a CM-A213 zero calibration plate (black calibration) to accurately measure translucent and transparent liquid samples, followed by distilled water in a 10 mm CM-A98 glass cuvette (white calibration). The research utilized the Hunter Lab scale, and reference standard L^*, a^*, b^* values were predefined to measure the oil color within the specified range. The L^* parameter ranged from 0 to 100, indicating the brightness of the color from black to white. Similarly, the a^* parameter determined the green (below 0) or red (above 0) tinge, depending on the range. Another parameter considered was the b^* parameter, where negative values defined the color blue and positive values represented yellow. All samples were analyzed three times for accuracy and reliability.

2.2.3 Chemical determination of oxidative stability

The p-anisidine value (pAV) measurements for oil samples, used to assess the level of secondary oxidative products, were conducted following the ISO standard (ISO 6885, 2016). Spectrophotometric measurements were taken using a quartz cuvette with a 10 mm optical path length. For each measurement, a sample weighing 3 ± 0.001 grams was used. The obtained values were then calculated using the following equation:

$$pAV = (25\,[1.2\,(A1 - A2 - Ao)])/m \qquad (2)$$

where Ao is the absorbance of the non-reacting sample, A1 is the absorbance of the reacting sample, A2 is an absorbance of the blank sample and m is the mass of the sample (g).

Peroxide value was determined by following the ISO standard (ISO 3960, 2010). A sample of 5 ± 0.001 grams was weighed for measurement. Calculations were performed using the following equation:

$$PV = ((V - Vo) \times Cthio \times F \times 1000)/m \quad (3)$$

where PV is peroxide value (meq O_2/kg), V-volume of titrant in test portion (ml), V_0-ml), Cthio-molar concentration of the sodium thiosulfate solution in mol/l, F-exact concentration of the 0.01 N thiosulfate solution, m-weighed portion of test substance (g).

In accordance with the ISO standard (ISO 3960, 2010), the total oxidation value (TOTOX) parameter was calculated, based on the pAV and PV values, by means of the following formula:

$$TOTOX = pAV + 2PV$$

expressing the overall rate of oil oxidation.

The acid value (AV), which indicates the extent of hydrolytic changes, was determined for five oils following the AOCS official method (AOCS, 2009). Each measurement involved weighing a sample of 10 ± 0.001 grams for analysis. The resulting values were calculated using the following equation:

$$AV = ((A - B) \times M \times 56.1)/W \quad (4)$$

where: AV-acid value (mg KOH/g of test portion), A-volume of standard alkali used in the titration (ml), B-volume of standard alkali used in titrating the blank (ml), M-molarity of standard alkali, W-mass of test portion (g).

2.2.4 Radical scavenging activity by DPPH (RSA DPPH)

The antioxidant activity of the oils was evaluated using the DDPH (2,2-diphenyl-1-pikrylhydrazyl) method (Larrauri et al., 1998). This method assesses the oil's ability to scavenge DPPH• radicals (0.04 mM). To carry out the evaluation, 10 µL of the oil was mixed with 990 µL of DPPH• radical in ethyl acetate (0.04 mM). The mixture was then incubated for one hour in the dark at room temperature. Spectrophotometric measurements at 517 nm were performed using a Varian Cary 1E spectrophotometer (Berlose, Australia), with ethyl acetate serving as a blank. The results were expressed as Trolox equivalents (TE) in mmol/L. A Trolox calibration curve, ranging

from 0 to 15 µM with a slope of 5.3668, was prepared for reference. All oils were analyzed twice to ensure accuracy and reliability of the antioxidant activity measurements.

2.2.5 Determination of oxidative stability by DSC

The oxidative stability of the oils was assessed using the ISO 11357-1 (ISO, 2013) and ASTM D3895-14 (ASTM International, 2019) methods. The measurements were conducted using a DSC 7 Perkin Elmer equipped with an Intracooler II and operated with Pyris software. Both isothermal and non-isothermal protocols were employed to determine the oxidative stability characteristics of the oils. Prior to analysis, the instrument was calibrated using indium (melting point 156.6 °C, ΔHf = 28.45 J/g) and n-dodecane (melting point -9.65 °C, ΔHf = 216.73 J/g). A high-purity nitrogen gas (99.99%) was used as the purge gas. For each analysis, approximately 6-7 mg of oil sample was weighed into open aluminum pans of 50 µL (Perkin Elmer, No. 02190041) and placed in the sample chamber, with an empty aluminum pan serving as the reference. In the isothermal program, the temperatures of 120, 140, and 160 °C were maintained, with a constant oxygen flow of 20 mL/min (purity 99.995%). The obtained curves provided parameters such as oxidation induction time (OIT), oxidation end time (OET), the length of oxidation (Δt = OET–OIT), and the rate of oxidation. The determination of OIT involved normalizing the oxidation DSC curve and finding the intersection of the extrapolated baseline and the tangent line to the descending exotherm. On the other hand, the OET value was measured at the minimum heat flow of the exotherm, indicating the end of the propagation and the beginning of the termination stage of oxidation.

The oxidation rate was calculated according to the following equation:

$$Oxidation\,rate = (Y1 - Y2)/\Delta t \quad (5)$$

where Y1-heat flow at OIT point (W/g, Y2-heat flow at OET (W/g), Δt-length of oxidation (min). The non-isothermal analyses were conducted using different heating rates of 1, 2, 5, 10, and 15 °C/min, while maintaining a constant oxygen flow of 20 mL/min. The oxidation curves obtained from these experiments allowed for the calculation of the onset temperature (Ton) and the end temperature (Tend) of the oxidative process. The Ton value was determined as the onset temperature, which was found at the intersection of the extrapolated baseline and the tangent line to the descending curve of the recorded exotherm. On the other hand, Tend value was measured as the temperature at which the heat flow reached its minimum value, indicating the end of the

propagation stage and the beginning of the termination stage of oxidation. To ensure accuracy and reliability, all DSC experiments were performed twice for the analysis of the oil samples.

2.2.6 DSC Melting and Crystallization Analysis

The melting and crystallization analysis of flaxseed oils was conducted with adaptations based on the method used for butterfat (American Oil Chemists' Society, 2000; Tomaszewska-Gras, 2016). The examination of the melting and crystallization properties was carried out using a Perkin Elmer differential scanning calorimeter DSC 8500 PerkinElmer (Waltham, Massachusetts, USA) equipped with an Intracooler II and operated with Pyris software (Perkin Elmer, Waltham, Massachusetts, USA). To examine the properties of the flaxseed oil, nitrogen gas of 99.999% purity was used as the purge gas. To calibrate the DSC calorimeter, indium (melting point 156.6 °C, ΔH_f = 28.45 J/g) and n-dodecane (melting point -9.65 °C, ΔH_f = 216.73 J/g) were used. For each measurement, samples weighing approximately 6–7 mg were placed in aluminum pans of 20 µL (Perkin Elmer, No. 0219-0062, Waltham, Massachusetts, USA) and hermetically sealed. An empty, hermetically sealed aluminum pan served as the reference. Before analysis, the samples were heated to 30 °C for 5 minutes to melt all crystals and nuclei. The samples were then cooled at scanning rates of 1 and 2 °C/min and heated at scanning rates of 1, 2, and 5 °C/min. Each measurement at a specific scanning rate was completed with the appropriate calibration procedure. Crystallization curves were recorded from 30 to -65 °C. The melting analysis commenced by cooling the oil sample at a scanning rate of 2 °C/min, starting from a temperature of 30 °C down to -65 °C. Subsequently, it was heated at scanning rates of 5 °C/min, covering the range from -65 °C to 30 °C. Each measurement at a specific scanning rate involved completing the calibration procedure with the appropriate scanning rate. After conducting the analysis, the DSC files were converted to the ASCII format and further analyzed using Origin Pro software, version 2023 (OriginLab Corporation, Northampton, MA, USA). To ensure consistent comparison, all curves were normalized, and the baseline was subtracted, allowing the projection of DSC curves for all investigated samples on the same scale. Various parameters were measured from the melting curves, including peak temperature (T, °C), peak heat flow or peak height (h, W/g), area of each peak of the transition (A), and enthalpy (ΔH, J/g). The peak temperature was determined at the maximum heat flow on the curve for the selected peak, while the peak heat flow was established as the maximum value of heat flow for the normalized peaks. Enthalpy was determined by

integrating the area under the curve of heat flow (J/s) versus temperature (°C). For each oil sample, two analytical repetitions were performed. Consequently, five samples of each cold-pressed oils were analyzed in duplicate, while three samples of each refined oils were analyzed in duplicate. In specific cases, the multicomponent DSC curves were deconvoluted using PeakFit and the nonlinear least squares fitting procedure included in the Origin Pro software.

2.2.7 Data analysis

Results were presented as mean and standard deviation. Statistical analysis of the obtained results was performed using Statistica 13.3 software (TIBCO Software Inc., Palo Alto, CA, USA) and SIMCA version 16.1 (Sartorius Stedim Data Analytics AB, Umea, Sweden). Verifications of statistical hypotheses were performed at the significance level of $\alpha = 0.05$. Analysis of variance (ANOVA) and Tukey's multiple comparisons test were used to assess the significance of differences between means. Linear regression analysis and Pearson's linear correlation coefficient was used to assess the significance and direction of the relationship between the selected variables. Multivariate data analysis methods were also used to verify the goals and hypotheses undertaken in the study. Classification and regression approaches were used to build predictive models for oils adulteration detection as it was proposed by authors for the food analysis purpose (Efenberger-Szmechtyk et al., 2018; Rocha et al., 2020). Principal component analysis (PCA) was used as an unsupervised method for pattern recognition and preliminary exploration of raw data. The following chemometric methods were used to build classification and regression models: Orthogonal Partial Least Squares Discriminant Analysis (OPLS-DA), Artificial Neural Networks (ANN), Support Vector Machines (SVM), Multivariate Adaptive Regression Splines (MARS), Linear Discriminant Analysis (LDA) and Multiple Linear Regression (MLR). Cross-validation was applied to build the models. To assess the quality of the classification models (LDA, SVM, MARS and ANN), a confusion matrix was used from which the performance parameters (accuracy, misclassification rate, precision, sensitivity, specificity and F1 score) were calculated. For the OPLS-DA model, the model's performance was evaluated based on the explained variability R^2(cum), representing the goodness of fit for the X and Y variables, and the predictive variability Q^2(cum), reflecting the predictive goodness of fit for the predicted variables. Correlation coefficient (r), coefficient of determination(R^2), adjusted R^2 (a modified version of R^2 was adjusted for the number of predictors in the model), Akaike information criterion (AIC), Bayesian

information criterion (BIC) and Root Mean Square Error (RMSE) were used to assess the goodness of fit of the regression models. In addition, such statistical process control (SPC) tools as X-bar and R (arithmetic mean and range) control charts were used to test the stability of selected melting profile parameters during oil storage. The X-bar chart calculated the average level of the monitored parameter, while the R chart showed the range, indicating the variation inside each sample at each storage time point. Control limits were set at the 3-sigma level, which represents the natural variability of the parameters monitored during storage.

3. Research goals and hypotheses

3.1 Research goals

The aim of this study was to investigate the possibility of using the instrumental technique of differential scanning calorimetry (DSC) in the comprehensive characterization of oils in terms of oxidative stability and authenticity assessment of three cold-pressed oils flaxseed, camelina, and hempseed oils of various cultivars.

The main goal was to be achieved by implementing specific goals:

- Comprehensive evaluation of the oxidative stability of cold-pressed oils by isothermal and non-isothermal DSC methods in relation to the analysis of the composition and chemical stability indicators of flaxseed oil (A1) and camelina oil (A2)
- Assessment by the DSC isothermal and non-isothermal tests changes of oxidative stability of three cold-pressed oils during six-month storage (A6)
- Evaluation of changes in DSC melting profiles of flaxseed oils during six-month storage using X bar and R control charts as statistical process control tools to identify markers of oil authenticity and deterioration (A3)
- Using the entire DSC melting profiles of three cold-pressed oils (flaxseed, camelina, hempseed) and three refined oils (rapeseed, soybean, sunflower) as unique fingerprints for an untargeted approach to oil authentication (A4)
- Comparison of different chemometric approaches for detecting adulteration of flaxseed oil with refined rapeseed oil added at various concentrations (5, 10, 20, 30 and 50% *w/w*) using DSC melting profiles (A5)

3.2 Research hypotheses

In this research the following hypotheses were verified:

- The DSC technique enables to assess the different oxidative stability of cold-pressed oils, by comparing flaxseed oil (A1) and camelina oil (A2).
- Deterioration of oil quality during storage causes a lowering of resistance to thermal oxidation measured by DSC parameters OIT and Ton (A6).
- The DSC phase transition profiles of melting and crystallization are affected by the factors of scanning rate (A1) and storage of oils (A3).
- The combination of untargeted DSC profiling and chemometric methods can provide the reliable tool for the discrimination and verification of the authenticity of selected oils (A4)
- Differential scanning calorimetry is suitable for adulteration detection of cold-pressed oil (flaxseed oil) with refined rapeseed oil by coupling with multivariate data analysis methods (A5)

4. Results

4.1 Determination of oxidative stability by DSC techniques

DSC offers versatile tools for assessing the oxidative stability of oils through both isothermal and non-isothermal methods. Given that oxidative stability stands as a pivotal quality determinant for edible fats and oils, influenced by temperature fluctuations, oxygen exposure, and fatty acid compositions, the diversified temperature regimens allow for a robust evaluation of the oils' performance. This study placed a primary focus on investigating the thermo-oxidative stability of cold-pressed oils, specifically flaxseed and camelina oils, employing a diverse range of analysis conditions. Utilizing DSC methods, the research aimed to comprehensively assess the oxidation characteristics of these oils under varying conditions, particularly accelerated temperature programs in relation to the time of exposure. By subjecting the oils to different temperature regimes and scanning rates, this approach allowed for a detailed examination of how these oils respond to oxidative processes.

4.1.1 Application of isothermal measurements by DSC to assess oxidative stability of cold pressed oils (A1, A2)

The selection of distinct temperature programs for measuring oxidative stability in flaxseed and camelina oils arises from the necessity to comprehensively scrutinize their behavior across a spectrum of conditions. In isothermal measurements, the oxidative stability of the oils is assessed at a constant temperature and the time of oil resistance to oxidation is measured. The influence of various temperatures (120, 140 and 160 °C) on the oxidation parameters measured isothermally has been presented in the publication (A1) for flaxseed oils and in the article (A2) for camelina oils. The parameters used for oxidative stability studies are fundamental markers of how oils behave at different temperatures. The indicators in a simultaneous evaluation of flaxseed and camelina oils include the oxidation induction time (OIT), oxidation end time (OET), length of oxidation (Δt), and rate of oxidation. While OIT and OET parameters indicate the initiation and end of the oxidation process, respectively, Δt indicates the length of oxidation. Meanwhile, the rate of oxidation provides a quantitative measure of how quickly oxidation occurs. These parameters work together to provide an accurate assessment and comparison of the oxidative stability of the oils, allowing for more informed decisions concerning their application and storage conditions.

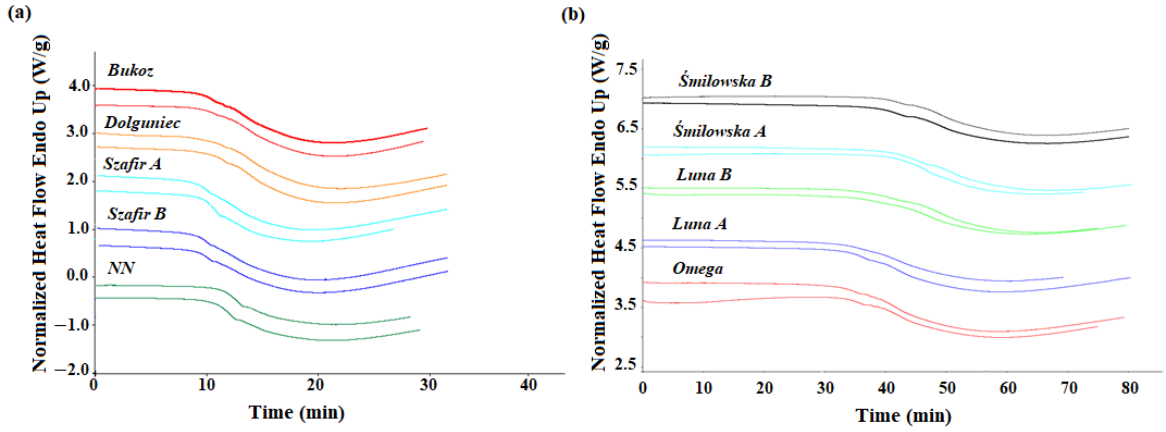

Figure 3. DSC oxidation curves obtained at 140 °C cold-pressed (a) flaxseed oils, and (b) camelina oils.

In Figure 3, to exemplify the nature of the oxidation, curves obtained from isothermal measurements of cold-pressed flaxseed and camelina oils have been presented, which were published in article (A1) for flaxseed oil, while for camelina oils in (A2). Initially, isothermal

experiments conducted at temperatures of 120 °C and 140 °C provided critical insights into the oxidation induction time (OIT) for both flaxseed and camelina oils, while also examining parameters such as OET values, Δt, and oxidation rates. Those results enabled to show the differences between oxidation profiles of these oils. For instance, at temperatures of 120 °C, for flaxseed oil, OIT values ranged from approx. 37.7 to 51.2 minutes, while camelina oil displayed a notably higher range, with values spanning from 61.4 to 76.2 minutes. Furthermore, at 140 °C, the OIT values for both flaxseed and camelina oils decreased significantly, for flaxseed oil, there was a reduction of approximately 4–5 times compared to the values observed at 120 °C, where OIT values ranging from 8.7 to 11.3 minutes. While for camelina oils values were reduced approx. 3.5 times, spanning from 17.0 to 20.7 minutes. Moreover, for camelina oils, the temperature program at 160 °C was also tested for assessing resistance to oxidation under extreme conditions. This was motivated by higher stability of this oil at 120 °C and 140 °C. In the case of camelina oils, OIT values measured at 160 °C ranged from 4.5 to 6.0 minutes, while for flaxseed oil it was not possible to measure OIT at this temperature due to the lower oxidative stability. Thus, the conditions for analysis of OIT parameter should be optimized for each oil individually.

The next parameter, length of oxidation (Δt) was analyzed for both oils. For flaxseed oils, at 120 °C, Δt ranged from 17.9 to 20.7 minutes, and when compared to the results obtained at 140 °C, it was evident that the oxidation rate tripled, ranging from 10.0 to 11.8 minutes. Similar trend was observed for camelina oils, at 120 °C, Δt spanned from 22.4 to 27.6 minutes, at 140 °C it was between 12.2 to 13.9 minutes, and at 160 °C, Δt ranged from 5.4 to 6.7 minutes. Additionally, the rate of oxidation, reflecting the speed of the oxidation process, was calculated from the DSC oxidation curve, at 120 °C, this rate ranged from 0.02 to 0.03 W/g·min, while at 140 °C it was in the range from 0.08 to 0.09 W/g·min. For camelina oils, it was noted that at 140 °C, the rate of oxidation (from 0.05 to 0.06 W/g·min) was four times higher than that observed at 120 °C (from 0.01 to 0.02 W/g·min). Furthermore, in the 160 °C program, the rate of oxidation was also three to four times higher, ranging from 0.11 to 0.21 W/g·min, compared to the 140 °C program. From the above results, it was observed that isothermal measurement mode by DSC technique can be efficiently employed to assess the OIT with good repeatability for both oils. Experimental trials encompassed various cultivars of both oils, serving to validate the unique traits associated with the oxidative stability profiles of flaxseed and camelina oils, distinguishing them from other types of

oil. The results obtained prove the notably higher oxidative stability traits exhibited by camelina oil when compared to flaxseed oil across various temperature programs.

Furthermore, in the article (A2), the relation between temperature of OIT analysis and the parameters gleaned from the isothermal DSC measurements for camelina oils, encompassing OIT, OET, Δt, and oxidation rate, was described by exponential functions (Figure 4). These intricate relationships furnish a prognostic framework that elucidates how these parameters change with temperature increase (120, 140 and 160 °C). High coefficients of determination (R^2= 0.99 for OIT, OET and Δt; R^2= 0.96 for oxidation rate) were obtained, that underscores the statistical goodness of fit (A2).

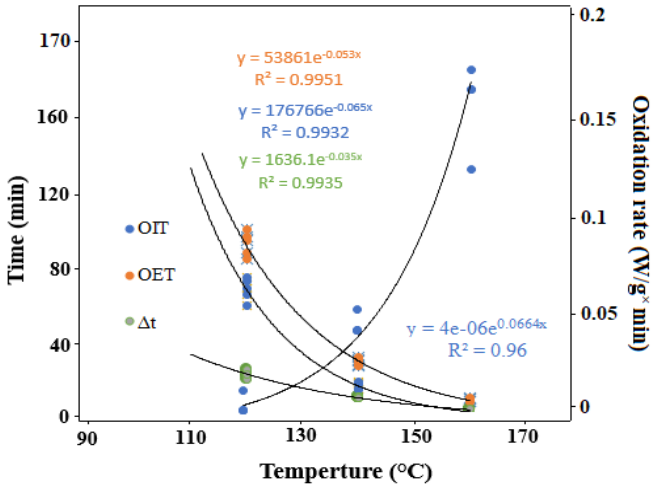

Figure 4. Relationship between temperature and parameters of isothermal DSC measurements: OIT, OET, oxidation duration (Δt) and rate of oxidation.

4.1.2 Application of non-isothermal measurements by DSC to assess oxidative stability of cold pressed oils (A1, A2)

The non-isothermal measurement by DSC technique was carried out to uncover distinctive resistance of oils to oxidation measured at dynamic conditions. The investigation was done based on flaxseed oil (A1) and camelina oils (A2) using various heating rates of 1, 2, 5, 10 and 15 °C/min. Two parameters were determined from the oxidation curves: the onset temperature (Ton), corresponding to the initiation of oxidation and the end temperature (Tend), which represents the end of the propagation stage and beginning of the termination stage, at which stable products are formed.

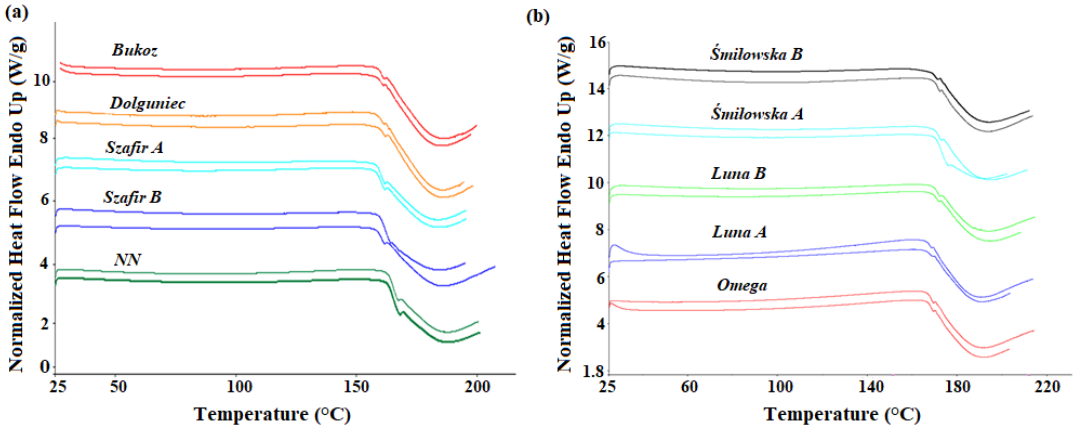

Figure 5. DSC non-isothermal oxidation curves obtained at scanning rate 5 °C/min for cold-pressed (a) flaxseed oils, and (b) camelina oils.

In Figure 5, examples of oxidation curves for flaxseed and camelina oils obtained at scanning rate 5 °C/min have been illustrated. It was observed for all oils higher Ton values were obtained when using a higher heating rate, for instance of 5 °C/min compared to 2 °C/min (A1, A2). This difference is likely due to the prolonged exposure of the oils to oxygen at the lower heating rate. Comparing parameters of Ton for flaxseed and camelina oil samples at different scanning rates it was shown that the differences in oxidative stability between two oils were not as distinct as in the measurement of oxidation induction time (OIT). For instance, for flaxseed oil, at a scanning rate of 2 °C/min, Ton values ranged from 144.0 to 146.6 °C among different cultivars, while for camelina oil from 152.14 to 155.9 °C. For parameter of Tend for both oils, the differences for both oils were similar, since values ranged between 157.3 to 160.8 °C for flaxseed oil and from 165.0 to 170.5 °C for camelina oil. In order to investigate the dependence of the Ton and Tend parameters on the applied heating rate, different conditions were tested (1, 2, 5, 10 and 15 °C/min) based on camelina oil (A2). Based on the abovementioned results for camelina oils, logarithmic relationship was possible to evaluate between the scanning rate and the parameters of Ton and Tend (Figure 7, A2). The data illustrates that as the scanning rate increases, the oils' onset temperature also rises. This relationship was expressed by logarithmic functions, with high coefficients of determination (R^2=0.99 for Ton, and R^2=0.90 for Tend). It was stated that these equations can serve as predictive tools to estimate oxidation temperatures at various scanning rates.

Additionally, in studies of oils oxidation, the kinetics of oxidation were examined, as shown in publication (A2), based on different cultivars of camelina oil and using all results obtained from non-isothermal measurements. The Ozawa-Flynn-Wall method (Flynn & Wall, 1966), adapted by

previous researchers (Adhvaryu et al., 2000; Qi et al., 2016; Ratusz et al., 2016), was applied to compare the kinetic parameters of oxidation for various cultivars of camelina oil. Different values were obtained for various cultivars of camelina oil for activation energy (Ea), which ranged from 96.49 kJ/mol to 92.17 kJ/mol, as well as for oxidation rate constants (k), which ranged from 0.25 1/min to 0.35 1/min and half-life times ($t_{1/2}$), from 2.0 1/min to 2.7 1/min. The most stable cultivars were characterized by the highest activation energy (Ea) and half-life times ($t_{1/2}$) and the lowest oxidation rate constants (k). Other researchers have reported comparable activation energy (Ea) values for camelina oil, falling within the range of 91.9 to 122 kJ/mol for camelina oil extracted using different methods (Belayneh et al., 2015). The successful application of DSC for camelina oil oxidation kinetics showed the possibility to predict by these kinetic parameters the behavior of oil during oxidation process. By tailoring the experimental conditions and analysis procedures to the specific characteristics of oil samples, a parallel investigation can be conducted, yielding valuable insights into the oxidation kinetics of this oil, and potentially contributing to a broader understanding of the thermal behavior and stability of edible oils.

4.1.3 Relationship between DSC oxidation stability parameters and chemical indicators of oxidative stability and fatty acid composition of cold-pressed oils

In parallel with DSC experiments on isothermal and non-isothermal oxidation, conventional chemical characterization of oils was also performed to understand the compositional characteristics of oils and the relationship between the two types of instrumental and traditional measurements. Traditional chemical oxidation measurements i.e., peroxide value (PV), p-anisidine value (pAV), TOTOX and acid value (AV) showed that both oils demonstrated good oxidative stability parameters as freshly pressed oils and fall within acceptable limits according to the Codex Alimentarius standards (Codex Alimentarius, 1999). Since all the peroxide values obtained were below 7 meqO2/kg, p-anisidine values were lower than 1.0 and TOTOX below 15, it was assumed that all the oils studied were of good quality. However, differences in oxidative stability indicators between various cultivars of flaxseed and camelina oil were observed, for instance TOTOX values were in the range from 3.2 to 14.8 for flaxseed (A1) and from 5.43 to 8.89 for camelina oil (A2). Considering those differences found between cultivars of fresh cold-pressed flaxseed oils, the analysis of the correlations between chemical indices and DSC parameters, was performed to provide insights into the factors influencing the oxidative stability. It was established that thermo-

oxidative stability DSC parameters (OIT, Ton) were negatively correlated with chemical indicators like PV and TOTOX, while no correlation with pAV was found (Figure 6a). The strongest negative correlations were observed for OIT (120 °C) and Ton (5 °C/min). It was demonstrated that higher peroxide values were associated with lower DSC parameters, indicating various thermo-oxidative stability in flaxseed oils depending on various cultivars (Figure 6a). The explanation for the different oxidative stability for different varieties was sought in the different composition of fatty acids, therefore the relationship between DSC parameters and the share of fatty acids was also examined. Understanding the fatty acid composition is crucial as it directly impacts the oxidative stability of the oils. In this study, both oils (flaxseed and camelina) are valued for their unsaturated fatty acids, such as α-linolenic acid (ALA) and linoleic acid. Flaxseed oil, as it was shown in article (A1) was characterized by its rich composition of polyunsaturated fatty acids, with α-linolenic fatty acid (ALA, C18:3, *n*-3) being the dominant and unique feature. Variations in ALA content existed among different flaxseed cultivars, ranging from 56% to 63%, which is similar to other studies findings (Choo et al., 2007; Daun et al., 2003; Łukaszewicz et al., 2004). The remaining unsaturated fatty acids i.e., linoleic acid (C18:2) made up the total amount of polyunsaturated fatty acid (PUFA) between 71 and 77%. Composition of camelina oils, presented in the article (A2), was characterized by its high content of PUFA, between 54 and 57%, among which the highest percentage was found for α-linolenic acid (ALA, C18:3, n-3), which made up from 30 to 37% of the total fatty acids. These results are consistent with other studies (Kurasiak-Popowska et al., 2019; Różańska et al., 2019; Zubr & Matthaus, 2002). Strong negative correlations were established between the percentage of α-linolenic acid and DSC parameters (OIT, Ton). For flaxseed oil Pearson's correlation coefficients were between -0.57 and -0.82 (Table 7, A1) and between -0.75 and -0.91 for camelina oil (Table 3, A2). This indicates that α-linolenic acid predominantly influences the thermo-oxidative stability of flaxseed and camelina oil, aligning with prior research findings (Mao et al., 2020). Additionally, strong positive correlations were noted between these unsaturated fatty acids and the oxidation rate constant (k), suggesting that higher levels of unsaturated fatty acids led to faster oxidation reactions (A2, Table 3). In addition, also the correlation analysis between antioxidant activity (RSA DPPH) and DSC oxidation parameters revealed strong positive correlations (r between 0.767 and 0.973), implying that greater antioxidant activity corresponded to higher DSC parameters (OIT, Ton), indicating enhanced thermo-oxidative stability (Table 5, A2).

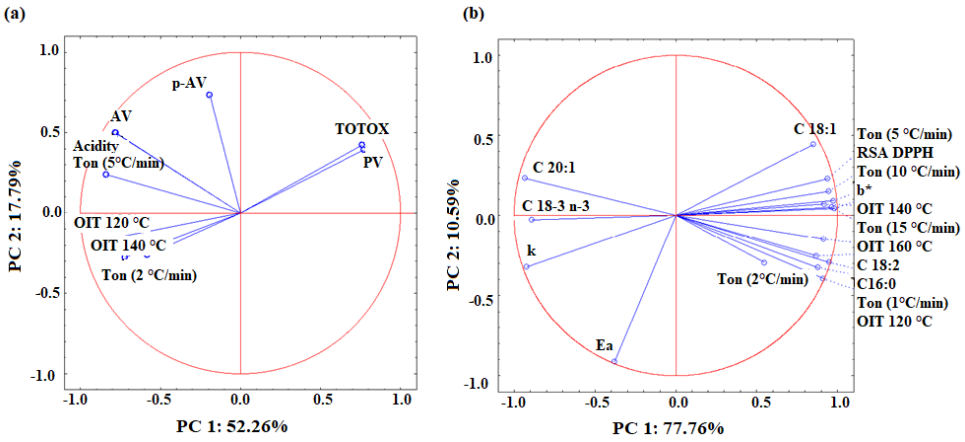

Figure 6. PCA analysis, the loading plots for PC1 and PC2 with projection of the variables: (a) DSC parameters, chemical indices for flaxseed oils, (b) DSC parameters, fatty acids content, RSA DPPH and b* for camelina oils.

The analysis of relationships between different parameters based on different cultivars of both flaxseed and camelina oils offers a comprehensive understanding of factors influencing their oxidative stability. The isothermal approach provides insights into oxidation initiation at specific temperatures, while the non-isothermal technique captures the oils' behavior under dynamic temperature conditions. These methodologies collectively provide valuable insights into the oils' performance at different temperatures and dynamic conditions, enabling informed choices for their applications and storage.

4.1.4 Influence of storage on DSC oxidative stability parameters of cold-pressed oils (A6)

Differential scanning calorimetry is a technique that enables resistance of oils to thermal oxidation to be measured by determining isothermally the oxidation induction time (OIT) or non-isothermally onset temperature (Ton). Deterioration in oil quality during storage can cause a lowering of resistance to thermal oxidation. However, there are no studies showing whether these parameters change during shelf life. Therefore, analysis of the oxidative stability of cold-pressed oils (flaxseed, camelina, hempseed) was conducted by considering storage time using isothermal and non-isothermal DSC methods. A study published in the article (A6) presented DSC as a promising alternative for assessing oxidative stability compared to conventional chemical analysis, which precision depends strongly on the technicians. DSC offers a non-toxic, cost-effective and environmentally friendly approach to monitor quality changes during storage. Traditionally, chemical methods such as peroxide value determination and TOTOX value were also used as

reference methods to monitor the deterioration in quality of oils. The study investigated the potential of isothermal and non-isothermal DSC tests to measure parameters such as OIT and Ton, respectively, as indicators of oxidative changes in oils. Another important aspect of this study was that the experiments were performed on stored samples that mimic conditions similar to those found on supermarket shelves. In Figure 7, the examples of DSC curves for a cold-pressed flaxseed oil (*Szafir* variety) are shown i.e., isothermal (120 °C) and non-isothermal (5 °C/min). These curves were analyzed to measure oxidative stability isothermally by oxidation induction time (OIT) and non-isothermally by onset temperature (Ton) during heating in the presence of oxygen. The results obtained throughout the experimental scheme revealed significant changes in these parameters during the six-month storage period for the three types of oils: flaxseed, camelina and hemp seed.

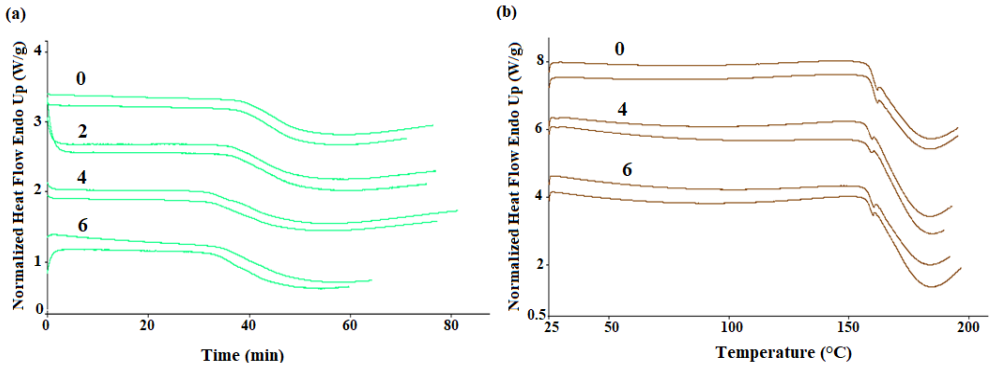

Figure 7. DSC oxidation curves for flaxseed oil (Szafir cultivar) during storage, determined (a) isothermally (OIT at 120 °C) and (b) non-isothermally (Ton 5 °C/min).

The oxidation profiles of all oils showed, a clear trend of shifting the oxidation induction time, (OIT) to lower values for every storage period. This shift indicates that storing oil samples for six months leads to a reduction in OIT, implying a decrease in resistance to thermal oxidation. Similarly, an alternative method for assessing thermal oxidation stability, namely non-isothermal, showed decreasing trend of Ton changes within storage was observed. In this approach, oil samples were subjected to increasing temperature at a constant heating rate (2 and 5 °C/min) (A6). The consistent trend of decreasing oxidative stability during storage, measured as oxidation induction time (OIT) values was confirmed for both temperatures 120 and 140 °C. Specifically, at 120 °C changes were most noticeable, the OIT level decreased for flaxseed oil, camelina oil and hempseed oil from 43, 72 and 51 minutes to 33, 65 and 41 minutes, respectively (Figure 3, A6). A similar trend was observed at 140 °C, although hempseed oil was an exception at this temperature. Non-

isothermal measurement (Ton) confirmed changes in oils stability observed by isothermal test. Ton values also indicated a trend of decreased oxidative stability during storage for all three oils. For example, average Ton values at 2 °C/min decreased from 147, 154 and 147 °C to 142, 152 and 144 °C for flaxseed, camelina and hempseed oil, respectively. Similar trends were observed when the heating rate was increased to 5 °C/min.

From the findings in Article A6, it's evident that the DSC parameters for measuring the oxidative stability of cold-pressed oils are highly repeatable, demonstrating their consistency across different cultivars of the same type of oil. The information regarding the coefficient of variation (CV) for OIT and Ton measurements, as provided in the supplementary material (Table S1, A6), further enhances the evaluation of the reliability of these measurements. Specifically, for the measurement of OIT at 120 °C, the CV values ranged from 0.68 to 2.56%, indicating relatively low variability among different cultivars. However, when the temperature was increased to 140 °C for OIT measurements, the CV values showed a higher range, from 1.17 to 5.85%, suggesting a slightly greater variability at this elevated temperature. Contrarily, for the non-isothermal determination of Ton, there were no significant differences in the CV between the two heating rates, 2 °C/min and 5 °C/min. The CV values were relatively consistent, ranging from 0.20 to 0.38% for the 2 °C/min rate and from 0.14 to 0.42% for the 5 °C/min rate. This consistency in the CV values for Ton, combined with the low CV values for OIT at 120 °C, suggests that the stability trends observed in these studies are reliable and can provide a solid basis for further statistical analysis. Overall, these results highlight the effectiveness of DSC parameters such as OIT and Ton as reliable indicators for monitoring the oxidative stability of cold-pressed oils over time.

For achieving the comprehensive understanding of the oils oxidation proneness, in parallel with the DSC measurements, the oxidative stability of cold-pressed oils during storage was also assessed using conventional chemical methods, including peroxide value (PV), acid value (AV), p-anisidine value (pAV), and TOTOX value. All chemical indicators of oxidative stability (PV, pAV, TOTOX, AV) for all three oils (flaxseed, camelina and hempseed oils) significantly increased ($p \leq 0.05$) during six months of storage (Figure 1, A6). The results obtained for the chemical indicators of deterioration in three types of oils are consistent with previous research in this field. The elevated values of PV and p-AV during storage were also documented for camelina seed oils in a separate study, even though the storage conditions (darkness at 8 °C for 3 weeks) differed from those for this investigation (Abramovič et al., 2007). Moreover, there were studies indicating a

significant increase in chemical indices (such as AV, PV, pAV) for stored flaxseed oil, which are comparable to the findings in our study (Hasiewicz-Derkacz et al., 2015; Tańska et al., 2016). In this part of the study the objective was to compare changes of DSC parameters (OIT and Ton) during storage of three oils with traditional chemical indicators (PV, pAV, AV, TOTOX). Results of Pearson's correlation coefficients (Table 1, A6) showed strong negative correlations between DSC parameters and chemical indices, especially for flaxseed and hemp seed oils. Furthermore, to assess the possibility of using DSC parameters to distinguish fresh from the deteriorated oils, a classification model was built using linear discriminant analysis (LDA). The LDA analysis (Figure 8) showed that for flaxseed and hempseed oils, the discrimination between fresh and stored oils was very distinct, and the classification was highly accurate, while for camelina oil, the distinction was less evident, as camelina oils proved to be more resistant to the oxidation process. The ability to accurately discriminate between fresh and stored oils, even when considering DSC data alone, highlights the potential of DSC analysis as a valuable tool for assessing oil stability and quality over time.

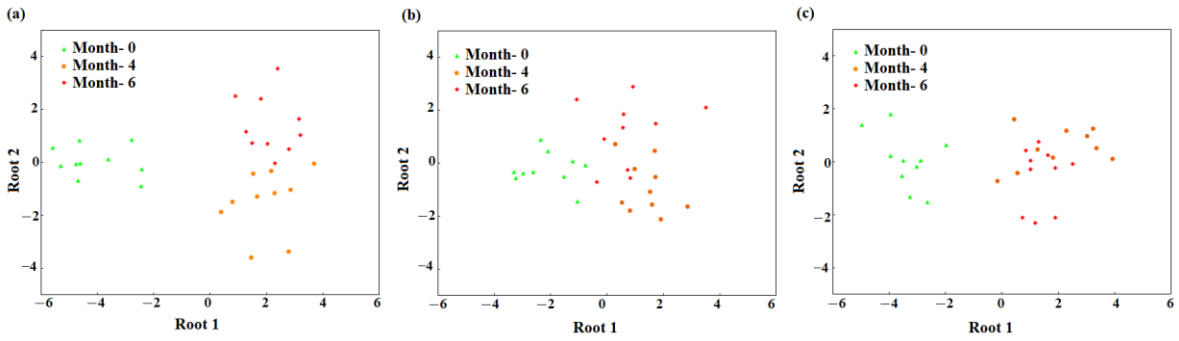

Figure 8. Linear discriminant analysis (LDA) performed using DSC parameters (OIT, OET, Δt, oxidation rate at 120 °C and 140 °C; Ton and Tend at 2 °C/min and 5 °C/min) for cold-pressed (a) flaxseed, (b) camelina and (c) hempseed oils during 0, 4- and 6- month storage time.

In this part of the study, it was proved that DSC parameters can effectively detect oxidative changes in oils caused by the storage, as can traditional chemical indicators such as PV, pAV and TOTOX value. Based on studies, significant correlations have been shown between DSC parameters and these chemical indicators, especially for flaxseed and hemp oils. This established DSC as a reliable tool for monitoring the oxidative degradation of oils. In regard to benefits, the use of DSC is an environmentally friendly alternative, as it does not require the use of harmful chemicals. It is also a time-efficient method that can measure multiple parameters, providing a comprehensive

overview of oil quality and stability. Furthermore, the study showed that DSC parameters are consistent across different varieties of the same oil type, increasing their reliability for further statistical analysis.

4.2 Determination of oils authenticity and stability using DSC phase transition

4.2.1 Factors influencing DSC phase transition profile

4.2.1.1 Influence of scanning rates on DSC phase transition curves (A1)

The goal of using the DSC technique to assess the authenticity of oils required first examining the factors influencing the change of the profile of the same oil sample. Specifically, it emphasizes the critical importance of selecting an appropriate scanning rate in DSC experiments when assessing the thermal properties of cold-pressed oils. The scanning rate represents the rate at which the sample is either heated or cooled. How the scanning rate can influence the obtained DSC curves was analyzed and presented in article (A1) based on cold-pressed flaxseed oil. Both crystallization and melting experiments were carried out, which paved the understanding for the phase transition phenomena occurred at different scanning rates. In this study, different parameters of phase transition i.e., peak temperature (T), the enthalpy of melting or crystallization ΔH (J/g) were calculated. The crystallization profiles are assessed to understand flaxseed oils phase transition from a liquid to a solid-state during cooling. In the provided study, two different scanning rates (1 °C/min and 2 °C/min) were employed to assess crystallization profiles of flaxseed oil (showed in Figure 1, A1). It was observed that the crystallization peak temperatures for various flaxseed oil cultivars were found to be in the range from -54.6 to -55.4 °C (1 °C/min) and from -59.1 to -60.2 °C (2 °C/min). The enthalpy was also measured, as the area under the peak provided information about the heat released during the phase transition. The mean enthalpy values ranged from -32.1 to -34.8 J/g for 1 °C/min and from -27.3 to -29.0 J/g for 2 °C/min. The mean enthalpy values ranged from -32.1 to -34.8 J/g for 1 °C/min and from -27.3 to -29.0 J/g for 2 °C/min. The results obtained for scanning rate 1 °C/min correlate well with the study presented by other authors for flaxseed oils (Teh & Birch, 2013).

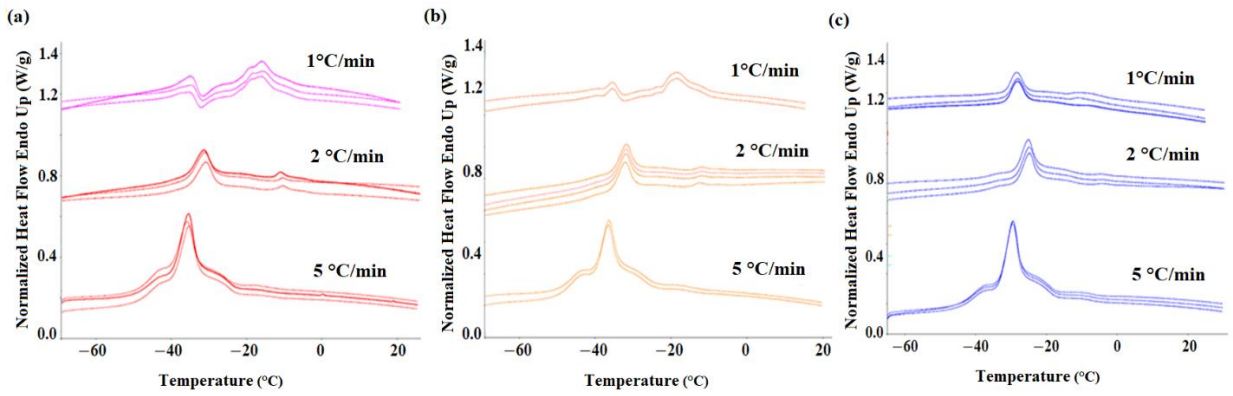

Figure 9. DSC melting curves obtained with a various heating rates (1, 2, and 5 °C/min) for cold-pressed flaxseed oils from different cultivars (a) *Bukoz*, (b) *Dolguniec*, and (c) *Szafir B*.

Example of phase transition melting profiles for various flaxseed cultivars, obtained at different heating rate (1, 2, 5 °C/min) is shown in Figure 9. Compared to the crystallization profiles, where one peak was detected, the melting profiles turned out to be more complex and therefore more informative. These multiple peaks indicate the presence of different triacylglycerols fractions as well as polymorphic forms. The variation in the melting profiles between flaxseed cultivars was most visible for the heating rate of 1 °C/min., for which some melting curves exhibited two pronounced peaks (Tm1 and Tm2), while others showed a reduction in the second peak (Tm2). This variation in the shape of melting profile was confirmed by the enthalpy values ranging from 34.3 to 127.9 J/g. The scanning rate of 2 °C/min led to alterations in peak shape compared to 1 °C/min. Moreover, compared to the heating rate of 1 °C/min, for which the second peak (Tm2) was detected in the range from -10.3 to -13.8 °C, for the scanning rate of 2 °C/min, higher similarity of melting curves between cultivars was observed, suggesting that higher heating rate reduces polymorphic transitions. While peak temperatures did not vary significantly among cultivars, the area of peaks differed, with a range of enthalpy values from 43.1 to 50.8 J/g. Similar observation for 1 and 2 °C/min melting profiles were found by other authors (Teh & Birch, 2013; Zhang et al., 2014). At the heating rate of 5 °C/min, all curves exhibited a high degree of similarity, meaning that polymorphic transitions for this scanning rate were more limited than for lower heating rates (1 and 2 °C/min). The main peak was detected for all cultivars, along with two pronounced shoulders peak on either side of the main peak. The temperature of the main peak (from -29.4 to -31.9 °C) and total enthalpy of melting phase transition (from 60.4 to 63.4 J/g) did not differ significantly among cultivars, which is in agreement with other findings (Zhang et al., 2011), where

peak temperatures were detected between -32.5 °C and -30.7 °C, and enthalpy between 62.2 J/g and 57.9 J/g.

The study has shown that the choice of scanning rate is crucial for each type of oil, thus preliminary study is necessary to establish how the heating rate affects the shape of curve, the number and position of peaks as well as the enthalpy of melting phase transition. The results obtained at different scanning rates suggested that the repeatability of the melting profiles was the highest at 5 °C/min, which can create a reliable fingerprint for authenticity assessment. Therefore, this heating rate was chosen for further study in the area of oils authentication.

4.2.1.2 Influence of storage time on DSC melting curves (A3)

The effect of storage time on the DSC melting curves of different flaxseed oil varieties was investigated to assess the stability of thermodynamic parameters and understand how storage time affects the melting behavior of cold-pressed flaxseed oil samples. Valuable insights into the melting profiles of phase transitions of flaxseed oils after 0, 2, 4 and 6 months of storage were obtained (article A3). Due to the complex, overlapping nature of the melting curves, a deconvolution analysis was performed to identify and calculate various parameters. Applying the deconvolution algorithm, it was possible to isolate and identify four distinct peaks in the melting curve of flaxseed oil, each corresponding to a specific phase transition or component (Figure 2, A3). This allowed for a more detailed and accurate characterization of the thermal behavior of flaxseed oil samples, including the identification of key parameters such as peak temperature (T), peak height (h), peak area (A) and percentage area (P A). In this study, published in article (A3), X-bar and R control charts tool was used to monitor changes of all those thermodynamic parameters of the melting curve during storage of oils, in order to select stable parameter for fingerprinting as well as to identify unstable parameters as indicators of oil deterioration. Figures 10 (a–b) demonstrates control charts for main peak height and area parameters (h2, A2, and PA2), which exhibited decreasing trend throughout the oil's shelf life. This trend was corroborated by the data presented in the article (A3) (Tables 3 and 4), showing significantly lower h2, A2, and PA2 values after six months of storage. Among four endothermic peaks, the main peak (T2) and the fourth peak (T4) exhibited a gradual shift to higher temperatures during storage. Comparing all peak height parameters, expressing the intensity of the phase transition phenomena, it was observed that the intensity of the main peak (h2) and the last peak (h4) decreased significantly after six months of

storage, while the other two smaller peaks (h1 and h3) remained relatively stable. In addition, changes in peak area and percentage of peak area over time were monitored. The area of the calculated for the second peak (A2) and the percentage of peak area (P A2), decreased significantly during storage, while the area of the first and third peak (A1, A3) remained relatively unchanged, contrasting with the increased percentages of the areas of the first and third peaks (P A1, P A3).

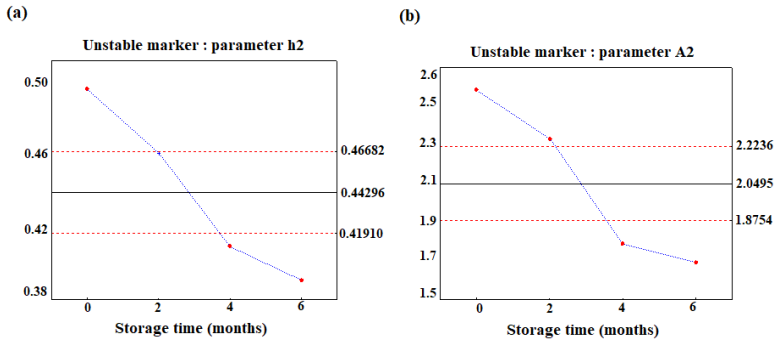

Figure 10. X-bar R control charts of unstable parameters calculated from DSC melting curves for the second peak: (a) h2, and (b) A2.

Moreover, the ratios calculated from the DSC parameters were also analyzed using control charts, for which decreasing or increasing trends were observed as it was shown in the Figures 5 and 6 of the article (A3). All the DSC parameters (in total 16), which were identified by control charts as unstable during storage with a decreasing or increasing trend, were considered as markers of oils deterioration .

Parameters that remained stable throughout the storage period were selected as potential markers of authenticity for fingerprinting purposes. A total of twelve parameters and their ratios were derived from these peaks, serving as indicators for authentication purposes. The utilization of X-bar and R control charts revealed that the first and third peak parameters, such as T1, h1, A1, T3, h3, and A3, remained stable and did not cross the upper and lower control limit lines, and as T1, h3, and A3 with minor variations (Figure 3, A3). Additionally, the ratios of those parameters were also calculated, such as h1/h3, A1/A3, P A1/P A3, for the first and the third peak as well as for the second and fourth peaks (h2/h4, A2/A4, and P A2/P A4) and were found to be stable (Figure 4, A3). Notably, this approach illustrates that, parameters responsible for the percentage of peak area (P A) did not exhibit coherent properties when examined individually, as they depend on the other peaks within the melting curve. However, when considered as ratios (P A2/P A4), these parameters proved to be a more reliable for assessing oil quality. The importance of the percentage

of area parameters lies in their ability to capture the overall shape and composition of the melting curve, offering a holistic perspective on the oil's characteristics. Achievement from the study underscored the critical importance of monitoring the melting profiles of oils, as changes in these parameters, especially in the second peak and specific parameter ratios, were indicative of oils authentication.

The importance of these findings lies in the potential to serve as effective indicators to characterize oil stability and quality, providing a valuable tool to monitor and assess oil deterioration over time, which can have significant implications for various industries dependent on oil quality control and product shelf life. The use of control charts therefore allowed both the selection of DCS parameters that are characteristic of flaxseed oil and do not change significantly during storage and the identification of parameters whose changes indicate a deterioration of oil quality during storage. These results highlight the effectiveness of DSC analysis in monitoring the stability of oils based on their thermal properties during storage.

4.2.2 Differentiation between cold-pressed and refined oils using DSC melting profile (A4)

This part of the experiment, published in the article (A4) will shade light on the innovative approach of using untargeted DSC analysis of the complete thermal spectrum for oil authentication as a novel and valuable tool for quality assessment and fraud detection in the edible oil industry. Analyzing both cold-pressed (flaxseed, camelina and hempseed) and refined (rapeseed, soybean and sunflower) oils for authenticity purposes was considered, assuming that each oil has a unique melting phase transition profile.

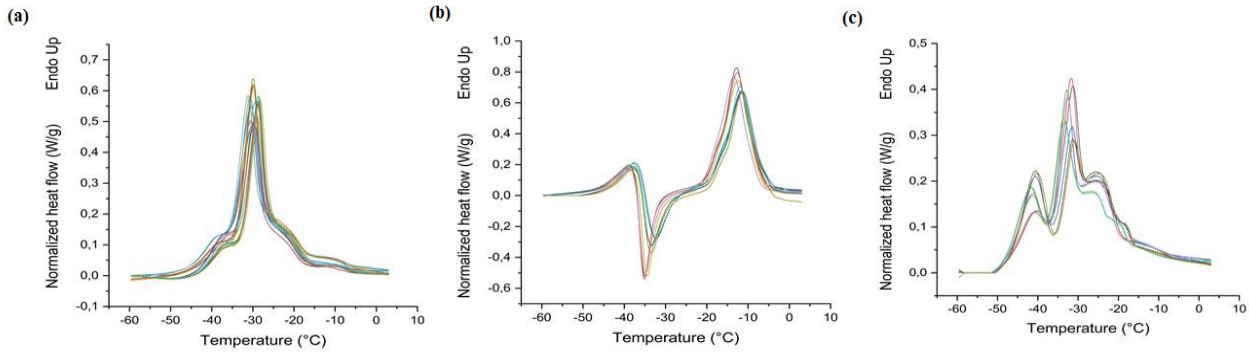

Figure 11. DSC melting curves of cold-pressed oils at scanning rate 5 °C/min; (a) flaxseed oils; (b) camelina oils; (c) hempseed oils.

As presented in Figure 11, the melting profiles of flaxseed, camelina, and hempseed oils are characterized by the appearance of multiple endothermic and exothermic (for camelina) peaks. The peaks appeared for flaxseed and hempseed oils are endothermic in nature, indicating heat absorption during the process, for instance, flaxseed oil exhibits four peaks at temperatures ranging from -36.4 to -12.8 °C, while hempseed oil shows peaks at temperatures ranging from -41.0 to -17.1 °C. Camelina oil, on the other hand, displays a unique profile with one exothermic peak at -33.6 °C and two endothermic peaks (at -38.1 °C and -12.0 °C). The presence of an exothermic peak during the melting phase transition of camelina seed oil was also reported at similar temperature of -34.6 °C by other authors (Rudakov et al., 2021). Moreover the results of determination of peak temperatures of the melting profiles of flaxseed were consistent with the results of the same authors (Rudakov et al., 2021).

Next step of this part of the study was to analyze the melting profile of refined oils (rapeseed, soybean and sunflower), as they are commonly used as adulterants due to their affordable price and widespread availability, but also because they are colorless and odorless. The melting profiles of the refined oils were characterized by the appearance of only endothermic peaks during the melting phase transition. The differences in peak profiles of these refined oils were illustrated in Figure 2 of the article (A4), where also parameters calculated from the DSC curves were presented (Table 2, A4). For rapeseed oil, two endothermic peaks were observed, with the second peak being the major one at -13.5 °C. In contrast, both soybean and sunflower oils display more complex melting profiles, however quite similar with four (-32.2, -24.1, -18.1, -5.2 °C) and three endothermic peaks (-32.2, -24.8, -8.6 °C) respectively. Comparable results obtained for the melting profiles for sunflower oils with three peaks (-36.4, -27.4, -10.7 °C) and rapeseed oil with two peaks (-23.0 °C and -15.4 °C) at a heating rate of 5 °C/min were reported (Rudakov et al., 2021).

Considering the above results for cold-pressed and refined oils, a chemometric analysis i.e., principal component analysis (PCA) and orthogonal partial least squares-discriminant analysis (OPLS-DA) were performed to differentiate and classify various oils based on their DSC melting profiles. The chemometric analysis focused on distinguishing between three cold-pressed from three refined oils (Figure 12a). PCA method effectively captured the underlying patterns of variation within the dataset. The first two principal components, t[1] and t[2], collectively

accounting for 80.8% of the total variation condensed the essential information required for distinguishing the oils, and their high cumulative contribution underscores their significance.

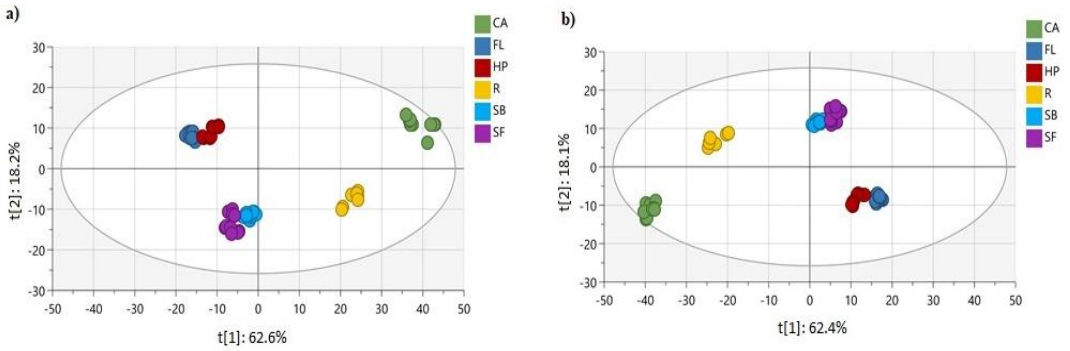

Figure 12. Distinguishing oils based on their DSC melting profiles; (a) PCA score plot; (b) OPLS-DA score plot; CA; camelina oil; FL, flaxseed oil; HP, hempseed oil; R, rapeseed oil; SB, Soybean oil; SF, sunflower seed oil.

OPLS-DA method (Figure 12b), on the other hand, successfully classified the oils into six distinct classes, representing each specific oil type. The model fit was assessed through coefficients such as $R^2X(cum)= 0.971$, $R^2(cum)= 0.916$, and $Q^2X(cum)= 0.887$, which collectively demonstrated the robustness and predictive accuracy of the model. The ultimate achievement of this study is the development of a novel approach for authenticating edible oils using their entire DSC melting profiles, effectively treating these profiles as unique fingerprints for each oil type. These distinctions were based on variations in the number and positions of peaks in the melting profiles, as well as differences in thermodynamic parameters like peak temperature, peak heat flow, and enthalpy for each oil type. The pragmatic significance of the findings lies in its potential for detecting fraudulent practices in the oil industry.

4.3 Detection of adulteration of cold-pressed flaxseed oil with refined rapeseed oil using DSC melting profiles (A5)

4.3.1 Changes of DSC melting profiles of flaxseed oil adulterated with rapeseed oil

DSC melting curves were analyzed to study the thermal properties of various flaxseed oil cultivars, both pure and adulterated with refined rapeseed oil at different concentrations: 0, 5, 10, 20, 30 and 50% *w/w* (Figure 13). The thermal profile of flaxseed oils was examined using DSC melting curves, which were first crystallized to the temperature -65 °C at a 2° C/min cooling rate

prior to the heating program. A shift to higher temperatures in all three endothermic peaks was observed as the concentration of rapeseed oil increased.

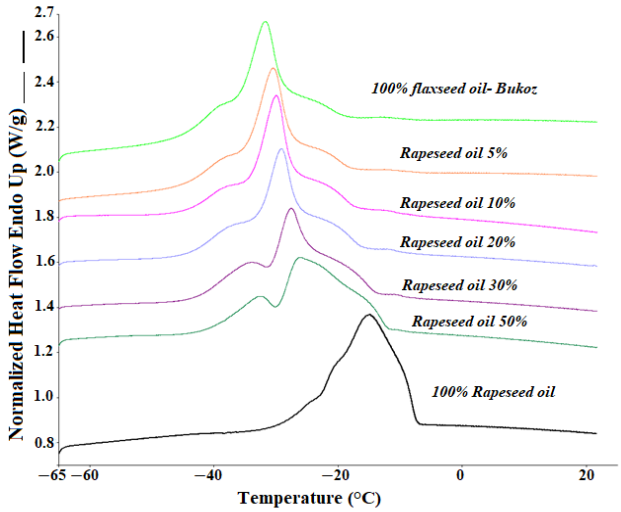

Figure 13. DSC melting curves obtained at a 5 °C/min heating rate for Bukoz cultivar of cold-pressed flaxseed oils adulterated with refined rapeseed oils in different concentrations (0, 5, 10, 20, 30, and 50% *w/w*).

In the article (A5), Table 1 quantified these changes, revealing varying behaviors in peak temperatures, peak heights and areas with increasing adulterant concentration. Regression analysis demonstrated a statistically significant ($p \leq 0.05$) correlation between DSC parameters and adulterant concentration (Figure 2, A5). Specifically, peak temperatures and the height of the third peak increased significantly, while the height of the second peak decreased.

4.3.2 Multivariate data analysis for adulteration study

The main idea of the research described in paper (A5) was to use differential scanning calorimetry (DSC) as an effective analytical technique for the detection of adulteration in edible oils, specifically focusing on cold-pressed flaxseed oil adulterated with refined rapeseed oil. The innovative aspect of this study lies in its integrative methodology, combining DSC-derived parameters with a range of chemometric techniques, including linear discriminant analysis (LDA), multiple linear regression (MLR), support vector machine (SVM), artificial neural networks (ANN), principal component analysis (PCA), orthogonal least squares discriminant analysis (OPLS-DA) and partial least squares (PLS). These techniques were used to construct both classification and regression models. The first is used to categorize the level of oil adulteration,

while the second quantifies the concentration of the adulterant. This approach allowed the effectiveness of different chemometric models to be assessed and compared.

4.3.2.1 Classification models for predicting oil adulteration levels

Four classification models (LDA, MARS, SVM, and ANNs) were evaluated for their ability to classify adulterated oil samples using DSC parameters. Among them LDA was identified as the most effective model, achieving a high accuracy of 99.46% and exceptional results in terms of precision, sensitivity, and specificity. A Wilks lambda of 0.00119 and a p-value of ≤ 0.05 confirmed the model's significance. Only one misclassification was observed in samples with 5% adulteration, as shown in Table 2 (A5).

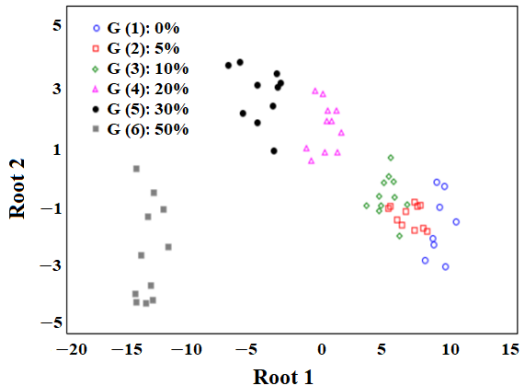

Figure 14. Linear discrimination analysis plot (LDA) for cold-pressed flaxseed oil adulterated with various concentrations of refined rapeseed oils (0, 5, 10, 20, 30, and 50% *w/w*).

The F1-score of 98.4% further confirmed the reliability of the model. Figure 14 illustrated the LDA model's effectiveness in distinguishing between different classes of oil adulteration. Other researchers also employed a LDA method to detect adulterations in peanut oil, achieving an identification accuracy of 97% (Peng et al., 2023). The high accuracy and precision of the LDA model make it a potential quality control tool in the food industry, especially to ensure the authenticity of edible oils. Its ability to correctly classify adulterated samples with a high degree of reliability provides the rationale for its use as a robust analytical method, suitable for both research and practical applications in food technology. The second classification model was a model constructed of Multivariate Adaptive Regression Splines (MARS). MARS is a non-parametric procedure that models the relationship between dependent and independent variables using a set of coefficients and basis functions. The model achieved a Generalized Cross-Validation (GCV) score

of 0.516 and allowed for 90.3% of correct classifications. Although it was the least effective among the models used, its non-parametric nature makes it flexible and capable of capturing complex relationships in the data. Next was the SVM model, which works by constructing hyperplanes in a multidimensional feature space to segregate samples into different classes. The SVM model achieved an accuracy rate of 97.3%, making it a potentially useful tool for classifying adulterated and unadulterated oil samples. In another study, the classification accuracy of SVM was reported as 96.25% while comparing chemometrics and AOCS official methods for predicting the shelf life of edible oil (Karami et al., 2020). Although the SVM model did not prove superior to the linear discriminant analysis (LDA) model, its high accuracy and suitability in multidimensional spaces make it a viable alternative for detecting adulteration in edible oils. The last classification model, ANN, employed a multilayer feed-forward neural network with various activation functions. The model's architecture consisted of an input layer with nine neurons, each representing a different DSC parameter. The hidden layer contained a variable number of neurons ranging from 4 to 11, and the output layer had 6 neurons representing the concentrations of the refined oil adulterants. In terms of performance, the ANN classification model achieved an impressive accuracy rate of almost 98%. This high accuracy indicates that the model is highly reliable for classifying oil samples based on their adulteration levels. Only three samples were misclassified, further attesting to the model's robustness. This discovery can be compared with the research conducted by (Firouz et al., 2022) where they utilized classification and quantification techniques to identify adulteration in sesame oil and achieved a 100% accuracy rate. Of all the models constructed, the LDA model was found to be the most effective, exhibiting the highest levels of accuracy (99.5%), precision (98.4%), sensitivity (98.4%), specificity (99.7%) and F1 score (98.4%). Contrarily, the MARS model was identified as the least effective, with the lowest levels of accuracy (95.7%), precision (87%), sensitivity (87%), specificity (97.4%) and F1 score (87%). In conclusion, the obtained classification models, in particular the LDA model, provide a strong analytical framework for the detection of adulteration in cold-pressed flaxseed oils. Their high accuracy and precision highlight their utility and importance in protecting the authenticity of edible oils.

The above discussion demonstrates that DSC results are very well fitted and highly relevant to the development of chemometric classification models for the detection of adulteration in oil samples. DSC generates multidimensional quantitative data that capture subtle thermal changes in oil composition caused by adulteration and, therefore, when combined with chemometric models

such as LDA, MARS, SVM and ANN, are able to establish complex relationships between DSC parameters and the possibility of oil adulteration.

4.3.2.2. Regression models for predicting the concentration of adulterants in cold-pressed flaxseed oils

The comprehensive study presented in the article (A5), four different regression models were evaluated to determine their ability to predict adulteration of cold-pressed flaxseed oil with refined rapeseed oil. The models analyzed were multiple linear regression (MLR), multivariate adaptive regression splines (MARS), support vector machine (SVM) and artificial neural networks (ANN). Each model was evaluated on selected statistics, including correlation coefficients, coefficients of determination and root mean square error (RMSE), among others. The Artificial Neural Networks (ANN) model emerged as the most effective among the four. It was characterized by the highest correlation coefficient (r=0.996) and determination coefficient (R^2=0.992), indicating that nearly 99.2% of the variability in the dependent variable could be explained by the independent variables in the model. The ANN model's RMSE value of 1.51 served as an additional metric for its predictive accuracy, further attesting to its robustness. The ANN model's performance was found to be particularly noteworthy when compared to a parallel study conducted by (Firouz et al., 2022), who also utilized ANNs and achieved a high accuracy rate in detecting adulteration in sesame oil.

The Multivariate Adaptive Regression Splines (MARS) model was found to be slightly less accurate than the ANN model. It showed a high correlation coefficient of r = 0.995 and a determination coefficient of R^2 = 0.990. These indices suggest that about 99% of the variation in the dependent variable can be explained by the independent variables in the model. The RMSE for the MARS model was calculated at 1.65, serving as an additional indicator of model fit and predictive accuracy. The complexity and adaptability of the MARS model in capturing non-linear relationships in the data was also highlighted, making it a strong contender for predicting levels of adulteration. The Support Vector Machine (SVM) model, although ranked third, still showed significant performance with a correlation coefficient of r = 0.992 and a coefficient of determination of R^2 = 0.985. The RMSE value of 2.10 for the SVM model served as an additional measure of its predictive accuracy. The model's ability to handle nonlinear relationships in the data was also noted, making it a viable alternative for such predictive tasks. The Multiple Linear Regression (MLR) model, despite its statistical significance and a high F-value, was the least

effective among the four models. It had a coefficient of determination R^2 of 0.9844, which, although high, was not as impressive as the other models. The model's performance was compared to a study by others researchers (Sim et al., 2018), which also employed MLR for predicting adulteration levels and found it to be feasible.

The combination of DSC results with regression models has allowed precise and reliable quantification of adulteration in oil samples, contributing significantly to quality assurance and authenticity verification in the food industry. The ability to quantify the extent of adulteration allows for more targeted interventions and product recalls, minimizing risk to consumers and potential damage to brand reputation. Furthermore, the predictive accuracy of these models has been found to be high, making them potentially reliable tools for both industrial and regulatory applications. Overall, the use of regression models in the detection of oil adulteration has proven both effective and suggests that they can make a significant contribution to oil quality and safety.

4.3.2.3 Other combined multivariate methods for adulteration study

In this study, more multivariate tools were employed for the discrimination of the genuine and adulterated flaxseed oils. Principal Component Analysis (PCA), which was used to visualize the data structure, identified two principal components, t[1] and t[2], explaining 91.1% of the data's variation. The model had high R^2X (cum) and Q^2 (cum) values (0.973 and 0.897 respectively), indicating good data capture (Figure 4a, A5). Next, Orthogonal Partial Least Squares Discriminant Analysis (OPLS-DA) was then applied to classify and differentiate various adulterant concentrations in flaxseed oil samples (Figure 4b, A5). The model used 15 variables, with nine DSC parameters as independent variables (X) and six adulterant concentrations as dependent variables (Y), representing six distinct classes. The scatter plot in Figure 4b (A5) visually represented the model's performance, with observations colored based on their respective class, corresponding to different adulterant concentrations. While the OPLS-DA model exhibited a good fit to the X data (DSC parameters) as indicated by the high R^2X (cum) value of 0.986, its predictive ability for Y data (adulterant concentrations) was somewhat limited with a Q^2 (cum) value of 0.33, as determined through cross-validation. This means that the model could predict approximately 33% of the variation in the Y data based on the DSC variables. Despite this limitation in predictive power, the OPLS-DA method effectively separated classes, allowing for classification of adulterated flaxseed oil samples based on DSC profiles. OPLS-DA was also evidently adopted by

other authors to determine important variables when detecting flaxseed oil multiple adulteration via near-infrared spectroscopy (Yuan et al., 2020). Partial Least Squares (PLS) modeling, an alternative technique, provided even better predictive modeling example (Figure 5a, A5), which not only effectively reduced the dimensionality of the dataset but also captured a substantial portion of the data's variation, as indicated by a high R^2X (cum) value of 0.953. Additionally, the model exhibited an excellent predictive ability, with a Q^2 (cum) value of 0.973, signifying its capacity to accurately estimate adulterant levels. This predictive power was further highlighted by the strong alignment between the observed and predicted values in the graphical representation, with a Pearson's correlation coefficient (r) of 0.995 indicating a strong linear relationship (Figure 6, A5). Utilizing the PLS method was reported by other researchers (Rocha et al., 2012), who employed it to classify and quantify various types of blended biodiesel derived from peanut, corn, and canola oils. Their findings revealed a strong correlation, with a Pearson's correlation coefficient of 0.969 between the actual and predicted concentrations. Overall, the PLS method demonstrated superior performance compared to other techniques, making it a valuable tool for detecting and quantifying adulteration in flaxseed oil samples. Moreover, the VIP plot (Figure 5b, A5) served as a tool for the selection of variables, which are crucial for the differentiation, by considering VIP values above 1. It was possible to pinpoint the key DSC parameters (T1, T2, T3, h2, h3, P2, P3) that played a substantial role in distinguishing between pure flaxseed oil and adulterated samples.

The most important achievements of this study include the successful development of chemometric models, for accurately predicting and classifying adulterant concentrations in flaxseed oil. These models provided a reliable means of detecting adulterations using selected most important DSC thermodynamic parameters of melting phase transition profile of flaxseed oil.

5. Conclusions

In conclusion, this research underscores the potential of Differential Scanning Calorimetry (DSC) as a reliable and versatile tool for characterizing and assessing the oxidative stability and authenticity of cold-pressed edible oils. By leveraging DSC oxidation curves as well as melting phase transition profiles as unique fingerprints, this approach offers a promising alternative to traditional chemical methods, enabling accurate discrimination of fresh and deteriorated oils or between pure and adulterated oils. The main conclusions of this research can be outlined as follows:

1. DSC isothermal (oxidative induction time, OIT) and non-isothermal (onset temperature, Ton) tests effectively measured differences in oxidative stability between flaxseed and camelina oils as well as between cultivars of each type of oil.

2. Strong negative correlations were found between DSC oxidation parameters (OIT, Ton) and traditional chemical indicators (PV, TOTOX) as well as with α-linolenic acid percentage.

3 The DSC oxidation tests were demonstrated to accurately monitor the deterioration process of three cold-pressed oils (flaxseed, camelina, hempseed) during storage. The most suitable for the discrimination of fresh and spoiled oils was isothermal test at temperature of 120 °C, which correlated strongly with all chemical indicators (PV, pAV, TOTOX).

4. In the study on the using DSC phase transition profile, it was shown that the scanning rate significantly affected the thermal behavior of oils, especially in terms of polymorphic transition, that occurred at the lowest heating rates. This finding stresses the need for careful selection of scanning rates for fingerprinting purposes.

5. The investigation on the effect of storage time on the DSC melting curves of flaxseed oil showed significant changes of some peaks (peak temperature, peak height and area) as was identified by X-bar and R control charts, which were applied to monitor the deterioration process of oils.

6. It was demonstrated that, utilization of DSC untargeted profiling enabled to distinguish between three cold-pressed oils (flaxseed, camelina, hempseed) and three refined oils (rapeseed, sunflower, soybean), by using the entire range of melting profiles as a unique fingerprint for each type of oil. Reliability and predictive accuracy of the OPLS-DA model was confirmed by a high coefficients of $R^2X(cum)= 0.971$ and $Q^2X(cum)= 0.887$.

7. The study found that thermodynamic parameters of DSC melting curves of flaxseed oil were highly sensitive to changes in oil composition caused by the adulteration with refined rapeseed oil.

8. Advanced chemometric methods (classification and regression), including LDA, MARS, SVM, ANNs and OPLS-DA, were successfully applied to DSC melting profiles to detect adulteration of cold-pressed flaxseed oil with refined rapeseed oil.

9. Comparing the various classification models tested, the Linear Discriminant Analysis (LDA) model exhibited exceptional performance (with 99.5% accuracy), making it a valuable tool for categorizing oil samples based on their adulteration levels.

10. Among the regression models for predicting adulteration, the ANN model distinguished itself with the highest correlation (R^2 = 0.996), followed by the PLS model, with a high ability to accurately estimate adulterant levels (R^2X (cum) = 0.986) and a strong relationship between observed and predicted values expressed.

11. This study highlights the significance of combining untargeted DSC method with chemometric tools for authentication of cold-pressed oils and emphasizes the importance of quality assessment and authenticity verification in the food industry.

Table of Figures

References

Abramovič, H., & Abram, V. (2005). Physico-chemical properties, composition and oxidative stability of camelina sativa oil. *Food Technology and Biotechnology*, *43*(1), 63–70.

Abramovič, H., Butinar, B., & Nikolič, V. (2007). Changes occurring in phenolic content, tocopherol composition and oxidative stability of Camelina sativa oil during storage. *Food Chemistry*, *104*(3), 903–909. https://doi.org/10.1016/j.foodchem.2006.12.044

Adhvaryu, A., Erhan, S. Z., Liu, Z. S., & Perez, J. M. (2000). Oxidation kinetic studies of oils derived from unmodified and genetically modified vegetables using pressurized differential scanning calorimetry and nuclear magnetic resonance spectroscopy. *Thermochimica Acta*, *364*(1–2), 87–97. https://doi.org/10.1016/S0040-6031(00)00626-2

American Oil Chemists' Society. (2000). *DSC melting properties of fats and oils. Cj 1-94* (Patent No. Cj 1-94).

AOCS. (1997). *AOCS Official Method Preparations of Methyl Esters of Fatty Acids*.

AOCS. (2009). *AOCS Official Method Acid Value. Cd 3d-63*.

ASTM International. (2019). *ASTM D3895-19. Test Method for Oxidative-Induction Time of Polyolefins by Differential Scanning Calorimetry*. ASTM Publisher.

Bao, R., Tang, F., Rich, C., & Hatzakis, E. (2023). A comparative evaluation of low-field and high-field NMR untargeted analysis: Authentication of virgin coconut oil adulterated with refined coconut oil as a case study. *Analytica Chimica Acta*, *1273*(May), 341537. https://doi.org/10.1016/j.aca.2023.341537

Barba, L., Arrighetti, G., & Calligaris, S. (2013). Crystallization and melting properties of extra virgin olive oil studied by synchrotron XRD and DSC. *European Journal of Lipid Science and Technology*, *115*(3), 322–329. https://doi.org/10.1002/ejlt.201200259

Belayneh, H. D., Wehling, R. L., Cahoon, E., & Ciftci, O. N. (2015). Extraction of omega-3-rich oil from Camelina sativa seed using supercritical carbon dioxide. *Journal of Supercritical Fluids*, *104*, 153–159. https://doi.org/10.1016/j.supflu.2015.06.002

Carter, O. C. S. (1885). On the Detection of Adulterations in Oils. In *JSTOR* (Vol. 22, Issue 120). American Philosophical Society. https://www.jstor.org/stable/982989

Choe, E., & Min, D. B. (2006). Mechanisms and factors for edible oil oxidation. *Comprehensive Reviews in Food Science and Food Safety*, *5*(4), 169–186. https://doi.org/10.1111/j.1541-4337.2006.00009.x

Choo, W. S., Birch, J., & Dufour, J. P. (2007). Physicochemical and quality characteristics of cold-pressed flaxseed oils. *Journal of Food Composition and Analysis*, *20*(3–4), 202–211. https://doi.org/10.1016/j.jfca.2006.12.002

Cichocki, W., Kmiecik, D., Baranowska, H. M., Staroszczyk, H., Sommer, A., & Kowalczewski, P. Ł. (2023). Chemical Characteristics and Thermal Oxidative Stability of Novel Cold-Pressed Oil Blends: GC, LF NMR, and DSC Studies. *Foods*, *12*(14), 2660. https://doi.org/10.3390/FOODS12142660

Codex Alimentarius. (1999). Standard for Named Vegetable Oils Codex Stan 210-1999. In *Codex Alimentarius*.

Coni, E., Di Pasquale, M., Coppolelli, P., & Bocca, A. (1994). Detection of animal fats in butter by differential scanning calorimetry: A pilot study. *Journal of the American Oil Chemists' Society*, *71*(8), 807–810. https://doi.org/10.1007/BF02540453

Daun, J. K., Barthet, V. J., Chornick, T. L., & Duguid, S. (2003). *Structure , Composition , and Variety Development of Flaxseed*.

De Souza, L. M., De Santana, F. B., Gontijo, L. C., Mazivila, S. J., & Borges Neto, W. (2015). Quantification of adulterations in extra virgin flaxseed oil using MIR and PLS. *Food Chemistry*, *182*, 35–40. https://doi.org/10.1016/j.foodchem.2015.02.081

Durazzo, A., Fawzy Ramadan, M., & Lucarini, M. (2022). Editorial: Cold Pressed Oils: A Green Source of Specialty Oils. *Frontiers in Nutrition*, *8*(February), 2021–2022. https://doi.org/10.3389/fnut.2021.836651

Efenberger-Szmechtyk, M., Nowak, A., & Kregiel, D. (2018). Implementation of chemometrics in quality evaluation of food and beverages. *Critical Reviews in Food Science and Nutrition*, *58*(10), 1747–1766. https://doi.org/10.1080/10408398.2016.1276883

Elzey, B., Pollard, D., & Fakayode, S. O. (2016). Determination of adulterated neem and flaxseed oil compositions by FTIR spectroscopy and multivariate regression analysis. *Food Control*, *68*, 303–309. https://doi.org/10.1016/j.foodcont.2016.04.008

European Commission. (2018). *European Commission The EU Food Fraud Network and the System for Administrative Assistance-Food Fraud*. https://eur-lex.europa.eu/legal-content/EN/TXT/?uri=COM:2018:772:FIN

FAO. (2021). *Food fraud-Intention, detection and management. Food safety technical toolkit for Asia and the Pacific No. 5. Bangkok*. https://www.fao.org/3/cb2863en/cb2863en.pdf

FDA. (2009). *Economically motivated adulteration; public meeting; request for comment. 74*(64), 69–71. https://www.federalregister.gov/documents/2009/04/06/E9-7843/economically-motivated-adulteration-public-meeting-request-for-comment

Firouz, M. S., Omid, M., Babaei, M., & Rashvand, M. (2022). Dielectric spectroscopy coupled with artificial neural network for classification and quantification of sesame oil adulteration. *Information Processing in Agriculture*, *9*(2), 233–242. https://doi.org/10.1016/j.inpa.2021.05.001

Flynn, J. H., & Wall, L. A. (1966). A quick, direct method for the determination of activation energy from thermogravimetric data. *Journal of Polymer Science Part C: Polymer Letters*, *4*, 323–328. https://doi.org/10.1098/rstb.1988.0133

Garrido-Delgado, R., Eugenia Muñoz-Pérez, M., & Arce, L. (2018). Detection of adulteration in extra virgin olive oils by using UV-IMS and chemometric analysis. *Food Control*, *85*, 292–299. https://doi.org/10.1016/j.foodcont.2017.10.012

Gelpí, E., Posada de la Paz, M., Terracini, B., Abaitua, I., Gómez de la Cámara, A., Kilbourne, E. M., Lahoz, C., Nemery, B., Philen, R. M., Soldevilla, L., & Tarkowski, S. (2002). The spanish

toxic oil syndrome 20 years after its onset: A multidisciplinary review of scientific knowledge. *Environmental Health Perspectives*, *110*(5), 457–464. https://doi.org/10.1289/ehp.02110457

Giese, E., Rohn, S., & Fritsche, J. (2019). Chemometric tools for the authentication of cod liver oil based on nuclear magnetic resonance and infrared spectroscopy data. *Analytical and Bioanalytical Chemistry*, *411*(26), 6931–6942. https://doi.org/10.1007/s00216-019-02063-y

Gordon, M. H. (2001). The development of oxidative rancidity in foods. In *Antioxidants in Food*. Woodhead Publishing Ltd. https://doi.org/10.1016/9781855736160.1.5

Grand View Reasearch. (2021). *Cold Pressed Oil Market Size, Share & Trends Analysis Report By Product (Coconut Oil, Palm Oil, Ground Nut Oil, Rapeseed Oil, Soybean Oil, Sunflower Oil), By Distribution Channel, By Region, And Segment Forecasts, 2022 - 2028*. https://www.grandviewresearch.com/industry-analysis/cold-pressed-oil-market-report

Hao, S., Zhu, L., Sui, R., Zuo, M., Luo, N., Shi, J., Zhang, W., He, X., & Chen, Z. (2019). Identification and quantification of vegetable oil adulteration with waste frying oil by laser-induced fluorescence spectroscopy. *OSA Continuum*, *2*(4), 1148. https://doi.org/10.1364/osac.2.001148

Hasiewicz-Derkacz, K., Kulma, A., Czuj, T., Prescha, A., Zuk, M., Grajzer, M., Łukaszewicz, M., & Szopa, J. (2015). Natural phenolics greatly increase flax (Linum usitatissimum) oil stability. *BMC Biotechnology*, *15*(1), 1–14. https://doi.org/10.1186/s12896-015-0178-0

Islam, M., Bełkowska, L., Konieczny, P., Fornal, E., & Tomaszewska-Gras, J. (2022). Differential scanning calorimetry for authentication of edible fats and oils - What can we learn from the past to face the current challenges? *Journal of Food and Drug Analysis*, *30*(2). https://doi.org/doi.org/10.38212/2224-6614.3402

ISO. (2013). EN ISO 11357-6:2013 Plastics - Differential scanning calorimetry (DSC) - Part 6: Determination of oxidation induction time (isothermal OIT) and oxidation induction temperature (dynamic OIT) (ISO 11357-6:2008). In *ISO*.

ISO 3960. (2010). *Animal and Vegetable Fats and Oils—Determination—Iodometric (Visual) Endpoint; International Organization for Standardization: Geneva, Switzerland, 2017*.

ISO 6885. (2016). *Animal and Vegetable Fats and Oils: Determination of Anisidine Value. ISO: Geneva, Switzerland 2016*.

Karami, H., Rasekh, M., & Mirzaee – Ghaleh, E. (2020). Comparison of chemometrics and AOCS official methods for predicting the shelf life of edible oil. *Chemometrics and Intelligent Laboratory Systems*, *206*(September), 104165. https://doi.org/10.1016/j.chemolab.2020.104165

Kerti, K. (2001). Investigating isothermal DSC method to distinguish between cocoa butter and cocoa butter alternatives. *Journal of Thermal Analysis and Calorimetry*, *63*(1), 205–219. https://doi.org/10.1023/A:1010157008213

Kozłowska, M., & Gruczyńska, E. (2018). Comparison of the oxidative stability of soybean and sunflower oils enriched with herbal plant extracts. *Chemical Papers*, *72*(10), 2607–2615. https://doi.org/10.1007/s11696-018-0516-5

Kozub, A., Nikolaichuk, H., Przykaza, K., Tomaszewska-Gras, J., & Fornal, E. (2023). Lipidomic Characteristics of Three Edible Cold-pressed Oils by LC / Q-TOF for Simple Quality and Authenticity Assurance. *Food Chemistry*, 135761. https://doi.org/10.1016/j.foodchem.2023.135761

Kurasiak-Popowska, D., Rynska, B., & Stuper-Szablewska, K. (2019). Analysis of distribution of selected bioactive compounds in camelina sativa from seeds to pomace and oil. *Agronomy*, *9*(4). https://doi.org/10.3390/agronomy9040168

Larrauri, A., Saura-calixto, F., & Sanchez-Moreno, C. (1998). *A Procedure to Measure the Antiradical Efficiency of Polyphenols*. *76*, 270–276.

Ligěza, M., Wyglădacz, D., Tobiasz, A., Jaworecka, K., & Reich, A. (2016). Natural cold pressed oils as cosmetic products. *Family Medicine and Primary Care Review*, *18*(4), 443–447. https://doi.org/10.5114/fmpcr.2016.63699

Łukaszewicz, M., Szopa, J., & Krasowska, A. (2004). Susceptibility of lipids from different flax cultivars to peroxidation and its lowering by added antioxidants. *Food Chemistry*, *88*(2), 225–231. https://doi.org/10.1016/j.foodchem.2003.12.042

Maggio, R. M., Cerretani, L., Barnaba, C., & Chiavaro, E. (2012). Application of Differential Scanning Calorimetry-Chemometric Coupled Procedure to the Evaluation of Thermo-Oxidation on Extra Virgin Olive Oil. *Food Biophysics*, *7*(2), 114–123. https://doi.org/10.1007/s11483-012-9248-1

Mao, X., Chen, W., Huyan, Z., Sherazi, S. T. H., & Yu, X. (2020). Impact of linolenic acid on oxidative stability of rapeseed oils. *Journal of Food Science and Technology*, *57*(9), 3184–3192. https://doi.org/10.1007/s13197-020-04349-x

Marina, A. M., Che Man, Y. B., Nazimah, S. A. H., & Amin, I. (2009). Monitoring the adulteration of virgin coconut oil by selected vegetable oils using differential scanning calorimetry. *Journal of Food Lipids*, *16*(1), 50–61. https://doi.org/10.1111/j.1745-4522.2009.01131.x

Momot, M., Stawicka, B., & Szydłowska-Czerniak, A. (2023). Physicochemical Properties and Sensory Attributes of Cold-Pressed Camelina Oils from the Polish Retail Market. *Applied Sciences (Switzerland)*, *13*(3). https://doi.org/10.3390/app13031924

Nina Naquiah, A. N., Marikkar, J. M. N., Mirghani, M. E. S., Nurrulhidayah, A. F., & Yanty, N. A. M. (2017). Differentiation of fractionated components of lard from other animal fats using different analytical techniques. *Sains Malaysiana*, *46*(2), 209–216. https://doi.org/10.17576/jsm-2017-4602-04

Peng, D., Shi, C., Nie, Q., Xie, S., Bi, Y., & Li, J. (2023). Qualitative and quantitative detection of peanut oils adulteration based on fatty acid information fusion coupled with chemometrics. *LWT*, *181*(February), 114785. https://doi.org/10.1016/j.lwt.2023.114785

Piravi-vanak, Z., Azadmard-Damirchi, S., Kahrizi, D., Mooraki, N., Ercisli, S., Savage, G. P., Rostami Ahmadvandi, H., & Martinez, F. (2022). Physicochemical properties of oil extracted from camelina (Camelina sativa) seeds as a new source of vegetable oil in different regions of Iran. *Journal of Molecular Liquids*, *345*(xxxx), 117043. https://doi.org/10.1016/j.molliq.2021.117043

Qi, B., Zhang, Q., Sui, X., Wang, Z., Li, Y., & Jiang, L. (2016). Differential scanning calorimetry study - Assessing the influence of composition of vegetable oils on oxidation. *Food Chemistry*, *194*, 601–607. https://doi.org/10.1016/j.foodchem.2015.07.148

Rajagukguk, Y. V., Islam, M., Siger, A., Fornal, E., & Tomaszewska-Gras, J. (2023). Oxidative stability assessment of industrial and laboratory-pressed fresh raspberry seed oil (Rubus idaeus L.) by differential scanning calorimetry. *Food Chemistry Advances*, *2*(August 2022), 100186. https://doi.org/10.1016/j.focha.2023.100186

Rajagukguk, Y. V., Utcu, M. A., Islam, M., Muzolf-Panek, M., & Tomaszewska-Gras, J. (2022). Authenticity Assessment from Sesame Seeds to Oil and Sesame Products of Various Origin by Differential Scanning Calorimetry. *Molecules*, *27*(21), 7496. https://doi.org/10.3390/molecules27217496

Ramadan, M. F. (2020). Introduction to cold pressed oils: Green technology, bioactive compounds, functionality, and applications. In *Cold Pressed Oils: Green Technology, Bioactive Compounds, Functionality, and Applications*. Elsevier Inc. https://doi.org/10.1016/B978-0-12-818188-1.00001-3

Ratusz, K., Popis, E., Ciemniewska-Żytkiewicz, H., & Wroniak, M. (2016). Oxidative stability of camelina (Camelina sativa L.) oil using pressure differential scanning calorimetry and Rancimat method. *Journal of Thermal Analysis and Calorimetry*, *126*(1), 343–351. https://doi.org/10.1007/s10973-016-5642-0

Rocha, W. F. C., Prado, C. B., & Niksa, B. (2020). Comparison of Chemometric Problems in Food Analysis using Non-Linear Methods. *Molecule*, *25*(3025). https://doi.org/10.3390/molecules25133025

Rocha, W. F. C., Vaz, B. G., Sarmanho, G. F., Leal, L. H. C., Nogueira, R., Silva, V. F., & Borges, C. N. (2012). Chemometric Techniques Applied for Classification and Quantification of Binary Biodiesel/Diesel Blends. *Analytical Letters*, *45*(16), 2398–2411. https://doi.org/10.1080/00032719.2012.686135

Różańska, M. B., Kowalczewski, P. Ł., Tomaszewska-Gras, J., Dwiecki, K., & Mildner-Szkudlarz, S. (2019). Seed-roasting process affects oxidative stability of cold-pressed oils. *Antioxidants*, *8*(8), 1–10. https://doi.org/10.3390/antiox8080313

Rudakov, O. B., Saranov, I. A., Van, A. N., Rudakova, L. V., & Polyanskiy, K. K. (2021). Differential Scanning Calorimetry as a Method for the Control of Vegetable Oils. *Journal of Analytical Chemistry*, *76*(2), 258–266. https://doi.org/10.1134/S1061934821020118

Saldana, M. D. A., & Martinez-Monteagudo, S. I. (2013). Oxidative Stability of Fats and Oils Measured by Differential Scanning Calorimetry for Food and Industrial Applications. In A. A. Elkarody (Ed.), *Applications of Calorimetry in a Wide Context - Differential Scanning Calorimetry, Isothermal Titration Calorimetry and Microcalorimetry* (pp. 445–474). https://doi.org/10.5772/54486

Sato, K., Bayés-García, L., Calvet, T., Cuevas-Diarte, M. À., & Ueno, S. (2013). External factors affecting polymorphic crystallization of lipids. *European Journal of Lipid Science and Technology*, *115*(11), 1224–1238. https://doi.org/10.1002/ejlt.201300049

Shahidi, F., & Wanasundara, U. N. (2002). Methods for measuring oxidative rancidity in fats and oils. In *Food lipids* (pp. 484–507). CRC Press.

Sim, S. F., Chai, M. X. L., & Jeffrey Kimura, A. L. (2018). Prediction of lard in palm olein oil using simple linear regression (SLR), multiple linear regression (MLR), and partial least squares regression (PLSR) based on fourier-transform infrared (FTIR). *Journal of Chemistry*, *2018*, 1–8. https://doi.org/10.1155/2018/7182801

Simopoulos, A. P. (2008). The importance of the omega-6/omega-3 fatty acid ratio in cardiovascular disease and other chronic diseases. *Experimental Biology and Medicine*, *233*(6), 674–688. https://doi.org/10.3181/0711-MR-311

Sun, X., Zhang, L., Li, P., Xu, B., Ma, F., Zhang, Q., & Zhang, W. (2015). Fatty acid profiles based adulteration detection for flaxseed oil by gas chromatography mass spectrometry. *LWT*, *63*(1), 430–436. https://doi.org/10.1016/j.lwt.2015.02.023

Tan, C. P., & Che Man, Y. B. (2002). Comparative differential scanning calorimetric analysis of vegetable oils: I. Effects of heating rate variation. *Phytochemical Analysis*, *13*(3), 129–141. https://doi.org/10.1002/pca.633

Tańska, M., Roszkowska, B., Skrajda, M., & Grzegorz, D. (2016). Commercial Cold Pressed Flaxseed Oils Quality and Oxidative Stability at the Beginning and the End of Their Shelf Life. *Journal of Oleo Science*, *January*. https://doi.org/10.5650/jos.ess15243

Teh, S. S., & Birch, J. (2013). Physicochemical and quality characteristics of cold-pressed hemp, flax and canola seed oils. *Journal of Food Composition and Analysis*, *30*(1), 26–31. https://doi.org/10.1016/j.jfca.2013.01.004

Tomaszewska-Gras, J. (2012). Detection of butter adulteration with water using differential scanning calorimetry. *Journal of Thermal Analysis and Calorimetry*, *108*(2), 433–438. https://doi.org/10.1007/s10973-011-1913-y

Tomaszewska-Gras, J. (2013). Melting and crystallization DSC profiles of milk fat depending on selected factors. *Journal of Thermal Analysis and Calorimetry*, *113*(1), 199–208. https://doi.org/10.1007/s10973-013-3087-2

Tomaszewska-Gras, J. (2016). Rapid quantitative determination of butter adulteration with palm oil using the DSC technique. *Food Control*, *60*, 629–635. https://doi.org/10.1016/j.foodcont.2015.09.001

Upadhyay, N., Goyal, A., Kumar, A., & Lal, D. (2017). Detection of adulteration by caprine body fat and mixtures of caprine body fat and groundnut oil in bovine and buffalo ghee using differential scanning calorimetry. *International Journal of Dairy Technology*, *70*(2), 297–303. https://doi.org/10.1111/1471-0307.12336

Vanstone, N., Moore, A., Martos, P., & Neethirajan, S. (2018). Detection of the adulteration of extra virgin olive oil by near-infrared spectroscopy and chemometric techniques. *Food Quality and Safety*, *2*(4), 189–198. https://doi.org/10.1093/fqsafe/fyy018

Visentainer, J. V., De Souza, N. E., Makoto, M., Hayashi, C., & Franco, M. R. B. (2005). Influence of diets enriched with flaxseed oil on the α-linolenic, eicosapentaenoic and docosahexaenoic fatty acid in Nile tilapia (Oreochromis niloticus). *Food Chemistry*, *90*(4), 557–560.

https://doi.org/10.1016/j.foodchem.2004.05.016

Yanty, N. A. M., Marikkar, J. M. N., & Long, K. (2011). Effect of varietal differences on composition and thermal characteristics of avocado oil. *JAOCS, Journal of the American Oil Chemists' Society*, *88*(12), 1997–2003. https://doi.org/10.1007/s11746-011-1877-x

Yuan, Z., Zhang, L., Wang, D., Jiang, J., Harrington, P. de B., Mao, J., Zhang, Q., & Li, P. (2020). Detection of flaxseed oil multiple adulteration by near-infrared spectroscopy and nonlinear one class partial least squares discriminant analysis. *LWT*, *125*(March), 109247. https://doi.org/10.1016/j.lwt.2020.109247

Zhang, L., Chen, J., Jing, B., Dong, Y., & Yu, X. (2019). New Method for the Discrimination of Adulterated Flaxseed Oil Using Dielectric Spectroscopy. *Food Analytical Methods*, *12*(11), 2623–2629. https://doi.org/10.1007/s12161-019-01620-6

Zhang, Z. S., Li, D., Zhang, L. X., Liu, Y. L., & Wang, X. De. (2014). Heating effect on the DSC melting curve of flaxseed oil. *Journal of Thermal Analysis and Calorimetry*, *115*(3), 2129–2135. https://doi.org/10.1007/s10973-013-3270-5

Zhang, Z. S., Wang, L. J., Li, D., Li, S. J., & Ozkan, N. (2011). Characteristics of flaxseed oil from two different flax plants. *International Journal of Food Properties*, *14*(6), 1286–1296. https://doi.org/10.1080/10942911003650296

Zubr, J., & Matthaus, B. (2002). Effects of growth conditions on fatty acids and tocopherols in Camelina sativa oil. *Industrial Crops and Products*, *15*(2), 155–162. https://doi.org/10.1016/S0926-6690(01)00106-6

Keywords

Thermal analysis, Differential scanning calorimetry, Plant oils, Cold-pressed oils, Flaxseed oils, Camelina oils, Hempseed oils, Thermo-oxidative stability, Isothermal test, Non-isothermal test, Oxidation induction time (OIT), Onset temperature (Ton), Oxidation kinetics, Storage analysis, Deterioration markers, Food authenticity, Crystallization profile, Melting profile, Phase transition, Deconvolution analysis, Untargeted analysis, Adulteration analysis, Refined oils, Rapeseed oil, Sunflower oil, Soybean oil, Chemometrics, Multivariate data analysis, Orthogonal partial least squares-discriminant analysis (OPLS-DA), Partial least squares regression (PLS), Linear discriminant analysis (LDA), Multiple linear regression, Classification model, Artificial neural networks (ANN), Multivariate adaptive regression splines (MARS), Support vector machine (SVM), Principle component analysis (PCA).

Publication no. A1

Tomaszewska-Gras, J.; Islam, M.; Grzeca, L.; Kaczmarek, A.; Fornal, E. Comprehensive Thermal Characteristics of Different Cultivars of Flaxseed Oil (Linum usittatissimum L.). Molecules 2021, 26, 1958. https://doi.org/10.3390/molecules26071958

molecules

MDPI

Article

Comprehensive Thermal Characteristics of Different Cultivars of Flaxseed Oil (*Linum usittatissimum* L.)

Jolanta Tomaszewska-Gras [1,*], Mahbuba Islam [1], Liliana Grzeca [1], Anna Kaczmarek [1] and Emilia Fornal [2]

[1] Department of Food Quality and Safety Management, Poznań University of Life Sciences, ul. Wojska Polskiego 31/33, 60-637 Poznań, Poland; mahbuba.islam@up.poznan.pl (M.I.); liliana.grzeca@up.poznan.pl (L.G.); anna.kaczmarek@up.poznan.pl (A.K.)

[2] Department of Pathophysiology, Faculty of Medicine, Medical University of Lublin, ul. Jaczewskiego 8b, 20-090 Lublin, Poland; emilia.fornal@umlub.pl

* Correspondence: jolanta.tomaszewska-gras@up.poznan.pl

Abstract: The aim of this study was to describe the thermal properties of selected cultivars of flaxseed oil by the use of the differential scanning calorimetry (DSC) technique. The crystallization and melting profiles were analyzed depending on different scanning rates (1, 2, 5 °C/min) as well as oxidative induction time (OIT) isothermally at 120 °C and 140 °C, and oxidation onset temperatures (Ton) at 2 and 5 °C/min were measured. The crystallization was manifested as a single peak, differing for a cooling rate of 1 and 2 °C/min. The melting curves were more complex with differences among the cultivars for a heating rate of 1 and 2 °C/min, while for 5 °C/min, the profiles did not differ, which could be utilized in analytics for profiling in order to assess the authenticity of the flaxseed oil. Moreover, it was observed that flaxseed oil was highly susceptible to thermal oxidation, and its stability decreased with increasing temperature and decreasing heating rate. Significant negative linear correlations were found between unsaturated fatty acid content (C18:2, C18:3 n-3) and DSC parameters (OIT, Ton). Principal component analysis (PCA) also established a strong correlation between total oxidation value (TOTOX), peroxide value (PV) and all DSC parameters of thermo-oxidative stability.

Keywords: flaxseed oil; melting; crystallization; oxidative stability; differential scanning calorimetry (DSC)

Citation: Tomaszewska-Gras, J.; Islam, M.; Grzeca, L.; Kaczmarek, A.; Fornal, E. Comprehensive Thermal Characteristics of Different Cultivars of Flaxseed Oil (*Linum usittatissimum* L.). *Molecules* **2021**, *26*, 1958. https://doi.org/10.3390/molecules26071958

Academic Editor: Francisco J. Barba

Received: 9 March 2021
Accepted: 27 March 2021
Published: 31 March 2021

1. Introduction

Flax (*Linum usitatissimum* L.) is an important plant known and cultivated all over the world mainly for oil and fiber. Originating from West Asia and the Mediterranean region, flaxseed (*Linum usitatissimum*, Latin; meaning "very useful") has long been cultivated as one of the oldest multi-purpose crops in history [1]. According to the latest report in 2017 from the Food and Agriculture Organization (FAO), the approximate annual flaxseed production worldwide reached about 2.8 million tons [2]. The cultivation of flaxseed and the quality of the oil yield are significantly influenced by factors such as the temperate climate zone, cultivation methods, genotype and biotic and abiotic stresses, seed moisture at harvest, agronomic treatment, etc. [3–7]. The use of flaxseed for human consumption dates back to ancient times, hence the revelation of the flax genome sequence in 2012 has added a new value and attention to the study [3]. The potential nutritional benefits of flaxseed oil are associated with its active biological compounds. Flaxseed oil comprises outstanding quantities of polyunsaturated fatty acids (PUFA), phytoestrogenic lignans (secoisolariciresinol diglucoside, SDG) [8], and an array of antioxidants such as phenolic acids and flavonoids. The beneficial PUFA of flax lipids are α-linolenic acid (ALA), C18:3, n-3 (30–70% of the total fatty acid content), linoleic, C18:2, n-6; (20% of the total fatty acid content), and oleic acid 18:1 (30% of the total fatty acid content) [3]. ALA in flaxseed can be metabolized to eicosapentaenoic acid (EPA) and docosahexaenoic acid (DHA) [9].

Nutrients present in flaxseed oil can play a pivotal role against various inflammatory autoimmune disorders, hypertension, diabetes, menopausal symptoms, and osteoporosis, and improve the condition of the nervous system and proper blood circulation [2,5,10]. Considering the compelling medicinal values, flaxseed and cold-pressed flaxseed oil have been introduced into the 9th edition of European Pharmacopoeia [11]. On the other hand, the presence of higher ALA content in flaxseed oil can make it distinctly susceptible to oxidation [12]. This oil is very sensitive to heat, light, exposure to oxygen and storage time, thus it can rapidly become rancid due to its higher concentration of ALA [11].

Different cultivars of flaxseed oil have been examined in various aspects. A low-linolenic variety, belonging to the Solin-type group (Solal), and a traditional linseed one rich in linolenic acid (Bethune) were compared in order to assess their agronomical and qualitative characteristics [11]. The yield, oil content and fatty acid profile of seven flax cultivars from Argentina were also tested [5]. The tocochromanols and fatty acid composition of two groups of flax genotypes were investigated by Trela et al. [3]. The seven cultivars from Russia, Poland, Uruguay, Great Britain and Canada [6] as well as the Szafir variety from Poland [13] and the three types of transgenic flax Linola [14] were examined in terms of the susceptibility of flaxseed oil to peroxidation.

According to Frega, Mozzon and Lercker [15], the most important parameter for oil quality is determined by its oxidative stability. In addition to the active oxygen method and Rancimat method [12], there are several other analytical methods that have been developed to estimate the freshness or oxidation ratio, i.e., peroxide value (PV), acid value (AV), p-anisidine value (pAV) [16]. However, to minimize the duration of experiments, laborious difficulty and the use of harmful chemicals, instrumental thermoanalytical methods are becoming popular for the characterization of fats and oils.

Taking into account the limited scientific data on the thermal properties of specified flaxseed cultivars, the aim of this study was to determine the melting and crystallization curves at various scanning rates, as well as thermo-oxidative stability based on isothermal and non-isothermal heating treatment by applying the differential scanning calorimetry (DSC) technique in order to establish comprehensive thermodynamic characteristics for assessing both the authenticity and stability of the flaxseed oil.

2. Results

2.1. Fatty Acid Composition

Fatty acid composition is substantial for the oxidative stability and physicochemical and nutritional properties, thus it was analyzed in five samples of cold-pressed flaxseed oils, the results of which are presented in Table 1. Three certified cultivars of flaxseed, i.e., Bukoz (FL BU), Dolguniec (FL DL), Szafir (FL SZA, FL SZB) and one sample of an unknown variety (FL NN) were taken for this study. The most abundant fatty acid in all flaxseed oils was α-linolenic fatty acid (ALA, C18:3, n-3), which is the dominant compound and unique feature of this oil. Flaxseed has a very high level of ALA, usually greater than 50% of the total fatty acids. Among the cultivars investigated, ALA varied from 55.91% for sample FL NN to 63.11% for FL SZA. It is notable that for each mean value, differences were significant ($p < 0.05$). The ALA content of five flaxseed oils was quite similar to other studies: in oil from the Szafir seed variety, ALA was found at the level of 65.4% [6]; from the Bukoz seed variety at 58% [3]; between 58.87 and 60.42% was determined in various flaxseed oils from New Zealand [17]; 64% was found in the Bethune variety from Italy [11]; between 50 and 60% in Ethiopian flaxseed cultivars, while in samples of the Canadian flaxseed, ALA was found to range from 52–63% [18], and the highest amount of ALA, which yields 69%, was determined in a recently registered cultivar in Canada (VT 50; Trademark: NuLin) [19]. In turn, a content of ALA below 50% was determined in the seven cultivars from Argentina [5], in five cultivars from Egypt [20], in the oil from fiber-flaxseed of an unknown variety from China (47%) [21] and from Poland [16]. The second most abundant fatty acid in flaxseed oil was oleic fatty acid (C18:1), which yielded between 14.64 and 18.71%, with significant differences between each examined cultivar. The oils FL NN

and FL SZB were characterized by the highest percentage of oleic acid (18.46 and 18.71%, respectively). Among the varieties, there were also significant differences in the percentage of linoleic acid (C18:2), for which the highest content (16.56%) was noted for sample FL BU and the lowest (11.14%) for FL SZA. In samples of flaxseed oils, saturated acids were also detected. The highest content of saturated FA (C16:0, C18:0) was found in samples FL NN and FL SZB, and these samples also had the lowest ratio of unsaturated to saturated fatty acids (9.0 and 9.1, respectively), while for FL BU this ratio was the highest, at around 11, which is in agreement with other published results [17]. In order to determine the relations between the content of fatty acids, correlation analysis was carried out, which showed high positive correlations between C18:1 and C18:0 (r = 0.93), between C18:1 and C16:0 (r = 0.85) and a negative correlation between C18:1 and C18:3 (r = −0.59). Similarly, a high positive correlation (r = 0.83) between oleic and palmitic acid was found by other researchers [6], while a negative correlation between oleic and linolenic acid was also confirmed by other studies [3,17,18].

Table 1. Fatty acid composition expressed as a percentage of total fatty acid (%). Saturated fatty acid (SFA), monounsaturated fatty acid (MUFA), polyunsaturated fatty acids (PUFA) and a ratio of n-3 to n-6 and unsaturated to saturated fatty acids (UFA /SFA) of different cultivars of cold-pressed flaxseed oils.

Fatty Acid	Flaxseed Variety				
	FL BU	FL DL	FL SZA	FL SZB	FL NN
12:0	0.04 ^{a} ± 0.00	0.03 ^{a} ± 0.00	0.03 ^{a} ± 0.00	0.04 ^{a} ± 0.01	0.04 ^{a} ± 0.01
14:0	0.02 ^{a} ± 0.00	0.02 ^{a} ± 0.01	0.02 ^{a} ± 0.01	0.02 ^{a} ± 0.00	0.02 ^{a} ± 0.00
16:0	4.86 ^{a} ± 0.03	4.96 ^{ab} ± 0.04	4.86 ^{a} ± 0.04	5.15 ^{c} ± 0.01	5.03 ^{bc} ± 0.05
16:1	0.05 ^{a} ± 0.01	0.06 ^{a} ± 0.00	0.06 ^{a} ± 0.00	0.06 ^{a} ± 0.01	0.09 ^{a} ± 0.02
17:0	0.07 ^{a} ± 0.00	0.05 ^{a} ± 0.00	0.06 ^{a} ± 0.01	0.07 ^{a} ± 0.01	0.08 ^{a} ± 0.04
17:1	0.04 ^{a} ± 0.01	0.04 ^{a} ± 0.01	0.04 ^{a} ± 0.00	0.04 ^{a} ± 0.00	0.04 ^{a} ± 0.01
18:0	3.00 ^{a} ± 0.01	4.01 ^{b} ± 0.01	3.99 ^{b} ± 0.04	4.30 ^{c} ± 0.02	4.54 ^{d} ± 0.02
18:1	14.64 ^{a} ± 0.01	16.64 ^{c} ± 0.01	16.13 ^{b} ± 0.03	18.46 ^{d} ± 0.06	18.71 ^{e} ± 0.00
18:2	16.56 ^{d} ± 0.03	14.77 ^{c} ± 0.07	11.14 ^{a} ± 0.14	11.88 ^{b} ± 0.01	14.92 ^{c} ± 0.08
18:3 n-6	0.21 ^{a} ± 0.03	0.20 ^{a} ± 0.03	0.18 ^{a} ± 0.00	0.17 ^{a} ± 0.02	0.20 ^{a} ± 0.01
18:3 n-3	59.96 ^{d} ± 0.05	58.77 ^{b} ± 0.05	63.11 ^{e} ± 0.16	59.39 ^{c} ± 0.06	55.91 ^{a} ± 0.15
20:0	0.15 ^{a} ± 0.05	0.15 ^{a} ± 0.034	0.14 ^{a} ± 0.01	0.15 ^{a} ± 0.01	0.14 ^{a} ± 0.01
20:1	0.14 ^{a} ± 0.01	0.10 ^{a} ± 0.03	0.09 ^{a} ± 0.01	0.12 ^{a} ± 0.01	0.13 ^{a} ± 0.04
20:3	0.06 ^{a} ± 0.00	0.05 ^{a} ± 0.01	0.03 ^{a} ± 0.04	0.02 ^{a} ± 0.03	0.02 ^{a} ± 0.03
22:0	0.13 ^{a} ± 0.01	0.12 ^{a} ± 0.01	0.12 ^{a} ± 0.01	0.12 ^{a} ± 0.00	0.14 ^{a} ± 0.01
24:0	0.08 ^{a} ± 0.01	0.08 ^{a} ± 0.00	0.05 ^{a} ± 0.06	0.05 ^{a} ± 0.06	0.05 ^{a} ± 0.06
ΣSFA	8.34	9.40	9.25	9.88	10.01
ΣMUFA	14.87	16.84	16.32	18.68	18.96
ΣPUFA	76.79	73.78	74.45	71.45	71.04
n-3/n-6	3.6	3.9	5.6	4.9	3.7
UFA/SFA	11.0	9.7	9.8	9.1	9.0

^{abcde}—values are mean ± standard deviations of three measurements (n = 3), different superscript letters within rows indicate significant differences ($p < 0.05$). ΣSFA—total of saturated fatty acid. ΣMUFA—total of monounsaturated fatty acid. ΣPUFA—total of polyunsaturated fatty acid. UFA/SFA—ratio of total of unsaturated fatty acid to total of saturated fatty acid. FL BU (Bukoz Flaxseed cultivar), FL DL (Dolguniec Flaxseed cultivar), FL SZA, FL SZB (Szafir Flaxseed cultivar), FL NN (Unknown Flaxseed cultivar).

2.2. Color Measurement

Color is an important quality determinant, significant for consumers' acceptability; therefore, in order to determine the parameters describing color, measurements of reflectance at a spectrum of wavelengths from 400 to 740 nm and the calculation of three parameters of L*, a*, b* were performed, with results given in Table 2. Among the five oil samples analyzed, significant differences were found in mean values of L*, a* and b*, and it is noticeable that flaxseed oil samples were characterized by a high value of b*, attributable to yellow color. The highest yellowness (b*), redness (a*) and lightness (L*) were noted for the Bukoz variety FL BU (136.58, 8.99, 87.86, respectively). Similar results were obtained by Choo, Birch and Dufour [17].

Table 2. CIE LAB L*, a*, b* values of cold-pressed flaxseed oils.

Seeds Variety	CIE LAB L*, a*, b* Values		
	L*	a*	b*
FL BU	87.86 ^{e} ± 0.06	8.99 ^{e} ± 0.07	136.58 ^{e} ± 0.06
FL DL	86.21 ^{b} ± 0.02	2.59 ^{a} ± 0.01	112.48 ^{b} ± 0.04
FL SZA	74.64 ^{a} ± 0.08	4.86 ^{c} ± 0.01	102.90 ^{a} ± 0.10
FL SZB	87.12 ^{d} ± 0.02	2.79 ^{b} ± 0.00	120.27 ^{c} ± 0.02
FL NN	86.64 ^{c} ± 0.00	5.09 ^{d} ± 0.01	128.31 ^{d} ± 0.03

^{abcde}—values are mean ± standard deviations of three (n = 3) measurements, different superscript letters within rows indicate significant differences ($p < 0.05$). FL BU (Bukoz Flaxseed cultivar), FL DL (Dolguniec Flaxseed cultivar), FL SZA, FL SZB (Szafir Flaxseed cultivar), FL NN (Unknown Flaxseed cultivar).

2.3. DSC Crystallization Profiles of Cold-Pressed Flaxseed Oils

The thermal properties of fats and oils can be described by measuring thermal behavior during the phase transition, such as crystallization or melting, but also by determining thermal stability during chemical reactions of oxidation. All these measurements were carried out using the analytical technique of differential scanning calorimetry. Since the DSC procedure for investigating phase transition involved first cooling the oil sample before heating, the crystallization curves will be discussed first. In Figure 1, the crystallization profiles of cold pressed flaxseed oils obtained by two different scanning rates are shown, and in Table 3 the results of crystallization temperature and enthalpy are presented. As can be seen on the cooling curves (Figure 1), one crystallization peak for both scanning rates (1 and 2 °C/min) was detected. Due to the high content of unsaturated fatty acids (Table 1), crystallization phase transition takes place for both scanning rates (1 and 2 °C/min) below a temperature of −50 °C, where for the scanning rate 1 °C/min it occurred for all five flaxseed oils being tested in a narrow range from −55.35 to −54.59 °C, while for the scanning rate 2 °C/min the temperature ranged from −60.24 to −59.1 °C. For both scanning rates (1 and 2 °C/min), the mean values of temperatures between cultivars did not differ significantly. However, it was observed that for the cultivar characterized by the highest UFA/SFA ratio (FL BU, ratio = 11, Table 1), the lowest crystallization temperature was observed for both scanning rates (1 and 2 °C/min). Correlation analysis between the ratio of UFA/SFA and crystallization temperature showed that there is a negative linear correlation with Pearson's correlation coefficient (r) −0.87 for rate 1 °C/min and −0.88 for rate 2 °C/min. The second parameter measured for the crystallization process was the enthalpy of the transition, which was measured as the area of the peak. The mean values of enthalpy did not differ significantly between the various cultivars of flaxseed oil for scanning rate 1 °C/min as well as for rate 2 °C/min. However, the values of enthalpy obtained for scanning rate 2 °C/min were lower than for rate 1 °C/min, for which the mean value calculated from all five cultivars was 34.12 J/g, while for scanning rate 2 °C/min it was −28.23 J/g. The results obtained for scanning rate 1 °C/min correlate well with the study presented by Teh and Birch [22], which reported a peak temperature at the value of

−53.79 °C and enthalpy 40.98 J/g. There are no studies performed using a scanning rate of 2 °C/min to compare the results obtained.

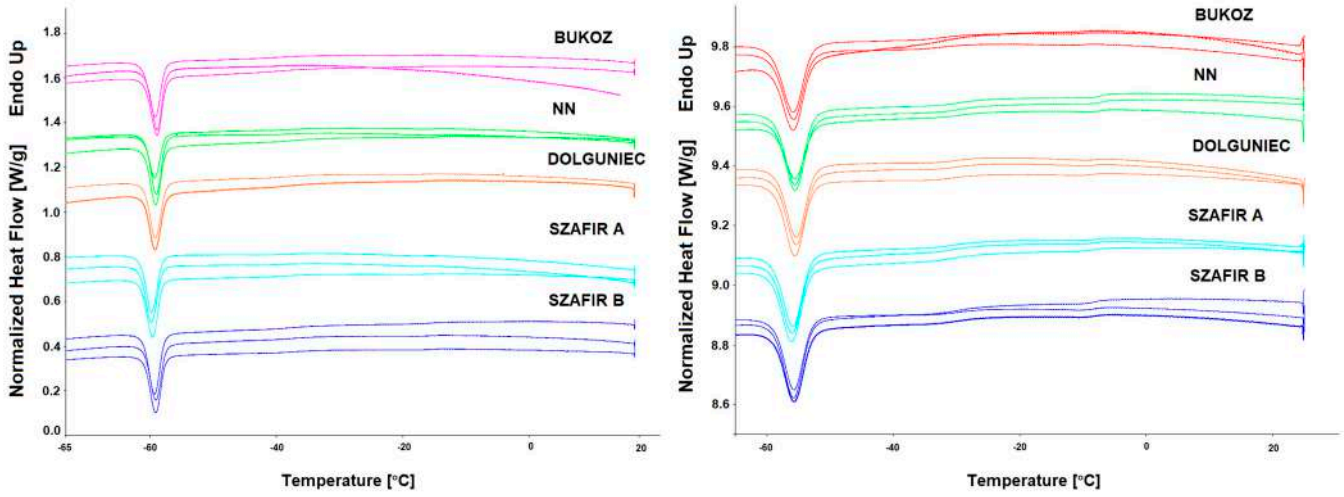

Figure 1. DSC crystallization curves of cold-pressed flaxseed oils from different cultivars obtained with various cooling rates: (**a**) Cooling rate 1 °C/min; (**b**) Cooling rate 2 °C/min.

Table 3. Differential scanning calorimetry (DSC) thermodynamic parameters of crystallization process of different cultivars of cold-pressed flaxseed oils obtained by different scanning rates.

Seeds Variety	Scanning Rate 1 °C/min		Scanning Rate 2 °C /min	
	Enthalpy	Peak Temperature	Enthalpy	Peak Temperature
	ΔH_c [J/g]	T_c [°C]	ΔH_c [J/g]	T_c [°C]
FL BU	−34.82 [a] ± 0.73	−55.35 [a] ± 2.01	−27.34 [a] ± 1.06	−60.24 [a] ± 1.90
FL DL	−34.33 [a] ± 0.42	−54.71 [a] ± 0.16	−27.87 [a] ± 0.54	−59.15 [a] ± 0.08
FL SZA	−34.71 [a] ± 0.21	−55.17 [a] ± 0.11	−28.49 [a] ± 0.90	−59.68 [a] ± 0.08
FL SZB	−34.66 [a] ± 1.31	−54.59 [a] ± 0.12	−28.99 [a] ± 1.06	−59.43 [a] ± 0.03
FL NN	−32.09 [a] ± 5.29	−54.74 [a] ± 0.01	−28.45 [a] ± 1.22	−59.10 [a] ± 0.07

[a] value is mean ± standard deviations of three (n = 3) measurements. The same superscript letters within columns indicate no significant differences ($p < 0.05$). FL BU (Bukoz Flaxseed cultivar), FL DL (Dolguniec Flaxseed cultivar), FL SZA, FL SZB (Szafir Flaxseed cultivar), FL NN (Unknown Flaxseed cultivar).

2.4. DSC Melting Profiles of Cold-Pressed Flaxseed Oils

Following the crystallization process, the melting phase transition of cold-pressed flaxseed oils was also investigated at different scanning rates. Figure 2a–c depicts melting curves obtained at different heating rates (1, 2, 5 °C/min). As can be seen in Figure 2, the melting profiles of flaxseed oil differ from crystallization curves. Firstly, the most discernible difference between crystallization and melting curves can be observed in the shape of the curves. Curves obtained during crystallization are manifested by only one peak, while melting curves are more complex because there are more peaks not separated. In contrast to the crystallization process, where the shape of the curves was similar for both scanning rates, in the melting process the shape of the curves and the size of the peaks (width and height) are affected by the scanning rate. Figure 2a shows that the melting profiles of five different cultivars of flaxseed differ for scanning rate 1 °C/min. In Table 4, the parameters of the melting peaks (temperatures and enthalpies) obtained by scanning rate 1 °C/min are given. The lowest values of melting temperatures and the highest of

total enthalpy (ΔHm total), significantly different from other mean values, were recorded for sample FL BU (Tm1 = −35.69 °C; Tm2 = −13.77 °C, ΔHm total = 127.91 J/g). All the melting curves of the five oil samples analyzed at this rate exhibited one common peak Tm1 in the range of −31.73 to −35.69 °C. The second peak Tm2, appearing within the range of −10.26 to −13.77 °C, differed in size among the cultivars (Figure 2a). Teh and Birch [22] reported similar results of temperature values obtained at rate 1 °C/min, i.e., −36.28 and −15.43 °C for both peaks.

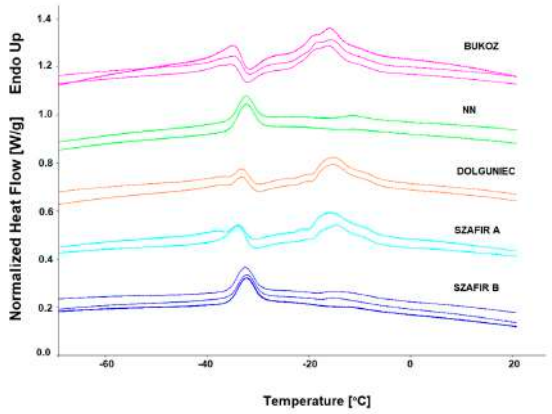

(**a**)

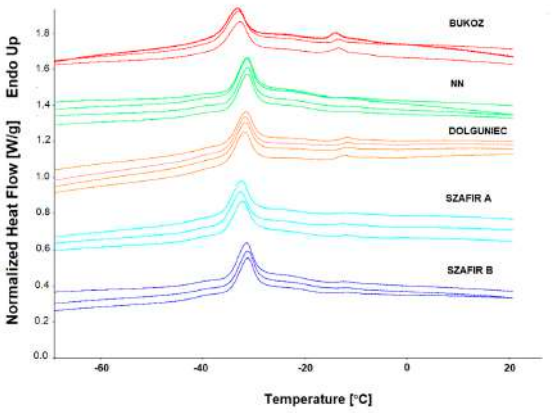

(**b**)

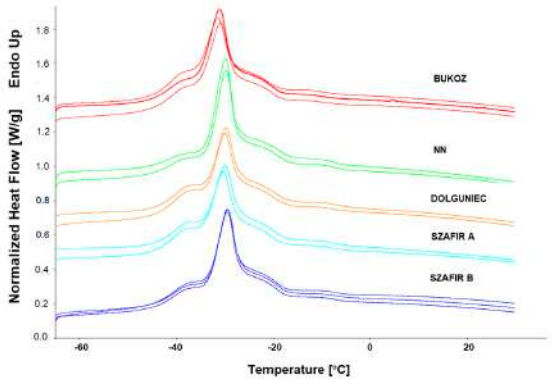

(**c**)

Figure 2. DSC melting curves of cold-pressed flaxseed oils from different cultivars obtained with various heating rates: (**a**) Heating rate 1 °C/min; (**b**) Heating rate 2 °C/min; (**c**) Heating rate 5 °C/min.

Table 4. DSC thermodynamic parameters of melting process of different cultivars of cold-pressed flaxseed oils obtained by a scanning rate of 1 °C/min.

Seeds Variety	Peak Temperature [°C]		Enthalpy [J/g]		
	Tm1	Tm 2	Δ Hm Peak 1	Δ Hm Peak 2	Δ Hm Total
FL BU	−35.69 ^{b} ± 1.71	−13.77 ^{b} ± 1.60	35.12 ^{b} ± 6.82	92.80 ^{d} ± 7.99	127.91 ^{c} ± 13.44
FL DL	−32.45 ^{a} ± 0.18	−12.42 ^{ab} ± 0.23	19.09 ^{a} ± 1.75	66.26 ^{a} ± 0.22	85.35 ^{b} ± 1.66
FL SZA	−33.26 ^{ab} ± 0.20	−12.44 ^{ab} ± 0.51	24.67 ^{ab} ± 6.38	71.46 ^{a} ± 6.48	71.46 ^{b} ± 4.90
FL SZB	−31.43 ^{a} ± 0.38	−10.87 ^{a} ± 1.10	26.17 ^{ab} ± 0.28	8.09 ^{b} ± 1.26	34.27 ^{a} ± 1.53
FL NN	−31.73 ^{a} ± 0.22	−10.26 ^{a} ± 0.24	19.60 ^{a} ± 3.04	23.85 ^{c} ± 1.63	43.45 ^{a} ± 4.67

^{abc} values are mean ± standard deviations of three measurements (n = 3), different superscript letters within columns indicate significant differences ($p < 0.05$). Tm1—peak temperature for peak 1, counting from the lower to the higher temperatures. FL BU (Bukoz Flaxseed cultivar), FL DL (Dolguniec Flaxseed cultivar), FL SZA, FL SZB (Szafir Flaxseed cultivar), FL NN (Unknown Flaxseed cultivar).

Comparing the shape of curves obtained by scanning rate 1 °C/min, it can be seen that the melting profiles for flaxseed cultivars of Bukoz, Dolguniec and Szafir A are similar, where two peaks, Tm1 and Tm2, are clearly visible. In the case of NN and Szafir B flaxseed oil samples, the huge reduction in the peak Tm2 at around −10 °C was observed.

Figure 2b shows the melting curves of five flaxseed oil samples obtained with a scanning rate of 2 °C/min. The shape of the curves differed from curves obtained with a scanning rate of 1 °C/min. The most significant difference compared to the curves with a rate of 1 °C/min is the reduction in the second peak or its complete disappearance, as in the case of the FL NN sample. This indicates that the heating rate of 2 °C/min is too fast for polymorphic transition to occur, as it was by the rate 1 °C/min. Table 5 presents the results of melting transition with a scanning rate of 2 °C/min. There are no significant differences between the five samples of oils in mean values of peak temperatures, although the values of melting enthalpy are significantly different. The highest total enthalpy was observed for sample FL SZA (50.84 J/g) and lowest for FL NN (43.12 J/g). Similarly, as for rate 1 °C/min, the lowest values of melting temperatures were noted for the Bukoz variety (FL BU), Tm1 = −32.89 °C and Tm2 = −11.08 °C, and the highest for sample FL NN, Tm1 = −30.34 °C, and a second peak was not detected.

Table 5. DSC thermodynamic parameters of melting process of different cultivars of cold-pressed flaxseed oils obtained by a scanning rate of 2 °C/min.

Seeds Variety	Peak Temperature [°C]		Enthalpy [J/g]		
	Tm1	Tm2	Δ Hm1	Δ Hm2	Δ Hm Total
FL BU	−32.89 ^{a} ± 2.03	−11.08 ^{a} ± 1.98	41.96 ^{c} ± 2.58	2.39 ^{b} ± 1.15	44.35 ^{bc} ± 1.88
FL DL	−30.66 ^{a} ± 0.19	−8.72 ^{a} ± 0.47	47.96 ^{ab} ± 2.00	1.28 ^{ab} ± 0.27	49.23 ^{a} ± 1.75
FL SZA	−31.49 ^{a} ± 0.19	−9.21 ^{a} ± 0.46	50.09 ^{b} ± 1.84	0.75 ^{ab} ± 0.14	50.84 ^{a} ± 1.76
FL SZB	−30.36 ^{a} ± 0.05	−8.56 ^{a} ± 0.26	48.14 ^{ab} ± 2.86	0.69 ^{a} ± 0.14	48.83 ^{ac} ± 2.97
FL NN	−30.34 ^{a} ± 0.07	nd	43.12 ^{ac} ± 1.95	nd	43.12 ^{b} ± 1.95

^{abc} values are mean ± standard deviations of three measurements (n = 3), different superscript letters within columns indicate significant differences ($p < 0.05$). nd: not detected. Tm1—peak temperature for peak 1, counting from the lower to the higher temperatures. Δ Hm1—enthalpy for peak 1, counting from the lower to the higher temperatures. FL BU (Bukoz Flaxseed cultivar), FL DL (Dolguniec Flaxseed cultivar), FL SZA, FL SZB (Szafir Flaxseed cultivar), FL NN (Unknown Flaxseed cultivar).

Figure 2c depicts the melting curves of five oil samples obtained with a heating rate of 5 °C/min. It can be seen that all the curves differ from the curves obtained by a scanning rate of 1 and 2 °C/min. However, they do not differ in shape among the cultivars. All curves are very similar and repeatable with the main peak at a temperature between −29.45 and −31.88 °C, as is shown in Table 6. There were no significant differences in the mean values of temperature nor in enthalpy. However, the lowest values of melting temperatures were obtained for FL BU and the highest values for sample FL NN, as in the case of a

heating rate of 1 and 2 °C/min. Moreover, it can be seen from all curves that the main peak is composed of more than one peak, and two pronounced shoulders on both sides of this peak are visible. The first shoulder is from around −47 °C to −35 °C, and the second is from −27 °C to −17 °C. Additionally, a small separate shoulder was identified at around—13 °C. The results are consistent with those obtained by Zhang et al. [10], who studied the effect of heating on the DSC melting curve of flaxseed oil. In their experiment, they similarly mentioned about one major peak at −31 °C and two endothermic shoulders with a maxima at −38 °C and at −24 °C. An endothermic event was also recognized at −13 °C. Our results obtained for scanning rate 5 °C/min also correlated well with the study of Zhang et al. [21], which reported a peak temperature at the value of −32.53 °C and −30.65 °C and enthalpies of 62.15 J/g and 57.85 J/g for two different flaxseed oils.

Table 6. DSC thermodynamic parameters of melting process of different cultivars of cold-pressed flaxseed oils obtained by a scanning rate of 5 °C/min.

Seeds Variety	Peak Temperature [°C]	Enthalpy [J/g]
	Tm1	Δ Hm
FL BU	−31.88 [a] ± 0.42	60.36 [a] ± 0.79
FL DL	−30.15 [a] ± 0.46	65.12 [a] ± 0.39
FL SZA	−30.53 [a] ± 0.62	61.33 [a] ± 1.20
FL SZB	−29.45 [a] ± 0.11	63.32 [a] ± 1.75
FL NN	−29.48 [a] ± 0.62	63.39 [a] ± 0.42

[a] value is mean ± standard deviations of three measurements (n = 3), the same superscript letters within columns indicate no significant differences ($p < 0.05$). nd: not detected. FL BU (Bukoz Flaxseed cultivar), FL DL (Dolguniec Flaxseed cultivar), FL SZA, FL SZB (Szafir Flaxseed cultivar), FL NN (Unknown Flaxseed cultivar).

Considering the impact of the fatty acid composition of flaxseed oils on the melting temperatures, Pearson's correlation analysis was performed between temperature value Tm1 and ratio UFA/SFA for each scanning rate. The analysis revealed that for all heating rates, Pearson's correlation coefficients were statistically significant ($p < 0.05$), and the values r were −0.98, −0.97, and −0.99, respectively, for scanning rates 1, 2, and 5 °C/min.

2.5. Isothermal Determination of Oxidative Stability by DSC Non-Isothermal Determination of Oxidative Stability by DSC

Oxidative stability is one of the most important quality features of all edible fats and oils because lipid peroxidation leads to their nutritional and sensory deterioration. Polyunsaturated fatty acids, the lipid compounds most prone to oxidation in the presence of light, oxygen or high temperature, can form free radicals, which are transformed into aldehydes and ketones responsible for undesirable flavor. Using the DSC technique, it is possible to create favorable conditions for lipid peroxidation, i.e., increased temperature and oxygen atmosphere. The DSC method provides information regarding oils' resistance to thermal oxidation, which can be measured isothermally and non-isothermally. Figure 3 depicts the DSC curves of the isothermal determination of oxidative stability at 120 °C of the five cold-pressed flaxseed oils. All DSC curves show a sharp exothermic decline at the initiation of the oxidation process due to heat evolving during the oxidation reaction. Only in the case of sample FL NN compared to other varieties was the point of the curve's decline shifted to a higher value of time. Figure 4 shows graphs with results calculated from oxidation curves presented in Figure 3. Various parameters of oxidative stability were analyzed, i.e., oxidation induction time (OIT), oxidation end time (OET), the length of the oxidation process Δt (OET-OIT) and the rate of oxidation. The time required for the decline in exotherm was taken as the induction time OIT (min). As can be seen in Figures 3 and 4, the best oxidative stability was exhibited by oil sample FL NN, for which oxidation started at 51 min, while significantly lower OIT values were registered for the sample FL DL at 43 min and FL BU at 41 min. The Szafir variety (FL SZA, FL SZB)

was characterized by the worst oxidative stability, with OIT values around 37–38 min, which was significantly different from the rest of the oil samples. Considering the second parameter OET, determined from the oxidation curve at 120 °C, it was noted that this parameter followed in the same order as was observed for OIT, and the mean values differed significantly between each other in a similar way as for OIT. On the other hand, another factor Δt, which measures the oxidation duration, ranged from 17 to 20 min with no significant differences among the cultivars. The last parameter calculated from the DSC oxidation curve at 120 °C was the rate of oxidation, which can express the speed of the oxidation process. Among the various cultivars, the mean values did not differ significantly, and ranged between 0.02 and 0.03.

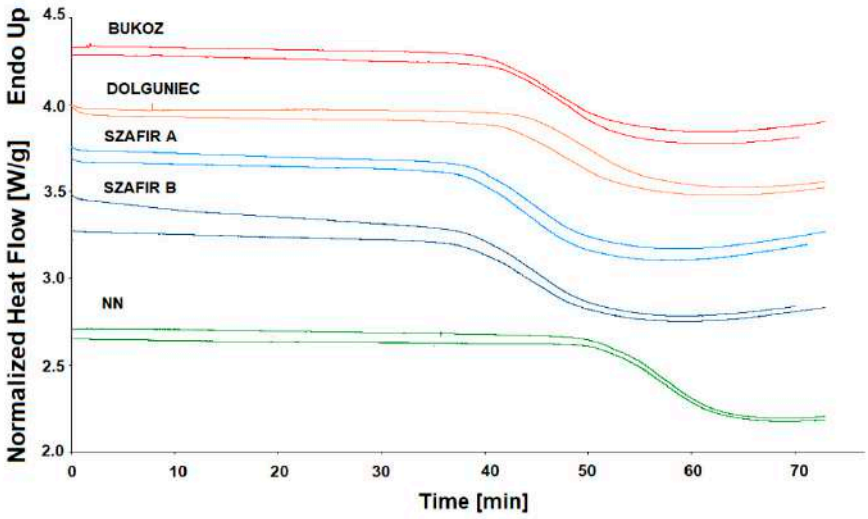

Figure 3. DSC isothermal oxidation curves obtained at 120 °C for cold-pressed flaxseed oils.

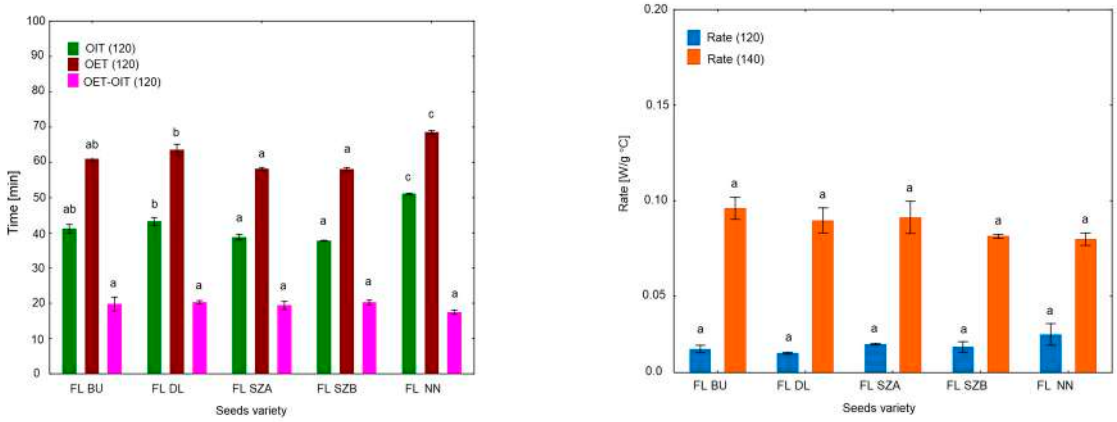

(**a**) (**b**)

Figure 4. Oxidative stability parameters of five cold-pressed flaxseed oils determined isothermally by DSC at 120 °C: (**a**) Oxidation induction time OIT (min), oxidation end time OET (min), the oxidation duration Δt (min). (**b**) Rate of oxidation at 120 and 140 °C. Different letters (a, b, c) indicate significant differences ($p < 0.05$). FL BU (Bukoz Flaxseed cultivar), FL DL (Dolguniec Flaxseed cultivar), FL SZA, FL SZB (Szafir Flaxseed cultivar), FL NN (Unknown Flaxseed cultivar).

In summary, five different samples of flaxseed oils started to be oxidized isothermally at 120 °C between 37 and 51 min, and oxidation finished between 58 and 68.5 min. The sample FL NN was characterized by the highest and significantly different values of OIT and OET. However, the duration and rate of oxidation at 120 °C did not differ significantly among the varieties.

To confirm the observed resistance of some flaxseed varieties to oxidation, a further measurement was carried out by isothermal DSC at higher temperatures than 120 °C, i.e., 140 °C. The curves are shown in Figure 5 and the results are presented in Figure 6. It was observed that the initiation point of oxidation appearing as the decline of exotherm (OIT) occurred much sooner in the case of 140 °C than at 120 °C. The mean values for 140 °C were five times lower than for 120 °C, and ranged between 8 and 11 min. It is also worth noting that the highest OIT values were observed for the FL NN sample and the lowest for the Szafir samples (FL SZA, FL SZB), as for the 120 °C. The values of the OET parameter were in a similar order as for OET at 120 °C and as for OIT at 120 °C and 140 °C; the highest values were noted for FL NN and FL DL (21.82 and 21.93 min, respectively), and the lowest for Szafir A and B (19.51 and 20.17 min, respectively). Subsequently, the results for the length of oxidation (Δt) at 140 °C were analyzed (Figure 6). It was observed that the Szafir variety (FL SZA) was completely oxidized in the shortest time, around 10 min, and this value was significantly different from the values obtained for the remaining four oil samples ($p < 0.05$). Figure 4b shows the results of calculating the oxidation rate for 140 °C. Compared to the results of the rate obtained at 120 °C, it can be noted that for 140 °C the oxidation rate was three times higher for all varieties. Samples FL SZA and FL BU were oxidized with the highest rate (0.09), whereas the other three varieties showed a rate of 0.08. However, as was the case at 120 °C, there were also no significant differences among cultivars ($p > 0.05$).

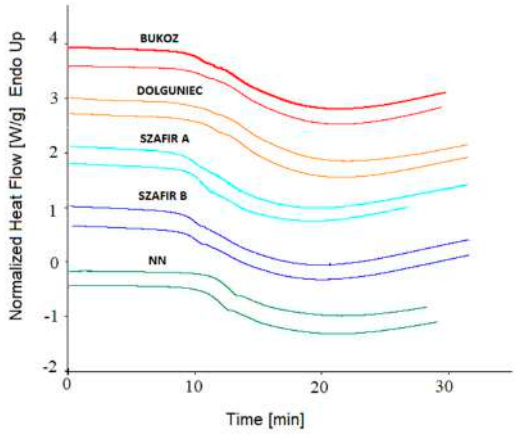

Figure 5. DSC isothermal oxidation curves obtained at 140 °C for cold-pressed flaxseed oils.

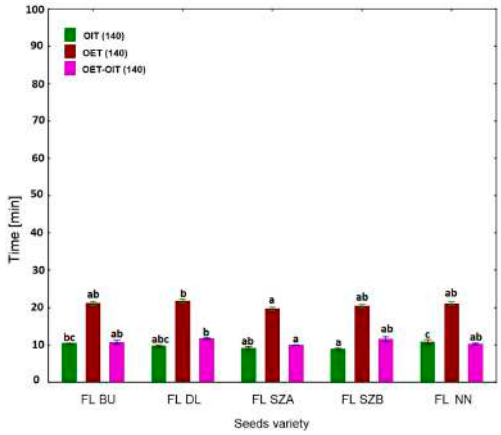

Figure 6. Oxidative stability parameters of five cold-pressed flaxseed oils determined isothermally by DSC at 140 °C: Oxidation induction time OIT (min), oxidation end time OET (min), the oxidation duration Δt (min). Different letters (a, b, c) indicate significant differences ($p < 0.05$). FL BU (Bukoz Flaxseed cultivar), FL DL (Dolguniec Flaxseed cultivar), FL SZA, FL SZB (Szafir Flaxseed cultivar), FL NN (Unknown Flaxseed cultivar).

By way of conclusion, it can be stated that for the DSC isothermal measurement of the oxidation stability of flaxseed oils, both measurements at 120 and 140 °C confirmed the best resistance to oxidation of sample FL NN and the worst of the Szafir variety (FL SZA, FL SZB).

2.6. Non-Isothermal Determination of Oxidative Stability by DSC

Figures 7 and 8 demonstrate the results of the non-isothermal measurements of thermal stability by DSC of the five samples of flaxseed oils carried out with a scanning rate of 2 and 5 °C/min, for which the values of onset temperature (Ton) and end temperature (Tend) were determined. Considering the scanning rate 2 °C/min, it can be observed that for the Szafir variety (FL SZA, FL SZB), the oxidation initiation temperature (Ton) was the lowest, i.e., 144.5 and 144.1 °C, respectively, while for sample FL NN, the highest value was noted at 146.6 °C. However, all mean values of Ton were not significantly different among the five flaxseed oil varieties. Along with the determination of Ton, Tend values were also collected, which express the end of the oxidation process. As in the case of Ton, for the Szafir variety (FL SZA, FL SZB) the values of Tend were the lowest, i.e., 157.8 and 157.3 °C, respectively, while the highest values were observed for FL BU and FL NN (160.8 and 160.6 °C). However, there were no significant differences between the mean values of Ton and Tend among the five oils at a scanning rate of 2 °C/min. The oxidative behavior of oils under increasing temperature was further tested for a higher heating rate, i.e., 5 °C/min (Figures 7 and 8). The determination of onset time (Ton) for rate 5 °C/min confirmed the best stability of the sample of FL NN, reaching the highest level and significantly different from the remaining four oils at a value of 162.50 °C ($p < 0.05$). The Ton values for the remaining oils ranged between 157.7 and 158.5 °C and they do not differ significantly. Similarly, the parameter of the end of oxidation (Tend) was highest and significantly different for FL NN. Summing up, the non-isothermal DSC technique showed that the Szafir seed variety was oxidized at the lowest temperatures for both 2 and 5 °C/min, along with the highest values for the sample FL NN variety, indicating significantly higher resistance to oxidation than for other varieties in both cases of rate.

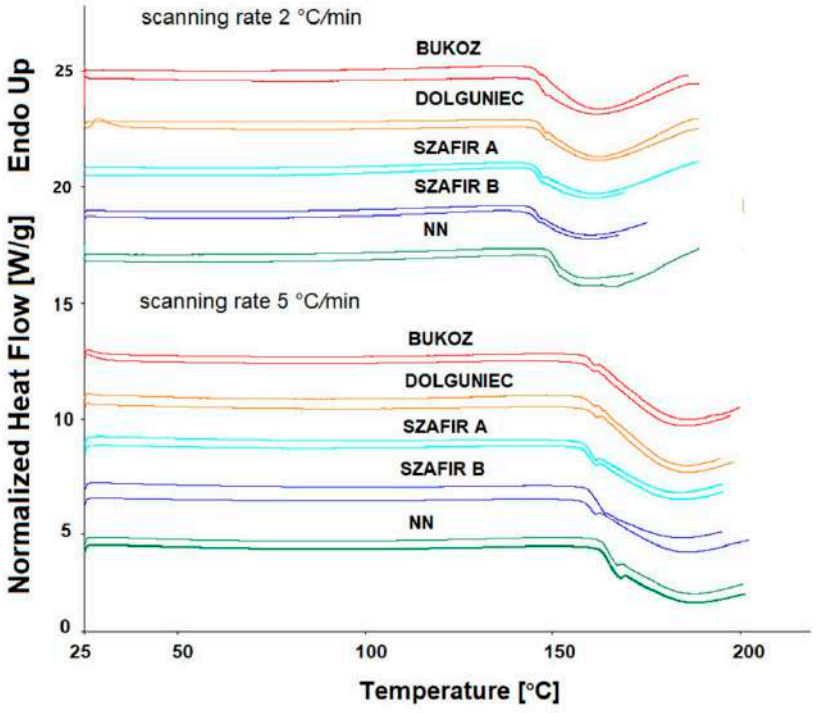

Figure 7. DSC non-isothermal oxidation curves obtained at a scanning rate 2 and 5 °C/min for cold-pressed flaxseed oils.

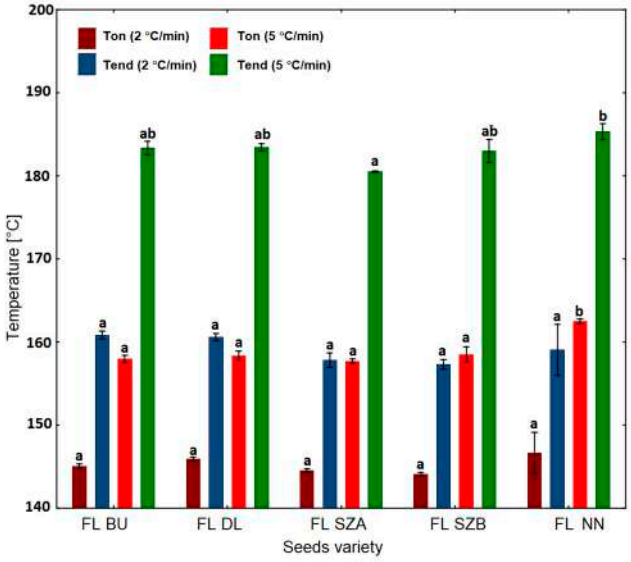

Figure 8. Oxidative stability parameters of five cold-pressed flaxseed oils determined non-isothermally by DSC at a scanning rate of 2 and 5 °C/min. Different letters (a, b) indicate significant differences ($p < 0.05$). FL BU (Bukoz Flaxseed cultivar), FL DL (Dolguniec Flaxseed cultivar), FL SZA, FL SZB (Szafir Flaxseed cultivar), FL NN (Unknown Flaxseed cultivar).

2.7. Peroxide, p-Anisidine, TOTOX and Acid Value

In order to compare the results of the oxidative stability determined by DSC with traditional chemical determinations, various analyses were carried out, i.e., peroxide value (PV), as a measure of primary oxidation products, p-anisidine value (pAV), as an indicator of nonvolatile secondary oxidation products, and acid value (AV) to measure the degree of hydrolytic changes. Moreover, the parameter of total oxidation value (TOTOX) was calculated based on the results of p-anisidine value and peroxide value (TOTOX = pAV+2 PV). Figure 9a depicts the values obtained from chemical analysis of pAV and PV, as well as the calculated parameter TOTOX. Since all the peroxide values obtained were below 7 meqO_2/kg, p-anisidine values were lower than 1.0 and TOTOX below 15, it can be assumed that all the oils studied were of good quality because the requirements of the Codex Alimentarius standard [23] for a peroxide value (<15 meqO_2/kg) and of pAV < 2.0 were met. Among all the cultivars, the highest values of all three parameters were noted for the sample FL SZB: pV = 6.9 mEqO_2/kg, pAV = 0.94, and TOTOX = 14.74. In turn, the lowest value of pV was 1.21 mEqO_2/kg and TOTOX was 3.17 for sample FL NN, although for the sample FL DL, the lowest value of pAV = 0.65 was measured. Only in the case of pAV did the mean values not differ significantly among the cultivars ($p < 0.05$). Figure 9b shows the results of acid value and acidity measurement. The acid value is the measure of free fatty acids as a result of the hydrolytic breakdown of triglyceride molecules. The results show that acid values ranged between 1.6 and 0.4 mg KOH/g. This confirmed that the flaxseed oil samples represent good quality, as their acid values did not exceed the maximum limit of 4.0 mg KOH/g of oil according to the Codex Alimentarius standard [23]. Similar results of peroxide, anisidine and TOTOX values were obtained for seven cold-pressed flaxseed oils sold in New Zealand by Choo, Birch and Dufour [17].

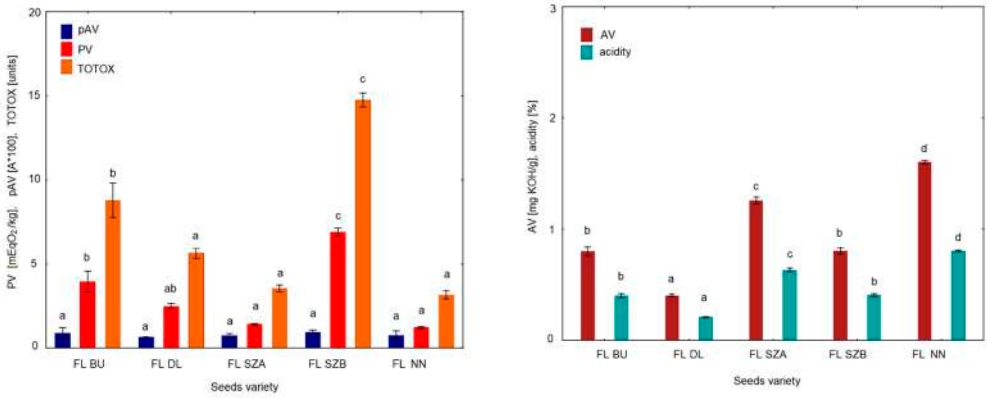

(**a**) (**b**)

Figure 9. Oxidative stability parameters of five cold-pressed flaxseed oils: (**a**) Peroxide value (PV), p-anisidine value (pAV), total oxidation rate (TOTOX) value; (**b**) Acid value (AV), acidity. Different superscript letters (a, b, c, d) indicate significant differences ($p < 0.05$). FL BU (Bukoz Flaxseed cultivar), FL DL (Dolguniec Flaxseed cultivar), FL SZA, FL SZB (Szafir Flaxseed cultivar), FL NN (Unknown Flaxseed cultivar).

3. Discussion

In this study, differential scanning calorimetry was used to characterize the thermal behavior of various cultivars of flaxseed oil in terms of melting and crystallization profiles as well as thermo-oxidative stability. The crystallization analysis showed that there were no significant differences between cultivars in peak temperature and enthalpy, although for oil with the highest UFA/SFA ratio, the lowest crystallization temperature was observed for both scanning rates (1 and 2 °C/min). Correlation analysis between the ratio of UFA/SFA and crystallization temperature showed a significant, negative linear correlation with coefficients r = −0.87 for rate 1 °C/min and r = −0.88 for rate 2 °C/min. This observation is in line with other studies carried out on various edible oils [24].

The effect of cooling rate on the crystallization peak temperatures and enthalpies was also found. The results obtained from crystallization indicated that the higher the cooling rate, the lower the peak temperatures and the lower the enthalpy of transition. This statement is in agreement with previous research conducted on butterfat [25] and other vegetable oils [26].

The melting profiles were also analyzed by using various heating rates. Despite variation in the shape of the melting profile between the various scanning rates, one common peak was found at around −30 °C (Tm1) for all heating rates. Interestingly, for heating rate 1 °C/min, differences in the shape of the melting curve were also observed between cultivars. For the cultivar of Bukoz, Dolguniec and Szafir A, two peaks were identified, while for NN and Szafir B the second peak was reduced. This can indicate that the first peak, appearing at lower temperatures (Tm1), is the result of melting a less stable α polymorph that was formed during cooling, and the second peak (Tm2) could arise from polymorphic transition. The lower enthalpy for peak Tm1 than for peak Tm2 in the case of samples FL BU, FL DL, and FL SZA can confirm this statement because the higher the enthalpy, the more stable the polymorph. The highest rate of polymorphic transition was observed for the cultivar Bukoz (FL BU), with an enthalpy (ΔHm Peak 2) noted for the peak Tm2 of 92.80 J/g and the lowest for the Szafir (FL SZB) of 8.09 J/g (Table 4). The lower enthalpy for the second peak was also observed for sample FL NN. The similar behavior of flaxseed oil with recrystallization and polymorphic transitions of metastable forms at a heating rate of 1 °C/min was noted by Teh and Birch [22]. Oomah and Sitter [27] also observed two similar transitions, the first between −35 and −33 °C and the second between −25 and −24 °C indicative of crystalline melting corresponding to the α and β polymorphic forms. Similarly, a minor transition at −14 °C was detected.

Analyzing these results, the question may arise as to what kind of compositional differences affect this different polymorphic behavior, particularly in the case of the sample FL SZB and FL NN. As the results of composition indicate (Table 1), for these two samples of oils (FL SZB and FL NN) the highest percentage of oleic fatty acid (18:1), i.e., 18.46 and 18.71%, respectively, and the lowest ratio of unsaturated to saturated fatty acids (9.1 and 9.0, respectively) were observed. In turn, for these samples the total saturated fatty acid level was highest (9.88 and 10.01%, respectively). This indicates that the content of saturated and unsaturated fatty acid is crucial for flaxseed triacylglycerols' polymorphic behavior, as well as for the peak melting temperatures. For samples with the highest percentage of saturated fatty acid (FL SZB and FL NN), the highest melting temperatures were observed (−31.43 and −31.73 °C, respectively, for Tm1, and −10.87 and −10.26 °C, respectively, for Tm 2). Regarding the influence of the composition of fatty acids on the melting temperatures, correlations analysis revealed that there was a strong negative linear correlation between melting temperature value (Tm1) and ratio UFA/SFA for all scanning rates. Statistically significant ($p < 0.05$) Pearson's correlation coefficients were obtained, i.e., −0.98, −0.97 and −0.99, respectively, for scanning rates 1, 2, and 5 °C/min. This observation was previously noted by Tan and Che Man [24].

Based on these results, it can be assumed that the heating rate 1 °C/min can be considered for the differentiation of flaxseed oil cultivars, while the heating rate 5 °C/min can be utilized as a fingerprint for the authenticity assessment of flaxseed oil.

The DSC technique is also a very convenient method for measuring thermo-oxidative resistance to oxidation caused by oxygen and elevated temperature. It can be measured isothermally at various temperatures or non-isothermally, in dynamic mode with various heating rates. Five different samples of flaxseed oils started to be oxidized isothermally at 120 °C between 37 and 51 min, and oxidation finished between 58 and 68.5 min, while at 140 °C the OIT values were around 4–5 times lower. Flaxseed oil sample FL NN exhibited significantly higher values of OIT and OET than the rest of the oils. The worst resistance to oxidation was noted for the Szafir variety (FL SZA, FL SZB). The non-isothermal DSC technique confirmed these observations. The Szafir seed variety oxidized at the lowest temperatures for both rates 2 and 5 °C/min (144 °C and 157 °C, respectively), along with the highest values for the sample FL NN variety (146.6 °C and 162.5 °C, respectively), thus confirming significantly higher resistance to oxidation than for other varieties in both cases of the rate. The duration and rate of isothermal oxidation analysis at 120 and 140 °C did not differ significantly among the cultivars. However, for 140 °C the rate was three times higher than for 120 °C. In another experiment with five flaxseed oils of the Szafir cultivar, pressure differential scanning calorimetry (PDSC) isothermally at various temperatures and with the oxygen flow rate of 100 mL/min was carried out by Symoniuk, Ratusz and Krygier [13]. They obtained OIT values at 120 °C between 21.20 and 24.34 min and at 140 °C between 4.33 and 4.97 min.

In order to explain the variation in thermal resistance to oxidation among the cultivars, correlation analysis between fatty acid composition and DSC isothermal and non-isothermal results was performed, the results of which are presented in Table 7. As can be seen, high Pearson's correlation coefficients were obtained between fatty acid C18:3 and all DSC parameters, except for the parameter of non-isothermally measured onset temperature (Ton) at the scanning rate of 2 °C/min. It can be concluded that α-linolenic acid is predominantly responsible for the thermal oxidation of flaxseed oil. This statement is in agreement with the findings of other researchers [28]. In order to establish the relations between thermo-oxidative stability and stability determined by chemical methods, principal component analysis was performed. This is a method for detecting structure in the relationships between variables and to classify the objects [29]. Principal component analysis (PCA) was used to describe the oxidative stability of flaxseed oil measured by different methods. Various variables were used for PCA: from isothermal DSC oxidation determination at 120 and 140 °C: OIT(120), OIT(140) and non-isothermal onset temperature at a heating rate of 2 and 5 °C/min: Ton (2), Ton (5), as well as from the chemical determination of oxidation

stability: PV, pAV, AV, acidity, TOTOX. Using the graphical criterion, the first six principal components, which explain 99.85% of the total variance, were derived. Figure 10 depicts the plot of loadings, which visualizes relations between variables by analyzing the first two principal components: PC1 and PC2. The horizontal axis corresponds to PC1, and the vertical to PC2. The closer the variable is to the circle, the more it is correlated with the component. The graph obtained shows that the first two PCs describe 70.05% of the initial variability, where the first PC1 explains the observed variability in 52.26% and PC2 in 17.79%. The first component (PC1) describes the thermo-oxidative stability measured by parameters such as OIT (120), OIT (140) and Ton (2), Ton (5), as well as PV and TOTOX. The first PC is positively correlated with PV and TOTOX, and negatively correlated with the rest of the variables, which were taken for the analysis, except pAV. From all sets of DSC variables which are related to PC1, with all being located on the negative side (negative correlations with PC1), the strongest factor loadings were noted for OIT (120), being −0.85, and for Ton (5) of −0.84. On the opposite side of PC1, the variables of PV and TOTOX are located, which means that there are negative correlations between them and DSC parameters. This observation confirms that the greater the peroxide value, the lower the DSC parameters, i.e., the lower the thermo-oxidative stability. However, it can also be seen that variables of PV and TOTOX are strongly related to PC1 (0.69 and 0.68, respectively), as well as to PC2 (0.56 and 0.58, respectively). Figure 10 also shows no correlation of DSC parameters with anisidine value (pAV), as they are located perpendicular to each other, thus the pAV variable is more related to PC2 with a factor loading of 0.73.

Table 7. Pearson's correlation coefficients between fatty acid composition and oxidative stability parameters measured by DSC.

	C16:0	C18:0	C18:1	C18:2	18:3 n-3
OIT (120 °C)	0.08	0.37	0.39	0.53	−0.82 *
OIT (140 °C)	−0.21	−0.16	−0.07	0.80 *	−0.63 *
T_{on} (2 °C/min)	−0.13	0.18	0.17	0.47	−0.57
T_{on} (5 °C/min)	0.40	0.59	0.66 *	0.27	−0.82 *

* marked correlations are significant at $p < 0.05$.

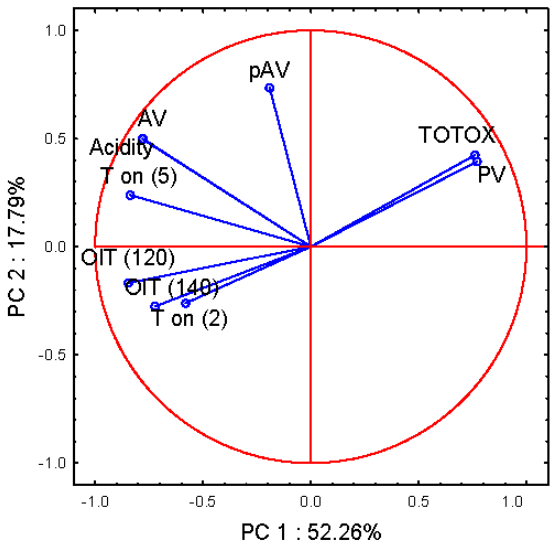

Figure 10. Oxidative stability parameters of five cold-pressed flaxseed oils.

4. Materials and Methods

4.1. Materials

We obtained three certified cultivars of flaxseed, i.e., Bukoz (FL BU), Dolguniec (FL DL), Szafir, from two different suppliers (FL SZA, FL SZB) and one sample of unknown variety (FL NN). All were brown-seeded flaxseed varieties, collected in 2019 from different parts of Poland, and were used for oil cold-pressing at a temperature under 50 °C. The pressed oils were left for 24 h for decantation and kept in brown glass bottles at freezing temperature (−80 °C).

4.2. Fatty Acid Composition

The percentage fatty acids composition was determined by GC-FID. Fatty acid methyl esters were prepared according to the AOCS Official Method Ce 2-66 [30]. Two drops of fat were dissolved in 1 mL of hexane (for HPLC, Sigma Aldrich, Sp. z o.o. Poznan, Poland). A total of 1 mL of 0.4 N sodium methoxide was added. Samples were stirred and left for 15 min, then 5 mL of distilled water was added after and the top layer was taken. Fatty acid methyl esters were analyzed using a Trace 1300 chromatograph (Thermo Fisher Scientific, Waltham, Massachusetts, USA). Separation was performed on a Supelcowax 10 capillary column (30 m × 0.2 mm × 0.2 µm). The injection was performed in splitless mode. The sample volume was 1 µL and hydrogen was used as the carrier gas. The initial furnace temperature was 160 °C, and was increased from 12 °C/min to 220 °C. A temperature of 220 °C was maintained for 20 min. Fatty acid methyl esters were identified on the basis of comparing the retention times in the sample and in the 37-Component FAME Mix (Supelco).

4.3. Color Measurement

Color measurements of oils were carried out according to [17], using the Konica Minolta CM-5 spectrophotometer (Konica Minolta, Inc., Tokyo, Japan) and SpectraMagicNx software (Konica Minolta, Inc., Tokyo, Japan). The instrument was calibrated prior to starting the analysis transmission chamber that can accurately measure both translucent and transparent liquid samples using a CM-A213 zero calibration plate (black calibration), followed by distilled water in a 10 mm CM-A98 glass cuvette (white calibration). The research was conducted using the Hunter Lab scale. Reference standard L*a*b* values were pre-defined and oil color was measured within the defined range. Parameter L* was in the range of 0–100, and denoted the brightness of the color from black to white. Similarly, the a* parameter, depending on the range, determined green (below 0) and red (above 0) tinge. Another parameter determined was the b* parameter, which in the case of negative values defined the color blue, but in the case of positive values—yellow. The samples used were analyzed in three replications.

4.4. DSC Melting and Crystallization Analysis

Melting and crystallization analysis of flaxseed oils was carried out with modifications according to the method used for butterfat [31]. A Perkin Elmer differential scanning calorimeter DSC 8500 PerkinElmer (Waltham, Massachusetts, USA), equipped with an Intracooler II and running under Pyris software (Perkin Elmer, Waltham, Massachusetts, USA), was used to examine the melting and crystallization properties of the flaxseed oil. Nitrogen (99.999% purity) was the purge gas. The DSC calorimeter was calibrated using indium (m.p. 156.6 °C, ΔH_f = 28.45 J/g) and n-dodecane (m.p. −9.65 °C, ΔH_f = 216.73 J/g). Samples of ca. 6–7 mg were weighed into aluminum pans of 20 µL (Perkin Elmer, No. 0219-0062, Waltham, Massachusetts, USA) and hermetically sealed. The reference was an empty, hermetically sealed aluminum pan. Prior to analysis, the samples were heated at 30 °C for 5 min to melt all crystals and nuclei. The samples were cooled at scanning rate 1 and 2 °C/min and heated at scanning rates 1, 2, 5 °C/min. For each measurement at a given scanning rate, the calibration procedure was completed with the correct scanning rate. Crystallization curves were recorded from 30 to −65 °C, then, following cooling, melting

curves were obtained from −65 to 30 °C. The temperature of each peak (Tp), the enthalpy of melting or crystallization ΔH [J/g] were measured from cooling or heating curves. All measurements were performed in triplicate for each sample.

4.5. Determination of Oxidative Stability by DSC

Oxidative stability was determined by following the ISO standard [32], and also implementing the ASTM procedure [33]. Oil samples were studied in a DSC 7 Perkin Elmer (Norwalk, Connecticut, USA) along with an Intracooler II operated with Pyris software (Perkin Elmer, Waltham, Massachusetts, USA). Both the isothermal and non-isothermal protocols were followed to determine the oxidative stability characteristics of the oils. The instrument was calibrated using indium (m.p. 156.6 °C, ΔH_f = 28.45 J/g) and n-dodecane (m.p. −9.65 °C, ΔH_f = 216.73 J/g), while 99.99% pure nitrogen gas was used as the purge gas. For the isothermal program, temperatures of 120 °C and 140 °C were maintained with a constant oxygen flow of 20 mL/min. For the non-isothermal program, curves were obtained by operating a scanning rate of 2 °C/min and 5 °C/min, respectively. Based on the resulting curves, parameters denoted as oxidation induction time (OIT), oxidation end time (OET), length of oxidation Δt (OIT-OET), and rate of oxidation were assayed. The oxidation rate was calculated according to the following equation:

$$\text{Oxidation Rate} = (Y1 - Y2)/\Delta t \quad (1)$$

where: Y1—heat flow at OIT point [W/g], Y2—heat flow at OET [W/g], Δt—length of oxidation.

4.6. Chemical Determination of Oxidative Stability

Measurements of p-anisidine value (pAV) for oil samples, as a measure of the level of secondary oxidative products, were carried out according to the ISO standard [34]. Spectrophotometric measurements were taken with a quartz cuvette with the 10 mm optical path length. A sample of 3 ± 0.001 g grams was weighed for measurement. The values obtained were calculated by means of the following equation:

$$pAV = (25\,[1.2\,(A1 - A2 - Ao)])/m \quad (2)$$

where Ao is the absorbance of the non-reacting sample, A1 is the absorbance of the reacting sample, A2 is an absorbance of the blank sample and m is the mass of the sample [g].

Peroxide value was determined by following the ISO 3960 standard [35]. A sample of 5 ± 0.001 g grams was weighed for measurement.

Calculations were performed using the following equation:

$$PV = ((V - Vo) \times C_{thio} \times F \times 1000)/m \quad (3)$$

where PV is peroxide value [meq O_2/kg], V—volume of titrant in test portion [ml], V0—volume of titrant in blank [ml], C_{thio}—molar concentration of the sodium thiosulfate solution in mol/l, F—exact concentration of the 0.01 N thiosulfate solution, m—weighed portion of test substance [g].

In accordance with the ISO 3960 standard [35], the total oxidation value (TOTOX) parameter was calculated, based on the pAV and PV values, by means of the following formula:

TOTOX = pAV + 2PV, expressing the overall rate of oil oxidation.

Acid value (AV), as an indicator of the degree of hydrolytic changes, was measured in five oils according to the AOCS official method [36]. A sample of 10 ± 0.001 g was weighed for measurement. The resulting values were calculated using the following equation:

$$AV = ((A - B) \times M \times 56.1)/W \quad (4)$$

where: AV—acid value [mg KOH/g of test portion], A—volume of standard alkali used in the titration [ml], B—volume of standard alkali used in titrating the blank [ml], M—molarity of standard alkali, W—mass of test portion [g].

4.7. Statistical Analysis of Results

The results were presented in the form of a mean and standard deviation. The first stage of the statistical analysis consisted of verifying ANOVA assumptions (variance homogeneity using the Hartley–Cochran–Bartlett test and data normality). If the assumptions were respected, one-way analysis of variance (ANOVA) was used and Tukey's test was applied to create statistically homogeneous groups. In turn, when one assumption was not confirmed, non-parametric tests were used, i.e., ANOVA and the Kruskal–Wallis rank test. Pearson's linear correlation coefficient was used to assess the significance of the relationship between selected variables. Additionally, principal component analysis (PCA) was used to assess the linear relationships between multiple variables. This analysis is an unsupervised pattern recognition method that is used for exploring raw data. This technique is also used to reduce the dimensionality of data sets. These methods define unique variances (principal components) using linear combinations of the original numeric variables, and these PCs are orthogonal (not correlated). Statistical analysis of the recorded results was performed using Tibco Statistica 13.3 software (Tibco Software Inc., Tulsa, Oklahoma, USA) at a significance level of $\alpha = 0.05$.

5. Conclusions

The DSC technique allowed differences in the shape of crystallization and melting profiles obtained by different scanning rates to be identified, and the oxidative stability of five different flaxseed oil cultivars at various thermal conditions to be measured. The crystallization process measured using the DSC technique was manifested as a single peak, which among the cultivars ranged between −55.35 and −54.59 °C for a cooling rate of 1 °C/min, while for the scanning rate of 2 °C/min, the temperature ranged from −60.24 to −59.1 °C. Analysis of the melting process at different scanning rates revealed that melting curves were more complex, and in the case of rates 1 and 2 °C/min, the cultivars differed in curve shape, while the profiles did not differ for a scanning rate of 5 °C/min. Considering the results obtained from the melting process, it can be concluded that the scanning rate had a significant influence on the behavior of the oil during melting. The lower scanning rate of 1 °C/min affected the different melting behaviors among various cultivars, depending on the small differences in composition (content of unsaturated and saturated fatty acids). In the case of a higher scanning rate of 5 °C/min, the curves for all cultivars were similar and this fact could be utilized in analytics for profiling in order to assess the authenticity of flaxseed oil. Comparing the differences among flaxseed cultivars, it was observed that lower melting and crystallization temperatures were noted for oils characterized by the highest ratio of unsaturated fatty acids. Highly significant, negative linear correlation coefficients were obtained for the relation between the crystallization and melting peak temperatures and the ratio of UFA/SFA. The investigation of oxidation stability by means of the DSC technique revealed that flaxseed oil is very susceptible to thermal oxidation. The mean value calculated from all cultivars of time needed to start oxidation (OIT) at 120 °C was 42 min, while at 140 °C it was 10 min, and for 140 °C the rate of oxidation was three times higher than for 120 °C. In the DSC non-isothermal mode, it was possible to measure at which temperature oxidation starts. For the heating rate of 2 °C/min, the mean value from all cultivars of onset temperature for oxidation was 145 °C, and for a rate of 5 °C/min it was 159 °C. Significant linear correlations were found between unsaturated fatty acid content (C18:2, C18:3 n-3) and DSC parameters of isothermally and non-isothermally determined stability of flaxseed oils (OIT, Ton). Using PCA, it was also established that there is a strong negative correlation between PV, TOTOX values and all DSC parameters of the thermo-oxidative stability of flaxseed oil.

Author Contributions: Conceptualization, J.T.-G.; methodology J.T.-G. and M.I.; formal analysis, J.T.-G. and M.I.; investigation, J.T.-G. and M.I.; resources, J.T.-G.; data curation J.T.-G. and M.I.; writing—original draft preparation, J.T.-G. and M.I.; writing—review and editing, J.T.-G., M.I., L.G., A.K., E.F.; visualization, J.T.-G., M.I., A.K.; supervision, J.T.-G., project administration, J.T.-G.; funding acquisition, J.T.-G., E.F. All authors have read and agreed to the published version of the manuscript.

Funding: This research was funded by NATIONAL SCIENCE CENTRE, POLAND, grant number: UMO 2018/31/B/NZ9/02762. Open access publication was co-financed within the framework of the Polish Ministry of Science and Higher Education's program: "Regional Initiative Excellence" in the years 2019–2022 (No. 005/RID/2018/19)", financing amount 12,000,000 PLN.

Institutional Review Board Statement: Not applicable.

Informed Consent Statement: Not applicable.

Data Availability Statement: The data presented in this study are available upon reasonable request.

Acknowledgments: The authors are grateful to the Polish Institute of Natural Fibers and Medicinal Plants (Poznań, Poland), SEMCO manufactory (Śmiłowo, Poland) and Hodowla Roślin STRZELCE Sp. z o.o. (Strzelce, Poland) for arranging seeds and cold-pressed oils from certified cultivars of flaxseeds.

Conflicts of Interest: The authors declare no conflict of interest.

Sample Availability: Not available.

References

1. Goyal, A.; Sharma, V.; Upadhyay, N.; Gill, S.; Sihag, M. Flax and flaxseed oil: An ancient medicine & modern functional food. *J. Food Sci. Technol.* **2014**, *51*, 1633–1653. [CrossRef] [PubMed]
2. Punia, S.; Sandhu, K.S.; Dhull, S.B.; Kaur, M.; Siroha, A.K. Kinetic, rheological and thermal studies of flaxseed (*Linum usitatissiumum* L.) oil and its utilization. *J. Food Sci. Technol.* **2020**, *57*, 4014–4021. [CrossRef] [PubMed]
3. Trela, A.; Silska, G.; Chyc, M.; Latowski, D.; Kruk, J.; Szymańska, R. Tocochromanols and fatty acid composition in flax (*Linum usitatissimum* L.) accessions. *Acta Soc. Bot. Pol.* **2019**, *88*, 1–12. [CrossRef]
4. Kumar, S.; You, F.M.; Duguid, S.; Booker, H.; Rowland, G.; Cloutier, S. QTL for fatty acid composition and yield in linseed (*Linum usitatissimum* L.). *Theor. Appl. Genet.* **2015**, *128*, 965–984. [CrossRef]
5. Gallardo, M.A.; Milisich, H.J.; Drago, S.R.; González, R.J. Effect of cultivars and planting date on yield, oil content, and fatty acid profile of flax varieties (*Linum usitatissimum* L.). *Int. J. Agron.* **2014**, *2014*, 150570. [CrossRef]
6. Łukaszewicz, M.; Szopa, J.; Krasowska, A. Susceptibility of lipids from different flax cultivars to peroxidation and its lowering by added antioxidants. *Food Chem.* **2004**, *88*, 225–231. [CrossRef]
7. Adugna, W.; Labuschagne, M.T. Association of linseed characters and its variability in different environments. *J. Agric. Sci.* **2003**, *140*, 285–296. [CrossRef]
8. Touré, A.; Xueming, X. Flaxseed lignans: Source, biosynthesis, metabolism, antioxidant activity, Bio-active components, and health benefits. *Compr. Rev. Food Sci. Food Saf.* **2010**, *9*, 261–269. [CrossRef]
9. Chen, J.; Mark Stavro, P.; Thompson, L.U. Dietary flaxseed inhibits human breast cancer growth and metastasis and downregulates expression of insulin-like growth factor and epidermal growth factor receptor. *Nutr. Cancer* **2002**, *43*, 187–192. [CrossRef]
10. Zhang, Z.S.; Li, D.; Zhang, L.X.; Liu, Y.L.; Wang, X. De Heating effect on the DSC melting curve of flaxseed oil. *J. Therm. Anal. Calorim.* **2014**, *115*, 2129–2135. [CrossRef]
11. Tavarini, S.; Castagna, A.; Conte, G.; Foschi, L.; Sanmartin, C.; Incrocci, L.; Ranieri, A.; Serra, A.; Angelini, L.G. Evaluation of chemical composition of two linseed varieties as sources of health-beneficial substances. *Molecules* **2019**, *24*, 3729. [CrossRef]
12. Rudnik, E.; Szczucinska, A.; Gwardiak, H.; Szulc, A.; Winiarska, A. Comparative studies of oxidative stability of linseed oil. *Thermochim. Acta* **2001**, *370*, 135–140. [CrossRef]
13. Symoniuk, E.; Ratusz, K.; Krygier, K. Comparison of the oxidative stability of linseed (*Linum usitatissimum* L.) oil by pressure differential scanning calorimetry and Rancimat measurements. *J. Food Sci. Technol.* **2016**, *53*, 3986–3995. [CrossRef] [PubMed]
14. Hasiewicz-Derkacz, K.; Kulma, A.; Czuj, T.; Prescha, A.; Zuk, M.; Grajzer, M.; Łukaszewicz, M.; Szopa, J. Natural phenolics greatly increase flax (*Linum usitatissimum*) oil stability. *BMC Biotechnol.* **2015**, *15*, 62. [CrossRef] [PubMed]
15. Frega, N.; Mozzon, M.; Lercker, G. Effects of free fatty acids on oxidative stability of vegetable oil. *JAOCS J. Am. Oil Chem. Soc.* **1999**, *76*, 325–329. [CrossRef]
16. Raczyk, M.; Popis, E.; Kruszewski, B.; Ratusz, K.; Rudzińska, M. Physicochemical quality and oxidative stability of linseed (*Linum usitatissimum*) and camelina (camelina sativa) cold-pressed oils from retail outlets. *Eur. J. Lipid Sci. Technol.* **2016**, *118*, 834–839. [CrossRef]
17. Choo, W.S.; Birch, J.; Dufour, J.P. Physicochemical and quality characteristics of cold-pressed flaxseed oils. *J. Food Compos. Anal.* **2007**, *20*, 202–211. [CrossRef]

18. Daun, J.K.; Barthet, V.J.; Chornick, T.L.; Duguid, S. Structure, Composition, and Variety Development of Flaxseed. In *Flaxseed in human nutrition*, 2nd ed.; Thompson, L., Cunanne, S., Eds.; AOCS Press: Champaign, IL, USA, 2003; pp. 1–40.
19. Marambe, H.; Purdy, S.; Tse, T.; Reaney, M.J.T. Flax Oil and High Linolenic Oils. *Bailey's Ind. Oil Fat Prod.* **2020**, 1–23. [CrossRef]
20. El-Beltagi, H.S.; Salama, Z.A.; El-Hariri, D.M. Fatty acids and secondary metabolites in flax seeds. *Gen. Appl. Plant Physiol.* **2007**, *33*, 187–202.
21. Zhang, Z.S.; Wang, L.J.; Li, D.; Li, S.J.; Ozkan, N. Characteristics of flaxseed oil from two different flax plants. *Int. J. Food Prop.* **2011**, *14*, 1286–1296. [CrossRef]
22. Teh, S.S.; Birch, J. Physicochemical and quality characteristics of cold-pressed hemp, flax and canola seed oils. *J. Food Compos. Anal.* **2013**, *30*, 26–31. [CrossRef]
23. Alimentarius, C. Codex Alimentarius Standard for Named Vegetable Oils Codex Stan 210-1999. *Codex Aliment.* **1999**, *210*, 1–13.
24. Tan, C.P.; Che Man, Y.B. Differential Scanning Calorimetric Analysis of Edible Oils: Comparison of Thermal Properties and Chemical Composition. *JAOCS J. Am. Oil Chem. Soc.* **2000**, *77*, 143–155. [CrossRef]
25. Tomaszewska-Gras, J. Melting and crystallization DSC profiles of milk fat depending on selected factors. *J. Therm. Anal. Calorim.* **2013**, *113*, 199–208. [CrossRef]
26. Che Man, Y.B.; Tan, C.P. Comparative differential scanning calorimetric analysis of vegetable oils: II. Effects of cooling rate variation. *Phytochem. Anal.* **2002**, *13*, 142–151. [CrossRef] [PubMed]
27. Oomah, B.D.; Sitter, L. Characteristics of flaxseed hull oil. *Food Chem.* **2009**, *114*, 623–628. [CrossRef]
28. Mao, X.; Chen, W.; Huyan, Z.; Sherazi, S.T.H.; Yu, X. Impact of linolenic acid on oxidative stability of rapeseed oils. *J. Food Sci. Technol.* **2020**, *57*, 3184–3192. [CrossRef]
29. Tomaszewska-Gras, J. DSC coupled with PCA as a tool for butter authenticity assessment. *J. Therm. Anal. Calorim.* **2016**, *126*. [CrossRef]
30. AOCS. *AOCS Official Method Preparations of Methyl Esters of Fatty Acids*; AOCS Press: Urbana, IL, USA, 1997; pp. 2–66.
31. Tomaszewska-Gras, J. Multivariate analysis of seasonal variation in the composition and thermal properties of butterfat with an emphasis on authenticity assessment. *Grasas Y Aceites* **2016**, *67*, 167. [CrossRef]
32. ISO. *ISO 11357-1:2016 Plastics—Differential Scanning Calorimetry—General Principles*; International Organization for Standardization: Geneva, Switzerland, 2016.
33. ASTM International. ASTM International. ASTM D3895-19. Test Method for Oxidative-Induction Time of Polyolefins by Differential Scanning Calorimetry. In *Annu. B ASTM Stand*; ASTM Publiher: West Conshohocken, PA, USA, 2019.
34. ISO 6885:2016. *Animal and Vegetable Fats and Oils. Determination of Anisidine Value*; International Organization for Standardization: Geneva, Switzerland, 2016.
35. ISO 3960:2010. *Animal and Vegetable Fats and Oils—Determination—Iodometric (Visual) Endpoint*; International Organization for Standardization: Geneva, Switzerland, 2017.
36. AOCS. *AOCS Official Method Cd 3d-63: Acid Value*; AOCS Press: Urbana, IL, USA, 2009.

Statement about the contribution of authors

Publication title A1: Tomaszewska-Gras, J.; Islam, M.; Grzeca, L.; Kaczmarek, A.; Fornal, E. Comprehensive Thermal Characteristics of Different Cultivars of Flaxseed Oil (*Linum usittatissimum* L.). Molecules 2021, 26, 1958. https://doi.org/10.3390/molecules26071958

Author	Contribution	Percentage contribution	Signature
Jolanta Tomaszewska-Gras	Conceptualization, Methodology, Formal analysis, Investigation, Resources, Data Curation, Writing- original draft preparation, Writing- review and editing, Visualization, Supervision, Project administration, Funding acquisition.	29	
Mahbuba Islam	Methodology, Formal analysis, Investigation, Data Curation, Writing- original draft preparation, Writing- review and editing, Visualization.	51	
Liliana Grzeca	Writing- review and editing.	5	
Anna Kaczmarek	Writing- review and editing, Visualization.	10	
Emilia Fornal	Writing- review and editing, Funding acquisition.	5	

Publication no. A2

Islam, M., Muzolf-Panek, M., Fornal, E. et al. DSC isothermal and non-isothermal assessment of thermo-oxidative stability of different cultivars of Camelina sativa L. seed oils. J Therm Anal Calorim 147, 10013–10026 (2022). https://doi.org/10.1007/s10973-022-11367-8

Journal of Thermal Analysis and Calorimetry
https://doi.org/10.1007/s10973-022-11367-8

DSC isothermal and non-isothermal assessment of thermo-oxidative stability of different cultivars of *Camelina sativa* L. seed oils

Mahbuba Islam[1] · Małgorzata Muzolf-Panek[1] · Emilia Fornal[2] · Jolanta Tomaszewska-Gras[1]

Received: 24 November 2021 / Accepted: 6 April 2022

Abstract
There is growing interest worldwide in the use of camelina oil for food as well as for biofuel purposes. For both of these applications, oxidative stability is an important feature of the oil. Therefore, the aim of this study was to test the thermal resistance to oxidation of three different cultivars of camelina oil i.e., *Omega*, *Luna* and *Śmiłowska* by means of isothermal and non-isothermal differential scanning calorimetry (DSC) oxidation measurement. For isothermal DSC analysis, different temperatures were tested (120, 140, 160 °C) and in the non-isothermal mode different scanning rates (1, 2, 5, 10, 15 °C min^{-1}) were used. To support the DSC data, chemical analyzes were also performed i.e., fatty acid composition, peroxide value, p-anisidine value, acid value and radical scavenging activity by 2,2-diphenyl-1-picrylhydrazyl (RSA DPPH). The isothermal test indicated that for all camelina oils the oxidation induction time (OIT) decreased with an increase in temperature on average from 69.83 min for 120 °C to 5.13 min for 160 °C. The OIT values corresponded very well with non-isothermal DSC results, for which the onset temperatures (T_{on}) increased with the increase of heating rate on average from 142.15 °C for 1 °C min^{-1} to 185.75 °C for 15 °C min^{-1}. The parameters of DSC oxidative stability i.e., OIT as well as T_{on} values were negatively correlated with some unsaturated fatty acids content e.g., α-linolenic acid (C18:3, n-3) and positively with yellowness b^* and RSA DPPH. Oil from camelina seeds of *Śmiłowska* cultivar, which was characterized by the lowest content of α-linolenic acid and the highest b^* value of color and RSA DPPH, was the most thermally stable oil.

Keywords Camelina oil · Oxidative stability · Differential scanning calorimetry · Antioxidant activity · Oxidation induction time · OIT · DSC non-isothermal oxidation test · Oxidation kinetics

Introduction

Recent research concerning fats and oils with diverse compositional characteristics and usage suggested a revised approach toward the *Camelina Sativa* (L.) oil crop. This is due to its unique agronomic features, promising and sustainable oilseed quality and it is being a condensed source of nutritive fatty acids. In the literature, *Camelina Sativa* (L.) has been described mostly as an ancient crop, hence it has been highlighted by the same authors as a good source of edible vegetable oil, which for decades was neglected in industrial and commercial usage [1–5]. As early as 3000 years ago the cultivation of this crop was documented in Europe [6], and in his early study on camelina, Budin et al. [1] mentioned its cultivation in central Europe as an oil-bearing crop from 600 B.C. onwards. This annual flowering oilseed plant belongs to the *Cruciferae (Brassicaceae)* family, which appears in spring and winter varieties [2, 5–7]. Other names of camelina that have been mentioned are dodder oil, German sesame oil [8] or, false flax, gold of pleasure, Siberian oilseed or wild flax [7, 9]. This yellow flowering plant exhibits similarities with rapeseed plants' generic characteristics, since they belong to the same family, and is similar to flaxseed oils in terms of two highly enriched essential n-3 fatty acids (C18:3, α-linolenic acid). Although studies have suggested that this plant is indigenous to Central European plain, it was replaced by the initiation of rapeseed plants after the 1940s [2]. Therefore, interest of camelina oil was been renewed, which resulted from the urge to find new potential uses for this oil, such as e.g., biofuels,

✉ Jolanta Tomaszewska-Gras
jolanta.tomaszewska-gras@up.poznan.pl

[1] Department of Food Quality and Safety Management, Poznań University of Life Sciences, ul. Wojska Polskiego 31/33, 60-624 Poznań, Poland

[2] Department of Bioanalytics, Medical University of Lublin, ul. Jaczewskiego 8b, 20-090 Lublin, Poland

Published online: 13 May 2022

jet fuel, bio based-products, and feed [10]. Moreover, the following two beneficial features of this plant contribute to the growing interest in it. The first of these is its very favorable composition of fatty acids (high content of unsaturated fatty acids, about 90%), and the content of antioxidant compounds that affect high stability [1], 7, 11, 12. The second feature is the unique ability of camelina to adapt to various climatic and soil conditions [10]. Camelina is most often cultivated in poor and very poor soils, probably the least sensitive to soil water deficiency of all the plants in the *Brassicaceae* [13] family. With its being one of the richest vegetal sources of n-fatty acids, the nutritional values of camelina oil have been studied and evaluated by scientists in recent years. It has been shown that daily consumption of this oil brings remarkable health benefits, which include the prevention and treatment of hypertension, cardiovascular disease, obesity and controlling blood glucose levels, LDL (low-density lipoprotein) oxidation, neurological dysfunction [7, 14–16]. At the same time, apart from its utility in the formulation of functional foods, and in nutraceuticals, pharmaceuticals and cosmetics industries, the raw camelina plant has been reported by many authors as being used as an excellent source of biodiesel compared to canola and soybean biodiesels for its unique fatty acid composition and low energy requirements during its agro life cycle [5, 15–18]. However, the fatty acid composition of this oil depends on the cultivation conditions [14, 18, 19] or extraction methods [13, 20, 21]. Among the different extraction methods, cold pressing is now relatively popular due to its ability to retain the bioactive compounds in the oils, which is of great importance from the nutritional point of view [14]. Several studies have compared the stability of cold-pressed camelina oils with other oils, where it has been found to be more stable than flaxseed oil and less stable than others [22–24]. Among the many different thermal analyzes used for oils and fats [25], differential scanning calorimetry (DSC) is very popular for testing the thermo-oxidative stability of oils under isothermal and non-isothermal conditions. Oxidative stability is one of the crucial parameters determining oil quality. Most methods for testing oxidative stability are based on analyzing the oil at room temperature and many studies have been performed using camelina based on the traditional chemical methods (i.e., p-anisidine value, peroxide value and acid value determination) [4, 14, 22, 25, 26]. Due to the wide range of applications of camelina oil, it is also important to investigate the thermal oxidation stability of this oil by means of differential scanning calorimetry in various temperature conditions. There is little research on this topic in the literature, and existing studies are either incomplete [20, 22, 27] or concern the conditions of altered pressure (pressure differential scanning calorimetry, PDSC) [5, 6, 23], which do not reflect the actual conditions of using the oil at high temperatures. The novelty of these studies consists in the investigation of the properties of oxidative stability of camelina varieties originating from the Wielkopolska region in Poland, which have not been tested in this respect so far using the DSC technique. In this part of Poland, camelina oil had been a traditional product since the ancient time, which is now registered under the name "Olej rydzowy tradycyjny" as a Traditional Speciality Guaranteed product in the European Union and the United Kingdom. Hence, the objective of this study was to determine the comprehensive characteristics of the thermo-oxidative stability of cold-pressed camelina oils procured from five different suppliers in Poland, and of various cultivars. The DSC isothermal and non-isothermal experiments in various conditions were performed and the oxidation kinetic parameters were calculated and compared with the results of peroxide value, p-anisidine value, acid value, RSA DPPH, color and fatty acids composition.

Experimental

Materials

Three cultivars of *Camelina Sativa* L. seeds were collected during 2019 from Greater Poland region in Poland from different suppliers i.e., SEMCO manufactory (Śmiłowo, Poland) and Poznan University of Life Sciences (Dłoń 4, Miejska Górka). Total five oils samples were investigated from three cultivars, i.e., *Omega* -spring variety (CA OM), *Luna* -winter variety (CA LUA, CA LUB) *and Śmiłowska* -spring variety (CA SMA, CA SMB). *Luna* and *Śmiłowska* cultivars were obtained from two suppliers of seeds (A and B). These seeds were cold-pressed at a temperature below 50 °C. After pressing, the oils were decanted for 24 h. During subsequent laboratory storage, they were kept at freezing temperature at − 80 °C in brown glass bottles.

Fatty acid composition

To determine the fatty acid composition of the camelina seed oils, gas chromatography-Flame Ionization Detector (GC-FID) was employed. All the samples were analyzed in two replications. Two drops of fat were dissolved in 1 mL of hexane (for HPLC, Sigma Aldrich). 1 mL of 0.4 N sodium methoxide was added. The samples were stirred and left for 15 min, then 5 mL of distilled water was added and the top layer was taken off. By following the AOCS official method [29], fatty acid methyl esters were analyzed using a Trace 1300 chromatograph (Thermo Fisher Scientific, Waltham, Massachusetts, USA). Separation was performed on a Supelcowax 10 capillary column (30 m × 0.2 mm × 0.2 µm), and injection was performed in split less mode. The sample volume was 1 µL. Hydrogen was used as the carrier gas. The

initial furnace temperature was 160 °C, and was increased from 12 °C min^{-1} to 220 °C. The temperature of 220 °C was maintained for 20 min. Fatty acid methyl esters were identified on the basis of comparing the retention times in the sample and in the 37-Component FAME Mix (Supelco).

Color measurement

Color measurements of oils were carried out using the Konica Minolta CM-5 spectrophotometer and SpectraMagicNx software. The instrument was calibrated prior to starting the analysis transmission chamber, which can accurately measure both translucent and transparent liquid samples using a CM-A213 zero calibration plate (black calibration) followed by distilled water in a 10 mm CM-A98 glass cuvette (white calibration). The research was conducted using the Hunter Lab scale. Parameter L* was in the range from 0 to 100, and denoted the lightness of the color black to white. Similarly, the a* parameter, depending on the range, was determined by a green (below 0) and red (above 0) tinge and the b* parameter, which in the case of negative values defined the color blue, but in the case of positive values, this was yellow. The samples used were analyzed in three replications.

Determination of oxidative stability by DSC

Oxidative stability was determined by following the ISO 11357-1 [30], and also implementing the ASTM D3895-14 [31]. Oil samples were analyzed in DSC 7 Perkin Elmer along with an Intracooler II, operated with Pyris software. Both isothermal and non-isothermal protocol was followed to determine the oxidative stability characteristics of the oils. The instrument was calibrated using indium (m.p. 156.6 °C, $\Delta H_f = 28.45$ J g^{-1}) and n-dodecane (m.p. − 9.65 °C, $\Delta H_f = 216.73$ J g^{-1}), while 99.99% pure nitrogen gas was used as the purge gas. Oils samples of approximately 6–7 mg were weighed into open aluminum pans of 50 µL (Perkin Elmer, No. 02190041) and placed in the equipment's sample chamber. The reference was the same open and empty aluminum pan. For the isothermal program, temperature of 120, 140 and 160 °C was maintained with a constant oxygen flow of 20 mL min^{-1} (purity 99.995%). Based on the obtained curves, parameters denoted as oxidation induction time (OIT), oxidation end time (OET), length of oxidation Δt = OET-OIT, and rate of oxidation were determined. Determination of OIT was done after normalization of oxidation DSC curve, as the intersection of the extrapolated baseline and the tangent line to the descending exotherm, while OET value was measured at the minimum value of the heat flow of the exotherm, which expresses the end of the propagation and beginning of the termination stage of oxidation.

The oxidation rate was calculated according to the following equation:

$$\text{oxidation rate} = (Y1 - Y2)/\Delta t \quad (1)$$

where *Y1*—heat flow at OIT point [W g^{-1}], *Y2*—heat flow at OET [W g^{-1}], Δt—length of oxidation [min].

The non-isothermal analyzes were carried out by applying the heating rate of 1, 2, 5, 10 and 15 °C min^{-1}, maintaining the oxygen flow 20 mL min^{-1}. From the oxidation curves the onset temperature (T_{on}) and the end temperature (T_{end}) were calculated. The value of T_{on} was the onset temperature determined as the intersection of the extrapolated baseline and the tangent line to the descending curve of the recorded exotherm, whilst, T_{end} was measured as the temperature at the minimum value of the heat flow, which represents the end of the propagation and start of the termination stage. Oils samples were analyzed in two replications for all DSC experiments.

Chemical determination of oxidative stability

Measurement of p-anisidine value (pAV) as a measure of the level of secondary oxidative products was carried out according to ISO 6885:2016 [32]. Spectrophotometric measurements were taken with a quartz cuvette with a 10 mm optical path length. Peroxide value (PV) was determined by following the ISO 3960:2007 procedure [33]. The total oxidation value (TOTOX) parameter was calculated based on the pAV and PV values by the following formula TOTOX = pAV + 2PV, expressing the overall rate of oil oxidation. Acid value (AV), as an indicator of the degree of hydrolytic changes, was measured according to the official AOCS method [34]. All chemical analyzes were done in three replications.

Radical scavenging activity by DPPH (RSA DPPH)

The DDPH (2,2-diphenyl-1-pikrylhydrazyl) method was used to evaluate the antioxidant activity of the oils. The method is based on the ability of the oil to scavenge the DPPH$^{\bullet}$ radicals (0.04 mM). In brief, 10 µL of the oil was added to 990 µL of DPPH$^{\bullet}$ radical in ethyl acetate (0.04 mM) and mixed. The mixture was incubated for one hour in the dark at ambient temperature. Then, the spectrophotometric measurements at 517 nm were performed with a Varian Cary 1E (Berlose, Australia) using ethyl acetate as a blanc. Results are expressed as Trolox equivalents (TE) in mmol L^{-1}. A Trolox calibration curve in the range from 0 to 15 µM was prepared with a slope of 5.3668. All oils were analyzed in two replications.

Statistical analysis of results

The results were presented in the form of mean and standard deviation. The first stage in the statistical analysis consisted in verifying variance homogeneity using the Hartley-Cochran-Bartlett test. In the case of variance homogeneity, one-way analysis of variance (ANOVA) was used and Tukey's test was applied to create statistically homogeneous groups. In turn, when variances were not homogeneous, non-parametric tests were used, i.e., ANOVA and the Kruskal–Wallis rank test. Additionally, principle component analysis (PCA) was performed to show the relationships between variables and detect some patterns between variables and objects. The analysis also enables the dataset to be reduced from a higher to a lower dimensional level. Statistical analysis of recorded results was performed using Statistica 13.3 software (TIBCO Software Inc. USA) at a significance level of $\alpha = 0.05$.

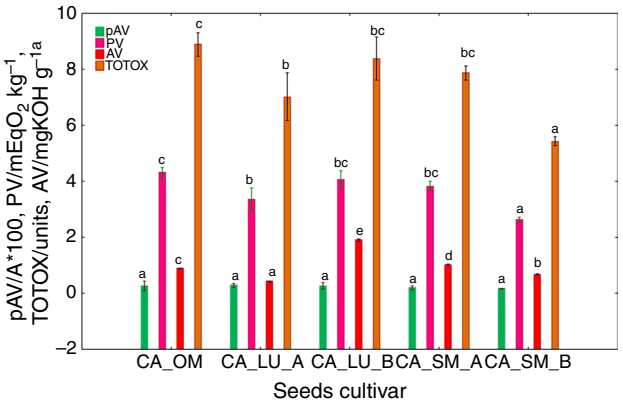

Fig. 1 Oxidative stability parameters of cold-pressed camelina seed oils: peroxide value (PV), p-anisidine value (pAV), total oxidation value (TOTOX) and acid value (AV). Different superscript letters (a, b, c, d) indicate significant differences between oils ($p \leq 0.05$). Camelina seed oils: CA OM (*Omega* cultivar), CA SMA, CA SMB (*Śmiłowska* cultivar) CA LUA, CA LUB (*Luna* cultivar). Vertical bars denote standard deviation

Results

Chemical characteristics of cold-pressed camelina oils

Fatty acid (FA) composition analysis is one of the most important for the characterization of edible oils. The FA profile of cold-pressed camelina seed oils is presented in Table 1, which shows its very high content of unsaturated fatty acids (UFA), around 90%, and low content of saturated fatty acids (SFA), varying between 8.73% to 10.36% for different cultivars. These results are in a similar range to those obtained by other authors [18, 23]. Among the UFAs, α-linolenic acid, C18:3, *n*-3 (ALA) showed prepotent presence, around 30–37%, which is consistent with other studies [5, 11, 28]. The highest amount of ALA (37.17%) was determined in the *Omega* cultivar. Similar content of ALA (36.88%) in this cultivar was also found by Kurasiak-Popowska et al. [30]. The next most abundant UFAs were linoleic acid, C18:2 (LA), ranging from 15.31 to 20.97% and oleic acid, C18:1 (15.16–18.29%). Comparing camelina cultivars, *Śmiłowska* had the highest content of LA, while other authors reported lower or a similar content of LA, for example, 16.1–18.6% was mentioned by Hrastar et al. [29], and 18.5% by Berti et al. [10]. Among the other unsaturated fatty acids, the eicosenoic acid C20:1 was found in a range from 13.26 to 15.83%, which is a specific fatty acid for camelina oil. At a relatively low level, the saturated fatty acids (SFA) were detected: palmitic acid, C16:0 with around 5% and stearic acid, C18:0 with around 2%. Another important parameter calculated from the results of FA composition is the ratio of fatty acids n-3 to n-6. In our study, it was found to be within the range from 1.4 to 2.4, where Ratusz et al. [6] reported the ratio in the range from 1.79 to 2.17. Figure 1 shows the results of peroxide (PV), p-anisidine (pAV), acid (AV) and TOTOX values determination in camelina oils. These chemical analyses confirmed the good quality of the freshly pressed camelina oil samples. As the oil samples are fresh, the pAV is expected to be low, since there was not enough time to form secondary oxidation products in the oil. For the camelina oil varieties, pAV ranged from 0.20 to 0.28, which is comparatively lower than the values obtained by Ratusz et al. [6] (0.22–1.48) and Symoniuk et al. [24] (0.45–0.67). Similarly, the peroxide values for all camelina cultivars did not exceed the required limits by the Codex Alimentarius standards [31], which states that the values for PV cannot be higher than 15 meq O_2kg^{-1}. All the camelina oil varieties were quite consistent with the PV value and ranged from 2.63 to 4.31, which is a slightly higher range than that obtained by Ratusz et al. [6] (0.89–3.49 meq O_2kg^{-1}), Ratusz et al. [5] (0.79–2.04 meq O_2kg^{-1}) and Symoniuk et al. [24] (2.37–3.00 meq O_2kg^{-1}). On the other hand, Raczyk et al. [23] obtained a similar range (1.20 to 4.88 meq O_2kg^{-1}), and Hrastar et al. [29] obtained an even higher range by experimenting with oils from different growing seasons (0.74 to 8.85 meq O_2kg^{-1}). For this experiment, though all the oils PV values were relatively low, the SM B variety had the lowest value (2.63 meq O_2 kg^{-1}) and the highest was for the *Omega* (CA OM) variety (4.31 meq O_2 kg^{-1}). The next measured parameter was the acid value (AV), ranging from 0.4 to 1.90 mg KOH kg^{-1}, which obviously indicates the low content of free acids in the oil, as they were freshly pressed. These values are similar to those obtained by Raczyk et al. [23] (0.53–0.89 mg KOH kg^{-1}). Among the oils, LU A had the lowest value at 0.43 and LU B had the highest value at

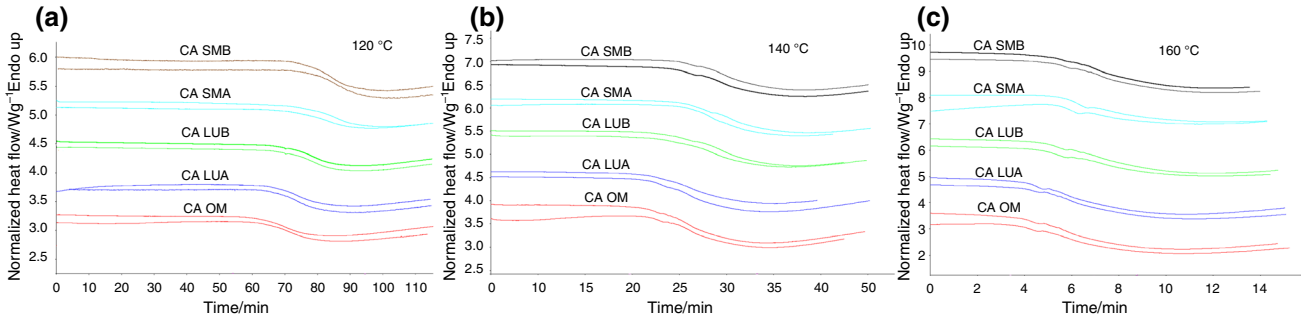

Fig. 2 DSC isothermal oxidation curves obtained at 120 °C (**A**), 140 °C (**B**), 160 °C (**C**) for cold-pressed camelina oils

1.90 mg KOH kg^{-1}. The total oxidation state (TOTOX) of these oils was also calculated and the range of values differed significantly between the varieties, ranging from 5.43 to 8.89. An almost similar range was obtained by Ratusz et al. [6] (2.40–7.83). Another study revealed values from 3.38 to 10.22 [23], and Symoniuk et al. [24] obtained results from 5.28 to 6.45. Among the varieties investigated in this study, the OM variety exhibited the highest TOTOX value (8.89) and the SM B variety the lowest (5.43).

DSC isothermal and non-isothermal thermo-oxidative stability of camelina oil

The thermo-oxidative stability of camelina oil was measured by means of the DSC technique in isothermal and non-isothermal (dynamic) mode. Figure 2 shows the curves for all camelina varieties obtained by isothermal oxidation at 120 °C (A), 140 °C (B), 160 °C (C). It can be seen that the higher the temperature, the faster the oxidation process, the start point of which is marked as the intersection of the baseline with the tangent to the descending curve (OIT). Figure 3 shows four graphs of oxidation parameters, calculated from the DSC curves: OIT (A), OET (B), the length of oxidation (C) and rate of oxidation (D). Oxidation induction time (OIT) is a parameter that shows the starting point of oxidation. Generally, for all camelina varieties, the OIT ranged between 61.38 and 76.20 min for 120 °C, between 17.02 and 20.67 min for 140 °C and between 4.48 and 5.87 min for 160 °C. This experiment revealed that for all temperatures (120, 140, 160 °C) the *Śmiłowska* variety turned out to be the most stable, as the highest OIT values were recorded for it. It also shows that for the OM and LU A varieties, the OIT values were the lowest, so they oxidized in the shortest time. Most of the research on the oxidative stability of camelina done by isothermal DSC was carried out under increased pressure, otherwise known as PDSC. In those conditions, lower oxidation induction times (OIT) were always recorded than in the case of DSC analysis under normal pressure. In the literature, only data on the stability of camelina oil pressed from roasted and unroasted seeds of unknown cultivars were found, which was done using the DSC technique under normal pressure. Różańska et al. [28] found as 8.96 min for unroasted seeds and 8.70 min for roasted seeds for spring camelina (SC) cultivation for 140 °C OIT values, while for winter camelina (WC) the OIT values were 7.79 min (unroasted seeds) and 9.98 min (roasted seeds). Oxidation end time (OET) parameter was also measured (Fig. 3B), which expresses the end of the propagation and beginning of the termination stage of oxidation. Data shows that for all isothermal conditions (120 °C, 140 °C and 160 °C), the lowest OET was recorded for the *Omega* variety and the highest for the *Śmiłowska* (SM B) variety, which corresponded with the OIT values. As it can be seen in Fig. 3B, for the temperature of 120 °C, the OET range was between 85.77 and 101.41 min, for 140 °C it was between 29.75 and 33.69 min, and for 160 °C between 10.36 and 12.34 min. However, Różańska et al. [28] also reported the OET for SC as 18.58 min (roasted) and 22.74 min (unroasted), in turn for WC as 14.96 min (roasted) and 17.94 min (unroasted) in a 140 °C temperature program. Ratusz et al. [5] tested samples of camelina oil obtained from the local market using the PDSC technique and several temperature programs were adopted (i.e., 90, 100, 110, 120, 130 °C) for studying oxidative stability, where for 130 °C values of OET were found between 14.08 and 16.83 min. In another experiment, Ratusz et al. [6] used the PDSC technique with 100 °C isothermal measurement, where the OET values ranged between 146.7 to 165.2 min. On the other hand, Symoniuk et al. [24] presented results obtained at 120 °C temperature using the PDSC technique for camelina oils, where the OET values were shown between 17 and 28 min. In a study of thermo-oxidative properties, along with OIT and OET parameters, the length of oxidation (Δt) parameter was calculated as a difference (Δt = OET-OIT) and presented in Fig. 3C. The values obtained for this parameter show that the lower the isothermal temperature, the longer the length of oxidation, as at 160 °C it was in the range of 5 to 6 min, at 140 °C between 12 to 13 min and at 120 °C, the range of Δt was between 22 to 27 min for different varieties. However, no significant differences ($p > 0.05$) were observed between

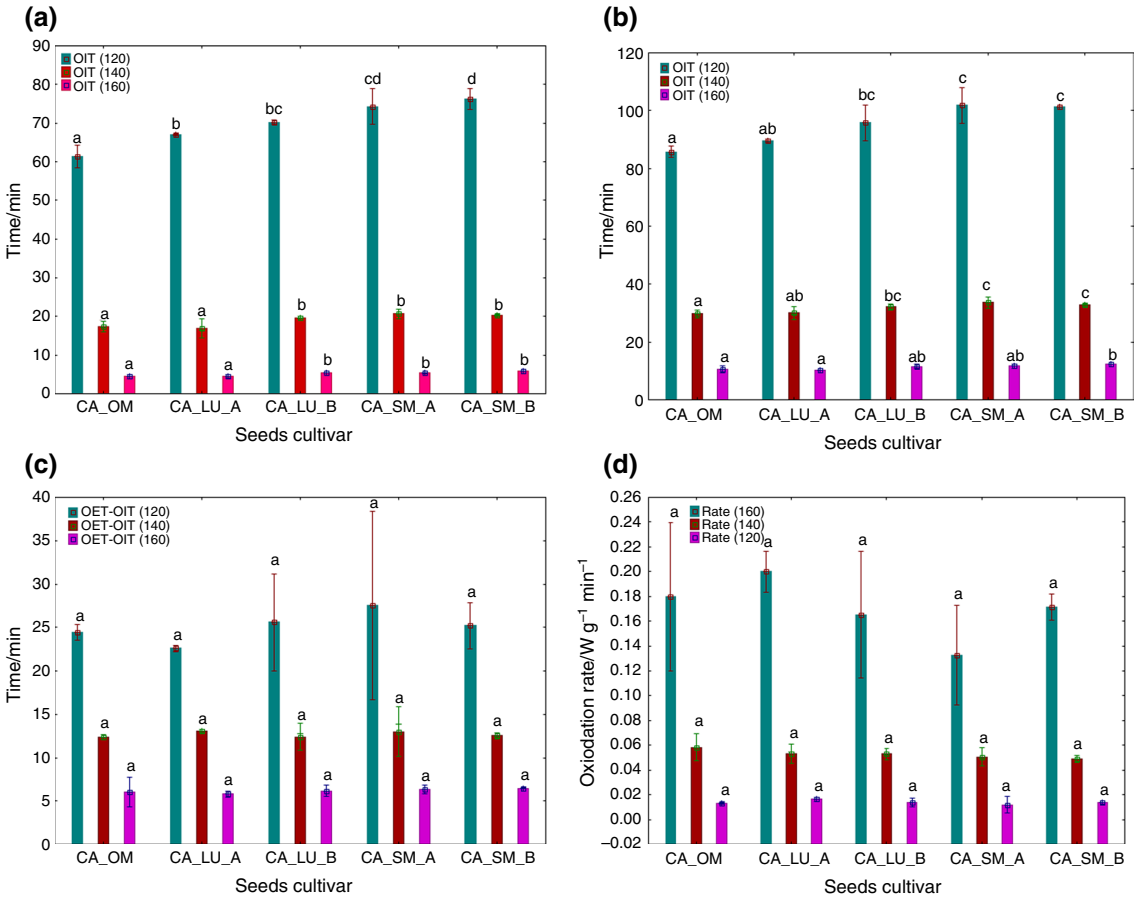

Fig. 3 Oxidative stability parameters of cold-pressed camelina oils determined isothermally by DSC at 120, 140, 160 °C: oxidation induction time (OIT) (**A**), oxidation end time (OET) (**B**), the oxidation length (Δt) (**C**), rate of oxidation (**D**). Different superscript letters (a, b, c, d) indicate significant differences between oils ($p \leq 0.05$). Camelina seed oils: CA OM (*Omega* cultivar), CA SMA, CA SMB (*Śmiłowska* cultivar) CA LUA, CA LUB (*Luna* cultivar). Vertical bars denote standard deviation

varieties. Unlike these results, Różańska et al. [28] established Δt for roasted camelina seeds oils as 4.98 min (WC) and 9.88 min (SC), and unroasted samples as 10.15 min (WC) and 13.78 min (SC) at 140 °C with statistically significant differences ($p \leq 0.05$). A study of the rate of oxidation was also presented in this study (Fig. 3D), which was calculated according to Eq. (1). By comparing the data for different temperature programs, oils analyzed at 140 °C were oxidized at a four times higher rate than at 120 °C. However, in the 160 °C program, the rate was also three to four times higher than in the 140 °C program. It is worth mentioning that among all the varieties, *Luna* (LU A) variety oxidized at a higher rate than any other varieties, however differences were not statistically significant. A comparative study for cold-pressed flaxseed oils was published by Tomaszewska-Gras et al. [32], where at 140 °C the oxidation rate was three times higher than at 120 °C for all varieties of flaxseed oils. Figure 4 shows the relationship between the DSC parameters measured (OIT, OET, Δt, oxidation rate) and the temperatures used for the analysis (120, 140, 160 °C). In Fig. 4A, the data fitted to the exponential function are shown for OIT, OET and Δt with high coefficient of determination of $R^2 = 0.99$, and in Fig. 4B fitting of oxidation rate curve to the exponential function with $R^2 = 0.96$. Equations are presented as they can be used for predicting the oxidation start point in different thermal conditions.

For comprehensive characteristics of thermo-oxidative stability measurements, analysis in non-isothermal (dynamic) mode was carried out at different heating rates i.e., 1, 2, 5, 10, 15 °Cmin^{-1} by means of DSC In Fig. 5 selected curves for 2, 5, 10 °Cmin^{-1} are presented. Two parameters were determined from the curves: the onset temperature (T_{on}), corresponding to the beginning of oxidation and the end temperature (T_{end}), which represents the end of the propagation stage and beginning of the termination stage, at which stable products are formed. On the basis of the obtained non-isothermal curves, it can be observed that the oxidation process proceeded in two different ways: for heating rate of 1, 2, 5 °C min^{-1} and for 10 and 15 °C min^{-1}. Differences can be noticed in the region of the curves around the minimum value of heat flow after the

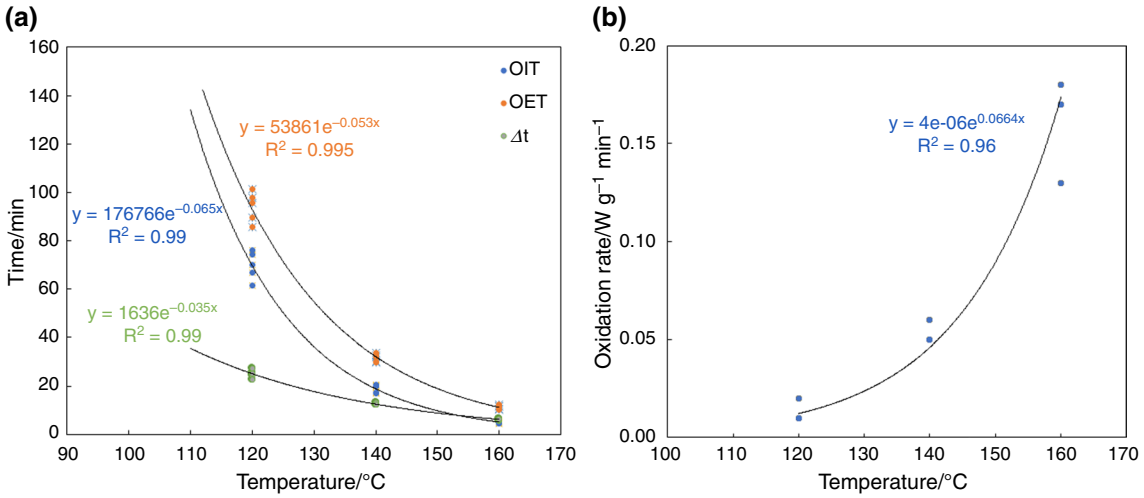

Fig. 4 Relationship between temperature and parameters of isothermal DSC measurements: OIT, OET, oxidation duration Δt **A** and rate of oxidation **B**

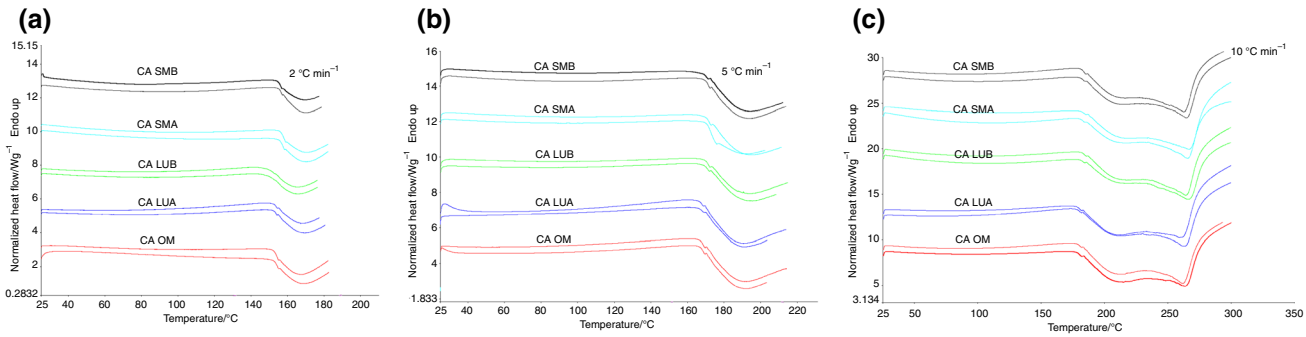

Fig. 5 DSC non-isothermal oxidation curves obtained at scanning rate: 2 °C min^{-1} (**A**), 5 °C min^{-1} (**B**), 10 °C min^{-1} (**C**) for cold-pressed camelina seed oils

decrease in exotherm i.e., T_{end}. For scanning rate 1, 2, 5 °C min^{-1} after reaching the T_{end} point, the curve rises sharply, while for scanning rate 10 and 15 °C min^{-1}, before reaching the T_{end} point, it can be observed that there is a plateau after the exotherm drop. Generally, it can be seen that as the heating rate increases, the temperature at which curves go downwards (T_{on}) also increases. In Fig. 6A, data obtained for the T_{on} parameter can be compared for the scanning rates 1, 2, 5, 10 and 15 °$Cmin^{-1}$. For various camelina oil cultivars, the T_{on} occurred at different ranges of temperatures upon exposure to various heating rates. In brief, data for scanning rate 1 °C min^{-1} shows that T_{on} was lowest for OM sample (139.64 °C) and highest for SM B sample (143.65 °C) and for 2 °C min^{-1}, T_{on} ranged between 152.14 °C for OM and 155.88 °C for the SM A. Temperature resistance increased for the 5 °$Cmin^{-1}$ scanning rate, where the range changed between 165.57 °C (LU A) and 169.98 °C (SM A) and for scanning rates 10 °$Cmin^{-1}$, 176.95 °C (LU A) and 181.31 °C (SM A). Whilst, for scanning rate 15 °$Cmin^{-1}$, temperature ranged from 183.01°C (OM) to 187.71 °C (SM A). However, for all the scanning rates (1, 2, 5, 10 and 15 °C min^{-1}) the differences between mean values of T_{on} were significant ($p \leq 0.05$) for the different varieties. Summarizing the results for all heating rates, the *Omega* and *Luna* (LU A) variety showed less stability, as the T_{on} values were lowest, and the *Śmiłowska* variety exhibited the highest stability with high T_{on} values. Values of temperatures measured at the T_{end} point are presented in Fig. 6B for different scanning rates. Observations from the dataset show no statistically significant differences between the varieties ($p > 0.05$), except for the scanning rate 1 °C min^{-1}, for which T_{end} values ranged from 152.25 °C to 155.46 °C and differed significantly between varieties ($p \leq 0.05$). In Fig. 7 logarithmic relationship is shown between scanning rate and parameters of T_{on} and T_{end}. It can be seen that with an increase in scanning rate, the thermal resistance of oils to oxidation increases, which can be expressed logarithmically with coefficient of determination of $R^2 = 0.99$ (T_{on}) and

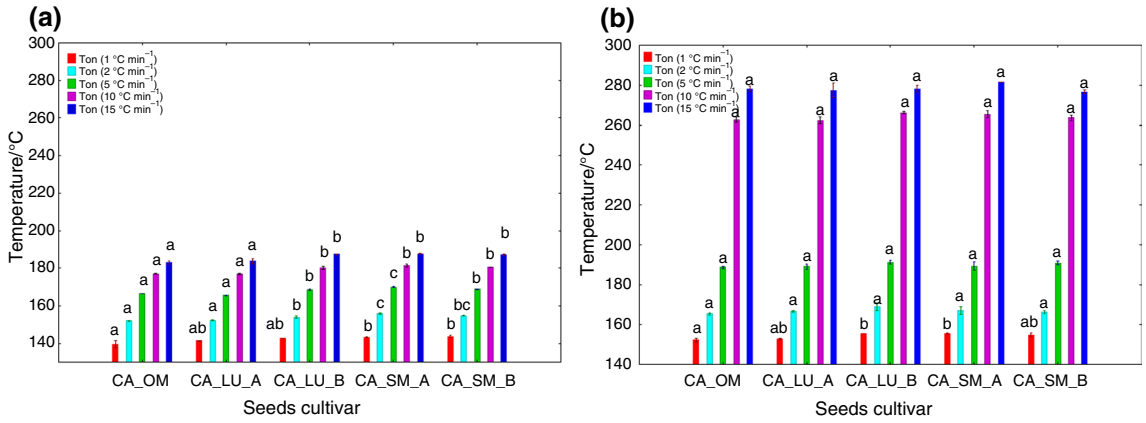

Fig. 6 Oxidative stability parameters: T_{on} **A** and T_{end} **B** of cold-pressed camelina oils determined non-isothermally by DSC at a scanning rate of T_{end} (1 °C min^{-1}) T_{end} (2 °C min^{-1}) T_{end} (5 °C min^{-1}) T_{end} (10 °C min^{-1}) and T_{end} (15 °C min^{-1}). Different superscript letters (a, b, c, d) indicate significant differences between cultivars ($p < 0.05$). Camelina seed oils: CA OM (*Omega* cultivar), CA SMA, CA SMB (*Śmiłowska* cultivar) CA LUA, CA LUB (*Luna* cultivar). Vertical bars denote standard deviation.

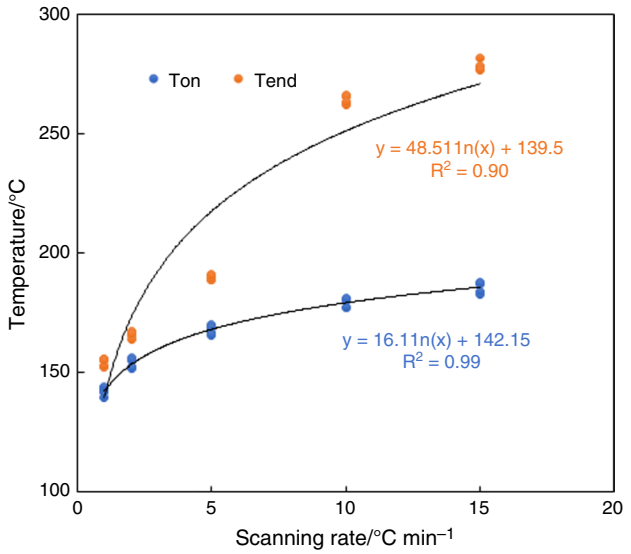

Fig. 7 Relationship between DSC parameters of non-isothermal measurements (T_{on}, T_{end}) and scanning rate (1, 2, 5, 10 and 15 °C min^{-1})

$R^2 = 0.90$ (T_{end}). The equations presented in the figure can be used for predicting the temperatures of oxidation at various scanning rates.

Discussion

Kinetics oxidation analysis

The results of DSC isothermal and non-isothermal measurements show that there are differences in oxidative stability depending on the variety and conditions of analysis i.e., temperature in isothermal DSC and scanning rate in non-isothermal DSC. In order to summarize the DSC results for different cultivars, kinetic analysis was carried out, the results of which are listed in Table 2.

Results obtained during the DSC experiments are recognized as a first order reaction, which resembles those of other studies [33–35]. To carry out the calculation, data was analyzed by following the Ozawa-Flynn-Wall method [36] adapted by other authors [5, 33, 37, 38]. To calculate activation energy E_a, first inversed values of onset temperature (T_{on}) expressed in Kelvin were plotted against scanning rates (β) of 1, 2, 5, 10 and 15 °C min^{-1}, expressed as log β. The value of the slope from the plot $\log\beta = f(T^{-1})$ for all varieties of camelina oils was calculated, since they are needed for further calculation of the activation energy (E_a, kJ mol^{-1}).

$$\log \beta = a\frac{1}{T} + b \tag{2}$$

where β is the heating rate (K min^{-1}), T is the onset temperature (K).

Activation energy, E_a was calculated from Eqs. (3):

$$Ea = -2.19R\frac{\mathrm{d}\log\beta}{\mathrm{d}T^{-1}} \tag{3}$$

and pre-exponential factor Z (min^{-1}) was calculated from the following equation

$$Z = \frac{\beta * Ea * \mathrm{e}\left(\frac{Ea}{RT}\right)}{RT^2} \tag{4}$$

After this, Z values was used for calculation of reaction rate constant (k, min^{-1}):

$$k = Ze^{\left(\frac{-Ea}{RT}\right)} \quad (5)$$

Additionally the half-life time ($t_{1/2}$) was calculated from the equation:

$$t_{1/2} = \frac{\ln 2}{k} \quad (6)$$

where R is the universal gas constant (8.31 J mol^{-1}). By plotting the values, it was possible to compute the activation energy (E_a, kJ mol^{-1}), reaction rate constant, (k, min^{-1}), pre-exponential factor (Z, min^{-1}), and half-life time as ($t_{1/2}$, min).

By considering the data obtained in Table 2, the values of activation energy E_a ranged from 96.49 kJ mol^{-1} (CA LU A) to 92.17 kJ mol^{-1} (CA LU B), respectively. The values descended in the following order CA LU A > CA SM B > CA SM A > CA OM > CA LU B. Coherently, the pre-exponential factor (Z) followed approximately the same order, as the CA LU A showed the highest Z value 9.65×10^{10}, while for the CA LU B it was 2.30×10^{10}. In Table 2 it has been shown that, there were no significant differences ($p > 0.05$) between the camelina oils varieties concerning the activation energy values. Similar results of E_a for camelina oil were obtained by other authors, ranging between 91.9 and 122 kJ mol^{-1} for camelina oil extracted by different methods [21], or between 87.63 and 93.61 kJ mol^{-1} for six different commercial camelina oils [5]. The results of E_a obtained by Adhvaryu et al. [39] ranged from 63 to 88 kJ mol^{-1} for different unmodified vegetable oils, such as cottonseed, corn, canola, sunflower oil, soybean oil and genetically modified high oleic sunflower and high oleic safflower oils. Adhvaryu et al. [33] suggested that the PUFA and SFA content does not fully explain the variation in E_a values or the other kinetic behaviors. Baokun et al. [37] showed that the SFA rich refined palm oil exhibited a noticeably high E_a value (134.7 kJ mol^{-1}), while PUFA rich safflower oil showed a lower E_a value (86.05 kJ mol^{-1}) for all experimented scanning rates at 5, 7.5, 10, 12.5, and 15 °C min^{-1}. Besides activation energy, it is recommended to evaluate the oxidative stability of the oils based on the other kinetic parameters. The values of the oxidation rate constant (k) and half-life time as ($t_{1/2}$) were also taken into consideration, as these parameters enable the thermal behavior of the oils in other thermal conditions to be predicted. In Table 2 the k values are presented for different camelina varieties calculated for the temperature of 441 K. The rate constant ranged from 0.25 min^{-1} for the *Śmiłowsk*a cultivar (CA SM A) to 0.35 min^{-1} for *Luna* cultivar (CA LU A). Statistically, rate constant k did not differ significantly for samples CA LUB, CA SMA, CA SMB ($p > 0.05$), while for the samples OM and CA LUA mean values were significantly different ($p \leq 0.05$). Similarly, the half-life time ($t_{1/2}$) values were lower for the low stable oils (CA OM and CA LUA), and higher for the more stable varieties (CA LU B, CA SM A, CA SM B). Table 2 shows that, all the oil varieties were showing significant differences ($p \leq 0.05$) regarding half-life time ($t_{1/2}$). The values of the k constant correspond well with the rate of oxidation calculated for the isothermal test, which are shown in Fig. 3D, where it can be seen that the same three samples of camelina oil (CA LU B, CA SM A, CA SM B) were characterized by the lowest values. In other study the reaction rate constant k of camelina oils, measured at a scanning rate from 2.5 to 15 °C min^{-1}, was reported between 0.19 and 0.41 min^{-1} [21]. Since the oxidation kinetic parameters presented in Table 2 show differences between the camelina cultivars, analysis of correlations between all the oxidation parameters and fatty acid composition was carried out (Table 3). As can be seen in Table 3, significant positive correlation coefficients were found between saturated and unsaturated fatty acids (C16:0, C18:0, C18:1, C18:2) and DSC oxidation parameters. In turn, between two unsaturated fatty acids (C20:1, C18:3, n-3) and DSC oxidation parameters a negative correlation was established, the higher the content of unsaturated fatty acids, the lower the OIT and T_{on} values and the lower the oxidative stability of the oils. Similarly, high positive correlation coefficients were found between those fatty acids (C20:1, C18:3, n-3) and oxidation rate constant k, so the higher content of unsaturated FA, the faster the oxidation reaction. It has also been proved in other studies that the oxidative properties of camelina oils rely on upon the MUFA and PUFA contents [5, 6, 23, 24, 27]. However, the question may arise as to whether differences between oxidative stability can only be explained by the fatty acid composition. The explanation for the differences in oxidative stability could also be found in the antioxidant activity of different camelina cultivars. In Table 4, the results of the RSA DPPH analysis and color measurement are presented. Color measurement can indicate the content of compounds responsible for the color of camelina oil like carotenoids, which are compounds of antioxidant activity. Color measurement was expressed as L^*, a^* *and* b^*, for which significant differences ($p \leq 0.05$) between the varieties were determined. The lowest values of L^*, representing the lightness of oil, were measured in sample CA SM B and the highest in sample CA OM. For three samples (CA LU B, CA SM A, CA SM B) very high values of b^* were observed, representing the yellowness of the oils. Among all the oils, the sample CA LU B had the highest b^* value (96.07), which can indicate the highest carotenoid content. This result can be compared with the study done by Itle et al. [39], where they found high correlation between b^* value with lutein carotenoid ($r = 0.87$), and also total carotenoids ($r = 0.75$). Another study has confirmed the presence of noticeable lutein content in *Luna* varieties of camelina oil as 9.35 mg L^{-1} [30]. Comparing to the results of the antioxidant activity RSA DPPH, shown

Table 1 Fatty acid composition expressed as a percentage of total fatty acid (%) for various cultivars of camelina seed oils

Fatty acids	Camelina cultivar				
	CA LUA	CA LUB	CA OM	CA SMA	CA SMB
FFA (%)	$0.45^{c} \pm 0.01$	$0.22^{a} \pm 0.01$	$0.95^{e} \pm 0.02$	$0.51^{d} \pm 0.01$	$0.34^{b} \pm 0.01$
C16:0	$5.01^{b} \pm 0.0$	$5.37^{c} \pm 0.04$	$4.61^{a} \pm 0.01$	$5.78^{d} \pm 0.01$	$5.78^{d} \pm 0.04$
C18:0	$1.93^{a} \pm 0.01$	$2.50^{e} \pm 0.01$	$2.16^{b} \pm 0.04$	$2.36^{d} \pm 0.00$	$2.33^{c} \pm 0.01$
C18:1	$15.16^{a} \pm 0.03$	$18.29^{d} \pm 0.00$	$16.19^{b} \pm 0.00$	$17.45^{c} \pm 0.02$	$17.50^{c} \pm 0.00$
C18:2	$18.85^{b} \pm 0.13$	$20.97^{d} \pm 0.06$	$15.31^{a} \pm 0.01$	$20.76^{c} \pm 0.06$	$20.45^{c} \pm 0.01$
C18:3, n-6	$0.14^{a} \pm 0.01$	$0.17^{a} \pm 0.04$	$0.14^{a} \pm 0.01$	$0.13^{a} \pm 0.00$	$0.14^{a} \pm 0.01$
C18:3, n-3	$34.39^{d} \pm 0.05$	$30.25^{a} \pm 0.09$	$37.17^{e} \pm 0.05$	$30.84^{b} \pm 0.01$	$32.51^{c} \pm 0.01$
C20:0	$1.37^{a} \pm 0.00$	$1.61^{bc} \pm 0.04$	$1.44^{ab} \pm 0.06$	$1.62^{c} \pm 0.00$	$1.54^{abc} \pm 0.07$
C20:1	$15.49^{d} \pm 0.12$	$14.33^{c} \pm 0.01$	$15.83^{a} \pm 0.01$	$14.02^{b} \pm 0.06$	$13.26^{a} \pm 0.00$
C20:2	$2.03^{c} \pm 0.03$	$1.56^{ab} \pm 0.01$	$1.52^{a} \pm 0.01$	$1.56^{ab} \pm 0.01$	$1.62^{b} \pm 0.02$
C20:3	$1.35^{c} \pm 0.01$	$0.94^{a} \pm 0.02$	$1.30^{c} \pm 0.01$	$0.97^{a} \pm 0.00$	$1.06^{b} \pm 0.02$
C22:0	$0.30^{a} \pm 0.01$	$0.36^{bc} \pm 0.01$	$0.34^{b} \pm 0.01$	$0.12^{a} \pm 0.01$	$0.35^{bc} \pm 0.00$
C22:1	$3.42^{c} \pm 0.06$	$3.01^{b} \pm 0.04$	$3.39^{c} \pm 0.01$	$3.42^{c} \pm 0.04$	$2.77^{a} \pm 0.00$
C22:2	$0.23^{b} \pm 0.01$	$0.18^{a} \pm 0.00$	$0.18^{a} \pm 0.01$	$0.21^{ab} \pm 0.01$	$0.20^{ab} \pm 0.02$
C24:0	$0.13^{a} \pm 0.00$	$0.22^{b} \pm 0.01$	$0.24^{b} \pm 0.01$	$0.22^{b} \pm 0.00$	$0.22^{b} \pm 0.01$
ΣSFA	8.73	10.06	8.77	10.36	10.22
ΣMUFA	34.07	36.63	35.41	34.88	33.53
ΣPUFA	56.97	54.05	55.60	54.46	55.96
n-3/n-6	1.8	1.4	2.4	1.5	1.6
UFA/SFA	10.4	8.9	10.4	8.6	8.8

All values are mean ± standard deviation of two measurements ($n=2$), $^{(abcde)}$ means with the same superscript within the raw are not different ($p>0.05$). ΣSFA—total of saturated fatty acid. ΣMUFA—total of monounsaturated fatty acid. ΣPUFA—total of polyunsaturated fatty acid. UFA/SFA—ratio of total of unsaturated fatty acid to total of saturated fatty acid. CA OM (*Omega* Cultivar), CA LUA and CA LUB (*Luna* Cultivar) and CA SMA and CA SMB (*Śmiłowska* Cultivar)

Table 2 Kinetic parameters for non-isothermal DSC oxidation test of cold-pressed camelina oil

Camelina Cultivar	Kinetic parameters				
	E_a /kJ mol^{-1}	Z/min^{-1}	k /min^{-1}	$t_{1/2}$ /min	R^2
CA OM	93.30 ± 2.65^{a}	4.01×10^{10}	0.31 ± 0.01^{b}	2.21 ± 0.07^{b}	0.9952
CA LUA	96.49 ± 1.38^{a}	9.65×10^{10}	0.35 ± 0.01^{c}	2.00 ± 0.05^{a}	0.9991
CA LUB	92.17 ± 1.34^{a}	2.30×10^{10}	0.27 ± 0.00^{a}	2.55 ± 0.04^{c}	0.9994
CA SMA	93.36 ± 1.04^{a}	2.94×10^{10}	0.25 ± 0.00^{a}	2.73 ± 0.03^{d}	0.9973
CA SMB	94.79 ± 1.67^{a}	4.89×10^{10}	0.28 ± 0.00^{a}	2.51 ± 0.02^{c}	0.9995

Ea—activation energy, *Z*—pre-exponential factor, *k*—oxidation rate constant, calculated for $T=441$ K, $t_{1/2}$—half-life time, R^2 –coefficient of determination. CA OM (*Omega* Cultivar), CA SMA, CA SMB (*Śmiłowska* cultivar), CA LUA, CA LUB (*Luna* cultivar). All values are mean ± SD, $^{(a-d)}$ means with the same superscript within the same column are not different ($p>0.05$)

in Table 4, the highest values were also observed for CA LUB and CA SM. Correlation analysis between the antioxidant activity (RSA DPPH) and DSC oxidation parameters (Table 5) revealed that for all the DSC parameters measured (OIT, T_{on}), high positive correlation coefficients were obtained, which means the greater the antioxidant activity, the higher the DSC parameters (time or temperature) and the more stable the oils. Significant correlation coefficients were also found between all DSC parameters measured and parameter a^* and b^* of color measurement. An analysis of the correlation between RSA DPPH and parameters of a^*, b^* revealed significant positive correlations with Pearson's coefficients $r=0.732$ and $r=0.885$, respectively.

Principle component analysis (PCA)

PCA was applied to investigate the structure of the relationships between all variables i.e., OIT (120, 140, 160 °C), T_{on} (1, 2, 5, 10 and 15 °C min^{-1}), fatty acids (C16:0, C18:1, C18:2, C18:3 n-3, C20:1), kinetic data parameters (E_a,

Table 3 Pearson's correlation coefficients between fatty acid composition and DSC oxidation parameters of cold-pressed camelina oil

Parameters	Fatty acids %					
	C16:0	C18:0	C18:1	C18:2	C20:1	C18:3n:3
OIT (120 °C)	0.977	0.525*	0.598*	0.871	−0.948	−0.783
OIT (140 °C)	0.878	0.761	0.784	0.746	−0.859	−0.776
OIT (160 °C)	0.880	0.736	0.800	0.778	−0.960	−0.747
T_{on} (1 °C min^{-1})	0.900	0.541*	0.609*	0.870	−0.866	−0.812
T_{on} (2 °C min^{-1})	0.922	0.699	0.724	0.760	−0.855*	−0.785
T_{on} (5 °C min^{-1})	0.836	0.858	0.866	0.681	−0.823	−0.772
T_{on} (10 °C min^{-1})	0.908	0.824	0.848	0.807	−0.890	−0.856
T_{on} (15 °C min^{-1})	0.887	0.809	0.844	0.864	−0.865	−0.912
E_a	−0.072*	−0.651	−0.590*	−0.064*	0.125*	0.274*
k	−0.755	−0.911	−0.907	−0.610	0.769	0.730

OIT—oxidation induction time for various temperatures: 120, 140, 160 °C, T_{on}—onset temperature for various heating rates 1, 2, 5, 10, 15 °C min^{-1}, E_a—activation energy (kJ mol^{-1}), k -oxidation rate constant (min^{-1}),

*Correlation not significant statistically, ($\alpha = 0.05$)

Table 4 Color measurement L*, a*, b* values and the antioxidant activity (RSA DPPH) of cold-pressed camelina oil

Camelina cultivar	Color			RSA DPPH /μmol TEg^{-1}
	L^*	a^*	b^*	
CA OM	$89.90^{e} \pm 0.03$	$-1.23^{b} \pm 0.00$	$45.93^{a} \pm 0.02$	$1.26^{a} \pm 0.02$
CA LU A	$82.73^{b} \pm 0.00$	$0.12^{a} \pm 0.00$	$55.52^{b} \pm 0.01$	$1.21^{a} \pm 0.01$
CA LU B	$86.69^{d} \pm 0.01$	$-3.2^{c} \pm 0.00$	$96.07^{e} \pm 0.02$	$1.39^{b} \pm 0.03$
CA SM A	$85.57^{c} \pm 0.01$	$0.11^{a} \pm 0.00$	$94.60^{d} \pm 0.01$	$1.52^{c} \pm 0.00$
CA SM B	$81.71^{a} \pm 0.02$	$0.82^{d} \pm 0.00$	$91.21^{c} \pm 0.01$	$1.42^{b} \pm 0.00$

All values are mean ± standard deviation of three ($n = 3$) for color measurements and ($n = 2$) for RSA DPPH measurements,$^{(abcde)}$ means with the same superscript within the same column are not different ($p > 0.05$). CA OM (*Omega* cultivar), CA SMA, CA SMB (*Śmiłowska* cultivar), CA LUA, CA LUB (*Luna* cultivar) varieties of camelina seed oils

Table 5 Pearson's correlation coefficients calculated between DSC oxidation parameters and L*, a*, b*, RSA DPPH for cold-pressed camelina oils

Parameters	RSA DPPH Color			
	L	a^*	b^*	
OIT (120 °C)	0.806	−0.669*	0.945	0.867
OIT (140 °C)	0.896	−0.244*	0.777	0.881
OIT (160 °C)	0.798	−0.467*	0.891	0.893
T_{on} (1 °C min^{-1})	0.767	−0.592*	0.908	0.856
T_{on} (2 °C min^{-1})	0.953	−0.283*	0.787	0.881*
T_{on} (5 °C min^{-1})	0.973	−0.073*	0.714	0.895
T_{on} (10 °C min^{-1})	0.958	−0.251*	0.833	0.947
T_{on} (15 °C min^{-1})	0.906	−0.304*	0.874	0.966
E_a	−0.382*	−0.542*	−0.030*	−0.325*
k	−0.946	−0.055*	−0.639	−0.863

OIT (min)—Oxidation induction time, T_{on}—onset temperature, E_a—activation energy (kJ mol^{-1}), k -oxidation rate constant (min^{-1}), *Correlation not significant statistically, ($\alpha = 0.05$)

k), b*, RSA DPPH and to classify the objects in terms of camelina varieties. Based on the eigenvalue plot, which showed that around 96.7% of the variation in the data can be explained by four principal components, since for the first two PCs 88.35% of total variance was explained. A projection of the variables and a projection of the cases on the principal component plane with PC1 and PC2 on the X and Y axes, respectively, are presented in Fig. 8. The plot in Fig. 8A depicts the relations between variables and the plot of scores (Fig. 8B), distribution of objects (samples). As can be seen from Fig. 8A, the first PC1 explains the observed variability in 77.76% and PC2 in 10.59%. For the first principal component (PC1), the highest correlations were observed for the variables of oxidation constant k (−0.92), fatty acid content i.e., C18:3 (−0.89) and C20:1 (−0.93), for which vectors were located on the negative side of X axis and on the opposite side were variables positively correlated with PC1 i.e., C16:0 (0.95), RSA DPPH (0.94), b^* (0.98),

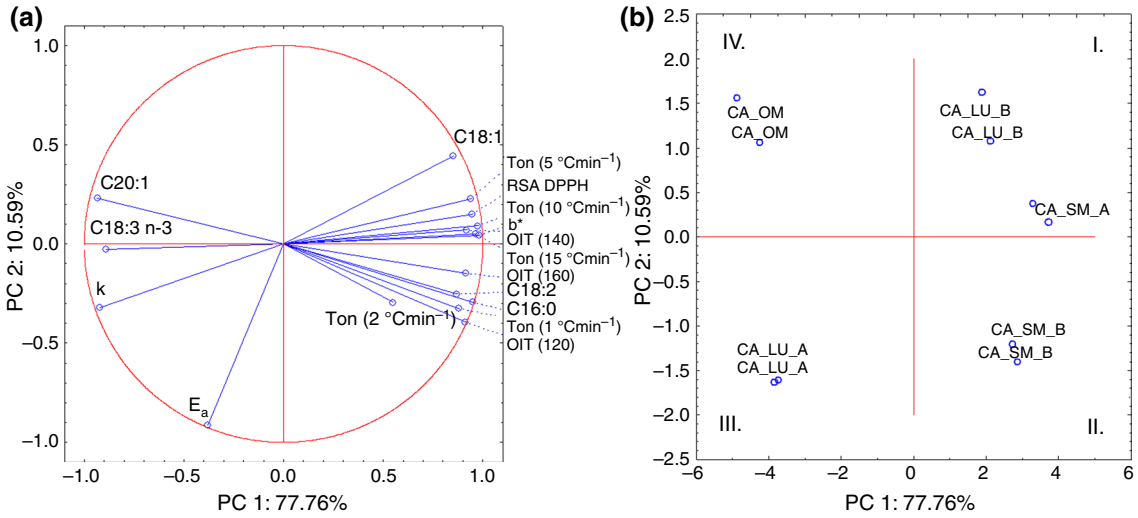

Fig. 8 PCA analysis with projection of the variables: DSC parameters, fatty acids content, RSA DPPH, *b** **A** PCA analysis with projection of cases showing distribution of camelina oils samples **B**

T_{on} (0.97), OIT (0.92). The distribution of camelina samples in terms of cultivars is shown in Fig. 8B. They were divided into four clusters. The first (CA SMA, CA LUB) and second (CA SMB) clusters, located on the positive side of X axis, consist of the most stable camelina oils characterized by the highest oxidative stability by means of RSA DPPH and OIT values. Those samples were placed on the opposite side to the third and fourth cluster (CA LUA, CA OM), for which the lowest values of PC1 were obtained (the lowest oxidative stability, the highest content of unsaturated fatty acids, the lowest b* and RSA DPPH).

Conclusions

The aim of this study was to assess the thermal stability of cold-pressed camelina seed oils by means of DSC isothermal and non-isothermal, dynamic tests. The results of oxidation induction time (OIT) obtained in isothermal mode at 120, 140 and 160 °C clearly show that *Omega* and *Luna* (CA LU A) cultivars were the least stable, while the *Śmiłowska* variety was the most resistant to oxidation. Generally, for all camelina oils, oxidation induction time (OIT) decreased with an increase in temperature (isothermal test) on average from 69.83 min for 120 °C to 5.13 min for 160 °C. In addition to the results of OIT, the oxidation rate was also calculated, which showed that the oxidation is faster at higher temperatures, increasing 3–4 times with every increase of 20 degrees in temperature. Findings from isothermal measurements corresponded very well with the results of non-isothermal experiments with heating rates of 1, 2, 5, 10, 15 °C min^{-1}. Analysis of the onset temperature showed the lowest values of T_{on} for *Omega* and *Luna* samples and the highest for the *Śmiłowska* cultivar at all heating rates. All correlation analyzes led to the conclusion that differences in oxidative stability between the cultivars were mainly caused by the content of some unsaturated fatty acids e.g., α-linolenic acid (C18:3, n-3) as well as by the antioxidative activity. Oil from camelina seeds of *Omega* cultivar, characterized by the highest content of fatty acid C18:3, n-3 (37.2%), was the least thermally stable oil. There was a strong and statistically significant positive correlation between this fatty acid and DSC oxidation parameters (OIT and T_{on}), which were also highly correlated with value *b** (yellowness) and the radical scavenging activity by 2,2-diphenyl-1-picrylhydrazyl (RSA DPPH). The lowest values of *b** and RSA DPPH were observed for the least stable oil (*Omega* cultivar), and the highest for *Śmiłowska* cultivar. Principal component analysis confirmed all observations, namely that the DSC thermal oxidation stability of camelina oil can be explained by the unsaturated fatty acid content, yellowness *b** and RSA DPPH, and can also be predicted by the oxidation rate constant *k*, which was negatively correlated to OIT and T_{on}.

Acknowledgements Part of the results published in this article was presented at the conference "7th International Congress on Thermal Analysis and Calorimetry; 8th Joint Czech-Hungarian-Polish-Slovakian Thermoanalytical Conference; 14th Conference on Calorimetry and Thermal Analysis of the Polish Society of Calorimetry and Thermal Analysis" on August 29– September 2, 2021.

Author Contributions Conceptualization: Mahbuba Islam, Jolanta Tomaszewska-Gras; methodology Mahbuba Islam, Jolanta Tomaszewska-Gras, Małgorzata Muzolf-Panek; formal analysis: Mahbuba Islam, Jolanta Tomaszewska-Gras, Małgorzata Muzolf-Panek; investigation: Mahbuba Islam, Jolanta Tomaszewska-Gras, Małgorzata Muzolf-Panek; resources: Jolanta Tomaszewska-Gras; data curation: Mahbuba Islam, Jolanta Tomaszewska-Gras; writing—original draft

preparation: Mahbuba Islam, Jolanta Tomaszewska-Gras; writing—review and editing: Mahbuba Islam, Jolanta Tomaszewska-Gras, visualization, Mahbuba Islam, Jolanta Tomaszewska-Gras; supervision: Jolanta Tomaszewska-Gras, project administration: Emilia Fornal, Jolanta Tomaszewska-Gras, funding acquisition: Emilia Fornal, Jolanta Tomaszewska-Gras. All authors have read and agreed to the published version of the manuscript.

Funding This research was funded by the NATIONAL SCIENCE CENTRE, POLAND, grant number: 2018/31/B/NZ9/02762.

Declarations

Conflict of interest The authors declare that they have no conflict of interest.

References

1. Budin JT, Breene WM, Putnam DH. Some compositional properties of camelina (camelina sativa L. Crantz) seeds and oils. J Am Oil Chem Soc. 1995;72:309–15.
2. Crowley JG, Fröhlich A. (1998) Factors affecting the composition and use of Camelina. End Proj Reports, Teagasc. 1–23
3. Ibrahim FM, El Habbasha SF. Chemical composition, medicinal impacts and cultivation of camelina (Camelina sativa): review. Int J PharmTech Res. 2015;8:114–22.
4. Abramovič H, Abram V. Physico-chemical properties, composition and oxidative stability of camelina sativa oil. Food Technol Biotechnol. 2005;43:63–70.
5. Ratusz K, Popis E, Ciemniewska-Żytkiewicz H, Wroniak M. Oxidative stability of camelina (Camelina sativa L.) oil using pressure differential scanning calorimetry and Rancimat method. J Therm Anal Calorim. 2016;126:343–51.
6. Ratusz K, Symoniuk E, Wroniak M, Rudzińska M. Bioactive compounds, nutritional quality and oxidative stability of cold-pressed camelina (Camelina sativa L.) oils. Appl Sci. 2018;8:1–17.
7. Piravi-vanak Z, Azadmard-Damirchi S, Kahrizi D, Mooraki N, Ercisli S, Savage GP, et al. Physicochemical properties of oil extracted from camelina (Camelina sativa) seeds as a new source of vegetable oil in different regions of Iran. J Mol Liq. 2021;345:117043.
8. Gunstone FD, Morris LJ. Fatty acids. Part VI. The oxygenated acid present in Camelina sativa (Crantz.) seed oil. J Chem Soc. 1959. https://doi.org/10.1039/jr9590002127.
9. Abramovič H, Butinar B, Nikolič V. Changes occurring in phenolic content, tocopherol composition and oxidative stability of Camelina sativa oil during storage. Food Chem. 2007;104:903–9.
10. Berti M, Gesch R, Eynck C, Anderson J, Cermak S. Camelina uses, genetics, genomics, production, and management. Ind Crops Prod. 2016;94:690–710.
11. Zubr J, Matthaus B. Effects of growth conditions on fatty acids and tocopherols in Camelina sativa oil. Ind Crops Prod. 2002;15:155–62.
12. Gugel RK, Falk KC. Agronomic and seed quality evaluation of Camelina sativa in western Canada. Can J Plant Sci. 2006;86:1047–58.
13. Kurasiak-Popowska D, Graczyk M, Przybylska-Balcerek A, Stuper-Szablewska K. Influence of variety and weather conditions on fatty acid composition of winter and spring Camelina sativa varieties in Poland. Eur Food Res Technol. 2021;247:465–73. https://doi.org/10.1007/s00217-020-03639-0.
14. Moslavac T, Jokić S, Šubarić D, Aladić K, Vukoja J, Prce N. Pressing and supercritical CO2 extraction of Camelina sativa oil. Ind Crops Prod. 2014;54:122–9.
15. Kiralan M, Kiralan SS, Subaşi I, Aslan Y, Ramadan MF. Fatty acids profile and stability of camelina (Camelina sativa) seed oil as affected by extraction method and thermal oxidation. Riv Ital delle Sostanze Grasse. 2018;95:223–8.
16. Urbaniak SD, Caldwell CD, Zheljazkov VD, Lada R, Luan L. The effect of seeding rate, seeding date and seeder type on the performance of Camelina sativa L. in the Maritime Provinces of Canada. Can J Plant Sci. 2008;88:501–8.
17. Ciubota-Rosie C, Ruiz JR, Ramos MJ, Pérez Á. Biodiesel from Camelina sativa: a comprehensive characterisation. Fuel Elsevier Ltd. 2013;105:572–7.
18. Yang J, Caldwell C, Corscadden K, He QS, Li J. An evaluation of biodiesel production from Camelina sativa grown in Nova Scotia. Ind Crops Prod. 2016;81:162–8.
19. Obeng E, Obour AK, Nelson NO, Moreno JA, Ciampitti IA, Wang D, et al. Seed yield and oil quality as affected by Camelina cultivar and planting date. J Crop Improv Taylor Francis. 2019;33:202–22.
20. Belayneh HD, Wehling RL, Cahoon EB, Ciftci ON. Effect of extraction method on the oxidative stability of camelina seed oil studied by differential scanning calorimetry. J Food Sci. 2017;82:632–7.
21. Belayneh HD, Wehling RL, Cahoon E, Ciftci ON. Extraction of omega-3-rich oil from Camelina sativa seed using supercritical carbon dioxide. J Supercrit Fluids. 2015;104:153–9.
22. Szterk A, Roszko M, Sosińska E, Derewiaka D, Lewicki PP. Chemical composition and oxidative stability of selected plant oils. JAOCS, J Am Oil Chem Soc. 2010;87:637–45.
23. Raczyk M, Popis E, Kruszewski B, Ratusz K, Rudzińska M. Physicochemical quality and oxidative stability of linseed (Linum usitatissimum) and camelina (camelina sativa) cold-pressed oils from retail outlets. Eur J Lipid Sci Technol. 2016;118:834–9.
24. Symoniuk E, Ratusz K, Ostrowska-Ligęza E, Krygier K. Impact of selected chemical characteristics of cold-pressed oils on their oxidative stability determined using the Rancimat and pressure differential scanning calorimetry method. Food Anal Methods. 2018;11:1095–104.
25. Tamási K, Marossy K. Combined thermal analysis of plant oils. J Therm Anal Calorim. 2021;147:2047–54. https://doi.org/10.1007/s10973-020-10470-y.
26. Eidhin DN, Burke J, O'Beirne D. Oxidative stability of ω3-rich Camelina oil and camelina oil-based spread compared with plant and fish oils and sunflower spread. J Food Sci. 2003;68:345–53.
27. Eidhin DN, O'Beirne D. Oxidative stability of camelina oil in salad dressings, mayonnaises and during frying. Int J Food Sci Technol. 2010;45:444–52.
28. Różańska MB, Kowalczewski PŁ, Tomaszewska-Gras J, Dwiecki K, Mildner-Szkudlarz S. Seed-roasting process affects oxidative stability of cold-pressed oils. Antioxidants. 2019;8:313. https://doi.org/10.3390/antiox8080313.
29. Hrastar R, Abramovič H, Košir IJ. In situ quality evaluation of Camelina sativa landrace. Eur J Lipid Sci Technol. 2012;114:343–51.
30. Kurasiak-Popowska D, Rynska B, Stuper-Szablewska K. Analysis of distribution of selected bioactive compounds in camelina sativa from seeds to pomace and oil. Agronomy. 2019;9:168.
31. Codex Alimentarius. (1999) Standard for named vegetable oils codex Stan 210–1999. Codex Aliment. 1–13.
32. Tomaszewska-Gras J, Islam M, Grzeca L, Kaczmarek A, Fornal E. Comprehensive thermal characteristics of different cultivars of flaxseed oil (Linum usittatissimum L.). Molecules. 2021;26:1–20.
33. Adhvaryu A, Erhan SZ, Liu ZS, Perez JM. Oxidation kinetic studies of oils derived from unmodified and genetically modified

vegetables using pressurized differential scanning calorimetry and nuclear magnetic resonance spectroscopy. Thermochim Acta. 2000;364:87–97.
34. Ostrowska-Ligeza E, Bekas W, Kowalska D, Lobacz M, Wroniak M, Kowalski B. Kinetics of commercial olive oil oxidation: dynamic differential scanning calorimetry and Rancimat studies. Eur J Lipid Sci Technol. 2010;112:268–74.
35. Tan CP, Che Man YB, Selamat J, Yusoff MSA. Application of Arrhenius kinetics to evaluate oxidative stability in vegetable oils by isothermal differential scanning calorimetry. JAOCS, J Am Oil Chem Soc. 2001;78:1133–8.
36. Flynn JH, Wall LA. A quick, direct method for the determination of activation energy from thermogravimetric data. J Polym Sci Part B Polym Lett. 1966;4:323–8.
37. Qi B, Zhang Q, Sui X, Wang Z, Li Y, Jiang L. Differential scanning calorimetry study - Assessing the influence of composition of vegetable oils on oxidation. Food Chem. 2016;194:601–7. https://doi.org/10.1016/j.foodchem.2015.07.148.
38. Saldana MDA, Martinez-Monteagudo SI. (2013) Oxidative Stability of Fats and Oils Measured by Differential Scanning Calorimetry for Food and Industrial Applications. In: Amal Ali Elkordy, (Eds) Appl Calorim a Wide Context - Differ Scanning Calorimetry, Isothermal Titration Calorim. Microcalorim. IntechOpen https://doi.org/10.5772/54486
39. Itle RA, Kabelka EA. Correlation between lab color space values and carotenoid content in Pumpkins and Squash (Cucurbita spp.). HortScience. 2009;44:633–7.

Statement about the contribution of authors

Publication title A2: Islam, M., Muzolf-Panek, M., Fornal, E. et al. DSC isothermal and non-isothermal assessment of thermo-oxidative stability of different cultivars of Camelina sativa L. seed oils. J Therm Anal Calorim 147, 10013–10026 (2022). https://doi.org/10.1007/s10973-022-11367-8

Author	Contribution	Percentage contribution	Signature
Mahbuba Islam	Conceptualization, Methodology, Formal analysis, Investigation, Data curation, Writing- original draft preparation, Writing—review and editing, Visualization.	45	
Małgorzata Muzolf-Panek	Methodology, Formal analysis, Investigation, Writing- review and editing.	10	
Emilia Fornal	Project administration, Funding acquisition.	10	
Jolanta Tomaszewska-Gras	Conceptualization, Methodology, Formal analysis, Investigation, Resources, Data curation, Writing- original draft preparation, Writing- review and editing, Visualization, Supervision, Project administration, Funding acquisition.	35	

Publication no. A3

Islam, M.; Kaczmarek, A.; Grygier, A.; Tomaszewska-Gras, J. DSC Phase Transition Profiles Analyzed by Control Charts to Determine Markers for the Authenticity and Deterioration of Flaxseed Oil during Storage. Foods 2023, 12, 2954. https://doi.org/ 10.3390/foods12152954

foods

MDPI

Article

DSC Phase Transition Profiles Analyzed by Control Charts to Determine Markers for the Authenticity and Deterioration of Flaxseed Oil during Storage

Mahbuba Islam [1], Anna Kaczmarek [1], Anna Grygier [2] and Jolanta Tomaszewska-Gras [1,*]

[1] Department of Food Quality and Safety Management, Poznań University of Life Sciences, ul. Wojska Polskiego 31/33, 60-624 Poznań, Poland; mahbuba.islam@up.poznan.pl (M.I.); anna.kaczmarek@up.poznan.pl (A.K.)
[2] Department of Food Technology of Plant Origin, Poznań University of Life Sciences, ul. Wojska Polskiego 31/33, 60-624 Poznań, Poland; anna.grygier@up.poznan.pl
* Correspondence: jolanta.tomaszewska-gras@up.poznan.pl

Abstract: An approach of implementing X-bar and R control charts as a statistical control tool to monitor the changes in the melting profile of fresh and stored flaxseed oils by differential scanning calorimetry (DSC) was used. Phase transition melting profiles were collected after 0, 2, 4, and 6 months of storing flaxseed oils, originating from five different cultivars. Four peaks at around −36, −30, −25, and −12 °C were identified using the deconvolution analysis procedure, which enabled the data to be collected at peak temperature (T), peak height (h), the peak area (A), and the percentages of the area (P A), as well as the ratio calculated from these parameters. Control charts obtained for the second peak of the melting profile showed a significant decrease of peak height (h2) from 0.50 to 0.39 W/g and the percentage of the area (P A2) from 50 to 38%, within the storage time ($p \leq 0.05$); thus, they were considered to be indicators of oil deterioration. Strong negative correlations of the unstable parameters of DSC with chemical indicators of the oils' oxidative stability (PV, p-AV, TOTOX) were found. For DSC parameters, related to the first peak (h1, A1) and the third peak (h3, A3), changes were statistically not significant within storage ($p > 0.05$); thus, they can be used as markers of flaxseed oil authenticity. The study demonstrated that X-bar and R control charts could effectively monitor changes in the specific peaks and calculated ratios from the DSC melting profile of fresh and stored flaxseed oils, serving as reliable indicators of oil deterioration.

Keywords: differential scanning calorimetry; melting profile; storage analysis; plant oils; stability; authenticity

Citation: Islam, M.; Kaczmarek, A.; Grygier, A.; Tomaszewska-Gras, J. DSC Phase Transition Profiles Analyzed by Control Charts to Determine Markers for the Authenticity and Deterioration of Flaxseed Oil during Storage. *Foods* **2023**, *12*, 2954. https://doi.org/10.3390/foods12152954

Academic Editor: Antonella De Leonardis

Received: 11 July 2023
Revised: 30 July 2023
Accepted: 2 August 2023
Published: 4 August 2023

1. Introduction

One of the most popular cold-pressed plant oils, found on the shelf of almost every supermarket, is flaxseed oil. The unique profile of fatty acids ranked this oil among the healthiest edible oils in terms of the content of polyunsaturated fatty acids (PUFA), especially from the n-3 (omega-3) group. Also called linseed, this multipurpose plant belongs to the Linaceae family and grows well in the temperate climate zone. According to FAOSTAT's report from 2020, annually, 738,940 thousand tons of flaxseed oil are produced to meet the increasing demand, with China dominating the production, followed by Belgium, the United States, Germany, and India [1]. Research has demonstrated that the quality and utility of the products obtained from this plant depends on the variety [2], climate [3], seed maturity [4], and extraction process [5]. Reasonably, edible flaxseed oil is formulated using the cold-pressing process, which enables the retention of an outstanding combination of triacylglycerols (TAG's) and acylglycerols (mono- and diacylglycerol), and other bioactive compounds (i.e., phenols, sterols, tocopherols, phospholipids, lignans, and pigments). Thus, the cold pressing of seeds has become popular nowadays, and some

of these valuable compounds, e.g., tocopherols and phenols, play a role in the stability of the oils and exert significant antioxidant properties upon consumption. Similar to *Lallemantia iberica*, [6] cold-pressed flaxseed oil has been acknowledged as one of the richest in polyunsaturated fatty acids (PUFA's), especially α-linolenic fatty acid (ALA; C18:3, n-3) and linoleic acid (LA; C18:2, n-6), amounting to 50–63% and 16–26%, respectively [2,7], which are crucial for the human diet. Accompanied to the fatty acids, the presence of fat-soluble vitamins such as vitamin E (mainly as γ-tocopherol), phyto-estrogenic lignans (secoisolariciresinol diglucoside; SDG), and dietary fiber has made this non-traditional oil very popular amongst researchers, due to its manifold applications [8–10]. Here it is worth noting that flaxseed oils are used not only as edible oils in bottles, but also in pharmacies as a carrier of fat-soluble supplements (e.g., vitamin D). Meanwhile, the benefits of cold-pressed flaxseed oil come with an inevitable oddity, since the presence of many PUFAs make this oil very prone to peroxidation, which can additionally be accelerated by other natural compounds present in the oil, such as chlorophylls or phospholipids. Thus, ongoing anti- and pro-oxidant interactions makes cold-pressed oils less predictable in terms of their shelf-life stability [11]. Although the regular shelf life for vegetable oils has been accepted as 6 to 12 months [11], instructions from flaxseed oil producers clearly state the oxidation proneness of this oil, as the stability time has been pinned down at 5 weeks to 3 months [12]. This uncertain shelf-life assumption urged researchers to find the reasons and indicators responsible for the deterioration of flaxseed oil quality. In chemical analysis, alongside p-anisidine (p-AV), acid (AV) and peroxide (PV) values are the most common indicators for observing the stage of rancidity. However, other methods were also used, for instance, conjugated diene (CD) and triene (CT) values [13,14], a Rancimat analysis [15], and an isothermal and dynamic analysis by DSC [14].

With the furtherance of achievements in food science, the ultimate strategy nowadays is to use instruments, which are supposed to be not only ecological and environmentally friendly, but also a time-saver. Recent advancements in thermo-analytical assessments have contributed substantially to the analysis of fats and oils characterization. Differential scanning calorimetry (DSC) is an advanced analytical instrument which has broad applications dedicated to explaining the thermal behavior of lipid compounds, and is thus able to provide significant data regarding the authenticity and stability profiles of fats and oils [16]. Several research studies have proven the effective use of the DSC technique to explore the oxidative deterioration resulting from normal or accelerated shelf-life tests [17–19]. Compared to conventional chemical analyses, an assessment by DSC offers a significant database, expressed as the exothermic/endothermic phase transition phenomena manifested by curve changes as a function of temperature, which is related to the lipids composition of the oil. Thus, the unique and specific DSC curves for flaxseed oils can also be obtained as the cooling and melting profile [2,20]. Bearing in mind that such a crystallization or melting profile could be used as a fingerprint to assess authenticity and to ensure the safety and quality of this oil, it is important to investigate whether these profiles are stable over the shelf life of the oils. So far, there have been no such studies showing how the crystallization or melting profile changes within the storage time. Considering that flaxseed oil may be nutritionally degraded due to adulteration with other less expensive oils or due to rancidity, it is important to monitor for both of these risks. Thus, in this study, the aim was to evaluate the changes in the DSC melting profiles of flaxseed oil of various cultivars over their shelf life using a control chart as one of the statistical process control tools. The novelty of this study lies in its distinctive approach of employing X-bar and R control charts to monitor the changes in the DSC melting profile of both fresh and stored flaxseed oils over a period of six months. This approach enables the identification of reliable indicators for oil deterioration and authenticity, utilizing specific peaks and calculated ratios. Moreover, this rapid and environmentally friendly method for assessing the oil quality and stability holds significant importance, especially for flaxseed oil, which is highly prone to oxidation during extended storage. To the best of the authors' knowledge, this particular approach has not been previously presented in any other study.

2. Materials

2.1. Materials

For the experiment, 15 kg of seeds of each cultivar, i.e., Bukoz (FL BU), Dolguniec (FL DL), Szafir (FL SZA, FL SZB) and of an unknown variety (FL NN) of flax were cold pressed to obtain the oils. All seeds were pressed in the SEMCO manufactory to obtain the oils at the same conditions by keeping the temperature below 50 °C. The pressed oils were left for 24 h for decantation and stored in brown glass bottles, which were used to store the oils as they offer excellent protection against light exposure, particularly harmful UV rays, and also to replicate the similar conditions as they are available in the market. A storage analysis was carried out for the samples from the fresh condition until the sixth month of shelf life. For every period of storage (0, 2nd, 4th, and 6th month) freshly opened bottles of flaxseed oil samples were used in order to perform all the analyses. During the shelf life, the samples were kept air-tight at room temperature (23–25 °C) by the window, where they were exposed to ambient natural sunlight with the aim to simulate real-life conditions that the oils may encounter during transportation, distribution, or in consumer households.

2.2. Methods

2.2.1. Fatty Acid Composition

A Gas Chromatography-Flame Ionization Detector (GC-FID) was employed for the determination of fatty acid composition. An amount of 15 mg of oil was dissolved in 1 mL of hexane (for HPLC, Sigma Aldrich, St. Louis, MO, USA), and 1 mL of 0.4 N sodium methoxide was added. The samples were stirred and left for 15 min, then 5 mL of distilled water was added, and the top layer was taken off. By following the AOCS official method [21], fatty acid methyl esters were analyzed using a Trace 1300 chromatograph (Thermo Fisher Scientific, Waltham, MA, USA). Separation was performed on a Supelcowax 10 capillary column (30 m × 0.2 mm × 0.2 µm), and an injection was performed in the splitless mode. The sample volume was 1 µL. Hydrogen was used as the carrier gas. The initial oven temperature was 160 °C and was increased to 220 °C with a rate of 12 °C. The temperature of 220 °C was maintained for 20 min. The quantification of fatty acids was performed using the percentage of the area method, where individual fatty acids were measured based on their retention times via a comparison with the standard of 37-Component FAME Mix (Supelco, Sigma Aldrich). All the samples were analyzed in two replications.

2.2.2. Chemical Analyses of the Oxidative Stability of Fresh and Stored Flaxseed Oil

The acid value (AV) was determined by using a volumetric titration formula following the standard AOCS method [22]. The peroxide value (PV) was measured by determining the milliequivalents of excess active oxygen content in the oil samples by following the standard ISO method [23]. The secondary oxidation products were determined by measuring the p-Anisidine values (p-AV) according to the standard [24]. The total oxidation rate of the oil samples was expressed as a TOTOX value and calculated from the formula based on the reported p-Anisidine and peroxide value data, TOTOX = p-AV + 2PV [23].

2.2.3. Melting Phase Transition Analysis by Differential Scanning Calorimetry (DSC) of Flaxseed Oil during Storage

A melting analysis of flaxseed oils was carried out with modifications according to the method used for butterfat [25]. A PerkinElmer differential scanning calorimeter (DSC 8500 PerkinElmer, Waltham, MA, USA), equipped with an Intracooler II and running with Pyris software (PerkinElmer, Waltham, MA, USA), was used. Samples of ca. 6–7 mg were weighed into aluminum pans of 20 µL (PerkinElmer, No. 0219-0062, Waltham, MA, USA) and hermetically sealed. The reference was an empty, hermetically sealed aluminum pan, and nitrogen (99.999% purity) was used as the purge gas. The analysis started with cooling the oil sample at a scanning rate of 2 °C/min from a temperature of 30 °C to −65 °C, after which it was heated at scanning rates of 5 °C/min from −65 °C to 30 °C. For each

measurement at a given scanning rate, the calibration procedure was completed with the correct scanning rate. After the analysis, the DSC files were converted into the ASCII format and were analyzed using Origin Pro software, version 2020 (OriginLab Corporation, Northampton, MA, USA). The temperature of each peak (T), the amplitude of each peak height (h), and area of each peak of the transition (A) were determined from the curves via the fitting procedures. The multicomponent DSC curves were deconvoluted with PeakFit, using the nonlinear least squares fitting procedure included in the Origin Pro software. All measurements were performed in duplicate for each sample.

2.2.4. Statistical Analysis

The results were presented in the form of mean and standard deviation. A statistical analysis of the recorded results was performed using Statistica 13.3 software (TIBCO Software Inc., Palo Alto, CA, USA) at a significance level of $\alpha = 0.05$. The first stage in the statistical analysis consisted of verifying the variance homogeneity using the Hartley–Cochran–Bartlett test. In the case of variance homogeneity, a one-way analysis of the variance (ANOVA) was used, and Tukey's test was applied to create statistically homogeneous groups. In turn, when the variances were not homogeneous, non-parametric tests were used, i.e., ANOVA and the Kruskal–Wallis rank test. Additionally, a principal component analysis (PCA) was performed to show the relationships between the variables and detect some patterns between the variables and the objects. X-bar and R (arithmetic mean and range) control charts were used to test the stability of selected melting profile parameters. The X-bar and R control chart were used with continuous/variable data when a subgroup or sample size was between 2 and 15. The X-bar chart is based on a calculation of the average level of the parameter being monitored, while the R chart showed the range, i.e., the difference between the smallest and the largest value in each sample at each time point of storage, revealing the variability of the variation.

3. Results

3.1. Physicochemical Characteristics of Fresh and Stored Flaxseed Oils

Physicochemical characteristics of fresh (0 month) and stored (6th month) flaxseed oils included the fatty acid composition and chemical analyses of the oxidative stability (AV, PV, p-AV, and TOTOX).

3.1.1. Fatty Acid Content

The abundance of PUFA (up to 73%) with 16% of monounsaturated fatty acids (MUFA) and 8% of saturated fatty acids (SFA) was determined in all flaxseed oils, as shown in Figure 1. The predominant fatty acid was α-linolenic acid (ALA, C18:3, n-3), which contributed up to 63% of the total fatty acids. Between the oil samples, FL_NN showed the lowest quantity of ALA (55%), of which FL_SZA showed the highest quantity of 63%. This quantity is comparatively higher than that found in other studies on commercial oils from the same region [15]. Nevertheless, the value aligns with the data reported for high-performing linseed cultivars. For instance, Florinda, Lirina, and Floriana cultivars, monitored over nine years, exhibited ALA levels accounting for 63.04%, 63.25%, and even 64.10%, respectively [26]. Despite the presence of three unsaturated carbon bonds, this fatty acid remained stable and showed no significant differences ($p > 0.05$) for all the oil samples after six months of storage. Next, the abundant PUFA, linoleic acid (C18:2, LA), was detected as the highest at 16% for the Bukoz variety. The data obtained are comparable to the results of other researchers [27]. Of the MUFAs, oleic acid is distributed amongst the varieties in a range from 14% to 18% of the total FA and no significant differences were observed between 0 and 6 months of storage for all the oil samples ($p > 0.05$). Concerning the presence of the two SFAs, i.e., palmitic acid (C16:0) and stearic acid (C18:0), up to 4% and 3%, respectively, was observed. Summing up the entire dataset for 0 and 6 months of oil storage showed that there were no significant differences in the composition of fatty acids between fresh and stored oils ($p > 0.05$). This finding about the changes in fatty acids

after the storage time analysis can be compared with another study on flaxseeds stored for 128 days, which found no changes in fatty acid composition after the storage time [28]. Also, another study showed that, cold-pressed flaxseed oils stored for six months at room temperature exhibited no significant differences for SFA, MUFA or PUFA, which is linear to the data found from our study [29].

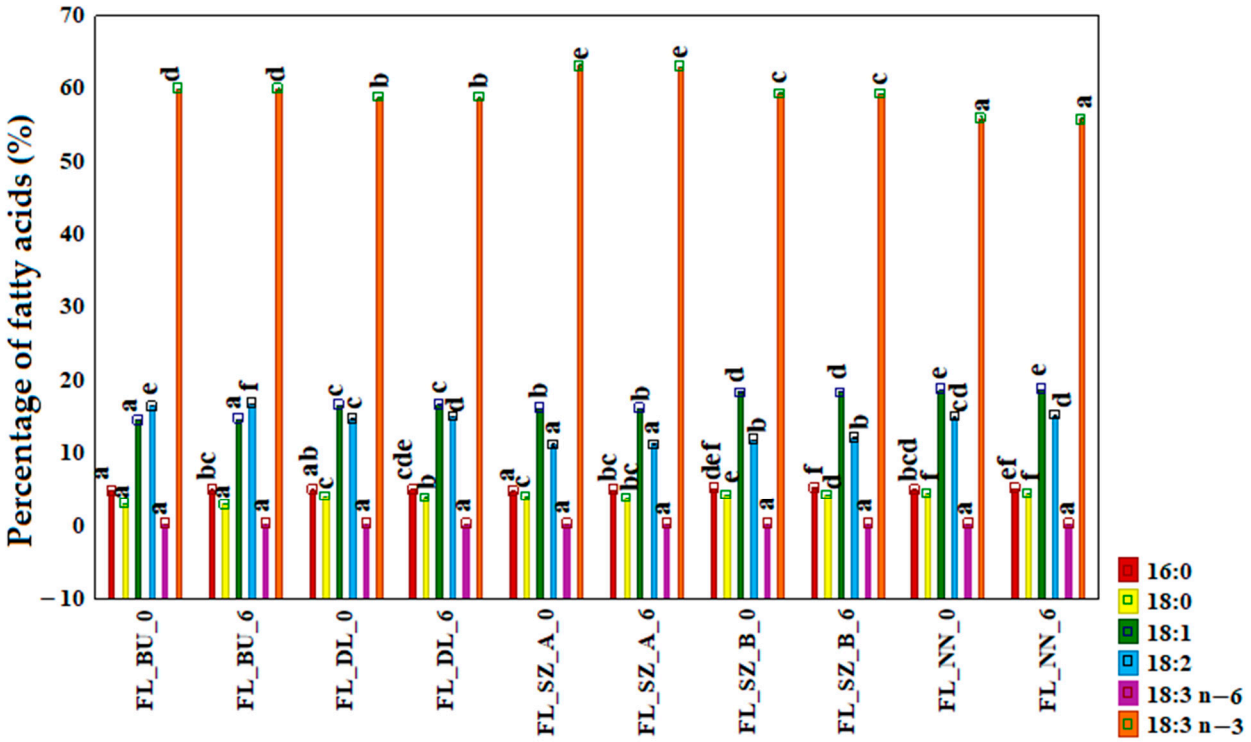

Figure 1. Fatty acids composition expressed as a percentage of total fatty acids (%) for fresh (0 month) and stored (6th month) flaxseed oils. a–f—different superscript letters above bars indicate significant differences analyzed for each fatty acid ($p \leq 0.05$). FL_BU_0 and FL_BU_6 (Bukoz variety at 0 month and after 6 months, analogously), FL_DL (Dolguniec variety), FL_SZA, FL_SZB (Szafir variety), and FL NN (Unknown variety).

3.1.2. Oxidative Stability Analysis of Flaxseed Oil

A conventional chemical analysis was carried out to detect any deterioration of the oil samples after six months of shelf life. The acid value (AV) measurement results, expressing the amount of free fatty acids, are shown in Table 1. The analyzed samples from the different varieties showed increased hydrolytic phenomena after six months, as the values increased for all of them. Particularly, the highest AV was found for the sample FL_NN, which was 3.25 (statistically significant at $p \leq 0.05$) after shelf life. However, none of the samples exceeded the standard limit (4.0 mg KOH/g oil) provided by the Codex Alimentarius [30]. A similar propensity was assessed for the peroxide values and p-Anisidine values obtained for all varieties. The peroxide values measured the primary oxidation compound formation in samples like aldehydes and ketones, which gradually generates a musty smell and promotes rancidity. After shelf life, the FL_SZB sample produced the highest ($p \leq 0.05$) level of the primary oxidation product (15.57), which is still within the range of the acceptable limit from the given standard (up to 15 milliequivalents of active oxygen/kg oil) [30]. For the storage time analysis, the p-Anisidine values are considered more reliable, as they provide information about secondary oxidation products (e.g., 2-alkenals and 2,4-alkadienals as a result of hydroperoxide decomposition, and unsaturated aldehydes) [31]. As an indicator of the oxidative rancidity, the p-AV values presented in Table 1 show that all samples presented an increased level of secondary oxidation phenomena, where the FL_NN sample was the highest at 2.47 ($p \leq 0.05$). The overall oxidation state can be assessed

by means of the TOTOX value, where the sample FL_SZB exhibits the highest level of oxidation (33.61) amongst all varieties after the shelf-life period. Changes in the oxidation states determined by other authors can be compared with this study. Similar results were found by authors who stored flaxseed oils at room temperature and presented a significant rise in the oxidative status determined by AV, PV, and p-AV values [13]. Authors from the same region [15] performed a storage analysis of the commercial oils after storing them in a refrigerator (4 ± 2 °C). Their results showed a significant level of increase for all AV, PV, and p-AV values after six months of shelf life.

Table 1. Acid values (AV), peroxide values (PV), p-anisidine values (p-AV), TOTOX values for cold-pressed flaxseed oils at fresh condition and after 6 months storage time.

Seeds Varieties	Time	Chemical Analysis			
		AV (mg KOH/g)	PV (meq O2/kg)	p-AV	TOTOX
FL_BU	0 month	0.80 ± 0.04 ^{b}	3.95 ± 0.63 ^{c}	0.87 ± 0.35 ^{a}	8.78 ± 1.02 ^{c}
	After 6 months	2.54 ± 0.02 ^{g}	14.44 ± 0.08 ^{h}	2.02 ± 0.02 ^{c}	30.90 ± 0.15 ^{h}
FL_DL	0 month	0.41 ± 0.01 ^{a}	2.49 ± 0.15 ^{b}	0.65 ± 0.01 ^{a}	5.63 ± 0.31 ^{b}
	After 6 months	1.59 ± 0.02 ^{d}	10.64 ± 0.11 ^{f}	1.70 ± 0.07 ^{bc}	22.76 ± 0.21 ^{f}
FL_SZA	0 month	1.27 ± 0.03 ^{c}	1.41 ± 0.06 ^{a}	0.73 ± 0.13 ^{a}	3.54 ± 0.20 ^{a}
	After 6 months	2.40 ± 0.02 ^{f}	9.73 ± 0.13 ^{e}	1.49 ± 0.01 ^{b}	21.09 ± 0.28 ^{e}
FL_SZB	0 month	0.81 ± 0.03 ^{b}	6.90 ± 0.23 ^{d}	0.94 ± 0.12 ^{a}	14.74 ± 0.41 ^{d}
	After 6 months	1.79 ± 0.02 ^{e}	15.57 ± 0.16 ^{i}	1.63 ± 0.02 ^{bc}	33.61 ± 0.30 ^{i}
FL_NN	0 month	1.60 ± 0.02 ^{d}	1.21 ± 0.06 ^{a}	0.76 ± 0.25 ^{a}	3.17 ± 0.24 ^{a}
	After 6 months	3.25 ± 0.10 ^{h}	11.69 ± 0.22 ^{g}	2.47 ± 0.03 ^{d}	25.08 ± 0.50 ^{g}

All values are mean ± standard deviation of three measurements (n = 3); (a–i)—means with the same letters within the column are not different ($p > 0.05$).

The unexpected results showed no changes in the percentage of individual fatty acids after 6 months of storage (Figure 1), and significant changes in the oxidative stability indicators (Table 1) may suggest that the oxidative changes that occur in the oils come from the fraction of free fatty acids or mono- or diacylglycerols. It should be noted here that the procedure for determining the fatty acids includes extraction with hexane, which dissolves only the TAG, unlike the free fatty acids and the rest of the acylglycerols.

3.2. Analysis of the DSC Melting Profiles of Flaxseed Oils during Shelf Life

DSC Melting Profile Changes during Storage of Flaxseed Oil

A DSC analysis of the melting profiles was carried out for all the flaxseed oil varieties throughout the shelf life (0, 2, 4, and 6 months) to determine the stability of the thermodynamic parameters. Figure 2a illustrates the endothermic curves generated from the phase transition of melting a flaxseed oil sample of the Szafir variety. The melting process for the samples was followed by prior crystallization of the samples at −65 °C with cooling at a scanning rate of 2 °C/min, after which the sample was heated with a scanning rate of 5 °C/min. Due to the complexity of the melting curves, which appear to be multicomponent, as the plethora of lipid components melt sequentially according to their increasing melting point, there was a need to use a peak deconvolution procedure, as shown in Figure 2b. For all the varieties, four peaks were identified during the melting process occurring from −65 °C to 30 °C. From the DSC curves presented in Figure 2, it is clear that the melting temperature initiated at around −40 °C, and the phase transition finished after the formation of the four encompassing peaks until the temperature reached around 0 °C. Among these four peaks, the second was considered to be the major peak, which occurred at around −30 °C. There are three more shoulder peaks along with the second peak, where the first peak can be detected at around −36 °C, and the comparatively smaller third and fourth peaks appeared at temperatures of approx. −25 °C and −12 °C, respectively. The melting behavior of the flaxseed oil is influenced by the composition

of fatty acids that are bound in acylglycerols, mainly DAG and TAG. As was shown in a lipidomic study, 39 DAGs and 110 TAGs in the flaxseed oil were identified [32], which differ in their melting points. The position of the unsaturated bonds and the length of the fatty acid chains regulates the energy involved in the phase transition of the polymorph [33]. The appearance of multiple peaks can be the consequence of two simultaneously occurring phenomena, i.e., the complex distribution of TAGs and the polymorphic rearrangement of crystals, which can especially take place during the slow melting of lipid components [34]. In this study, a fast-scanning rate (5 °C/min) was used, which limits the polymorphic transitions. Furthermore, the distribution of the TAG's as polymorphs cannot be surmised using the DSC curves, and research rather suggests that the X-ray diffraction method might be an effective tool to understand the in-depth cognition of each crystal packed in a TAG molecule and their discrete melting behavior [35,36]. However, the DSC curves can provide us with the paradigm of heat transition from one physical state to another [37].

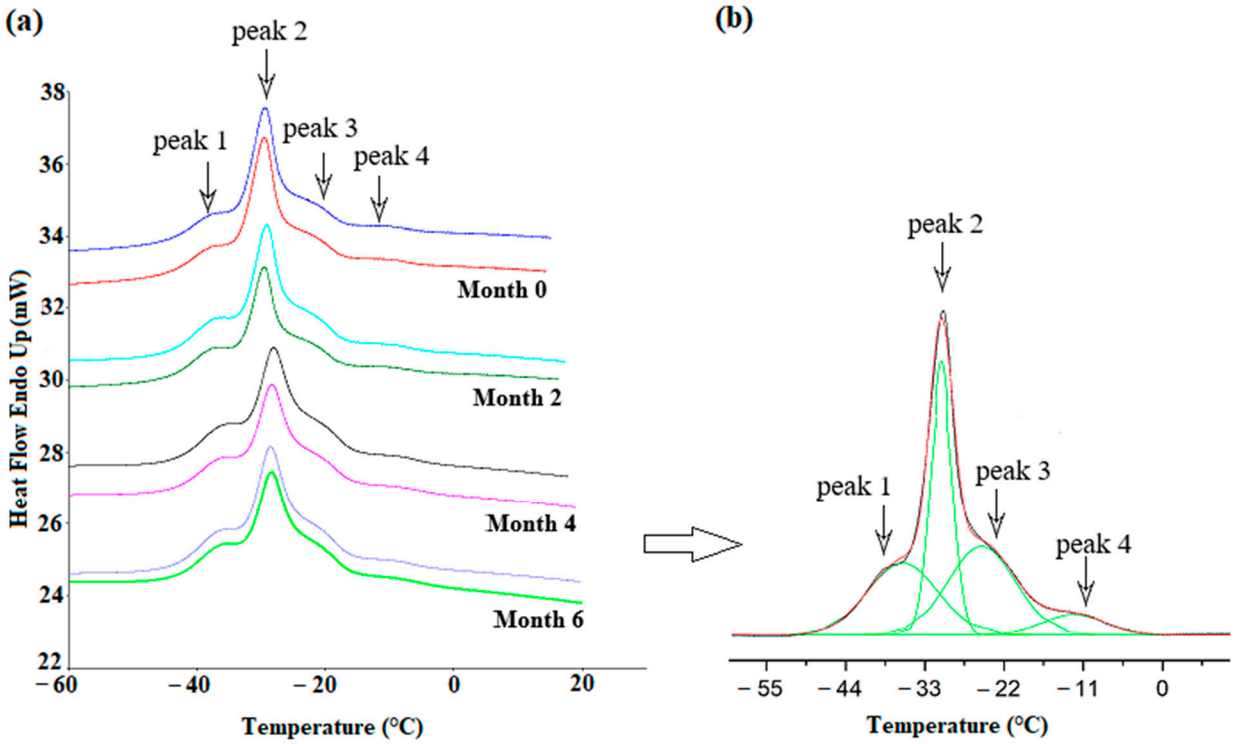

Figure 2. (**a**) Melting curves obtained from DSC analysis of cold-pressed flaxseed oil (FL_SZB) with heating rate of 5 °C/min during whole shelf life (0, 2, 4, and 6 months); (**b**) and deconvolution of melting curve of fresh flaxseed oil.

In order to assess the parameters describing the melting curves, a deconvolution procedure was carried out to separate the four peaks. Over the decades, a computational method using a deconvolution algorithm has been employed by authors to analyze the complex DSC profiles [38,39]. Several parameters were taken under consideration to access the melting phase transition occurring in the flaxseed oil samples, i.e., peak temperature, peak height, peak area, and the percentage of the area. As a result, the various parameters of each peak were obtained, i.e., peak temperatures (T1, T2, T3, and T4), which are shown in Table 2; the peak heights (h1, h2, h3, and h4), which are presented in Table 3; the peak areas (A1, A2, A3, and A4); and the calculated percentages of the peak areas (P A1, P A2, P A3, and P A4), which are shown in Table 4.

Table 2. Peak temperature changes (T, °C) of DSC melting curves of flaxseed oils during storage (0, 2, 4, and 6 months).

Peak Temperature (°C)	Time	FL_BU	FL_DL	FL_SZA	FL_SZB	FL_NN
T1	0	−36.85 ± 0.11 ^{aA}	−36.37 ± 0.12 ^{aAB}	−36.65 ± 0.22 ^{aAB}	−36.36 ± 0.07 ^{aA}	−36.55 ± 0.93 ^{aA}
	2	−37.19 ± 0.37 ^{abA}	−36.93 ± 0.27 ^{abcA}	−37.57 ± 0.36 ^{aA}	−36.2 ± 0.18 ^{cA}	−36.44 ± 0.32 ^{bcA}
	4	−36.72 ± 0.62 ^{aA}	−36.58 ± 0.06 ^{aAB}	−36.44 ± 0.18 ^{aB}	−35.69 ± 0.46 ^{abA}	−34.80 ± 0.17 ^{bB}
	6	−36.55 ± 0.18 ^{aA}	−36.12 ± 0.29 ^{abB}	−36.38 ± 0.20 ^{aB}	−35.59 ± 0.11 ^{bA}	−35.59 ± 0.06 ^{bAB}
T2	0	−31.67 ± 0.09 ^{aA}	−30.10 ± 0.11 ^{abAB}	−30.37 ± 0.25 ^{abB}	−29.72 ± 0.05 ^{bA}	−30.01 ± 0.97^{a} ^{bA}
	2	−31.54 ± 0.2 ^{aA}	−30.50 ± 0.29 ^{bcA}	−31.06 ± 0.21 ^{abA}	−29.64 ± 0.23 ^{dA}	−30.00 ± 0.25 ^{cdA}
	4	−30.88 ± 0.27 ^{aB}	−29.31 ± 0.28 ^{bcB}	−29.53 ± 0.12 ^{bC}	−28.35 ± 0.20 ^{dB}	−28.66 ± 0.03 ^{cdA}
	6	−30.22 ± 0.11 ^{aB}	−29.39 ± 0.24 ^{bB}	−29.67 ± 0.08 ^{abC}	−28.6 ± 0.13 ^{cB}	−28.55 ± 0.08 ^{cA}
T3	0	−25.12 ± 0.00 ^{aA}	−24.94 ± 0.18 ^{abA}	−24.96 ± 0.2 ^{abA}	−24.19 ± 0.12 ^{bA}	−24.58 ± 0.54 ^{abA}
	2	−25.01 ± 0.00 ^{aA}	−25.05 ± 0.09 ^{aA}	−25.14 ± 0.00 ^{aA}	−24.85 ± 0.08 ^{abA}	−24.55 ± 0.22 ^{bA}
	4	−24.98 ± 0.16 ^{aA}	−25.10 ± 0.00 ^{aA}	−25.11 ± 0.00 ^{aA}	−24.63 ± 0.66 ^{aA}	−23.31 ± 0.16 ^{bB}
	6	−25.12 ± 0.00 ^{aA}	−24.55 ± 0.77 ^{aA}	−25.13 ± 0.00 ^{aA}	−24.47 ± 0.04 ^{aA}	−22.99 ± 0.07 ^{bB}
T4	0	−13.63 ± 0.24 ^{aA}	−12.50 ± 0.49 ^{abA}	−12.64 ± 0.34 ^{abA}	−12.20 ± 0.06 ^{bA}	−13.87± 0.18 ^{aA}
	2	−13.57 ± 0.16 ^{aA}	−12.84 ± 0.18 ^{abA}	−13.27 ± 0.20 ^{aA}	−11.76 ± 0.42 ^{cA}	−12.21 ± 0.61 ^{bcB}
	4	−14.02 ± 0.00 ^{aA}	−10.62 ± 0.23 ^{bcB}	−11.13 ± 0.24 ^{bB}	−10.40 ± 0.29 ^{bcB}	−9.94 ± 0.15 ^{cC}
	6	−12.05 ± 0.24 ^{bB}	−11.24 ± 0.16 ^{aB}	−11.13 ± 0.04 ^{abB}	−10.54 ± 0.28 ^{cB}	−10.49 ± 0.08 ^{cC}

FL_BU (Bukoz cultivar), FL_DL (Dolguniec cultivar), FL_SZA, FL SZB (Szafir cultivar), FL_NN (Unknown Flaxseed cultivar). T1—peak temperature for first peak, counting from lower to higher temperature as T2, T3, and T4. All values are mean ± standard deviation of the two replicates. (a–d) means with the same superscript within the same row are not different ($p > 0.05$); (A–C) means with the same superscript within the same column are not different ($p > 0.05$).

Table 3. Peak height changes (h, W/g) of DSC melting curves of flaxseed oils during storage (0, 2, 4, and 6 months).

Peak Height (W/g)	Time	FL_BU	FL_DL	FL_SZA	FL_SZB	FL_NN
h1	0	0.15 ± 0.008 ^{bB}	0.13 ± 0.008 ^{abA}	0.14 ± 0.005 ^{abA}	0.12 ± 0.008 ^{aA}	0.08 ± 0.014 ^{aA}
	2	0.17 ± 0.007 ^{cB}	0.15 ± 0.006 ^{bA}	0.15 ± 0.008 ^{bcA}	0.13 ± 0.004 ^{aA}	0.12 ± 0.003 ^{aA}
	4	0.12 ± 0.004 ^{abcA}	0.14 ± 0.008 ^{bcA}	0.15 ± 0.002 ^{cA}	0.11 ± 0.006 ^{abA}	0.11 ± 0.013 ^{aA}
	6	0.15 ± 0.006 ^{aB}	0.13 ± 0.024 ^{bA}	0.15 ± 0.011 ^{abA}	0.12 ± 0.000 ^{cA}	0.12 ± 0.001 ^{cA}
h2	0	0.47 ± 0.033 ^{aB}	0.52 ± 0.099 ^{aA}	0.46 ± 0.003 ^{aB}	0.52 ± 0.002 ^{aC}	0.51 ± 0.062 ^{aAB}
	2	0.43 ± 0.016 ^{aB}	0.46 ± 0.008 ^{abA}	0.46 ± 0.012 ^{abB}	0.48 ± 0.013 ^{bB}	0.48 ± 0.031 ^{bB}
	4	0.45 ± 0.005 ^{cB}	0.37 ± 0.005 ^{abA}	0.37 ± 0.000 ^{aA}	0.40 ± 0.005 ^{bA}	0.46 ± 0.016 ^{cAB}
	6	0.36 ± 0.007 ^{aA}	0.42 ± 0.040 ^{aA}	0.39 ± 0.013 ^{aA}	0.41 ± 0.010 ^{aA}	0.38 ± 0.000 ^{aA}
h3	0	0.14 ± 0.006 ^{aA}	0.14 ± 0.006^{a} ^{A}	0.14 ± 0.000 ^{aA}	0.15 ± 0.005 ^{aA}	0.13 ± 0.000 ^{aA}
	2	0.14 ± 0.002 ^{aA}	0.15 ± 0.006 ^{bAB}	0.15 ± 0.001 ^{bB}	0.16 ± 0.006 ^{bA}	0.16 ± 0.002 ^{bB}
	4	0.14 ± 0.003 ^{aA}	0.17 ± 0.003 ^{bB}	0.16 ± 0.008 ^{abB}	0.15 ± 0.010 ^{abA}	0.14 ± 0.008 ^{aA}
	6	0.14 ± 0.001 ^{aA}	0.14 ± 0.002 ^{aA}	0.15 ± 0.001 ^{aB}	0.15 ± 0.008 ^{aA}	0.14 ± 0.001 ^{aA}
h4	0	0.02 ± 0.001 ^{cAB}	0.01 ± 0.001 ^{aA}	0.02 ± 0.001 ^{bAB}	0.02 ± 0.001 ^{bcB}	0.02 ± 0.002 ^{bcB}
	2	0.03 ± 0.002 ^{cB}	0.02 ± 0.001 ^{abA}	0.02 ± 0.001 ^{bcB}	0.02 ± 0.001 ^{aB}	0.02 ± 0.003 ^{abB}
	4	0.02 ± 0.002 ^{bA}	0.02 ± 0.001 ^{abA}	0.02 ± 0.000 ^{abA}	0.01 ± 0.002 ^{bA}	0.01 ± 0.002 ^{bA}
	6	0.02 ± 0.000 ^{bA}	0.01 ± 0.004 ^{abA}	0.01 ± 0.003 ^{abA}	0.01 ± 0.003 ^{abA}	0.01 ± 0.000 ^{aA}

FL_BU (Bukoz cultivar), FL_DL (Dolguniec cultivar), FL_SZA, FL_SZB (Szafir cultivar), FL_NN (Unknown cultivar). h1—peak height for first peak, counting from first to fourth peak as h2, h3, and h4. All values are mean ± standard deviation of the two replicates. (a–c) means with the same superscript within the same row are not different ($p > 0.05$); (A–C) means with the same superscript within the same column are not different ($p > 0.05$).

Table 4. Peak area (A) and percentage of peak area (P A) changes of DSC melting curves for flaxseed oils during storage (0, 2, 4, and 6 months).

Peak Area	Time	FL_BU	FL_DL	FL_SZA	FL_SZB	FL_NN
A1	0	1.39 ± 0.07^{bB}	1.18 ± 0.07^{abA}	1.19 ± 0.04^{abA}	1.03 ± 0.07^{aA}	0.86 ± 0.12^{aA}
	2	1.45 ± 0.06^{cB}	1.27 ± 0.05^{bA}	1.33 ± 0.07^{bcA}	1.12 ± 0.04^{aA}	1.04 ± 0.02^{aA}
	4	1.09 ± 0.03^{abA}	1.14 ± 0.1^{abA}	1.30 ± 0.02^{bA}	0.10 ± 0.07^{aA}	0.93 ± 0.11^{aA}
	6	1.36 ± 0.05^{aB}	1.12 ± 0.21^{aA}	1.30 ± 0.04^{aA}	1.07 ± 0.00^{aA}	1.08 ± 0.01^{aA}
A2	0	2.50 ± 0.20^{aB}	2.68 ± 0.73^{aB}	2.22 ± 0.01^{aB}	2.70 ± 0.05^{aC}	2.42 ± 0.04^{aA}
	2	2.20 ± 0.08^{aB}	2.19 ± 0.04^{aAB}	2.28 ± 0.03^{aB}	2.21 ± 0.14^{aB}	2.42 ± 0.26^{aA}
	4	2.29 ± 0.04^{bB}	1.23 ± 0.11^{aA}	1.40 ± 0.09^{aA}	1.61 ± 0.05^{aA}	2.31 ± 0.20^{bA}
	6	1.41 ± 0.06^{aA}	1.74 ± 0.16^{abAB}	1.62 ± 0.18^{abA}	1.72 ± 0.05^{abA}	1.89 ± 0.02^{bA}
A3	0	1.20 ± 0.00^{aA}	1.35 ± 0.06^{abA}	1.32 ± 0.00^{abA}	1.44 ± 0.05^{bA}	1.25 ± 0.00^{aA}
	2	1.29 ± 0.03^{aB}	1.44 ± 0.06^{bAB}	1.41 ± 0.06^{abA}	1.50 ± 0.06^{bA}	1.48 ± 0.02^{bB}
	4	1.29 ± 0.02^{aB}	1.58 ± 0.02^{bB}	1.49 ± 0.08^{abA}	1.44 ± 0.09^{abA}	1.32 ± 0.08^{bA}
	6	1.38 ± 0.01^{aC}	1.38 ± 0.02^{aA}	1.47 ± 0.01^{aA}	1.41 ± 0.08^{aA}	1.34 ± 0.01^{aA}
A4	0	0.21 ± 0.01^{bB}	0.14 ± 0.02^{aAB}	0.18 ± 0.02^{abB}	0.18 ± 0.02^{abB}	0.22 ± 0.02^{bB}
	2	0.22 ± 0.01^{bB}	0.19 ± 0.01^{abB}	0.23 ± 0.01^{bC}	0.15 ± 0.02^{aB}	0.20 ± 0.04^{abB}
	4	0.18 ± 0.02^{bAB}	0.12 ± 0.01^{aA}	0.13 ± 0.00^{abA}	0.08 ± 0.02^{aA}	0.08 ± 0.02^{aA}
	6	0.14 ± 0.00^{bA}	0.11 ± 0.02^{abA}	0.11 ± 0.02^{abA}	0.09 ± 0.02^{abA}	0.06 ± 0.00^{aA}
% peak area						
P A1	0	26.21 ± 0.07^{bB}	22.18 ± 2.33^{abA}	24.25 ± 0.57^{abA}	19.23 ± 0.99^{aA}	18.16 ± 2.17^{aA}
	2	28.16 ± 1.30^{cB}	25.02 ± 0.20^{bA}	25.33 ± 1.09^{bcA}	22.54 ± 0.74^{abB}	20.33 ± 1.62^{aA}
	4	22.49 ± 0.13^{aA}	28.01 ± 1.06^{bcA}	30.20 ± 0.25^{cB}	24.11 ± 1.49^{abB}	20.13 ± 2.37^{aA}
	6	31.65 ± 0.36^{bC}	25.58 ± 2.89^{aA}	28.97 ± 0.47^{abB}	24.93 ± 0.04^{aB}	24.67 ± 0.15^{aA}
P A2	0	48.21 ± 1.32^{aC}	50.03 ± 5.48^{aC}	45.91 ± 0.42^{aB}	52.65 ± 1.66^{aC}	51.71 ± 1.92^{aA}
	2	42.67 ± 1.12^{aB}	43.03 ± 0.59^{aBC}	43.40 ± 0.70^{aB}	44.35 ± 0.95^{abB}	47.08 ± 2.32^{bA}
	4	47.15 ± 0.22^{bcC}	30.07 ± 1.38^{aA}	32.45 ± 1.88^{aA}	38.94 ± 0.73^{abA}	49.70 ± 4.3^{cA}
	6	32.99 ± 0.62^{aA}	40.01 ± 0.65^{bcB}	35.88 ± 2.1^{abA}	40.12 ± 1.26^{bcA}	43.37 ± 0.45^{cA}
P A3	0	22.68 ± 1.15^{aA}	25.49 ± 3.05^{aA}	26.85 ± 0.41^{aA}	26.85 ± 0.45^{aA}	26.36 ± 0.49^{aA}
	2	24.87 ± 0.47^{aAB}	28.21 ± 0.24^{bcA}	26.87 ± 1.32^{abA}	30.03 ± 0.41^{cAB}	28.80 ± 1.28^{abAB}
	4	26.63 ± 0.26^{aB}	38.92 ± 2.47^{cB}	34.43 ± 2.14^{abcB}	34.95 ± 2.58^{bcB}	28.35 ± 1.59^{abAB}
	6	32.18 ± 0.98^{aC}	31.80 ± 2.79^{aAB}	32.77 ± 1.96^{aB}	32.86 ± 1.88^{aB}	30.68 ± 0.24^{aB}
P A4	0	3.94 ± 0.10^{bcAB}	2.61 ± 0.11^{aA}	3.67 ± 0.26^{bcB}	3.45 ± 0.22^{abB}	4.55 ± 0.25^{cB}
	2	4.30 ± 0.24^{bB}	3.74 ± 0.16^{abA}	4.40 ± 0.14^{bC}	3.07 ± 0.20^{aAB}	3.78 ± 0.61^{abB}
	4	3.73 ± 0.36^{cAB}	2.99 ± 0.03^{bcA}	2.92 ± 0.01^{abcAB}	1.99 ± 0.39^{abA}	1.81 ± 0.34^{aA}
	6	3.17 ± 0.01^{bA}	2.61 ± 0.76^{abA}	2.37 ± 0.33^{abA}	2.09 ± 0.58^{abA}	1.27 ± 0.06^{aA}

FL_BU (Bukoz cultivar), FL_DL (Dolguniec cultivar), FL_SZA, FL SZB (Szafir cultivar), FL_NN (Unknown cultivar). A1—peak area for first peak, counting from first to fourth peak as A2, A3, and A4. and P A1—percentage of peak area for first peak, counting from first peak to fourth peak as P A2, P A3, and P A4. All values are mean ± standard deviation of the two replicates. (a–c) means with the same superscript within the same row are not different ($p > 0.05$); (A–C) means with the same superscript within the same column are not different ($p > 0.05$).

Table 2 presents the peak temperature data of the four peaks identified for the five fresh and stored (2, 4, and 6 months) flaxseed oils samples. Four endothermic peaks appeared around the same temperature range for all varieties, which confirms the similarity of the thermal profiles for the flaxseed oils. The statistical exploration was based on a comparison of the variances between the varieties and between the different storage times. Generally, the comparison of varieties for the fresh oils showed that the temperatures of peaks T2, T3, and T4 were significantly higher only for sample FL_SZB than for the rest of the samples ($p \leq 0.05$), although these differences were not greater than 2 °C. Temperature peak differences among the varieties are associated with the composition of PUFA, MUFA, and SFA in the flaxseed oils. As shown in Table 2, samples FL_SZB and FL_NN were characterized by the lowest content of PUFA, which justifies the highest peak temperatures for those

varieties with a lower count of unsaturated C=C bonds (i.e., MUFA and PUFA). Other authors also stated that for canola oil, those peaks, which represent a lower temperature transition, are associated with the melting of unsaturated fatty acids [30]. Additionally, four peak temperatures throughout the storage time (0, 2, 4, and 6 months) were compared, as presented in Table 2. These data show that the main peak (T2) always gradually shifted towards a higher temperature until six months of storage (significantly, $p \leq 0.05$), except for the FL_NN sample, for which the parameter T2 increased with time, but the changes were not significant ($p > 0.05$). The peak temperature T4 was significantly higher for all oil samples after six months ($p \leq 0.05$). In comparison, T1 and T3 seemed to be more stable throughout the storage time analysis, since no significant changes took place for the measurements taken in different months ($p > 0.05$).

Table 3 presents the results of the measurement of the peak height of the four peaks calculated from the DSC curves. The parameter of the peak height expresses in the DSC analysis the intensity of the phase transition phenomena, which is dependent on the scanning rate used; the higher the scanning rate, the higher the peak height [2]. Thus, the parameters of the peak height that were obtained with the same scanning rate can only be compared, since the peak height is proportional to the rate of the heat transfer, which was also confirmed by other authors [40]. Generally, the parameters of the peak height (h1, h2, h3, and h4) for the fresh flaxseed oils did not differ significantly between the oil varieties, except for sample FL_BU, for which h1 was significantly different from the rest of the oil varieties ($p \leq 0.05$). Among all the flaxseed oils samples, the peak height of the main peak (h2) and the last peak (h4) were significantly ($p \leq 0.05$) lowered after six months of storage. On the other hand, two other minor peaks, h1 and h3, were quite stable during the storage period.

Table 4 presents the results of the calculations of the peak area of the four peaks (A1, A2, A3, and A4) determined by the deconvolution analysis. Comparing the parameters of the peak area between the oil samples, it can be seen that the area of the second peak (A2), determined between 2.2 and 2.7 for the fresh oils, makes the greatest contribution to the melting phenomena of the complex TAG structures. For the fresh flaxseed oils, A2 did not differ significantly between the oil varieties ($p > 0.05$).

Analyzing the influence of the storage time, it can be seen that the area of the first and third peaks (A1, A3) did not change significantly within the six months of storage, in contrast to the values for the second (A2) and fourth (A4) peaks, for which a significant lowering of values was observed within the storage time ($p \leq 0.05$). It is noticeable that the changes in the area of the peaks (A2, A4) observed during storage are in line with the changes in the peak height values (h2, h4). As shown in Table 4, the percentage of each peak area was also calculated based on the accumulated values of the total area of the endothermic peaks of the melting curves. Comparing the values of the percentage of the area within the storage time, it can be seen that for the first, second, and third peaks, the parameters P A1 and P A3 increased significantly ($p \leq 0.05$), while PA2 decreased after six months. This is because the values of the peak areas (A1, A2, A3, and A4) are expressed as absolute values and the percentages of the area (P A1, P A2, P A3, P A4) are relative values, depending on the changes in the area of other peaks. The difference between the area and the percentage of the area is visible in the example of the first and third peaks (A1 and A3), which did not change significantly within the six months of storage, whereas the percentage of the peak area (P A1, P A3) increased, due to the decrease in the area of the second peak (A2). This observation implies that the changes in the percentage of the area (P A) should be considered only when all the peaks are analyzed together.

4. Discussion

4.1. Determination of DSC Parameters as Markers of Authenticity and Deterioration of Flaxseed Oil

For the purposes of this study, control charts were used to select the DSC parameters which remained stable throughout the shelf-life period, which can be used for fingerprinting

as authenticity markers. On the other hand, all DSC parameters changing within the time of storage can be recognized as indicators of deterioration. Control charts are a common statistical tool for monitoring the conformity of products or processes with a reference value [41,42]. Referring to the study conducted on the stability of the DSC profile, monitoring with a control chart means that if the storage time does not affect the changes of the selected parameters, its level will not exceed the control limits ($\pm 3\sigma$), and it will then be considered as a stable parameter during storage. Therefore, it appears reasonable to suggest the possibility of determining the limits that these parameters can reach regardless of the storage time of the oils. They will be characteristic for the different types of oils. In this study, X-bar and R (arithmetic mean and range) control charts were used to test the stability of the selected melting profile parameters. The X-bar chart and the R chart are actually two different graphs that must be considered in tandem to understand the behavior of the parameter being measured. The X-bar chart shows the average level of the parameter being monitored, while the R chart shows the range, i.e., the difference between the smallest and largest value in each sample, at each time point of storage, thus explaining the variability of the variation. In fact, to the best of the authors' knowledge, there is no published research where a control chart was used to monitor the changes in the parameters within the storage time of cold-pressed oils. Using control charts, 16 variables were determined from the melting curves (T, h, A, and P A for the four peaks), and 18 variables were determined as ratios calculated for parameters h, A, and P A and were tested by using X-bar charts and the R charts.

4.1.1. Determination of Stable DSC Parameters as Markers of Oils' Authenticity during Storage

As it was shown in Tables 2–4, various parameters of the melting curve for flaxseed oils, i.e., peak temperature (T1, T2, T3, and T4), peak height (h1, h2, h3, and h4), peak area (A1, A2, A3, and A4), and the percentage of the peak area (P A1, P A2, P A3, and P A4) were analyzed within six months of storage. It was shown that for the first and third peaks, all DSC parameters (T, h, A, P A) did not change significantly within the storage time ($p > 0.05$). From a total amount of 16 variables (4 DSC parameters $\times$ 4 peaks) analyzed, the parameters that were remaining and anchored within the control limit in the X-bar chart were selected and denoted as 'stable parameters'. Figure 3 shows that the control charts for these parameters were found to be stable during storage, which are pertinent for all oil samples. No point exceeded the control lines on either the X-bar charts or on the R charts between "0 month" and "6 months" of storage. This means that the average level of the parameter, as well as its variability, was stable throughout the storage period. The control limits on the X-bar charts can therefore be considered as a range that is characteristic and not changeable during storage for a particular melting profile parameter of the flaxseed oil. In Figure 3a–c, stable parameters associated with the first peak are presented (i.e., T1, h1, and A1), while Figure 3d–f illustrates the parameters for the third peak (i.e., T3, h3, and A3). Based on the data acquired from the melting curves, these multivariate X-bar charts show that the first and third peak areas, heights, and temperatures did not cross the limits between the upper control limit line (ULC) and the lower control limit line (LLC), except for the T1, h3, and A3 parameters, where one control point appeared outside the range.

However, after careful observation of those points, it can be seen that the differences between the ULC and LLC are extraordinarily minimal compared to the range of undisputed parameters like A1, h1, and T3. Meanwhile, Figure 4a–f also shows a graph with the X-bar control charts prepared on the basis of the calculated ratio of DSC parameters. It can be observed that in addition to the ratio of parameters calculated for the first and third peaks, i.e., h1/h3, A1/A3, and P A1/P A3 (Figure 4a–c), there are other parameters fitting to the control limits, such as h2/h4, A2/A4, and P A2/PA4, which are calculated for the second and fourth peak (Figure 4d–f). The pivotal role of the first and third peaks regarding the authenticity analysis can be seen, and the ratio of the parameters for these two peaks are also persistently framed within the control limits. Furthermore, Figure 4

shows that the ratios calculated for the second and fourth peaks also abide by the rules to be considered as the stable parameters (h2/h4, A2/A4, and P A2/P A4), despite the fact that these individually considered parameters were not stable. It is worth noting that the parameters accountable for the percentage of the area (P A) do not have coherent properties when analyzed separately, since they depend on the other peaks, but the ratio calculated from parameters P A appeared to be a better option in this respect.

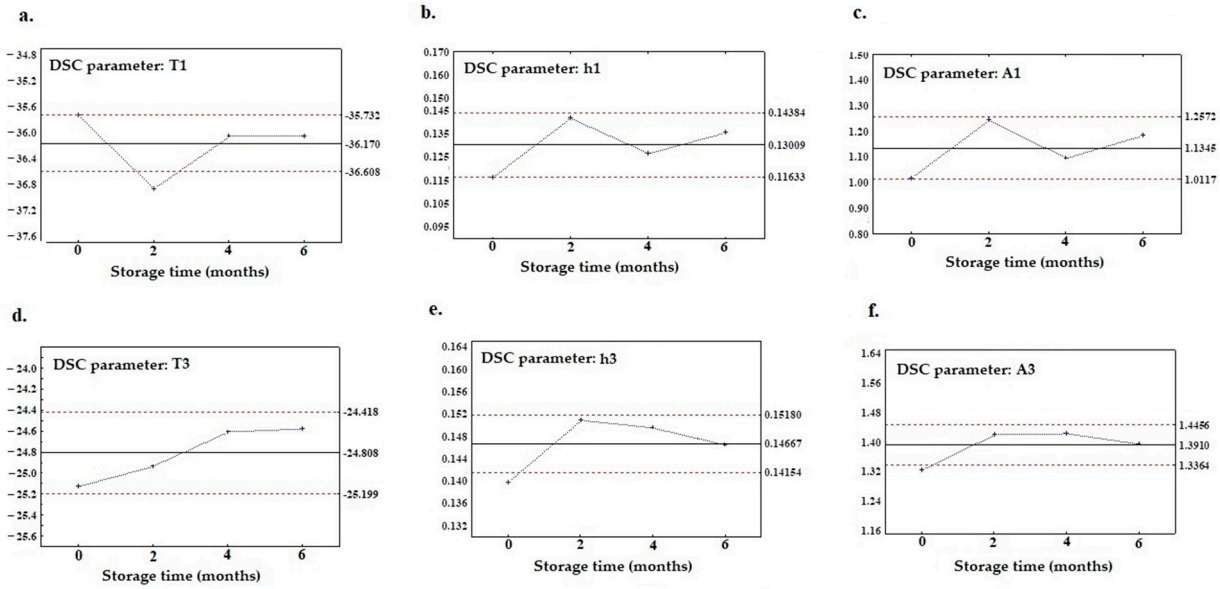

Figure 3. X-bar control charts of DSC parameters recognized as stable within six months storage; for the first peak: (**a**) T1, (**b**) h1, and (**c**) A1, and for the third peak: (**d**) T3, (**e**) h3, and (**f**) A3.

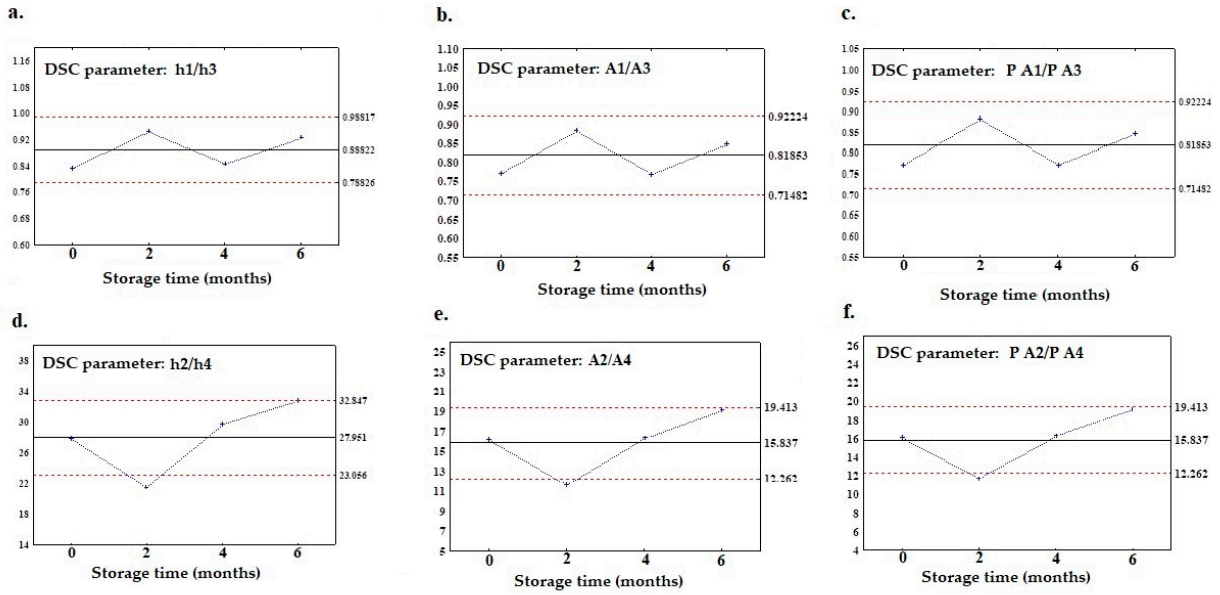

Figure 4. X-bar control charts of DSC parameters recognized as stable within six months of storage; for the ratio calculated for the first and third peaks: (**a**) h1/h3, (**b**) A1/A3, and (**c**) P A1/P A3, and for the second and fourth peaks: (**d**) h2/h4, (**e**) A2/A4P, and (**f**) P A2/P A4.

4.1.2. Detection of Flaxseed Oil Deterioration by Unstable DSC Parameters during Storage

The second purpose of this study was to recognize the DSC melting profile parameters that changed within the storage time. However, only the parameters with increasing or decreasing trends indicating changes caused by storage were considered. In order to

establish these, the control charts were analyzed in terms of the parameters for which the two control lines for the fresh and stored oils were exceeded via crossing the ULC and LLC from both ends. Figure 5a–c illustrates the control charts with the parameters of the main peak height and area (h2, A2, and PA2) for which the values decrease throughout the shelf life of the oil. From Tables 3 and 4, it is clearly seen that for all the flaxseed oil varieties, the values h2, A2, and P A2 are significantly lower after six months of storage, which coincides with the control charts presented in Figure 5a–c.

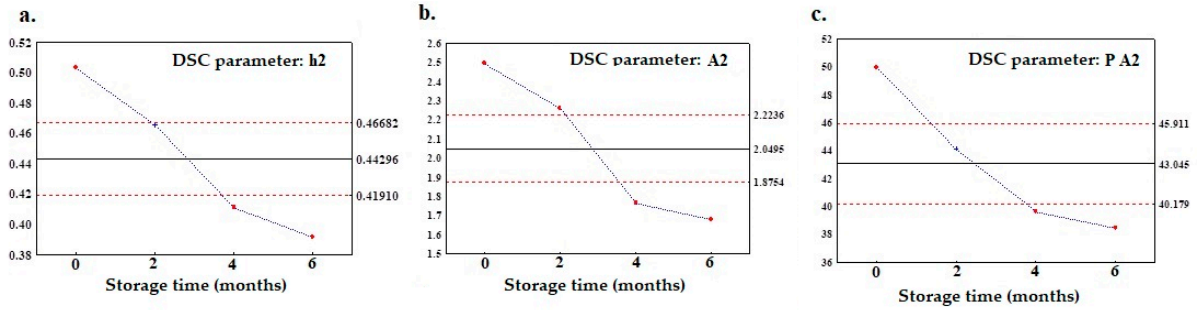

Figure 5. X-bar control charts of unstable parameters calculated from DSC melting curves for the second peak: (**a**) h2, (**b**) A2, and (**c**) P A2.

The trend within the storage time of the ratio calculated for the parameters of the peak height (h2/h1, h2/h3, h1/h4, and h3/h4), as well as the ratio of the peak area (A2/A1, A2/A3, A1/A4, and A3/A4) was also analyzed using the control charts (Figure 6a–h). can be seen, a downward trend was observed for ratios h2/h1 and h2/h3 (Figure 6a,b), as well as for A2/A1 and A2/A3 (Figure 6c,d). In turn for the parameters of h1/h4, h3/h4, A1/A4, and A3/A4, an increasing trend was shown (Figure 6e–h). Analogously, as for the ratios of the peak area (A2/A1, A2/A3, A1/A4, and A3/A4), the same trend was observed for the ratio of the percentage of the area (PA2/PA1, PA2/PA3, PA1/PA4, and PA3/PA4), which means that the values increased or decreased by the same pattern (Figure S1; Supplementary Data).

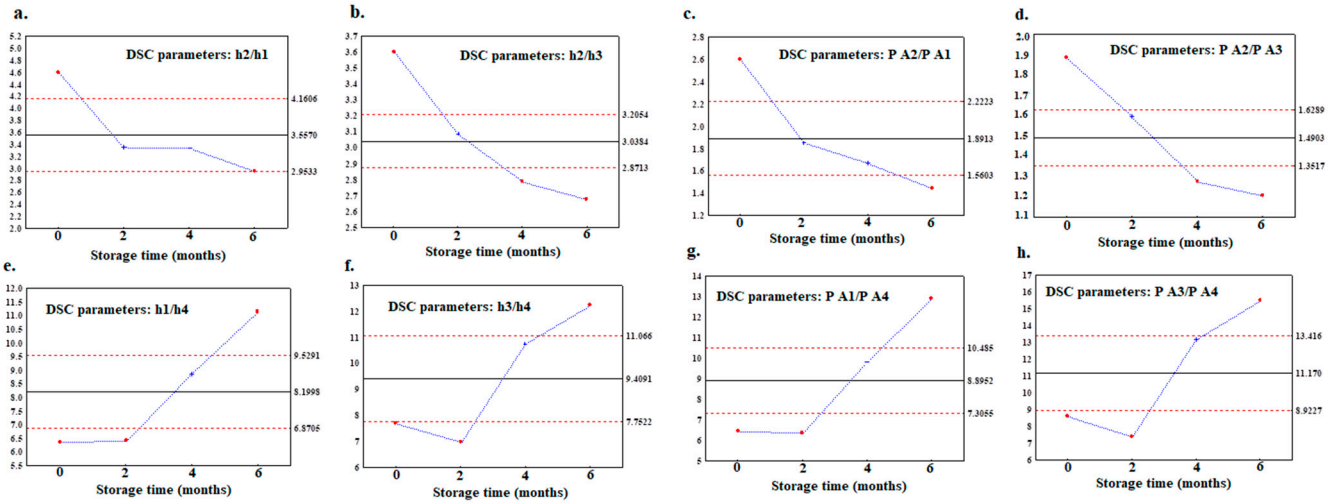

Figure 6. X-bar control charts of ratios calculated from DSC melting curves with downward trends: (**a**) h2/h1, (**b**) h2/h3, (**c**) A2/A1, (**d**) A2/A3, and with upward trends: (**e**) h1/h4, (**f**) h3/h4, (**g**) A1/A4, and (**h**) A3/A4.

In addition, a PCA analysis was applied with all the unstable parameters obtained from the DSC and fatty acid content (∑SFA, ∑MUFA, ∑PUFA) (Figure 7a,c); and also, for the DSC unstable parameters and chemical indicators (PV, p-AV, AV, TOTOX) (Figure 7b,d)

for the fresh oil samples and the ones that were stored for 6 months. It was shown that for both approaches, two distinctive clusters were separated, with a differentiation between the two groups of oils, i.e., fresh and stored (Figure 7c,d). In the graph of the variable projection (Figure 7a,b), it can be seen that the parameters connected with the second peak (h2, A2, and P A2) were the highest for fresh oil and the lowest after 6 months, in contrast to the parameters of the ratios calculated for the first and fourth peaks, as well as for the third and fourth peaks. Chemical indicators of the oxidative stability of the oil (PV, p-AV, AV, and TOTOX) were found to have strong negative correlations with the DSC unstable parameters connected to the second peak of the melting profile (for instance h2, A2, and P A2). Significant correlations ($p \leq 0.05$) were observed between p-AV, PV, AV, TOTOX, and DSC parameters that were determined for the second peak, as the Pearson correlation coefficients were, e.g., for h2: −0,63, −0.64, −0.57, and −0.64, and for A2: −0.51, −0.51, −0.64, and −0.55, respectively.

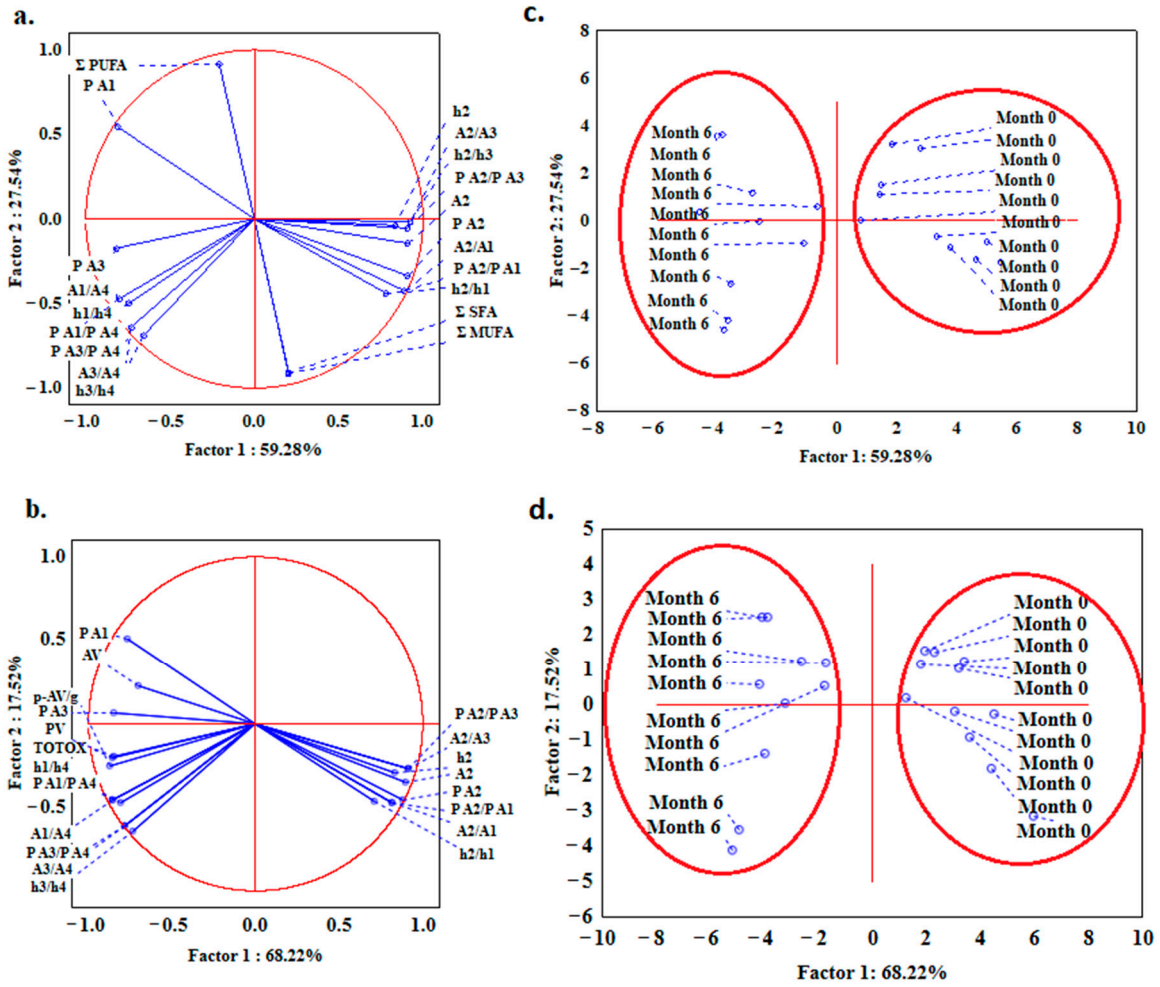

Figure 7. PCA analysis with projection of the variables: (**a**) DSC unstable parameters and fatty acids content; (**b**) DSC unstable parameters and chemical indicators (PV, p-AV, AV, and TOTOX); PCA analysis with projection of the cases showing distribution and separation of flaxseed oil samples based on their stability control by means of (**c**) DSC parameters and fatty acids content; and (**d**) DSC parameters and chemical indicators.

5. Conclusions

In the age of the global food market, rapid and ecological methods which will facilitate a fast authentication assessment are crucial. At the same level, controlling the quality of flaxseed oil is important, since it is highly susceptible to the oxidation process occurring during prolonged storage. Chemical analysis of the oxidative stability (AV, PV, p-AV, and

TOTOX) showed the changes occurring during the storage of flaxseed oil for six months, since all parameters measured increased for all the oil samples. This study proposed an approach using X-bar and R control charts to monitor the stability and changes of the DSC melting profiles of flaxseed oil stored for six months in conditions similar to the supermarket shelf. By implementing the procedure of deconvolution, four peaks were identified in the melting profile, for which the peak temperature, peak height, peak area, and the percentage of peak area were analyzed. Analysis by means of control charts enabled stable parameters of the melting profile of flaxseed oil to be determined, which were connected to the first and third peak. In total, twelve parameters calculated based on those peaks were selected, which can be considered as indicators for authentication. On the other hand, it was also possible to indicate from the melting profile those parameters that changed throughout the shelf life with an increasing or decreasing tendency. Those parameters were mainly connected with the major second peak, as well as with the ratios calculated for the first to fourth and third to fourth peak. Sixteen parameters calculated from the melting profile were found to be unstable parameters, which can be used as indicators for the deterioration of oil. In the case of the percentage of peak area (PA), values of this parameter should be considered all together, since they depend on the other peaks. Strong negative correlations of the DSC unstable parameters with chemical indicators of the oils' oxidative stability were found.

Supplementary Materials: The following supporting information can be downloaded at: https://www.mdpi.com/article/10.3390/foods12152954/s1, Figure S1: Control charts of unstable parameters (calculated from the ratio of peak's percentage of area) from DSC melting curves. (a) Ratio of parameters P A2/P A1, (b) ratio of parameters P A2/P A3, (c) ratio of parameters P A1/P A4, and (d) ratio of parameters P A3/P A4.

Author Contributions: Conceptualization, M.I. and J.T.-G.; methodology, M.I., J.T.-G., A.K. and A.G.; formal analysis, M.I., A.K. and J.T.-G.; investigation, M.I., J.T.-G. and A.G.; resources, J.T.-G.; data curation, M.I., A.K. and J.T.-G.; writing—original draft preparation, M.I. and J.T.-G.; writing—review and editing, M.I., A.K. and J.T.-G.; visualization, M.I., A.K. and J.T.-G.; supervision, A.K. and J.T.-G.; project administration, J.T.-G.; funding acquisition, J.T.-G. All authors have read and agreed to the published version of the manuscript.

Funding: This research was funded by the National Science Centre, Poland, grant number: 2018/31/B/NZ9/02762.

Data Availability Statement: Data is contained within the article and supplementary material.

Conflicts of Interest: The authors declare no conflict of interest.

References

1. FAO. Production/Yield Quantities of Oil of Linseed in World + (Total). Available online: https://www.fao.org/faostat/en/#data/QCL/visualize (accessed on 23 May 2023).
2. Tomaszewska-Gras, J.; Islam, M.; Grzeca, L.; Kaczmarek, A.; Fornal, E. Comprehensive Thermal Characteristics of Different Cultivars of Flaxseed Oil (*Linum usittatissimum* L.). *Molecules* **2021**, *26*, 1958. [CrossRef]
3. Obranović, M.; Škevin, D.; Kraljić, K.; Pospišil, M.; Neđeral, S.; Blekić, M.; Putnik, P. Influence of Climate, Variety and Production Process on Tocopherols, Plastochromanol-8 and Pigments in Flaxseed Oil. *Food Technol. Biotechnol.* **2015**, *53*, 496–504. [CrossRef]
4. Herchi, W.; Bouali, I.; Bahashwan, S.; Rochut, S.; Boukhchina, S.; Kallel, H.; Pepe, C. Changes in Phospholipid Composition, Protein Content and Chemical Properties of Fl Axseed Oil during Development. *Plant Physiol. Biochem.* **2012**, *54*, 1–5. [CrossRef]
5. Khattab, R.Y.; Zeitoun, M.A. Quality Evaluation of Flaxseed Oil Obtained by Different Extraction Techniques. *LWT Food Sci. Technol.* **2013**, *53*, 338–345. [CrossRef]
6. Komartin, R.S.; Stroescu, M.; Chira, N.; Stan, R.; Stoica-Guzun, A. Optimization of Oil Extraction from Lallemantia Iberica Seeds Using Ultrasound-Assisted Extraction. *J. Food Meas. Charact.* **2021**, *15*, 2010–2020. [CrossRef]
7. Teh, S.S.; Birch, J. Physicochemical and Quality Characteristics of Cold-Pressed Hemp, Flax and Canola Seed Oils. *J. Food Compos. Anal.* **2013**, *30*, 26–31. [CrossRef]
8. El-Beltagi, H.S.; Salama, Z.; El-Hariri, D.M. Evaluation of Fatty Acids Profile and the Content of Some Secondary Metabolites in Seeds of Different Flax Cultivars (*Linum usitatissimum* L.). *Gen. Appl. Plant Physiol.* **2007**, *33*, 187–202.
9. Tavarini, S.; Castagna, A.; Conte, G.; Foschi, L.; Sanmartin, C.; Incrocci, L.; Ranieri, A.; Serra, A.; Angelini, L.G. Evaluation of Chemical Composition of Two Linseed Varieties as Sources of Health-Beneficial Substances. *Molecules* **2019**, *24*, 3729. [CrossRef]

10. Gallardo, M.A.; Milisich, H.J.; Drago, S.R.; González, R.J. Effect of Cultivars and Planting Date on Yield, Oil Content, and Fatty Acid Profile of Flax Varieties (*Linum usitatissimum* L.). *Int. J. Agron.* **2014**, *2014*, 150570. [CrossRef]
11. Choe, E.; Min, D.B. Mechanisms and Factors for Edible Oil Oxidation. *Compr. Rev. Food Sci. Food Saf.* **2006**, *5*, 169–186. [CrossRef]
12. Choo, W.S.; Birch, J.; Dufour, J.P. Physicochemical and Quality Characteristics of Cold-Pressed Flaxseed Oils. *J. Food Compos. Anal.* **2007**, *20*, 202–211. [CrossRef]
13. Hasiewicz-Derkacz, K.; Kulma, A.; Czuj, T.; Prescha, A.; Zuk, M.; Grajzer, M.; Łukaszewicz, M.; Szopa, J. Natural Phenolics Greatly Increase Flax (*Linum usitatissimum*) Oil Stability. *BMC Biotechnol.* **2015**, *15*, 62. [CrossRef] [PubMed]
14. Islam, M.; Muzolf-Panek, M.; Fornal, E.; Tomaszewska-Gras, J. DSC Isothermal and Non-Isothermal Assessment of Thermo-Oxidative Stability of Different Cultivars of Camelina Sativa L. Seed Oils. *J. Therm. Anal. Calorim.* **2022**, *147*, 10013–10026. [CrossRef]
15. Tańska, M.; Roszkowska, B.; Skrajda, M.; Grzegorz, D. Commercial Cold Pressed Flaxseed Oils Quality and Oxidative Stability at the Beginning and the End of Their Shelf Life. *J. Oleo Sci.* **2016**, *65*, 111–121. [CrossRef]
16. Islam, M.; Bełkowska, L.; Konieczny, P.; Fornal, E.; Tomaszewska-Gras, J. Differential Scanning Calorimetry for Authentication of Edible Fats and Oils—What Can We Learn from the Past to Face the Current Challenges? *J. Food Drug Anal.* **2022**, *30*, 185–201. [CrossRef]
17. Islam, M.; Rajagukguk, Y.V.; Siger, A.; Tomaszewska-Gras, J. Assessment of Hemp Seed Oil Quality Pressed from Fresh and Stored Seeds of Henola Cultivar Using Differential Scanning Calorimetry. *Foods* **2023**, *12*, 135. [CrossRef]
18. Cichocki, W.; Kmiecik, D.; Baranowska, H.M.; Staroszczyk, H.; Sommer, A.; Kowalczewski, P.Ł. Chemical Characteristics and Thermal Oxidative Stability of Novel Cold-Pressed Oil Blends: GC, LF NMR, and DSC Studies. *Foods* **2023**, *12*, 2660. [CrossRef] [PubMed]
19. Rajagukguk, Y.V.; Islam, M.; Tomaszewska-Gras, J. Influence of Seeds' Age and Clarification of Cold-Pressed Raspberry (*Rubus idaeus* L.) Oil on the DSC Oxidative Stability and Phase Transition Profiles. *Foods* **2023**, *12*, 358. [CrossRef]
20. Zhang, Z.S.; Li, D.; Zhang, L.X.; Liu, Y.L.; Wang, X.-D. Heating Effect on the DSC Melting Curve of Flaxseed Oil. *J. Therm. Anal. Calorim.* **2014**, *115*, 2129–2135. [CrossRef]
21. AOCS. AOCS Official Method Preparations of Methyl Esters of Fatty Acids. 1997. Available online: https://www.coursehero.com/file/53583244/AOCS-Official-Method-Ce-2-66-Preparation-of-Methyl-Esters-of-Fatty-Acidspdf/ (accessed on 20 May 2023).
22. AOCS. AOCS Official Method Acid Value. Cd 3d-63. 2009. Available online: https://myaccount.aocs.org/PersonifyEbusiness/Store/Product-Details/productId/111545 (accessed on 20 May 2023).
23. *ISO 3960*; Animal and Vegetable Fats and Oils—Determination—Iodometric (Visual) Endpoint. International Organization for Standardization: Geneva, Switzerland, 2017.
24. *ISO 6885*; Animal and Vegetable Fats and Oils: Determination of Anisidine Value. ISO: Geneva, Switzerland, 2016.
25. Tomaszewska-Gras, J. Rapid Quantitative Determination of Butter Adulteration with Palm Oil Using the DSC Technique. *Food Control* **2016**, *60*, 629–635. [CrossRef]
26. Anastasiu, A.E.; Chira, N.A.; Banu, I.; Ionescu, N.; Stan, R.; Rosca, S.I. Oil Productivity of Seven Romanian Linseed Varieties as Affected by Weather Conditions. *Ind. Crop. Prod.* **2016**, *86*, 219–230. [CrossRef]
27. Cantele, C.; Bertolino, M.; Bakro, F.; Giordano, M.; Jędryczka, M.; Cardenia, V. Antioxidant Effects of Hemp (*Cannabis Sativa* L.) Inflorescence Extract in Stripped Linseed Oil. *Antioxidants* **2020**, *9*, 1131. [CrossRef] [PubMed]
28. Malcolmson, L.J.; Przybylski, R.; Daun, J.K. Storage Stability of Milled Flaxseed. *JAOCS J. Am. Oil Chem. Soc.* **2000**, *77*, 235–238. [CrossRef]
29. Prescha, A.; Grajzer, M.; Dedyk, M.; Grajeta, H. The Antioxidant Activity and Oxidative Stability of Cold-Pressed Oils. *JAOCS J. Am. Oil Chem. Soc.* **2014**, *91*, 1291–1301. [CrossRef]
30. Codex Alimentarius. Standard for Named Vegetable Oils Codex Stan 210-1999. In *Codex Alimentarius*; FAO: Rome, Italy, 1999; pp. 1–13.
31. Gordon, M.H. *The Development of Oxidative Rancidity in Foods*; Woodhead Publishing Ltd.: Sawston, UK, 2001. [CrossRef]
32. Kozub, A.; Nikolaichuk, H.; Przykaza, K.; Tomaszewska-Gras, J.; Fornal, E. Lipidomic Characteristics of Three Edible Cold-Pressed Oils by LC/Q-TOF for Simple Quality and Authenticity Assurance. *Food Chem.* **2023**, *415*, 135761. [CrossRef] [PubMed]
33. Mcelhaney, R.N. The Use of Differential Scanning Calorimetry and Differential Thermal Analysis in Studies of Model and Biological Membranes. *Chem. Phys. Lipids* **1982**, *30*, 229–259. [CrossRef]
34. Tan, C.P.; Che Man, Y.B. Comparative Differential Scanning Calorimetric Analysis of Vegetable Oils: I. Effects of Heating Rate Variation. *Phytochem. Anal.* **2002**, *13*, 129–141. [CrossRef]
35. Minato, A.; Ueno, S.; Yano, J.; Smith, K.; Seto, H.; Amemiya, Y.; Sato, K. Thermal and Structural Properties of Sn-1,3-Dipalmitoyl-2-Oleoylglycerol and Sn-1,3-Dioleoyl-2-Palmitoylglycerol Binary Mixtures Examined with Synchrotron Radiation X-Ray Diffraction. *JAOCS J. Am. Oil Chem. Soc.* **1997**, *74*, 1213–1220. [CrossRef]
36. Pratama, Y.; Burholt, S.; Baker, D.L.; Sadeghpour, A.; Simone, E.; Rappolt, M. Polymorphism of a Highly Asymmetrical Triacylglycerol in Milk Fat: 1-Butyryl 2-Stearoyl 3-Palmitoyl-Glycerol. *Cryst. Growth Des.* **2022**, *22*, 6120–6130. [CrossRef]
37. Tan, C.P.; Che Man, Y.B. Differential Scanning Calorimetric Analysis of Edible Oils: Comparison of Thermal Properties and Chemical Composition. *JAOCS J. Am. Oil Chem. Soc.* **2000**, *77*, 143–155. [CrossRef]

38. Konieczny, P.; Tomaszewska-Gras, J.; Andrzejewski, W.; Mikołajczak, B.; Urbańska, M.; Mazurkiewicz, J.; Stangierski, J. DSC and Electrophoretic Studies on Protein Denaturation of Anodonta Woodiana (Lea, 1834). *J. Therm. Anal. Calorim.* **2016**, *126*, 69–75. [CrossRef]
39. Vega, S.; Garcia-Gonzalez, M.A.; Lanas, A.; Velazquez-Campoy, A.; Abian, O. Deconvolution Analysis for Classifying Gastric Adenocarcinoma Patients Based on Differential Scanning Calorimetry Serum Thermograms. *Sci. Rep.* **2015**, *5*, 7988. [CrossRef] [PubMed]
40. Saito, Y.; Saito, K.; Ataké, T. Theoretical Analysis of Peak Height in Classical DTA, Power-Compensated DSC and Heat-Flux DSC. *Thermochim. Acta* **1986**, *107*, 277–282. [CrossRef]
41. Lim, S.A.H.; Antony, J.; Albliwi, S. Statistical Process Control (SPC) in the Food Industry—A Systematic Review and Future Research Agenda. *Trends Food Sci. Technol.* **2014**, *37*, 137–151. [CrossRef]
42. Pudjihardjo, I.; Mulyana, I.J.; Asrini, L.J. Autocorrelated Multivariate Control Chart in Cooking Oil Industry. *Proc. Int. Conf. Ind. Eng. Oper. Manag.* **2019**, *2019*, 1440–1448.

Statement about the contribution of authors

Publication title A3: Islam, M.; Kaczmarek, A.; Grygier, A.; Tomaszewska-Gras, J. DSC Phase Transition Profiles Analyzed by Control Charts to Determine Markers for the Authenticity and Deterioration of Flaxseed Oil during Storage. Foods 2023, 12, 2954. https://doi.org/10.3390/foods12152954

Author	Contribution	Percentage contribution	Signature
Mahbuba Islam	Conceptualization, Methodology, Formal analysis, Investigation, Data curation, Writing- original draft preparation, Writing—review and editing, Visualization.	45	
Anna Kaczmarek	Methodology, Formal analysis, Data curation, Writing- review and editing, Visualization, Supervision.	20	
Anna Grygier	Methodology, Investigation.	5	
Jolanta Tomaszewska-Gras	Conceptualization, Methodology, Formal analysis, Investigation, Resources, Data curation, Writing- original draft preparation, Writing- review and editing, Visualization, Supervision, Project administration, Funding acquisition.	30	

Publication no. A4

Islam, M., Montowska, M., Fornal, E., Tomaszewska-Gras, J. (2023). Discrimination of Selected Cold-Pressed and Refined Oils by Untargeted Profiling of Phase Transition Curves of Differential Scanning Calorimetry. Polish Journal of Food and Nutrition Sciences, 224-232.
https://doi.org/10.31883/pjfns/169425

ORIGINAL ARTICLE
http://journal.pan.olsztyn.pl

Polish Journal of Food and Nutrition Sciences
2023, Vol. 73, No. 3, 224–232
DOI: 10.31883/pjfns/169425
ISSN 1230-0322, e-ISSN 2083-6007

Discrimination of Selected Cold-Pressed and Refined Oils by Untargeted Profiling of Phase Transition Curves of Differential Scanning Calorimetry

Mahbuba Islam[1], Magdalena Montowska[2], Emilia Fornal[3], Jolanta Tomaszewska-Gras[1]*

[1]Department of Food Quality and Safety Management, Poznan University of Life Sciences, ul. Wojska Polskiego 31/33, 60-637 Poznan, Poland
[2]Department of Meat Technology, Poznan University of Life Sciences, ul. Wojska Polskiego 31, 60-624 Poznan, Poland
[3]Department of Bioanalytics, Faculty of Biomedicine, Medical University of Lublin, Jaczewskiego 8b, 20-090 Lublin, Poland

The authenticity assessment of edible oils is crucial to reassure consumers of product compliance. In this study, a new approach was taken to combining untargeted profiling by using differential scanning calorimetry (DSC) with chemometric methods in order to distinguish cold-pressed oils (flaxseed, camelina, hempseed) from refined oils (rapeseed, sunflower, soybean). The whole spectrum of DSC melting profiles was considered as a fingerprint of each oil. Flaxseed and hempseed oils exhibited four endothermic peaks, while three peaks with one exothermic event were detected for camelina seed oil. In the case of refined oils, two endothermic peaks were detected for rapeseed oil, three for sunflower oil and four for soybean oil. Thermodynamic parameters, such as peak temperature, peak heat flow and enthalpy, differed for each type of oil. Principal component analysis (PCA) and orthogonal partial least squares-discriminant analysis (OPLS-DA) were used for processing data consisting of the whole spectrum of heat flow variables of melting phase transition. PCA demonstrated a clear separation between refined and cold-pressed oils as well as six individual oils. The OPLS-DA showed a distinct classification in six classes according to the types of oils. High OPLS-DA coefficients including $R^2X(cum)=0.971$, $R^2(cum)=0.916$ and $Q^2X(cum)=0.887$ indicated good fitness of the model for oil discrimination. Variables influence on projection (VIP) plot indicated the most significant variables of the heat flow values detected at temperatures around −29°C, −32°C, −14°C, −10°C, −24°C and −41°C for the differentiation of oils. The study ultimately demonstrated great potential of the untargeted approach of using the whole melting DSC profile with chemometrics for the discrimination of cold-pressed and refined oils.

Key words: authentication, plant oils, chemometrics, multivariate data analysis, melting profiles, orthogonal partial least squares-discriminant analysis, differential scanning calorimetry

INTRODUCTION

Authentication of cold-pressed oils can be carried out by means of adulteration detection and quality assessment. Edible oils are susceptible to adulteration with lower-quality oils or substances, which can have a detrimental effect on their nutritional value, safety, and sensory properties [Islam *et al.*, 2022]. Authenticity analysis employs a combination of chemical and physical tests to determine the composition, purity, and quality of the oil. The authenticity analysis becomes increasingly important in the case of the high-value oils, like cold-pressed oils (*e.g.*, flaxseed oil, camelina seed oil, hemp seed oil, olive oil, and avocado oil), which are commonly targeted by fraudulent practices, including

***Corresponding Author:**
tel.: +48 618487512; e-mail: jolanta.tomaszewska-gras@up.poznan.pl (J. Tomaszewska-Gras)

Submitted: 3 June 2023
Accepted: 10 July 2023
Published on-line: 2 August 2023

adulteration with other substances or blending with cheaper oils [De Souza *et al.*, 2015; Jović & Jović, 2017; Nikolaichuk *et al.*, 2022; Van Wetten *et al.*, 2015; Yanty *et al.*, 2011]. Refined oils, characterized by a neutral flavor, high smoke point and longer shelf life, have been one of the most commonly used and cheapest oils. Therefore, it is also crucial to know the characteristics of widely consumed refined oils (*e.g.*, rapeseed, soybean, sunflower oils), since they can be used as adulterants.

Several factors should be considered when evaluating the authenticity of cold-pressed and refined oils, for instance, the oil's origin can provide insights into its authenticity [Karim *et al.*, 2015; Piravi-vanak *et al.*, 2022; Rajagukguk *et al.*, 2022; Zhang *et al.*, 2011]. Cold-pressed oils are usually extracted from high-quality seeds or nuts, while refined oils may be sourced from raw materials of average quality. Furthermore, the oil's color and clarity can be crucial in authenticity assessment. Cold-pressed oils tend to have a darker and cloudier appearance, whereas refined oils have a lighter color due to the elimination of impurities and color pigments during the refining process [Aydeniz Güneser *et al*., 2017; Gharby, 2022; Vaisali *et al*., 2015]. The authenticity of an oil can be inferred from its chemical composition. Cold-pressed oils, for instance, may contain more antioxidants and other beneficial compounds than refined oils [Gogolewski *et al*., 2000; Wroniak *et al.*, 2008].

The analysis of the authenticity of cold-pressed and refined oils usually entails a list of physical, chemical, and sensory tests. Several analytical techniques are employed for this purpose, *e.g.*, gas chromatography (GC) [Xu *et al.*, 2015], high-performance liquid chromatography (HPLC) [Ratusz *et al.*, 2018], and various spectroscopy methods such as UV-visible spectroscopy [Karbasian *et al.*, 2015], nuclear magnetic resonance (NMR) [Siudem *et al.*, 2019], and Fourier transform infrared spectroscopy (FTIR) [Moigradean *et al.*, 2015] being the most widely deployed. However, thermal analysis is an emerging technique that has proved useful in authenticating oil products. Differential scanning calorimetry (DSC) is a thermal analysis technique that measures the amount of heat absorbed or released by a sample as it is heated or cooled, which is often used to analyze oil melting behavior and thermal stability. This information can provide insight into the oil's purity and authenticity, as well as its thermal stability. Different exothermic or endothermic curves obtained by DSC technique can provide information about the energy changes that occur inside fats or oils during phase transitions, such as melting [Islam *et al.*, 2023] or crystallization [Brożek *et al.*, 2022]. These curves are determined by the structure and behavior of triacylglycerols (TAG), which are the major constituents of fats and oils. Assessment of TAG components showed their influence on polymorphic behavior during phase transition, which affects unique DSC curves [Rousseau *et al.*, 2005; Sato *et al.*, 2013]. Furthermore, degree of unsaturation, indicated by the number of double bonds in the fatty acid chains, influences the energy required for crystallization or melting phase transition [Zhang *et al.*, 2022]. Thus, any added adulterants, such as low-quality oils or other substances, can affect the oil's thermal properties and can be detected through thermal analysis. In brief, if an oil sample has been adulterated with a lower-grade oil or a non-food-grade substance, the melting and solidification points of the sample will be different from those of the pure oil, and this difference can be detected using DSC [Angiuli *et al.*, 2009; Marikkar, 2014; Dyszel & Baish, 1992; Rudakov *et al.*, 2021].

The aim of this study was to use the whole thermal profiles of melting phase transition of selected edible oils (both cold-pressed and refined oils) for discrimination purposes. A novel approach was taken to combining an untargeted method of DSC with chemometrics in order to distinguish three cold-pressed oils, *i.e.*, flaxseed, camelina, and hempseed oils from such refined oils as rapeseed, sunflower, and soybean oil. Multivariate data analysis tools, *i.e.*, principal component analysis (PCA) and orthogonal partial least squares-discriminant analysis (OPLS-DA), were used to investigate a dataset with a large number of variables. The originality of this study lies in the fact that chemometric methods (PCA, OPLS-DA) were employed for the first time to analyze the whole thermal spectrum of melting phase transition to authenticate cold-pressed oils. To the best of the authors' knowledge, the use of untargeted analysis of the whole DSC spectrum for the authentication of edible oils has never been reported and is yet to be fully explored.

MATERIALS AND METHODS

Materials

For the experiment, primarily 15 kg of seeds of each cultivar or batch of flax, camelina and hemp were obtained from different sources and then cold-pressed to obtain oils. In the case of flax (*Linum usitatissimum* L.), seeds of *Bukoz* cultivar from the Polish Institute of Natural Fibers and Medicinal Plants (Poznań, Poland), *Dolguniec* cultivar from SEMCO manufactory (Śmiłowo, Poland), *Szafir* cultivar from two different suppliers, *i.e.*, from SEMCO manufactory and Hodowla Roślin Strzelce Sp. z o.o. (Strzelce, Poland) and seeds of unknown variety from VitaCorn company (Poznań, Poland) were collected. All hemp (*Cannabis sativa* L.) seeds of the *Henola* cultivar originated from five different suppliers and were collected from the Polish Institute of Natural Fibers and Medicinal Plants. Three cultivars of camelina (*Camelina sativa*) seeds originated from five suppliers; seeds of a spring *Omega* cultivar were purchased from the Poznań University of Life Sciences (Agriculture Research Station Dłoń, Miejska Górka); two camelina seed cultivars (*Luna* and *Śmiłowska*) were collected from SEMCO manufactory, which purchased seeds from different suppliers: *Luna* – a winter variety from two different suppliers and *Śmiłowska* – a spring variety from two different suppliers. All seeds were pressed in the SEMCO manufactory to obtain the oils at the same conditions, *i.e.*, keeping the temperature below 50°C. The pressed oils were left for 24 h for decantation and stored in brown glass bottles. A total of nine refined oils (three for each type of oil: rapeseed, sunflower, and soybean) were purchased from local Polish markets.

Melting phase transition analysis by differential scanning calorimetry

Melting phase transition analysis of oils was carried out according to the method used for butterfat [Tomaszewska-Gras, 2016] with

some modifications, using a DSC 8500 Perkin Elmer differential scanning calorimeter (Waltham, MA, USA), equipped with an Intracooler II and running with Pyris software. Nitrogen (99.999% purity) was the purge gas. Oils (6–7 mg) were weighed into 20-µL aluminum pans (Perkin Elmer, No. 0219-0062) and hermetically sealed. The reference was an empty, hermetically sealed aluminum pan. Analysis started with the oil sample being cooled at a scanning rate of 2°C/min from a temperature of 30°C to –65°C, after which it was heated at a scanning rate of 5°C/min from –65°C to 30°C. For each measurement at a given scanning rate, the calibration procedure was completed with the correct scanning rate. After the analysis, the DSC files were converted to the ASCII format and then analyzed using Origin Pro software, version 2023 (OriginLab Corporation, Northampton, MA, USA). All curves were normalized and the baseline was subtracted to project the DSC curves of all investigated samples in the same scale. Peak temperature (T, °C), peak heat flow (h, W/g), and enthalpy (ΔH, J/g) were measured from the melting curves. Peak temperature was determined at the maximum heat flow on the curve for the selected peak. Peak heat flow was established as the maximum value of heat flow for the normalized peaks. Enthalpy was determined by integrating the area under the curve of the heat flow (J/s) *vs.* temperature (°C). The number of analytical repetitions was two for each oil sample. Therefore, for each cold-pressed oils, five samples were analyzed in duplicate, and for each refined oils, three samples were analyzed in duplicate.

Statistical analysis

Mean and standard deviation were calculated in order to present results that were obtained from ten measurements (n=10) for each cold-pressed oil and from six measurements (n=6) for each refined oil. The SIMCA software version 16.1 (Sartorius Stedim Data Analytics AB, Umea, Sweden) was used to conduct multivariate data analysis, *i.e.*, PCA and OPLS-DA. Both PCA and OPLS-DA models were cross-validated, and the OPLS-DA models were also validated using permutation testing. For these models, X represents the normalized heat flow data matrix obtained from 7471 variables, Y represents the types of oils, and the predictive variables in X were used to classify and predict the oil types. To assess the quality of the models, the model statistics parameters: R^2X(cum), R^2(cum), R^2Y(cum), Q^2(cum), were obtained through cross-validation. Model performance was evaluated by examining the explained variation R^2(cum), which represents the goodness of fit for X- and Y-variables, and the predictive variation Q^2(cum), which represents the goodness of prediction for the fit of predicted variables.

RESULTS AND DISCUSSION

DSC melting profiles of cold-pressed and refined oils

Cold-pressed (flaxseed, camelina seed and hempseed) and refined (rapeseed, soybean and sunflower seed) oils were analyzed for phase transition during heating to establish their melting profile by considering the full spectrum of the DSC curves as fingerprint of the oil. DSC is a highly regarded thermal analysis technique that can explain various properties of these oils,

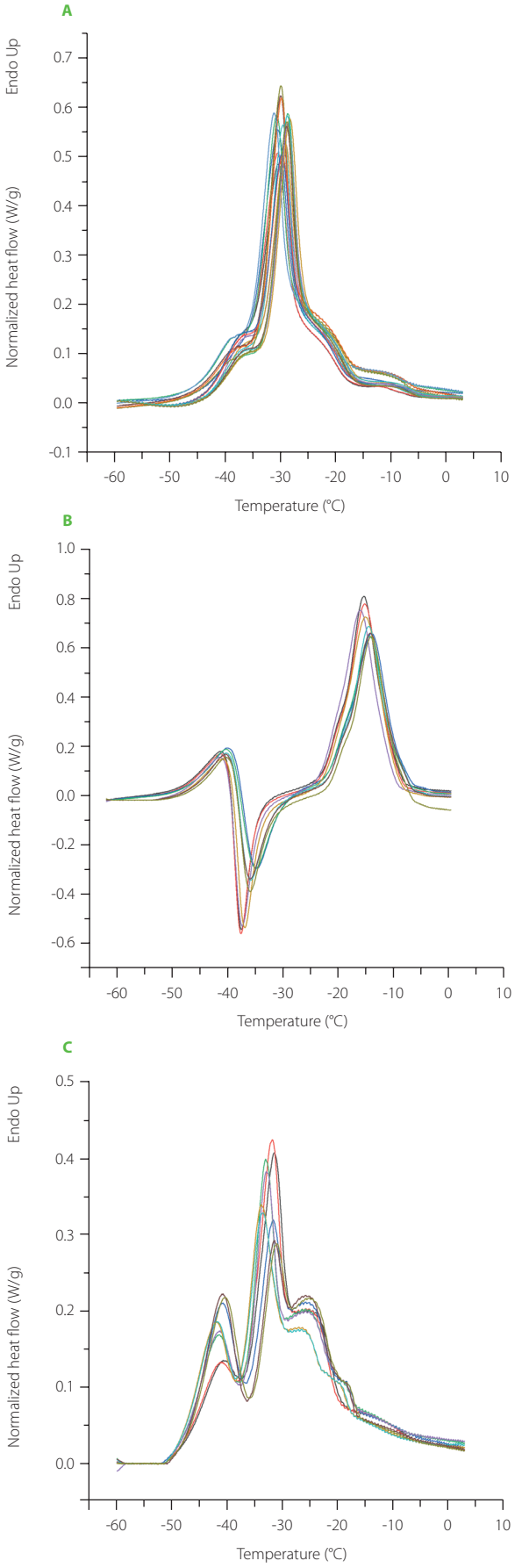

Figure 1. Differential scanning calorimetry (DSC) melting curves of cold-pressed oils at a scanning rate 5°C/min; (**A**) flaxseed oils; (**B**) camelina seed oils; (**C**) hempseed oils. Different color curves represent oil samples from different suppliers.

such as their phase transition temperature and magnitude of the thermal effect (heat flow) during individual processes of transition, and enthalpy as energy changes involved in the process. Figure 1 presents the melting curves of cold-pressed oils. To plot the melting curves, all those oils were subjected to crystallization before starting the heating program. The formation of peaks during the melting phase transition is a manifestation of the energy required to overcome the intermolecular forces holding the crystals together, which is absorbed by the sample during heating, resulting in endothermic peaks. As can be seen from Figures 1A and 1C, four peaks appeared on the melting curves, *i.e.*, at −36°C, −30°C, −25°C and −13°C for flaxseed oil; and at −41°C, −32°C, −24°C and −17°C for hempseed oil. In turn, the melting profiles of seed oils of all camelina cultivars were definitely different compared to the profiles of flaxseed and hempseed oils. The second peak was manifested as an exothermic thermal event at −34°C, whereas the other two peaks at −38°C and −12°C were clearly endothermic in nature (Figure 1B). The exothermic peak appeared as a downward deflection in the baseline of the DSC curve of camelina seed oil, which indicates that the sample is undergoing a polymorphic transition by recrystallization. The presence of an exothermic peak during the melting phase transition of camelina seed oil was also reported by other authors [Rudakov *et al.*, 2021]. Recrystallization of the polymorphic crystals of triacylglycerols into a more stable form was observed for flaxseed, hempseed and canola oil, especially at lower heating rates, *i.e.*, 1°C/min [Teh & Birch, 2013]. Although seeds of different plant cultivars were analyzed in the experiment, melting curves showed similarities between the samples of individual oil types, thus unique thermal profiles were obtained for each oil type. The melting process of flaxseed oils of all cultivars started at the temperature around −48°C, after which the initiation of the first peak occurred. The second peak appeared at around −30°C, which is the major peak of the transition, with two more shoulder peaks as the third and fourth peak at the end of transition (at temperatures of −25 and −13°C, respectively). For camelina and hempseed oils, the onset of the melting process was earlier than for flaxseed oils (for both at around −52°C). Although the curves for hempseed oils show the same number of endothermic peaks as for flaxseed oils (four peaks), their melting profile was noticeably different from that of flaxseed oils.

The behavior of oils during the phase transitions was quantified by the thermodynamic parameters, such as peak temperature, peak heat flow and enthalpy. Results are presented in Table 1. These parameters can be substantial for the authenticity assessment of oils. The peak temperatures are presented as T1, T2, T3 and T4 from the first to the fourth peak appearing while oil crystals were melted. The magnitude of transition measured as peak heat flow was also calculated for all peaks after the normalization of the melting curve. A normalized heat flow of the major peak (h2) for flaxseed oil was higher (0.49 W/g) than that of the major peak (h2) for hempseed oil (0.35 W/g). However, the greatest magnitude of transition was observed for the fourth peak (h4) of camelina oils (0.70 W/g). The first and third peak identified for hempseed oil had the higher heat flows (0.20 and 0.19 W/g, respectively) than those of flaxseed oils (0.13 and 0.14 W/g, respectively). For flaxseed and hempseed oil, the major peak (h2) appeared when the peak temperature reached approximately −30°C and −32°C, whereas for camelina oil the main peak was observed at the end of the melting transition when peak temperature reached approximately −12°C. In turn, the exothermic peak of camelina oil had peak heat flow minimum (h2) of −0.40 W/g. Enthalpy can provide insight into the degree of crystallinity or molecular weight, or amorphousness of the samples. Amongst the cold-pressed oils, flaxseed oils showed the lowest ΔH value (62.73 J/g), compared to camelina seed oil (65.09 J/g) and hempseed oil (69.53 J/g). Other authors determined the melting enthalpy for different transformants of camelina oil in the range from 42 to 57 J/g [Rodríguez-Rodríguez *et al.*, 2021] and for flaxseed oil from 54 to 62 J/g [Punia *et al.*, 2020; Zhang *et al.*, 2011].

The melting profiles of flaxseed and camelina seed oils in our study are consistent with the results obtained by Rudakov *et al.*

Table 1. Differential scanning calorimetry (DSC) parameters of the melting curves of cold-pressed oils.

Parameter		Flaxseed oil	Camelina seed oil	Hempseed oil
Peak temperature (°C)	T1	−36.37±0.72	−38.07±0.66	−40.96±0.56
	T2	−30.26±0.83	−33.61±1.08	−32.03±1.06
	T3	−24.66±0.50	-	−24.11±0.74
	T4	−12.79±0.91	−11.97±0.71	−17.11±2.88
Peak heat flow (W/g)	h1	0.13±0.02	0.20±0.01	0.20±0.03
	h2	0.49±0.06	−0.40±0.11	0.35±0.05
	h3	0.14±0.01	-	0.19±0.01
	h4	0.02±0.00	0.70±0.06	0.08±0.02
Enthalpy (J/g)	ΔH	62.73±2.05	65.09±2.69	69.53±1.52

All values are mean ± standard deviation (n=10); T1, T2, T3 and T4 represent the first, second, third and fourth peak temperatures, respectively; h1, h2, h3 and h4 mean heat flow for the first, second, third and fourth peak, respectively; ΔH represents enthalpy for the whole melting phase transition.

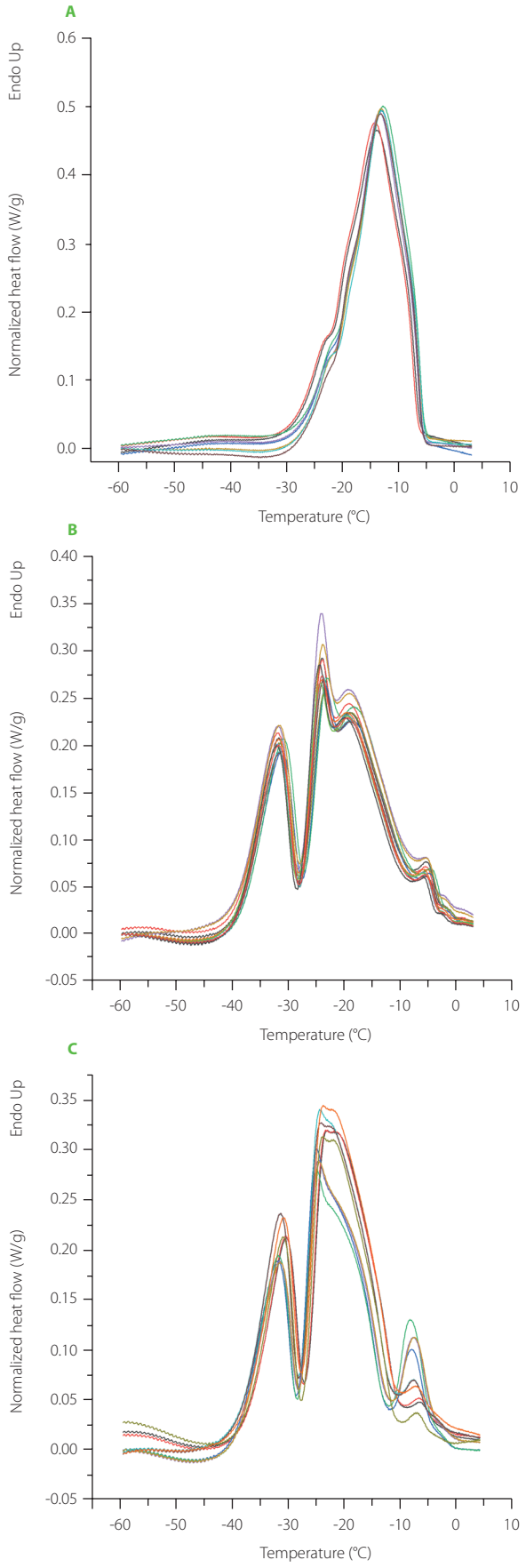

Figure 2. Differential scanning calorimetry (DSC) melting curves of refined oils at a scanning rate 5°C/min; (**A**) rapeseed oils; (**B**) soybean oils; (**C**) sunflower seed oils. Different color curves represent oil samples from different suppliers.

[2021] who used DSC at 5°C/min heating rate. These authors mentioned that the characteristics of the melting curves depended on the triacylglycerol (TAG) profile of the oil samples, which causes differences in the number of peaks, peak temperature values, and the magnitude and temperature ranges of melting transition, as well as enthalpy of transition. Similarly to this study, they also observed four endothermic peaks appearing for flaxseed oils, and three peaks for camelina seed oils (where the second peak was exothermic). Similar four peaks at −38, −31, −24, −13°C were identified by Zhang *et al.* [2014] for the melting profiles of flaxseed oil obtained with the same heating rate of 5°C/min. Our previous study showed that the melting profiles of oils were very strongly influenced by the scanning rate used for heating [Islam *et al.*, 2023; Tomaszewska-Gras *et al.*, 2021]. In turn, Teh & Birch [2013] compared the melting profiles of cold-pressed flaxseed and hempseed oils at a lower heating rate of 1°C/min, for which they determined two endothermic peaks at −40°C and −18°C for hempseed oil and at −36°C and −15°C for flaxseed oil, as well as one exothermic peak at −39°C for hempseed and at −30°C for flaxseed oils. They suggested that the polymorphic transitions indicating the recrystallization of unstable structures were due to the low heating rate. Another study, carried out with a higher scanning rate of 10°C/min, showed that flaxseed hull oils exhibited three peaks of the melting transitions at −33°C, −25°C and −14°C [Oomah & Sitter, 2009], which indicates that a higher heating rate may reduce peak resolution.

Authentication of cold-pressed oils requires knowledge and verification of the characteristics of oils which can be used as adulterants. These most often used ones include refined oils, because they are colorless and odorless, but also because they are cheap and widely available. The melting characteristics of refined rapeseed, soybean and sunflower oils are presented in Figure 2. The melting curves of rapeseed oils were characterized by two endothermic peaks, where the second peak was the major peak, appearing at −13°C, while the melting temperature range was from −30°C to −5°C. In the case of DSC profiles of soybean and sunflower oils, four and three endothermic peaks were identified, respectively, within the transition temperature range from −45°C to 0°C for both oils. For soybean and sunflower oils, the main peak was at a similar temperature, around −24°C. However, there were two peaks (at −18°C and −5°C) after the main peak for soybean oil and one peak at −9°C for sunflower oil. For soybean and sunflower oils, the curves showed differences in the number of peaks; however, corresponding peaks had similar magnitudes of transition and there was a similar temperature range of melting transition. These can be more explicitly described by analyzing the results shown in Table 2 collating DSC parameters, like peak temperature, peak heat flow and enthalpy of the refined oils. The highest transition magnitude was observed for the second peak (h2) of the rapeseed oil samples, *i.e.*, 0.48 W/g, whereas the main peak heat flows of the soybean oils and sunflower oils were 0.28 and 0.31 W/g, respectively. Additionally, during melting transition, two more shoulder peaks were detected for soybean oils, and one for sunflower oils. Comparing ΔH determined for the whole melting process, soybean oils show

Table 2. Differential scanning calorimetry (DSC) parameters of the melting curves of refined oils.

Parameter		Rapeseed oil	Soybean oil	Sunflower oil
Peak temperature (°C)	T1	−23.18±0.50	−32.23±0.68	−32.16±0.28
	T2	−13.49±0.65	−24.09±0.40	−24.83±0.87
	T3	-	−18.06±0.47	−8.57±0.33
	T4	-	−5.20±0.39	-
Peak heat flow (W/g)	h1	0.13±0.01	0.20±0.01	0.21±0.02
	h2	0.48±0.01	0.28±0.02	0.31±0.02
	h3	-	0.23±0.01	0.06±0.04
	h4	-	0.06±0.01	-
Enthalpy (J/g)	ΔH	63.91±0.94	58.42±2.78	61.14±3.18

All values are mean ± standard deviation (n=6); T1, T2, T3 and T4 represent the first, second, third and fourth peak temperatures, respectively; h1, h2, h3 and h4 mean heat flow for the first, second, third and fourth peak, respectively; ΔH represents enthalpy for the whole melting phase transition.

the lowest value (58.42 J/g), in contrast to rapeseed oils, for which the highest enthalpy was measured (63.91 J/g). A similar experimental approach was presented by other authors [Tan & Che Man, 2000], who characterized canola, soybean and sunflower oils after heating at a rate of 5°C/min and identified two peaks for canola and four peaks for the soybean and sunflower oils, where the position of peaks differed from that found in our study. Comparable results obtained for the melting profiles at a heating rate of 5°C/min for sunflower oils with three peaks (−36°C, −27°C, and −11°C) and rapeseed oil with two peaks (−23°C and −15°C) were reported by Rudakov *et al.* [2021]. Other authors [Teh & Birch, 2013] reported two major endothermic peaks at −23°C and −9°C for cold-pressed canola oils with a 1°C/min program, which is comparable to the results of our study.

Chemometric analysis of melting profiles of cold--pressed and refined oils

The main goal of this study was to use data obtained from the DSC technique to authenticate three cold-pressed oils and to differentiate them from the refined oils by analyzing the melting phase transitions. Since it could be seen (Figure 1 and 2) that the DSC profiles obtained for all oils (cold-pressed and refined) were visually different, it was necessary to decide at this stage which results and methods to choose for discrimination. To solve this problem, two potential approaches were considered in this study. The first was to compare the parameters determined from the curves, which are presented in Table 1 and Table 2. The second approach was based on comparing the entire phase transition spectrum using chemometric methods. The disadvantage of the first approach was the fact that melting profiles consist of a different number of peaks at different positions, which makes it difficult to compare them with each other. Thus, the authors decided to compare the whole melting profiles of oils expressed by normalized heat flow (W/g), which were tested as variables using SIMCA software. Multivariate data analyses, *i.e.*, PCA and OPLS-DA, were conducted to assess the usability of DSC melting profiles in classifying and distinguishing cold-pressed and refined oils. The first step was to compare two groups of oils, refined oils *vs.* cold-pressed oils. PCA – a widely used, unsupervised analysis – was employed to uncover and visualize the underlying patterns of variations within a dataset. Figure 3A shows a score plot with oils separated into two groups: refined and cold-pressed ones. Based on the DSC data matrix, the two principal components, t[1] and t[2] were established, which accounted for 80.8% of the variation in the values of normalized heat flow of the melting profiles. Next, an OPLS-DA model was built on the same data matrix, which focused on the separation of two oil classes: refined and cold-pressed ones (Figure 3B). The OPLS-DA is a multivariate statistical method that is commonly used for the classification and prediction of data with multiple variables. The OPLS-DA model separates the systematic variation in X (normalized heat flow) into two parts: one that is linearly related (and therefore predictive) to Y (representing classes), and one that is orthogonal to Y. The Y-predictive part represents the between-class variation and the Y-orthogonal part constitutes the within-class variation. A score plot of cold-pressed and refined oils classified into six classes in the space of two components: t[1] – predictive and t_o[1] – orthogonal, is shown in Figure 3B. The model fit was described by the coefficient R^2X(cum)=0.807, which is the cumulative R^2X of the fractions of the X variation modeled in the component, using the X model, the R^2(cum)=0.978, which is the cumulative R^2 of the fractions of Y variation modeled in the component, using the X model, and Q^2(cum)=0.977, which is cumulative Q^2 of fractions of Y variation predicted according to cross-validation in the component, using the X model. It can also be noticed that the separation in both classes, occurring relative to components t[1] and t[2], is additionally connected with the appearance of two subclasses for each class, which are located on opposite sides (Figure 3A). However, the difference between subclasses is smaller for refined oils compared to cold-press oils. This suggests some similarities inside both classes, leading to their differentiation. The existence of subclasses inside each class was confirmed

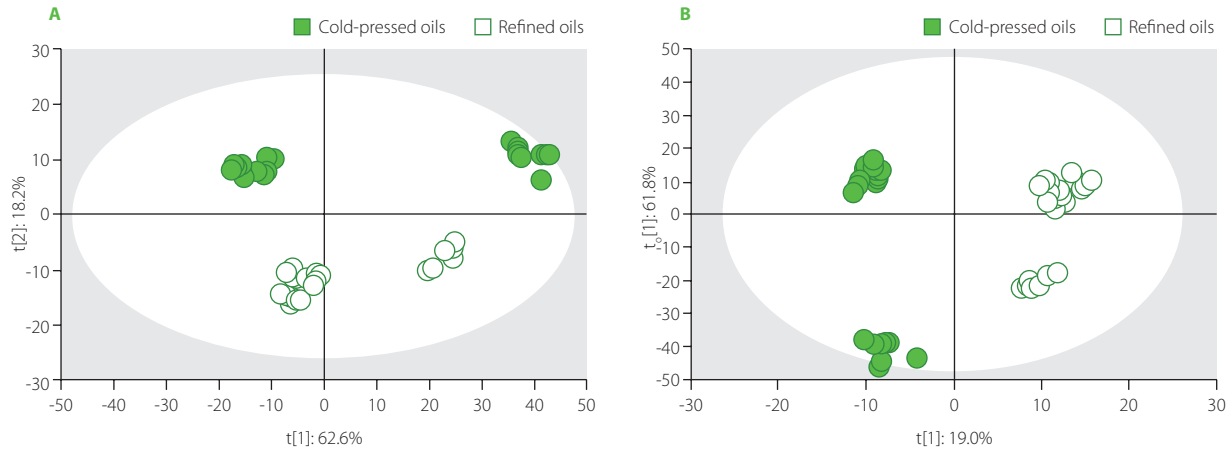

Figure 3. Differentiation between cold-pressed and refined oils based on their differential scanning calorimetry (DSC) melting profiles; (**A**) principal component analysis (PCA) score plot; where t[1] and t[2] are the first and second principal components, respectively; (**B**) orthogonal partial least square-discriminant analysis (OPLS-DA) score plot; where t[1] and t_o[1] are predictive and orthogonal components, respectively.

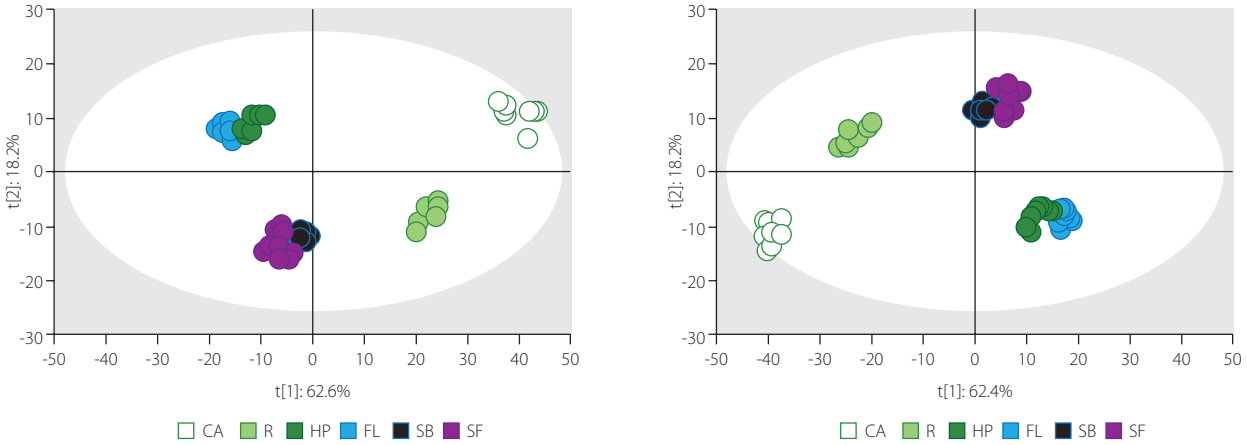

Figure 4. Distinguishing oils based on their differential scanning calorimetry (DSC) melting profiles; (**A**) principal component analysis (PCA) score plot; where t[1] and t[2] are the first and second principal components, respectively; (**B**) orthogonal partial least square-discriminant analysis (OPLS-DA) score plot; where t[1] and t[2] are predictive and orthogonal components, respectively. CA, camelina seed oil; FL, flaxseed oil; HP, hempseed oil; R, rapeseed oil; SB, soybean oil; SF, sunflower seed oil.

by the OPLS-DA method, where orthogonal component t_o[1] also shows differentiation inside the class of unrefined oils (Figure 3B).

Since the orthogonal component in X was significant ($R^2X = 0.618$), indicating that the variation within the class of cold-pressed oils and within the class of refined oils was high (Figure 3B), the next step was to analyze all six types of oils as six classes by using PCA (Figure 4A) and OPLS-DA (Figure 4B). Figure 4A shows a score plot of the PCA results with the oils separated into six groups: three refined oils (rapeseed, soybean and sunflower) and three cold-pressed oils (flaxseed, camelina, hempseed), in the space of the two first principal components t[1] and t[2], which accounted for 80.8% of the total variation. The score plot with the clear classification and discrimination of six types of oils conducted by means of the OPLS-DA is shown in Figure 4B. Five predictive components (P1-P5) and two orthogonal components in X (O1, O2) were calculated by the OPLS-DA. The variation modelled for X using all predictive components and orthogonal components in X gave the value of $R^2X(cum)=0.971$, which is a measure of model fit. The next parameters of OPLS-DA, $R^2(cum)$ and $Q^2X(cum)$, were equal to 0.916 and 0.887, respectively. Individual values of Q^2 calculated for five components are the fractions of the Y variation predicted according to cross-validation in the component using the X model. All Q^2 values were in the range from 0.143 to 0.198 and all were higher than the limit of 0.01, which is the critical value of Q^2 below which the component is insignificant.

Summing up, it can be stated that all parameters ($R^2X(cum)$, $R^2(cum)$ and $Q^2X(cum)$) indicated that the model established by the OPLS-DA fitted the data of DSC profiles and enabled reliable classification of oils into six classes. The variables influence on projection (VIP) plot shown in Figure 5 reflects selected variables, which are of the highest importance for oil differentiation. Normalized VIP values were in the range from 0.3 to 1.6, while the average squared VIP value was 1. Since only variables with VIP values above 1 are important, only such variables are shown in Figure 5. It can be seen that, in this model, the most important

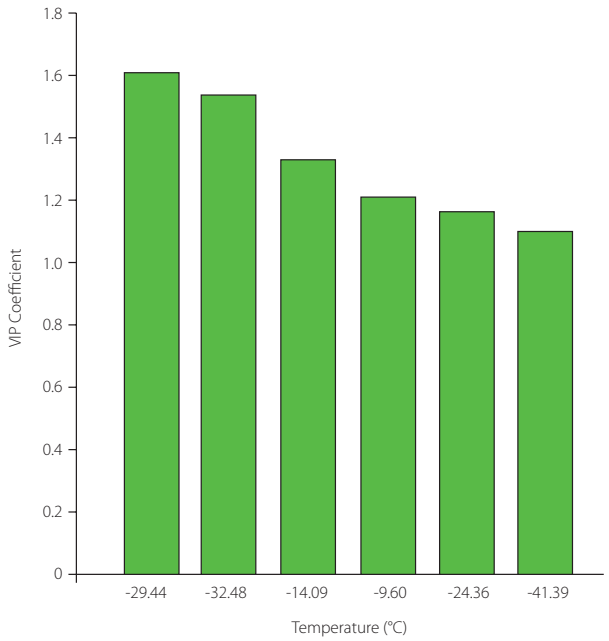

Figure 5. Variables influence on projection (VIP) plot showing the most important variables of heat flow values detected at different temperatures.

for oil discrimination were the heat flow values of the DSC profiles measured at temperatures of −29.44±0.32°C, −32.48±1.80°C, −14.09±1.61°C, −9.60±0.71°C, −24.36±0.94°C, and −41.39±0.77°C.

CONCLUSIONS

This study presents a novel approach for authenticating oils by using the whole spectrum of their DSC melting profiles. The DSC profiles combined with advanced chemometric methods of OPLS-DA were used to distinguish cold-pressed oils (flaxseed, camelina, hempseed) from refined oils (rapeseed, sunflower, soybean) in order to establish a model for their classification. The results showed that the DSC melting profiles can be considered as a fingerprint of each oil, since they differed in the number of peaks and their position. Flaxseed and hempseed oils exhibited four endothermic peaks, in contrast to camelina seed oil, for which three peaks with one exothermic event were detected. For the refined oils, two endothermic peaks were detected for rapeseed oil, three for sunflower oil and four for soybean oil. Additionally, it was stated that thermodynamic parameters, such as peak temperature, peak heat flow and enthalpy, differed for each type of oil. The results from the PCA and OPLS-DA showed successful classification of different edible oils into two classes (refined and cold-pressed), as well as into six classes according to the oil type. The model fitted the data well, as indicated by the R^2X(cum), R^2(cum), and Q^2X(cum) values, which assessed the variation in the X (normalized heat flow) and Y (classes) data. Furthermore, it was shown that certain heat flow values measured at specific temperatures were crucial for differentiating the oils. These variables played a significant role in the discrimination of oils based on their melting profiles.

The study provides practical information on the utility and the potential of the DSC profiles for the detection of frauds, as it was in the case of olive oil scandal in Western Europe in 2019, where refined sunflower oil was colored with chlorophylls and beta-carotene to mirror olive oil and sold as extra virgin olive oil. The approach presented in this study could lead to future research addressing more expensive and highly nutritious plant fats and oils available on the market, to build a database of their fingerprints to be analyzed by chemometric methods for authentication.

RESEARCH FUNDING

This research was funded by the National Science Centre, Poland, grant number: 2018/31/B/NZ9/02762.

CONFLICT OF INTERESTS

The authors declare that they have no competing interests.

ORCID IDs

E. Fornal https://orcid.org/0000-0002-0503-0706
M. Islam https://orcid.org/0000-0003-1860-3718
M. Montowska https://orcid.org/0000-0002-6331-5726
J. Tomaszewska-Gras https://orcid.org/0000-0003-3964-8093

REFERENCES

1. Angiuli, M., Bussolino, G.C., Ferrari, C., Matteoli, E., Righetti, M.C., Salvetti, G., Tombari, E. (2009). Calorimetry for fast authentication of edible oils. *International Journal of Thermophysics*, *30*(3), 1014–1024. https://doi.org/10.1007/s10765-009-0592-4
2. Aydeniz Güneser, B., Yilmaz, E., Ok, S. (2017). Cold pressed *versus* refined winterized corn oils: Quality, composition and aroma. *Grasas y Aceites*, *68*(2), art. no. e194. https://doi.org/10.3989/gya.1168162
3. Brożek, O., Kiełczewska, K., Bohdziewicz, K. (2022). Characterisation of selected emulsion phase parameters in milk, cream and buttermilk. *Polish Journal of Food and Nutrition Sciences*, *72*(1), 5–15. https://doi.org/10.31883/pjfns/144223
4. De Souza, L.M., De Santana, F.B., Gontijo, L.C., Mazivila, S.J., Borges Neto, W. (2015). Quantification of adulterations in extra virgin flaxseed oil using MIR and PLS. *Food Chemistry*, *182*, 35–40. https://doi.org/10.1016/j.foodchem.2015.02.081
5. Dyszel, S.M., Baish, S.K. (1992). Characterization of tropical oils by DSC. *Thermochimica Acta*, *212*(C), 39–49. https://doi.org/10.1016/0040-6031(92)80218-L
6. Gharby, S. (2022). Refining vegetable oils: Chemical and physical refining. *Scientific World Journal*, *2022*, art. no. 6627013. https://doi.org/10.1155/2022/6627013
7. Gogolewski, M., Nogala-Kalucka, M., Szeliga, M. (2000). Changes of the tocopherol and fatty acid contents in rapeseed oil during refining. *European Journal of Lipid Science and Technology*, *102*(10), 618–623. https://doi.org/10.1002/1438-9312(200010)102:10<618::aid-ejlt618>3.3.co;2-y
8. Islam, M., Bełkowska, L., Konieczny, P., Fornal, E., Tomaszewska-Gras, J. (2022). Differential scanning calorimetry for authentication of edible fats and oils - What can we learn from the past to face the current challenges? *Journal of Food and Drug Analysis*, *30*(2), art. no. 2. https://doi.org/10.38212/2224-6614.3402
9. Islam, M., Kaczmarek, A., Tomaszewska-Gras, J. (2023). DSC melting profile of cold-pressed hemp seed oil as an authenticity fingerprint influenced by scanning rate. *Applied Sciences, 13*(6), art. no. 3975. https://doi.org/10.3390/app13063975
10. Jović, O., Jović, A. (2017). FTIR-ATR adulteration study of hempseed oil of different geographic origins. *Journal of Chemometrics*, *31*(12), art. no. e2938. https://doi.org/10.1002/cem.2938
11. Karbasian, M., Givianrad, M.H., Ramezan, Y. (2015). A rapid method for detection of refined olive oil as adulterant in extra virgin olive oil by Differential Scanning Calorimetry. *Oriental Journal Of Chemistry*, *31*(3), 1735–1739. https://doi.org/10.13005/ojc/310354
12. Karim, M., Karim, S., Rana, A., Masum, S., Mondol, A., Israt, S. (2015). ATR-FTIR spectroscopy and chemometric techniques for the identification of edible vegetable oils. *Bangladesh Journal of Scientific and Industrial Research*, *50*(4), 233–240. https://doi.org/10.3329/bjsir.v50i4.25830

13. Marikkar, M.N., (2014). DSC as a valuable tool for the evaluation of adulteration of oils and fats. In E. Chiavaro (Ed.) *Differential Scanning Calorimetry: Applications in Fat and Oil Technology*, 1st ed., CRC Press, Boca Raton, USA. https://doi.org/10.1201/b17739
14. Moigradean, D., Poiana, M.A., Gogoasa, I. (2015). Use of ATR-FTIR spectroscopy to detect the changes in extra virgin olive oil by adulteration with soybean oil and high temperature heat treatment. *Open Chemistry*, *13*(1), 689–698. https://doi.org/10.1515/chem-2015-0110
15. Nikolaichuk, H., Przykaza, K., Kozub, A., Montowska, M., Wójcicka, G., Tomaszewska-Gras, J., Fornal, E. (2022). Shotgun lipidomic analysis for differentiation of niche cold pressed oils. *Molecules*, *27*(6), art. no. 1848. https://doi.org/10.3390/molecules27061848
16. Oomah, B.D., Sitter, L. (2009). Characteristics of flaxseed hull oil. *Food Chemistry*, *114*(2), 623–628. https://doi.org/10.1016/j.foodchem.2008.09.096
17. Piravi-vanak, Z., Azadmard-Damirchi, S., Kahrizi, D., Mooraki, N., Ercisli, S., Savage, G.P., Rostami Ahmadvandi, H., Martinez, F. (2021). Physicochemical properties of oil extracted from camelina (*Camelina sativa*) seeds as a new source of vegetable oil in different regions of Iran. *Journal of Molecular Liquids*, *345*, art. no. 117043. https://doi.org/10.1016/j.molliq.2021.117043
18. Punia, S., Sandhu, K.S., Dhull, S.B., Kaur, M., Siroha, A. K. (2020). Kinetic, rheological and thermal studies of flaxseed (*Linum usitatissiumum* L.) oil and its utilization. *Journal of Food Science and Technology*, *57*(11), 4014–4021. https://doi.org/10.1007/s13197-020-04434-1
19. Rajagukguk, Y.V., Utcu, M.A., Islam, M., Muzolf-Panek, M., Tomaszewska-Gras, J. (2022). Authenticity assessment from sesame seeds to oil and sesame products of various origin by Differential Scanning Calorimetry. *Molecules*, *27*(21), art. no. 7496. https://doi.org/10.3390/molecules27217496
20. Ratusz, K., Symoniuk, E., Wroniak, M., Rudzińska, M. (2018). Bioactive compounds, nutritional quality and oxidative stability of cold-pressed camelina (*Camelina sativa* L.) oils. *Applied Sciences (Switzerland)*, *8*(12), art. no. 2606. https://doi.org/10.3390/app8122606
21. Rodríguez-Rodríguez, M.F., Moreno-Pérez, A.J., Makni, S., Troncoso-Ponce, M.A., Acket, S., Thomasset, B., Sánchez, R., Venegas-Calerón, M., Garcés, R., Martínez-Force, E., Salas, J.J. (2021). Lipid profiling and oil properties of *Camelina sativa* seeds engineered to enhance the production of saturated and omega-7 fatty acids. *Industrial Crops and Products*, *170*, art. no. 113765. https://doi.org/10.1016/j.indcrop.2021.113765
22. Rousseau, D., Hodge, S.M., Nickerson, M.T., Paulson, A.T. (2005). Regulating the beta prime to beta polymorphic transition in food fats. *JAOCS – Journal of the American Oil Chemists' Society*, *82*(1), 7–12. https://doi.org/10.1007/s11746-005-1035-z
23. Rudakov, O.B., Saranov, I.A., Van, A.N., Rudakova, L.V., Polyanskiy, K.K. (2021). Differential Scanning Calorimetry as a method for the control of vegetable oils. *Journal of Analytical Chemistry*, *76*(2), 258–266. https://doi.org/10.1134/S1061934821020118
24. Sato, K., Bayés-García, L., Calvet, T., Cuevas-Diarte, M.À., Ueno, S. (2013). External factors affecting polymorphic crystallization of lipids. *European Journal of Lipid Science and Technology*, *115*(11), SI, 1224–1238. https://doi.org/10.1002/ejlt.201300049
25. Siudem, P., Wawer, I., Paradowska, K. (2019). Rapid evaluation of edible hemp oil quality using NMR and FT-IR spectroscopy. *Journal of Molecular Structure*, *1177*, 204–208. https://doi.org/10.1016/j.molstruc.2018.09.057
26. Tan, C.P., Che Man, Y.B. (2000). Differential scanning calorimetric analysis of edible oils: Comparison of thermal properties and chemical composition. *JAOCS – Journal of the American Oil Chemists' Society*, *77*(2), 143–155. https://doi.org/10.1007/s11746-000-0024-6
27. Teh, S.S., Birch, J. (2013). Physicochemical and quality characteristics of cold-pressed hemp, flax and canola seed oils. *Journal of Food Composition and Analysis*, *30*(1), 26–31. https://doi.org/10.1016/j.jfca.2013.01.004
28. Tomaszewska-Gras, J. (2016). Multivariate analysis of seasonal variation in the composition and thermal properties of butterfat with an emphasis on authenticity assessment. *Grasas y Aceites*, *67*(4), art. no. e167. https://doi.org/10.3989/gya.0453161
29. Tomaszewska-Gras, J., Islam, M., Grzeca, L., Kaczmarek, A., Fornal, E. (2021). Comprehensive thermal characteristics of different cultivars of flaxseed oil (*Linum usittatissimum* L.). *Molecules*, *26*(7), art. no. 1958. https://doi.org/10.3390/molecules26071958
30. Vaisali, C., Charanyaa, S., Belur, P.D., Regupathi, I. (2015). Refining of edible oils: A critical appraisal of current and potential technologies. *International Journal of Food Science and Technology*, *50*(1), 13–23. https://doi.org/10.1111/ijfs.12657
31. Van Wetten, I.A., Van Herwaarden, A.W., Splinter, R., Boerrigter-Eenling, R., Van Ruth, S.M. (2015). Detection of sunflower oil in extra virgin olive oil by fast differential scanning calorimetry. *Thermochimica Acta*, *603*, 237-243. https://doi.org/10.1016/j.tca.2014.11.030
32. Wroniak, M., Krygier, K., Kaczmarczyk, M. (2008). Comparison of the quality of cold pressed and virgin rapeseed oils with industrially obtained oils. *Polish Journal of Food and Nutrition Sciences*, *58*(1), 85–89.
33. Xu, B., Li, P., Ma, F., Wang, X., Matthäus, B., Chen, R., Yang, Q., Zhang, W., Zhang, Q. (2015). Detection of virgin coconut oil adulteration with animal fats using quantitative cholesterol by GC × GC-TOF/MS analysis. *Food Chemistry*, *178*, 128–135. https://doi.org/10.1016/j.foodchem.2015.01.035
34. Yanty, N.A.M., Marikkar, J.M.N., Long, K. (2011). Effect of varietal differences on composition and thermal characteristics of avocado oil. *JAOCS – Journal of the American Oil Chemists' Society*, *88*(12), 1997–2003. https://doi.org/10.1007/s11746-011-1877-x
35. Zhang, Z., Wei, Y., Guan, N., Li, B., Wang, Y. (2022). Changes in chemical composition of flaxseed oil during thermal-induced oxidation and resultant effect on DSC thermal properties. *Molecules*, *27*(20), art. no. 7135. https://doi.org/10.3390/molecules27207135
36. Zhang, Z.S., Li, D., Zhang, L.X., Liu, Y.L., Wang, X.D. (2014). Heating effect on the DSC melting curve of flaxseed oil. *Journal of Thermal Analysis and Calorimetry*, *115*(3), 2129–2135. https://doi.org/10.1007/s10973-013-3270-5
37. Zhang, Z.S., Wang, L.J., Li, D., Li, S.J., Ozkan, N. (2011). Characteristics of flaxseed oil from two different flax plants. *International Journal of Food Properties*, *14*(6), 1286–1296. https://doi.org/10.1080/10942911003650296

Statement about the contribution of authors

Publication title A4: Islam, M., Montowska, M., Fornal, E., Tomaszewska-Gras, J. (2023). Discrimination of Selected Cold-Pressed and Refined Oils by Untargeted Profiling of Phase Transition Curves of Differential Scanning Calorimetry. Polish Journal of Food and Nutrition Sciences, 224-232. https://doi.org/10.31883/pjfns/169425

Author	Contribution	Percentage contribution	Signature
Mahbuba Islam	Conceptualization, Methodology, Formal analysis, Investigation, Data curation, Writing- original draft preparation, Writing- review and editing, Visualization.	45	
Magdalena Montowska	Data curation, Writing- review and editing	15	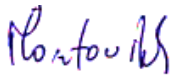
Emilia Fornal	Project administration, Funding acquisition.	5	
Jolanta Tomaszewska-Gras	Conceptualization, Methodology, Formal analysis, Investigation, Resources, Data curation, Writing- original draft preparation, Writing- review and editing, Visualization, Supervision, Project administration, Funding acquisition.	35	

Publication no. A5

Islam, M.; Kaczmarek, A.; Montowska, M.; Tomaszewska-Gras, J. Comparing Different Chemometric Approaches to Detect Adulteration of Cold-Pressed Flaxseed Oil with Refined Rapeseed Oil Using Differential Scanning Calorimetry. Foods 2023, 12, 3352. https://doi.org/10.3390/foods12183352

foods

MDPI

Article

Comparing Different Chemometric Approaches to Detect Adulteration of Cold-Pressed Flaxseed Oil with Refined Rapeseed Oil Using Differential Scanning Calorimetry

Mahbuba Islam [1], Anna Kaczmarek [1], Magdalena Montowska [2] and Jolanta Tomaszewska-Gras [1,*]

[1] Department of Food Quality and Safety Management, Poznań University of Life Sciences, ul. Wojska Polskiego 31/33, 60-624 Poznań, Poland; mahbuba.islam@up.poznan.pl (M.I.); anna.kaczmarek@up.poznan.pl (A.K.)
[2] Department of Meat Technology, Poznan University of Life Sciences, ul. Wojska Polskiego 31/33, 60-624 Poznań, Poland; magdalena.montowska@up.poznan.pl
* Correspondence: jolanta.tomaszewska-gras@up.poznan.pl

Abstract: Flaxseed oil is one of the best sources of *n*-3 fatty acids, thus its adulteration with refined oils can lead to a reduction in its nutritional value and overall quality. The purpose of this study was to compare different chemometric models to detect adulteration of flaxseed oil with refined rapeseed oil (RP) using differential scanning calorimetry (DSC). Based on the melting phase transition curve, parameters such as peak temperature (T), peak height (h), and percentage of area (P) were determined for pure and adulterated flaxseed oils with an RP concentration of 5, 10, 20, 30, and 50% (*w*/*w*). Significant linear correlations ($p \leq 0.05$) between the RP concentration and all DSC parameters were observed, except for parameter h1 for the first peak. In order to assess the usefulness of the DSC technique for detecting adulterations, three chemometric approaches were compared: (1) classification models (linear discriminant analysis—LDA, adaptive regression splines—MARS, support vector machine—SVM, and artificial neural networks—ANNs); (2) regression models (multiple linear regression—MLR, MARS, SVM, ANNs, and PLS); and (3) a combined model of orthogonal partial least squares discriminant analysis (OPLS-DA). With the LDA model, the highest accuracy of 99.5% in classifying the samples, followed by ANN > SVM > MARS, was achieved. Among the regression models, the ANN model showed the highest correlation between observed and predicted values (R = 0.996), while other models showed goodness of fit as following MARS > SVM > MLR. Comparing OPLS-DA and PLS methods, higher values of $R^2X(cum) = 0.986$ and $Q^2 = 0.973$ were observed with the PLS model than OPLS-DA. This study demonstrates the usefulness of the DSC technique and importance of an appropriate chemometric model for predicting the adulteration of cold-pressed flaxseed oil with refined rapeseed oil.

Keywords: DSC melting profile; multivariate analysis; oils authenticity; plant oils; multiple linear regression; classification model; artificial neural networks (ANN); orthogonal partial least squares discriminant analysis (OPLS-DA); MARS; SVM

Citation: Islam, M.; Kaczmarek, A.; Montowska, M.; Tomaszewska-Gras, J. Comparing Different Chemometric Approaches to Detect Adulteration of Cold-Pressed Flaxseed Oil with Refined Rapeseed Oil Using Differential Scanning Calorimetry. *Foods* **2023**, *12*, 3352. https://doi.org/10.3390/foods12183352

Academic Editor: Mircea Oroian

Received: 16 August 2023
Revised: 31 August 2023
Accepted: 5 September 2023
Published: 7 September 2023

1. Introduction

Recent studies have provided convincing evidence that combining chemometric methods with analytical measurements can produce remarkable results in assessing food quality, in particular its authenticity. This novel approach provides for a more thorough and accurate evaluation of foodstuffs, allowing for the detection of any adulteration or mislabeling [1–3]. These findings highlight the need to combine data and use multivariate statistical analysis tools to verify the authenticity and quality in the food supply chain. Adulteration of high-priced edible oils continues to be a major concern for both the edible oil industry and consumer health, despite the fact that experts recognized the problem centuries ago [4]. This deceptive technique is primarily motivated by individuals seeking

to increase their revenues by boosting the volume of the product [5] by taking advantage of the lack of effective quality assessment tools for unreliable food products, as suggested by the Food and Agricultural Organization (FAO) [6]. Food adulteration occurs frequently in many wealthy countries around the world, despite researchers' attention to the fraudulent phenomenon [7]. Addressing food fraud poses a significant financial burden, with estimates suggesting that the global food industry incurs an annual cost of approximately EUR 30 billion. This substantial expense highlights the economic impact of combating fraudulent practices in the food sector [8].

Several approaches to investigating and detecting adulterations in food products have been proposed by various food scientists. Researchers have shown the successful application of combining analytical techniques with linear and non-linear chemometric tools [9] to build classification and regression models for oil samples, which clearly demonstrates the importance of different uses of chemometric techniques, i.e., linear discriminant analysis (LDA) [10], multiple linear regression (MLR) [2], multivariate adaptive regression splines (MARS) [11], support vector machine (SVM) [12], artificial neural networks (ANNs) [13], principle component analysis (PCA) [14], orthogonal partial least squares discriminant analysis (OPLS-DA) [15], and partial least squares regression (PLS) [16]. For instance, to detect adulteration in extra virgin olive oils, UV-IMS (ultraviolet ion mobility spectrometry) combined with chemometric analyses like PCA and LDA [17], near-infrared spectroscopy with chemometric techniques [18], and DSC combined with SVM [19] were used. The detection of adulteration in flaxseed oil has also been reported by other authors using different analytical methods coupled with a statistical approach, e.g., mid-infrared spectroscopy (MIR) associated with the chemometric technique of PLS [20], low-field nuclear magnetic resonance relaxation fingerprints [21], gas chromatography–mass spectrometry (GC-MS) coupled with PCA and recursive support vector machine (R-SVM) [22], HPLC-ELSD profiling of triacylglycerols and chemometrics [23], dielectric spectroscopy with PCA and LDA analysis [10], and Fourier transform infrared spectroscopy (FTIR) and MLR [24]. Most of these studies emphasized the importance of using multivariate methods to efficiently detect the adulteration. Different studies were also conducted to show the applicability of using the DSC technique for the adulteration assessment of different fats and oils, which are comparatively expensive and acclaimed as being nutritious, e.g., olive oils and other vegetable oils [25–30] and animal fats [31–34]. In pursuit of the idea of gap analysis, DSC stands out as an analytical method with the ability to detect changes associated with changes in the composition of triacylglycerols, which makes it possible to use it as a "at-a-glance" method for oil authentication. This method measures the thermodynamic parameters of temperature and enthalpy of phase transition without the use of any chemicals, which is not possible in the case of liquid chromatography. Unlike other methods like FTIR [24], XRD [35], and NMR [14], the thermal behavior of the material can be studied under different conditions, e.g., scanning rate. The ability of the DSC technique has already been proven to provide quantitative thermal data in fields such as pharmaceuticals [36], polymers [37], and food science [38].

Derived from the flax plant (*Linum usitatissimum* L.), flaxseed is a seed that is widely grown in countries like Canada, America, China, and India [39]. The oil obtained from cold-pressing flaxseeds, known as flaxseed oil, is highly regarded for its exceptional content of α-linolenic acid (ALA) [40,41], an essential fatty acid that can be converted into beneficial compounds like eicosapentaenoic acid (EPA) and docosahexaenoic acid (DHA) in the human body [42]. Additionally, flaxseed contains abundant phenolic compounds such as lignans, ferulic acid, and p-coumaric acid, as well as mucilage. These bioactive components have demonstrated positive effects on intestinal function [43]. Flaxseed oil has been found to offer numerous health benefits, particularly for the cardiovascular and skeletal systems. It has also shown positive effects in inflammatory conditions like rheumatoid arthritis, psoriasis, ulcerative colitis, and colon tumor [44,45]. An authenticity analysis is crucial for cold-pressed oils like flaxseed oil, as they are commonly targeted by fraudulent practices, such as adulteration with lower-quality oils or blending with cheaper oils. Refined

rapeseed oil can be used as an adulterant to flaxseed oil, since it is cheaper and widely used as cooking oil known for its neutral flavor, high smoke point, and longer shelf life. Adulteration of flaxseed oil with refined rapeseed oil compromises its authenticity and can lead to a reduction in its nutritional value and overall quality [46]. Therefore, the aim of the study was to study the feasibility of the DSC technique combined with chemometric methods for the detection of adulteration of cold-pressed flaxseed with refined rapeseed oils in different concentrations. The novelty of the study lies in evaluating the potential of DSC coupled with various chemometric methods, which were employed to create predictive classification and regression models for the detection of oil adulteration. The classification approach categorized the level of oil adulteration, while the regression approach treated the concentration of refined rapeseed oils as a continuous variable. A number of chemometric methods, i.e., LDA, MLR, MARS, SVM, ANNs, PCA, OPLS-DA, and PLS were used to classify, describe, and generate prediction models of the adulteration phenomena. The originality of the study is evidenced by the pioneering comparative analyses of different chemometric models, which show both the good results of the LDA model in identifying adulterated flaxseed oil samples and the regression model in which ANN excels at predicting adulterated concentrations. This systematic exploration of various chemometric techniques highlights the researchers' innovative approach to increasing the accuracy of the detection and classification of adulterated oils.

2. Materials and Methods

2.1. Materials

Sample oil seeds for cold-pressed flaxseed oils were obtained from different Polish cultivars and then pressed mechanically. Seeds from four different cultivars were purchased, i.e., *Bukoz* (Polish Institute of Natural Fibers and Medicinal Plants in Poznan), *Dolguniec*, *Szafir* (SEMCO manufactory in Śmiłowo, the Hodowla Roślin Strzelce Sp. z o.o. in Strzelce), and one sample of an unidentified variety from the VitaCorn company in Poznan. The oils were obtained through screw-pressing the seeds while keeping temperature below 50 °C at the SEMCO manufactory (Śmiłowo, Poland). After the pressing process, the oils were left for 24 h for decantation and subsequently stored in brown glass bottles. Refined rapeseed oil was purchased from the market. Cold-pressed flaxseed oil samples were adulterated by adding refined rapeseed oils in varying concentrations (0, 5, 10, 20, 30, and 50% *w*/*w*). Prepared samples were analyzed in three replications.

2.2. Methods

2.2.1. Melting Phase Transition Analysis via Differential Scanning Calorimetry (DSC)

Melting analysis of oil samples was carried out with modifications according to the method used for butterfat [3,47]. A Perkin Elmer differential scanning calorimeter DSC 8500 PerkinElmer (Waltham, MA, USA), equipped with an Intracooler II and running with Pyris software 11 (Perkin Elmer, Waltham, MA, USA), was used. Nitrogen (99.999% purity) was the purge gas. Samples of ca. 6–7 mg were weighed into aluminum pans of 20 µL (Perkin Elmer, No. 0219-0062, Waltham, MA, USA) and hermetically sealed. An empty, hermetically sealed aluminum pan was used as reference. Analysis started with cooling the oil sample at a scanning rate of 2 °C/min from a temperature of 30 °C to −65 °C, after which it was heated at scanning rates 5 °C/min from −65 °C to 30 °C. For each measurement at a given scanning rate, the calibration procedure was completed with the correct scanning rate. After the analysis, the DSC files were converted to the ASCII format and then were analyzed using Origin Pro software, version 2023 (OriginLab Corporation, Northampton, MA, USA). The Origin PeakFit module was used to project the DSC curves of all investigated samples. Different DSC parameters, i.e., peak temperature (T, °C), peak height (h, W/g), and percentage of area (P, %), were measured from the melting curves. Peak temperature (T) was determined on the temperature axis (X) by locating the maximum point of heat flow for each peak. Peak height (h) was determined at the heat flow maximum

on the axis Y for each peak. The percentage of each peak area (P) was calculated as the ratio of the area of each peak to the total area of the melting phase transition curve.

2.2.2. Data Analysis

The recorded data were subjected to statistical analysis using Statistica 13.3 software, developed by TIBCO Software Inc. in the USA. A significance level of $\alpha = 0.05$ was chosen for the analysis. The outcomes were reported as the mean and standard deviation. The initial step in the statistical analysis involved assessing the assumptions of ANOVA, which included testing for variance homogeneity and checking data normality. If these assumptions were met, one-way analysis of variance (ANOVA) was performed, followed by the application of Tukey's test to establish statistically homogeneous groups. To assess the impact of adding adulterants at varying percentages to cold-pressed flaxseed oils, linear regression analysis was employed, utilizing the least squares estimation method. This analysis considered the DSC parameters extracted from the melting curves. Classification and regression approaches were used to build predictive models for oils adulteration detection as it was proposed by authors for the food analysis purpose [9,48]. For all models, the predictors were DSC parameters, while the dependent variable was the level of oil adulteration. In the classification approach, the dependent variable (level of oil adulteration) was categorial (6 classes—one for each level of oil adulteration), while in the regression approach, the dependent variable was a continuous variable (concentration of refined rapeseed oils). Artificial neural networks (ANNs), support vector machine (SVM), and multivariate adaptive regression splines (MARS) were used to build classification as well as regression models. In addition, linear discriminant analysis (LDA) was used to build a classification model and multiple linear regression analysis (MLR) to build a regression model. The leave-one-out cross-validation was used. The goodness of fit of the regression models was estimated based on R (correlation coefficient), R^2 (determination coefficient), adjusted R^2 (modified version of R^2 was adjusted for the number of predictors in the model), Akaike information criterion (AIC), Bayesian information criterion (BIC), and Root Mean Square Error (RMSE). The confusion matrix was used for selecting the best classification model. The confusion matrix represents the counts of predicted and true values. The score "TN" stands for True Negative, which shows the number of correctly classified negative examples. Similarly, "TP" stands for True Positive, which indicates the number of correctly classified positive examples. "FP" stands for False Positive, which is the number of actual negative examples classified as positive, and "FN" stands for False Negative, which is the number of actual positive examples classified as negative. Based on the confusion matrix, the performance parameters (Accuracy, Misclassification Rate, Precision, Sensitivity, Specificity, and F1-score) of the classification models were calculated. To perform PCA and OPLS-DA, the SIMCA software version 16.1 (Sartorius Stedim Data Analytics AB, Umea, Sweden) was utilized. Cross-validation was performed on both the PCA and OPLS-DA models, and the OPLS-DA models were validated using permutation testing. For these models, DSC parameters were considered as X variables, and Y variables consisted of different levels of concentrations added as adulterants to the flaxseed oils. The metrics (R^2X, R^2 and Q^2) were analyzed from the models to collectively provide information about how well the OPLS-DA model fits the X data (DSC parameters).

3. Results

3.1. DSC Melting Profiles of Cold-Pressed Flaxseed Oil Adulterated with Refined Rapeseed Oil

In Figure 1, the DSC melting curves obtained for all cultivars of flaxseed oils (pure and adulterated) are presented. Figure 1a–e each demonstrate the melting curves for different cultivars of flaxseed oils (*Bukoz*, *Dolguniec*, *Szafir* (A, B), and unknown variety, respectively) with different concentrations of refined rapeseed oil (0, 5, 10, 20, 30, and 50% *w*/*w*). In this study, the thermal profile of flaxseed oils was examined using melting DSC curves to track the alterations resulting from the addition of adulterants (rapeseed oil). All the samples were first crystallized to −65 °C at a 2 °C/min cooling rate prior to the heating program. On

the melting curve of pure flaxseed oil, three endothermic peaks were identified as a result of the melting of crystals and nuclei. The first shoulder peak was detected at around −36 °C; the second, as a major peak, occurred at around −30 °C; and the third peak appeared at a temperature of approx. −25 °C (Figure 1). Apart from the flaxseed oil, the melting curves of refined rapeseed oil, which gives two endothermic peaks, are also shown.

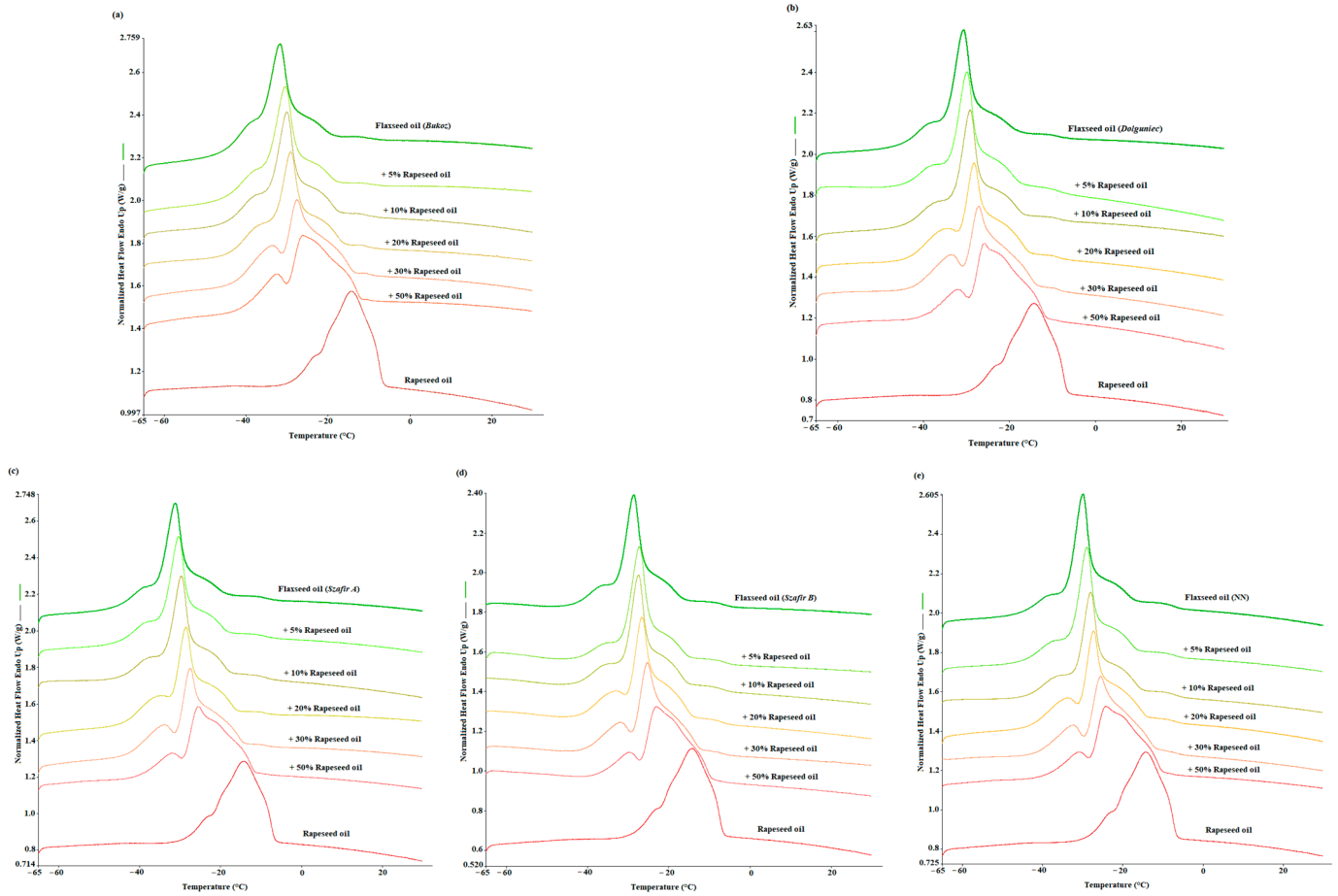

Figure 1. DSC melting curves obtained at a 5 °C/min heating rate for different cultivars of cold-pressed flaxseed oils adulterated with refined rapeseed oils in different concentrations 0, 5, 10, 20, 30, and 50% *w*/*w*. (**a**) *Bukoz* cultivar, (**b**) *Dolguniec* cultivar, (**c**) *Szafir A* cultivar, (**d**) *Szafir B* cultivar, and (**e**) unknown cultivar.

Between the DSC curve for flaxseed oil and refined rapeseed oil curves, the curves of adulterated flaxseed oil with rapeseed in different concentrations are shown. Comparing Figure 1a–e, it can be seen that all the varieties have shown similar changes of thermal transition profile upon the addition of refined rapeseed oil. With an increasing refined oil concentration, gradual changes in the formation of all peaks can be observed in Figure 1. Apparently, all three peaks' positions were shifted to a higher temperature with the gradual addition of rapeseed oil. Consequently, the peak height also changed, because the main peak decreased, while the height of the side peaks (first and third) increased with the increase in the concentration of rapeseed oils in the mixture. Alterations in the thermodynamic characteristics of the target samples with the addition of adulterants have been reported in other studies as well. A similar approach to adulterating cold–pressed oils with refined and cheaper oils was taken by other authors studying adulteration. For instance, using mid-infrared spectroscopy (MIR), authors performed a quantitative analysis of soybean oil and sunflower oil as adulterants with concentrations from 3.5 to 30% (*w*/*w*) in extra virgin flaxseed oil [20]. Another study showed the possibility of detecting the

adulteration of flaxseed oil samples with various concentrations of sunflower oil (10, 20, 30, 50, 70, and 90% *v*/*v*) using magnetic resonance fingerprinting (MRF) [21].

In Table 1, changes in DSC parameters are presented within an increasing concentration of refined rapeseed oil. An ANOVA analysis was performed to show si5gnificant differences between six concentrations of refined rapeseed oil for all the parameters measured, i.e., peak temperature (T1, T2, and T3); peak height (h1, h2, and h3); and the percentage of the peak area (P1, P2, and P3).

Table 1. DSC thermodynamic parameters of melting phases for cold-pressed flaxseed oils adulterated with different concentrations of refined rapeseed oils.

DSC Parameters	Concentrations					
	0%	5%	10%	20%	30%	50%
T1	-36.15 ± 0.35^{a}	-35.44 ± 0.23^{bc}	-34.95 ± 0.35^{bc}	-35.32 ± 0.36^{b}	-34.57 ± 0.59^{c}	-32.39 ± 0.6^{d}
T2	-30.67 ± 0.69^{a}	-30.26 ± 0.67^{ab}	-29.55 ± 0.68^{b}	-28.31 ± 0.54^{c}	-27.08 ± 0.61^{d}	-24.78 ± 0.77^{e}
T3	-24.73 ± 1.04^{a}	-24.08 ± 0.84^{ab}	-23.44 ± 0.72^{bc}	-22.92 ± 0.81^{c}	-22.53 ± 0.48^{c}	-19.12 ± 1.07^{d}
h1	0.12 ± 0.02^{a}	0.14 ± 0.02^{abc}	0.14 ± 0.02^{abc}	0.14 ± 0.01^{bc}	0.15 ± 0.01^{c}	0.13 ± 0.02^{ab}
h2	0.60 ± 0.03^{e}	0.57 ± 0.03^{de}	0.55 ± 0.02^{d}	0.50 ± 0.02^{c}	0.44 ± 0.03^{b}	0.37 ± 0.02^{a}
h3	0.16 ± 0.01^{a}	0.16 ± 0.01^{a}	0.17 ± 0.01^{a}	0.21 ± 0.02^{b}	0.23 ± 0.02^{c}	0.27 ± 0.02^{d}
P1	24.12 ± 3.58^{bc}	27.50 ± 4.00^{c}	27.55 ± 3.17^{c}	24.41 ± 3.04^{bc}	23.09 ± 1.74^{b}	17.08 ± 1.84^{a}
P2	39.77 ± 2.16^{c}	38.32 ± 1.96^{c}	37.49 ± 2.51^{c}	34.52 ± 2.35^{b}	32.43 ± 1.69^{ab}	30.27 ± 2.00^{a}
P3	30.49 ± 2.57^{a}	28.78 ± 3.07^{a}	30.75 ± 2.31^{a}	38.30 ± 2.52^{b}	41.50 ± 2.26^{b}	48.71 ± 2.96^{c}

All values are mean ± standard deviation (n = 10), (a–e)—means with the same letters within the column are not different ($p > 0.05$). T1, T2, and T3 represent the first, second, and third peak temperatures, respectively; h1, h2, and h3 means peak height for the first, second, and third peak, respectively; P1, P2, and P3 represent percentage of peak area for first, second, and third peak, respectively.

Considering the changes in peak temperatures resulting from a 0 to 50% addition, it can be seen that the first peak (T1) shifted from −36 to −32 °C, the second from −31 to −25 °C, and the third peak from −25 to −19 °C. In contrast, peak height (h) did not change in the same way for all peaks. The first (h1) and third (h3) peaks increased with the addition of an adulterant, while the main peak, the second peak (h2), reduced from a value 0.6 W/g for pure flaxseed oil to 0.37 W/g for a sample with 50% of refined rapeseed oil (Table 1). Similarly, different characteristics were exhibited by the percentage of area parameter (P), where P3 was increased while P1 and P2 decreased with the addition of refined oil.

3.2. Changes in DSC Parameters of Flaxseed Oil Melting Phase Transition Depending on Adulterant Concentrations

Parameters determined from the DSC curve for three peaks, i.e., peak temperature (T), peak height (h), and percentage of peak area (P) versus rapeseed oil concertation were analyzed using linear regression (Figure 2).

Linear regression analysis was also used by other authors to explain adulteration phenomena [3,30,49]. Thus, in this study, all variables were analyzed with the linear regression model to find out the trend of changes in DSC parameters resulting from the addition of the adulterant. The data in Figure 2a indicate that peak temperatures always rose to higher temperatures linearly with an increasing concentration of refined rapeseed oil added to the target oil, and it can be seen that all changes were significant ($p \leq 0.05$). Among the three peaks, the strongest correlation was observed for the second peak, T2 (r = 0.95). In Figure 2b, the parameter of peak height (h1) for the first peak is comparatively stable (slightly increased, which is not statistically significant at that level ($p > 0.05$) upon addition of refined oils. In contrast, for the third peak, h3 increased significantly ($p \leq 0.05$) and correlated strongly with the concentration of adulterant (r = 0.92). On the other hand, for the second peak, h2 was significantly lowered with the increment of added adulterant, with strong negative correlation, r = −0.96. The parameters for percentage of area calculated for each peak P1, P2, and P3 were also plotted against concentration of refined rapeseed

oil. Clearly, the first and second peaks' area proportion to the total melting curve area decreased significantly, while the percentage area of the third peak increased significantly ($p \leq 0.05$), with a strong correlation to the adulterant concentration (r = 0.92).

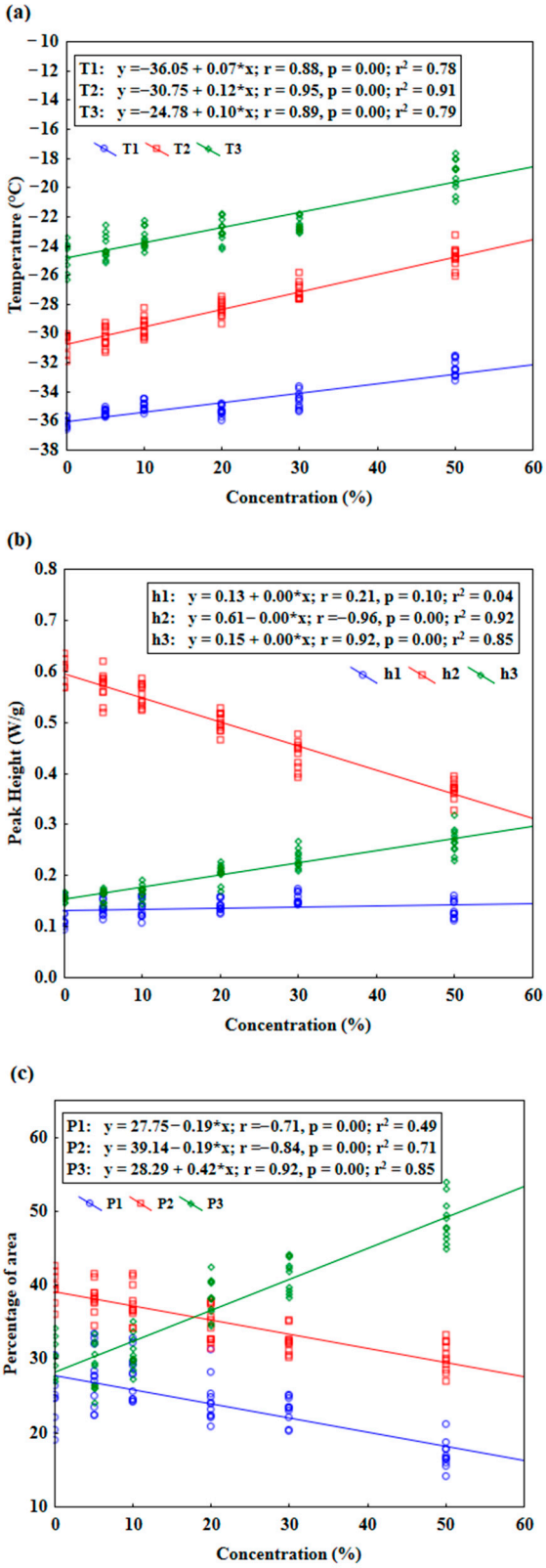

Figure 2. Regression analysis of adulterated flaxseed oil samples for DSC parameters. (**a**) Peak temperature (T, °C), (**b**) peak height (h, W/g), and (**c**) percentage of area (P).

4. Discussion

4.1. Classification Models for Predicting Cold-Pressed Flaxseed Oil Adulteration Levels

In order to assess the ability to build models that classify adulterated oil samples into appropriate classes, the LDA, MARS, SVM, and ANNs methods were used. Linear discriminant analysis (LDA) was used to build the first classification model. LDA and the related Fisher's linear discriminant (FLD) are used in machine learning to find the linear combination of features that best distinguish between two or more classes of objects. The resulting combinations are used as a linear classifier. Discriminant analysis resulted in a statistically significant model with Wilks' Lambda = 0.00119 and $p \leq 0.05$. All variables (DSC parameters) except h3 have significant statistical discriminant power. From our study, five discrimination functions were obtained based on Wilks' Lambda statistics, with $p \leq 0.05$ for the first three functions. For the purposes of classifying the cases, six classification functions were calculated. Each classification function represents a linear equation that combines the input variables (DSC parameters) to discriminate between six groups (G_1 to G_6) and thus provides different classes (C1 to C6). The case is classified by evaluating the values of the classification functions for that case and assigning it to the class associated with the highest C value. The six classification functions are as follows:

$$C1 = -71.3*T1-48.9*T2-127.8*T3 + 2483*h1 + 2487.6*h2 + 2172.7*h3 + 175.4*P1 + 206.1*P2 + 170*P3-13{,}488.8 \quad (1)$$

$$C2 = -68.7*T1-47.6*T2-125.2*T3 + 2672.8*h1 + 2442.4*h2 + 2240.3*h3 + 175.8*P1 + 206.1*P2 + 170.4*P3-13{,}326.2 \quad (2)$$

$$C3 = -65.5*T1-46.6*T2-125.1*T3 + 2740.0*h1 + 2413.7*h2 + 2284.9*h3 + 177.4*P1 + 207.5*P2 + 172.2*P3-13{,}332.2 \quad (3)$$

$$C4 = -69.5*T1-44.8*T2-121.4*T3 + 3034.4*h1 + 2242.8*h2 + 2478.0*h3 + 176.9*P1 + 207.6*P2 + 173.2*P3-13{,}341.7 \quad (4)$$

$$C5 = -67.6*T1-40.9*T2-119.8*T3 + 3346.2*h1 + 2059.7*h2 + 2606.5*h3 + 175.4*P1 + 207.1*P2 + 173*P3-13{,}058.4 \quad (5)$$

$$C6 = -59.4*T1-52.2*T2-103.2*T3 + 3328.9*h1 + 1783.4*h2 + 2843.7*h3 + 168.8*P1 + 198.3*P2 + 168.8*P3-12{,}082.0 \quad (6)$$

where variables (i.e., T1, T2, T3, h1, h2, h3, P1, P2, and P3) are DSC parameters related to the case being classified, the constants (e.g., −71.3, −48.9, −127.8, etc.) are regression coefficients (slope), the constant term (e.g., −13,488.8, −13,326.2, etc.) represents the intercept in the linear equation.

Figure 3 presents the results of the discriminant analysis. From each classification function, the value C can be calculated based on the linear combination of the DSC variables and their corresponding coefficients. The higher the C value, the more likely the case belongs to the corresponding class. It is important to note that the coefficients in the classification functions are obtained through the LDA algorithm, which allowed the separation between classes to be maximized, based on the available data from DSC melting curves. The confusion matrix indicated (Table 2) that only one oil sample with 5% adulteration was classified as a 10% adulterated sample. Thus, the accuracy of the LDA model was 99.5%. A similar approach to detecting adulterations in peanut oil was adopted by other authors, where the identification accuracy was 97% [12].

MARS regression was used to build the second classification model. Multivariate adaptive regression splines (MAR Splines) is the implementation of a generalization of a technique introduced into wide use by Friedman [50] and used to solve both regression and classification problems. MARS is a non-parametric procedure requiring no assumptions about the functional relationship between the dependent and independent variables. MAR Splines model this relationship with a set of coefficients and so-called basis functions that are entirely determined from the data. In this study, MARS models created for the data matrix included a maximum of 21 basis functions. The penalty was set to 2, and the threshold to 0.0005. The MARS model of the first order was created for classification purposes, and the maximum number of terms was limited by pruning. The model has

six basis functions and seven terms with GCV = 0.516. Increased numbers of the basis functions did not decrease the GCV error. MARS model coefficients and knots are presented in Table 3. The model developed here allows 90.3% of correct classifications to be obtained. The confusion matrix indicated that six samples were incorrectly classified. Therefore, the accuracy of the model based on MARS analysis was about 95.7%, as presented in Table 4. The MARS regression model was also used by other researchers to define the discriminant surface for studying the authentication of cod liver oil [13].

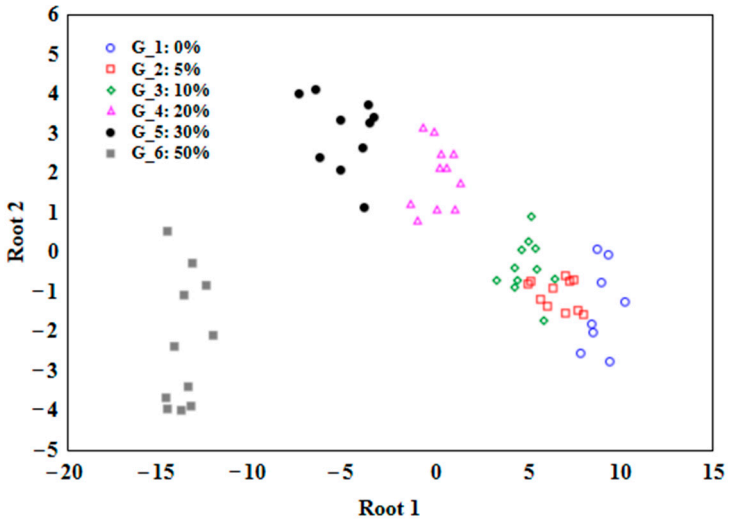

Figure 3. Linear discrimination analysis plot (LDA) for cold-pressed flaxseed oil adulterated with various concentrations of refined rapeseed oils (0, 5, 10, 20, 30, and 50% w/w).

Another model that was examined for its usefulness in classifying oil samples into different adulteration classes was the support vector machines (SVM) model. SVM is a method for classifying samples on the basis of the variables (predictors) that describe them. It is a supervised technique, that is, with a supervisor, i.e., there are both variables describing the samples, and their membership is in defined classes in the learning sample. The support vector method performs classification tasks by constructing hyperplanes in a multidimensional space that separates samples belonging to different classes. For SVM model calculations, the datasets were divided into three subsets in a ratio of 2:1:1 (training, validation, and test set). Samples were classified via the C-SVM method with a linear Kernel type. As a result of learning, a model was obtained that allowed an almost 92% (Table 2) correct classification of oil samples with 97.3% accuracy (Table 4). Another study showed the classification accuracy of SVM as 96.25% while comparing chemometrics and AOCS official methods for predicting the shelf life of edible oil [51].

The last classification model built was an artificial neural network model (ANN). For calculating the ANN model, the datasets were divided into three subsets in a ratio of 2:1:1 (training, validation, and test set). The ANN model was trained using selected parameters from the dataset and was subsequently validated using an independent dataset. A multilayer feed-forward connected ANN was trained with the Broyden–Fletcher–Goldfarb–Shanno (BFGS) learning algorithm (200 epoch). The search for an appropriate ANN model was conducted using multilayer perceptron (MLP) and radial basis function (RBF) networks. In total, 20 networks were evaluated, and the best 5 were retained. The neural network consists of an input layer, one hidden layer, and one output layer. The network architecture, mainly the size of the hidden layer, was selected empirically, taking into consideration the accuracy of predicting the results. The best five ANN-MLP networks are presented in Table 5.

Table 2. Confusion matrix of cold-pressed flaxseed oils adulterated with different concentrations of refined rapeseed oils.

Predicted	Observed	0%	5%	10%	20%	30%	50%
0%	LDA	8	0	0	0	0	0
	ANN	8	0	0	0	0	0
	SVM	6	2	0	0	0	0
	MARS	7	1	0	0	0	0
5%	LDA	0	10	1	0	0	0
	ANN	0	10	1	0	0	0
	SVM	0	10	1	0	0	0
	MARS	0	9	2	0	0	0
10%	LDA	0	0	11	0	0	0
	ANN	0	3	8	0	0	0
	SVM	0	2	9	0	0	0
	MARS	0	1	10	0	0	0
20%	LDA	0	0	0	11	0	0
	ANN	0	0	0	11	0	0
	SVM	0	0	0	11	0	0
	MARS	0	0	0	9	2	0
30%	LDA	0	0	0	0	10	0
	ANN	0	0	0	0	10	0
	SVM	0	0	0	0	10	0
	MARS	0	0	0	2	8	0
50%	LDA	0	0	0	0	0	11
	ANN	0	0	0	0	0	11
	SVM	0	0	0	0	0	11
	MARS	0	0	0	0	0	11

Table 3. MARS model coefficients and knots calculated for classification of cold-pressed flaxseed oils adulterated with different concentrations of refined rapeseed oils.

	Intercept	Term 1	Term 2	Term 3	Term 4	Term 5	Term 6
0%	-1.01	-3.39	-9.46×10^{-1}	8.85×10^{-1}	2.39×10^{-2}	9.37×10^{-1}	8.68
5%	1.27	-1.39	1.35	-9.96×10^{-1}	3.12×10^{-1}	-1.28	4.00
10%	-1.02×10^{-1}	1.81×10^{1}	-3.68×10^{-1}	-2.01×10^{-1}	-7.60×10^{-2}	2.72×10^{-1}	-2.12×10^{1}
20%	3.38×10^{-1}	2.92	1.83×10^{-1}	3.18×10^{-1}	-3.07×10^{-1}	-2.26×10^{-1}	-9.92
30%	5.08×10^{-1}	-1.58×10^{1}	-6.08×10^{-1}	-1.67×10^{-2}	4.51×10^{-2}	2.55×10^{-1}	1.79×10^{1}
50%	1.39	-2.29	5.25×10^{-1}	-1.03×10^{-1}	3.13×10^{-2}	-8.92×10^{-2}	4.43
Knots T1			-3.44×10^{1}	-3.44×10^{1}		-3.55×10^{1}	
Knots T2					-2.88×10^{1}		
Knots h2		4.83×10^{-1}					5.28×10^{-1}

Table 4. Performance parameters of models for classification of cold-pressed flaxseed oils adulterated with different concentrations of refined rapeseed oils.

Performance Parameter / Model	Accuracy	Misclassification Rate	Precision	Sensitivity	Specificity	F1-Score
LDA	99.46%	0.54%	98.39%	98.39%	99.68%	98.39%
ANN	97.85%	2.15%	93.55%	93.55%	98.71%	93.55%
SVM	97.31%	2.69%	91.94%	91.94%	98.39%	91.94%
MARS	95.70%	4.30%	87.10%	87.10%	97.42%	87.10%

Table 5. ANN models calculated for the classification of cold-pressed flaxseed oils adulterated with different concentrations of refined rapeseed oils.

Net Architecture	Training Accuracy	Test Accuracy	Validation Accuracy	Training Algorithm	Error Function	Hidden Activation	Output Activation
MLP 9-9-6	88.636	100.000	77.778	BFGS 10	Entropy	Linear	Softmax
MLP 9-11-6	88.636	88.889	100.000	BFGS 11	Entropy	Linear	Softmax
MLP 9-8-6	81.818	88.889	100.000	BFGS 9	Entropy	Linear	Softmax
MLP 9-9-6	84.091	77.778	100.000	BFGS 32	SOS	Exponential	Exponential
MLP 9-4-6	84.091	88.889	88.889	BFGS 15	Entropy	Tanh	Softmax

In the neural network obtained for oil sample classification, the Linear, Exponential, and Tanh functions were used in the hidden layer, while Softmax and Exponential functions were used in the output layer. In the input layer, there are nine neurons, which are DSC parameters. The number of neurons in hidden layer varies from 4 to 11, while the output layer contains six neurons representing each class of oil adulteration. A model consisting of the best five networks was used for oil sample classification. The accuracy of the resulting ANN model is almost 98% (Table 4) with only three samples misclassified (Table 2). This finding can be compared with the study conducted by Firouz et al. [52], who employed the classification and quantification of sesame oil adulteration and acquired 100% accuracy.

On the basis of the models' performance parameters, it was determined that the best model is the LDA model, with the highest values for accuracy (99.5%), precision (98.4%), sensitivity (98.4%), specificity (99.7%), and F1-score (98.4%), and the lowest value of misclassification rate equals 0.54%. In contrast, the worst one was the MARS model, which had the lowest values for accuracy (95.7%), precision (87%), sensitivity (87%), specificity (97.4%), and F1-score (87%), and the highest value of misclassification rate equals 4.3%. The second-best model was the ANN model, and the third was the SVM model. The accuracy of all these models was very high, which suggested its ability to predict adulterated oil samples into appropriate classes.

4.2. Regression Models for Predicting the Concentration of Refined Rapeseed Oil in Cold-Pressed Flaxseed Oil

Multiple regression analysis (MLR) was performed to formulate a general linear equation that would fit the variables from DSC melting curves against different concentrations of adulterants. This would provide the possibilities to detect the percentage of adulterants in any sample. The MLR model that was obtained was statistically significant with $F(9.52) = 364.57$ ($p \leq 0.05$), $R^2 = 0.9844$, and adjusted $R^2 = 0.9817$. The standard error of estimation was 2.3028.

Table 6 demonstrates the summary of DSC parameters, where (b*) values refer to the standardized regression coefficient, and (b) values refer to the regular regression coefficient. Determining (b*) allowed for a direct comparison of the magnitude and importance of the independent variables, where we can see the highest values are presented for h2, T3, and h3 as −0.32, 0.27, and 0.16, respectively. On the other hand, (b) values signify the slope coefficient associated with an independent variable. It represents the change in the dependent variable for a one-unit change in the corresponding independent variable while holding all other independent variables constant. Table 6 shows that the h2 (−65.52) variable has the strongest negative relationship with the concentration variables, indicating that with a decreased value of h2, the concentration of adulterants increased. On the other hand, h3 and T2 variables consequently increased or decreased linearly with the concentration values of adulterants. Accordingly, a model with statistically significant predictors was built.

$$\%\ \text{adulterant} = 2.185*T3 - 109.995*h2 + 96.576*h3 + 105.319 \pm 2.567 \quad (7)$$

where T3 represents the third strongest significant independent variable (p = 0.000), h2 represents the highest strongest significant independent variable (p = 0.000), and h3 represents the second strongest significant independent variable (p = 0.000).

Table 6. Summary of independent variables in multiple regression analysis.

DSC Parameters	b* (Standardized Co-Efficient)	b (Raw Co-Efficient)	*p*-Value
		145.3464 *	0.000059 *
T1	0.090680	1.2225	0.126748
T2	−0.052531	−0.4175	0.627294
T3	0.273274 *	2.3374 *	0.000332 *
h1	0.080773	73.6583	0.056670
h2	−0.324189 *	−65.5228 *	0.000014 *
h3	0.168666 *	65.1633 *	0.004121 *
P1	−0.128623	−0.4718	0.151392
P2	−0.145236	−0.6314	0.083058
P3	0.019714	0.0435	0.896428

* Coefficients are significant statistically ($p \leq 0.05$).

The goodness of fit of the model to the experimental data and the coefficient of determination R2 and the coded coefficient of determination were 0.978 and 0.977, respectively. Equation no. 7 can be used to estimate the percentage of adulterants (for this study, refined rapeseed oil) in a cold-pressed flaxseed oil sample based on three dependent variables: T3, h2, and h3. The equation implies that the variables T3, h2, and h3 are assumed to have a linear relationship with a percentage of the adulterant. The correlation between observed and predicted values was 0.992 with a low RMSE value of 2.12 (Table 7). A similar study by Sim et al. [2] showed that it was possible to predict adulteration of lard in palm oil olein using the MLR model, where the prediction performance was measured based on the percentage root mean square error (%RMSE).

Table 7. Goodness of fit parameters between observed and predicted regression models for the prediction of concentrations of refined rapeseed oils in cold-pressed flaxseed oil.

Model	R	R^2	Adjusted R^2	AIC	BIC	RMSE
ANN	0.996	0.992	0.992	233	240	1.51
MARS	0.995	0.990	0.990	244	251	1.65
SVM	0.992	0.985	0.984	274	280	2.10
MLR	0.992	0.984	0.984	275	281	2.12

MARS regression was used to build the second regression model. In this study, MARS models created for the data matrix included a maximum of 21 basis functions. The penalty was set to 2 and the threshold to 0.0005. The MARS model of the first order was created for classification purposes, and the maximum number of terms was limited by pruning. The model has 10 basis functions and 11 terms with GCV = 6.252. Equation (8) represents the MARS model for predicting the concentration of refined oil in the samples.

$$\begin{aligned}\%\ \text{adulterant} = {} & 1.955e - 1.9203*\max(0;\ T2 + 2.763e) - 3.192*\max(0;\ -2.763e - T2) + \\ & 3.6434*\max(0;\ T1 + 3.437e) + 4.572*\max(0;\ T3 + 2.254e) + 3.465e^{2}*\max(0;\ h1 - 1.241e^{-1}) - \\ & 4.490e^{2}*\max(0;\ h1 - 1.4729e^{-1}) + 2.214*\max(0;\ 3.240e - P2) - 7.047e^{-1}*\max(0;\ P1 - 2.769e) \\ & + 4.543e^{-1}*\max(0;\ 2.769e - P1) - 7.618e*\max(0;\ h2 - 4.510e^{-1})\end{aligned} \quad (8)$$

The correlation between the observed and predicted value was 0.995 with a low RMSE value of 1.65 (Table 7).

Another model that was examined for its usefulness in predicting oil sample adulteration was the support vector machines (SVM) model. SVM can be used for both classification and regression problems. In SVM regression, the search is for a functional dependence

of the dependent variable y (% of adulteration) on a set of independent variables x (DSC parameters). For calculating the SVM model, the datasets were divided into three subsets in a ratio of 2:1:1 (training, validation, and test set) for model regression type 1 (C = 10.000000, epsilon = 0.100000) with radial basis function (gamma = 0.111111) kernel type. Samples were classified using the C-SVM method with linear kernel type. The correlation between the observed and predicted values was 0.992 with a low RMSE value of 2.1 (Table 7).

The last regression model built was an artificial neural network model (ANN). For calculating the ANN model, the datasets were divided into three subsets in a ratio of 2:1:1 (training, validation, and test set). The ANN was trained using selected parameters from the dataset and was subsequently validated using an independent dataset. A multilayer feed-forward connected ANN was trained with the Broyden–Fletcher–Goldfarb–Shanno (BFGS) learning algorithm (200 epoch). The search for an appropriate ANN model was performed using multilayer perceptron (MLP) and radial basis function (RBF) networks. In total, 20 networks were evaluated, and the best 5 were retained. The neural network consists of an input layer, one hidden layer, and one output layer. The network architecture, mainly the size of the hidden layer, was selected empirically, taking into consideration the accuracy of the results prediction. The five best ANN-MLP networks are presented in Table 8.

Table 8. ANN models calculated for the prediction of refined rapeseed oil concentrations in cold-pressed flaxseed oils.

Net Architecture	Training Accuracy	Test Accuracy	Validation Accuracy	Training Algorithm	Error Function	Hidden Activation	Output Activation
MLP 9-9-1	0.9957	0.9919	0.9901	BFGS 43	SOS	Logistic	Logistic
MLP 9-13-1	0.9964	0.9961	0.9941	BFGS 46	SOS	Logistic	Tanh
MLP 9-11-1	0.9965	0.9913	0.9885	BFGS 61	SOS	Logistic	Exponential
MLP 9-13-1	0.9961	0.9899	0.9866	BFGS 54	SOS	Logistic	Exponential
MLP 9-11-1	0.9963	0.9937	0.9972	BFGS 37	SOS	Tanh	Tanh

In the neural network obtained for predicting oil adulteration, the Logistic and Tanh functions were used in the hidden layer, while Logistic, Tanh, and Exponential functions were used in the output layer. In the input layer, there are nine neurons, which are DSC parameters. The number of neurons in the hidden layer varies from 9 to 13, while the output layer contains 14 neurons representing the refined oil concentration. A model consisting of the best five networks was used for prediction purposes. The correlation between the observed and predicted values was 0.996 with a low RMSE value of 1.51 (Table 7). The study found that the ANN regression analysis demonstrated robust models for adulteration phenomena in sesame oil generated using sunflower oil, canola oil, and sunflower + canola oils, quantitatively [52]. Another study stated that using ANN as a pattern recognition technique for the data obtained from electronic nose could not detect the proportion of adulteration in camellia seed oil but successfully quantified adulteration in sesame oil [53].

Table 7 presents the goodness of fit parameters of the regression models obtained. The best model is based on ANN algorithms and exhibits the highest R (0.996), R2 (0.992), adjusted R2 (0.922) values with the lowest values of AIC (233), BIC (240), and RMSE (1.51). The MARS model was next, followed by the SVM, and the least fitting was the MLR model.

Principle Component Analysis (PCA) and Orthogonal Partial Least Squares Discriminant Analysis (OPLS-DA)

This adulteration detection study involves analyzing multiple variables of DSC parameters simultaneously. Chemometric techniques like PCA and OPLS-DA are designed to handle multivariate data, allowing for a comprehensive analysis of the oil samples. For instance, PCA presented in Figure 4a reduced the dimensionality of the dataset by transforming the variables into a smaller set of principal components, capturing the most important variations in the data. Hence, as an unsupervised method, PCA represents the

combinations of the original variables and can be difficult to interpret in the context of class separation. To solve this issue, OPLS-DA analysis was adopted for assessing the discrimination and classification of the adulterated flaxseed oil samples. As a fast and efficient screening tool for large datasets, OPLS-DA allowed us to evaluate the effectiveness of DSC melting profiles of adulterated flaxseed oils in classifying and detecting the percentage of adulterants concentration by differentiating them (Figure 4b).

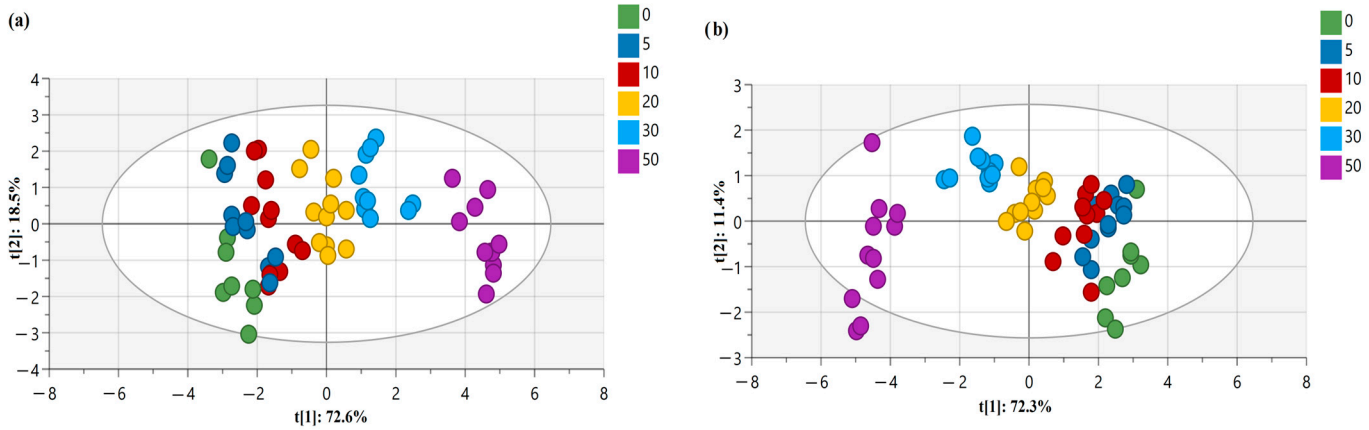

Figure 4. Score plots obtained via (**a**) PCA and (**b**) OPLS-DA for cold-pressed flaxseed oil adulterated with various concentrations of refined rapeseed oils (0, 5, 10, 20, 30, and 50% *w*/*w*).

In Figure 4a, the DSC data matrix serves as the basis for conducting PCA analyses, which provided a visual representation of the data pattern for six concentrations of adulterants mixed with pure flaxseed oils. In the score plot, each point represents a sample (a specific concentration of adulterant mixed with flaxseed oil) in the space of two principal components, t[1] and t[2], which were able to explain 91.1% of the variation of the normalized heat flow results. Additionally, R^2X (cum) and Q^2 (cum) values (Table 9) are the quantities useful for PC model diagnostics as the fraction of the explained variation R^2X and the fraction of predicted variation Q^2. The more significant a principal component, the closer its R^2X and R^2X (cum) will be to value 1 for a PC model with a sufficient number of components. For the PCA analysis presented in Figure 4a, the R^2X (cum) value was 0.973, which indicates that the retained principal components capture a larger proportion of the overall variation in the dataset. This finding can help in determining the appropriate number of components to retain for further analysis. Besides this, the Q^2 (cum) value was 0.897 for the PCA model, which shows that the cumulative sum of the cross-validated predictive ability is high for the variables of the normalized heat flow of phase transition curves. This approach of employing PCA analysis can be compared to other studies, where researchers detected (with 100% accuracy) adulteration of flaxseed oil with rapeseed, corn, peanut, sunflower seed, soybean, and sesame oils [23], or adulteration of virgin coconut oil with refined coconut oil [14].

Table 9. Summary of the fit of different models for discrimination (differentiation) of samples with different concentrations of adulterants (refined rapeseed oil).

Model	R^2X (cum)	R^2 (cum)	Q^2 (cum)
PCA	0.973		0.897
OPLS-DA	0.986	0.465	0.330

The next chemometric approach was analyzing the dataset of multiple variables using OPLS-DA, which can effectively enhance the separation of classes while maintaining the predictive power of the model by utilizing orthogonal projection in the score plot. The analysis aims to classify and distinguish different concentrations of adulterants (ranging

from 0% to 50%) added to pure flaxseed oil. The model consists of 15 variables, where a total of nine DSC parameters are considered as X variables and six different concentrations of adulterants added are considered as Y variables representing the six classes. Five predictive components (P1 to P5) capture the between-class variation, meaning they account for the differences between the different concentrations of adulterants. The orthogonal components capture the within-class variation, representing similarities within each concentration group. Within the framework of the OPLS-DA model, the systematic variation in data was described by two distinct components. The first component, known as the predictive component, exhibits a linear relationship with the classes (Y) and possesses the ability to make accurate predictions. In Figure 4b, the *x*-axis represents the first component (t1 = 72.3%), and the Y-axis the second principal component [t2 = 11.4%]. The observations in the scatter plot are colored, based on their class, which corresponds to the different concentrations of adulterants added to pure flaxseed oil. The scatter plot serves as a visualization of how the modeled observations in the X space are positioned relative to each other. Observations that are close to each other in the plot indicate a higher degree of similarity compared to those that are farther apart.

Also, in Table 9, the R^2X (cum) value was presented as 0.986, indicating that the OPLS-DA model fits the X data well, capturing a large portion of the variation present in the DSC parameters. On the other hand, a Q^2 (cum) value of 0.33 indicates that the OPLS-DA model can predict approximately 33% of the variation in the Y data, according to cross-validation. The range of Q^2 values suggests that the model has reasonable predictive ability for the concentration of adulterants based on DSC variables. OPLS-DA was also adopted by other authors to determine important variables when detecting flaxseed oil multiple adulteration via near-infrared spectroscopy. These authors also adopted the one-class partial least squares (OCPLS) method to build a detection model, which provided a high accuracy of 95.8% [15].

Although the model demonstrates a good fit to the X data (DSC parameters), a low Q^2 (cum) value (0.33) indicates that the model's ability to explain and predict the variation for the Y data (adulterant concentrations) was poor. Thus, the authors decided to explore an alternative modeling technique, i.e., the partial least squares (PLS) technique. In Figure 5a, a loading plot of PLS analysis is presented for DSC parameters obtained from the melting curves. To obtain a comprehensive understanding of the model's performance and predictive ability, the R^2X (cum) value was calculated at a level of 0.953 and was lower than for OPLS-DA, while the predictive Q^2 (cum) value was higher than for OPLS-DA (0.973). The results obtained for R2X (cum) and Q^2 (cum) indicate that the PLS model had higher predictive power than OPLS-DA. Additionally, Figure 5b presents the variables' influence on the projection (VIP) plot, which provides information about the importance of variables (DSC parameters) that are above value 1. As was the case with the MLR model (Table 6), the parameter for the first peak height (h1) and percentage area (P1) were not significant.

In addition to the approaches presented in the study, the observed and predicted value graph from the PLS model is presented in Figure 6. By plotting the observed concentrations of adulterants (actual values) against the predicted concentrations (values predicted using the PLS model) on a graph, it was possible to assess visually how well the model predicts the adulterant levels in the flaxseed oil samples, based on the DSC parameters from melting curves. We can see that the observed and predicted values align closely along a diagonal line, which indicates that the PLS model accurately predicts the adulterant concentrations based on the DSC parameters. A Pearson's correlation coefficient (r) of 0.995 between the observed and predicted values indicates an extremely strong positive linear relationship between the two sets of values. This graph also shows that this model can effectively differentiate between pure flaxseed oil and adulterated samples, providing a reliable means of detecting and estimating the adulterant concentrations. By assessing this graph, it is also evident that the PLS model has successfully learned the relationship between the DSC parameters and the adulterant concentrations, which validates the model for this purpose. This finding can be compared with the study conducted by Rocha et al., who

adopted the PLS method for the classification and quantification of different types of blended biodiesel synthesized from peanut, corn, and canola oils and observed a Pearson's correlation coefficient of 0.969 between the real and predicted concentrations [11].

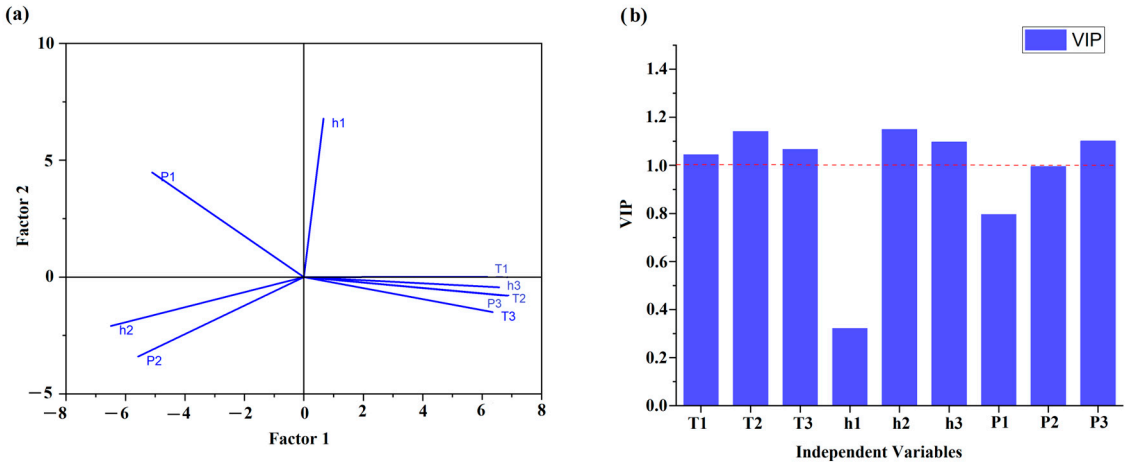

Figure 5. Loading plot of (**a**) PLS analysis for all DSC parameters determined for cold-pressed flaxseed oils adulterated with various concentrations of refined rapeseed oil (0, 5, 10, 20, 30, and 50% *w*/*w*). (**b**) The variables' influence on the projection (VIP) graph.

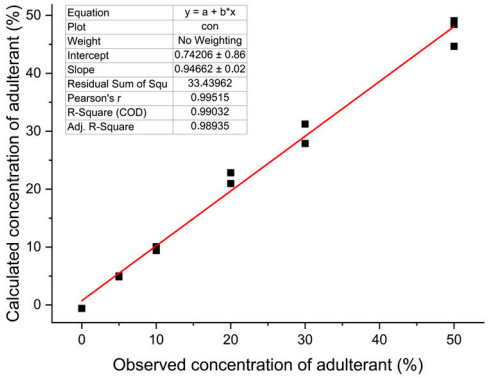

Figure 6. Observed and predicted values in a partial least squares (PLS) model based on the DSC parameters.

5. Conclusions

By developing a method for detecting adulteration of flaxseed oil, this study contributes to solving the problem of food adulteration and its economic impact on the global food industry. The DSC melting curves provided unique and substantial information about the thermal behavior of the flaxseed oil and showed distinct changes when adulterants were added. The second peak in the DSC profiles was identified as the major peak, and its characteristics, such as peak temperature, peak height, and percentage of peak area, were found to be significantly affected by the concentration of adulterants. Moreover, the findings demonstrate the efficacy of coupling DSC with chemometric methods in detecting and classifying adulterations in cold-pressed flaxseed oil. Of the classification models built, the LDA model exhibited the best performance, underlining its potential for accurate identification of adulterated oil samples. On the other hand, the regression model based on the ANN algorithm showed the best goodness of fit for DSC parameters regarding the prediction of adulterant concentrations. The equation and PMML codes derived from the MLR, MARS, SVM, and ANN regression analyses can be used to estimate the percentage of adulterants in flaxseed oil samples based on the values of peak temperature, peak height, and percentage of peak area. The study also employed other chemometric techniques, such as PCA, OPLS-DA, and PLS to effectively classify and describe the adulteration

phenomena. The resulting plots demonstrated that the PLS model showed the greatest accuracy in predicting adulterant levels in flaxseed oil samples based on DSC parameters, as indicated by a strong positive linear relationship (Pearson's correlation coefficient of 0.995). The PLS model effectively differentiated between pure flaxseed oil and adulterated samples, providing a reliable means of detecting and estimating adulterant concentrations. This study highlights the significance of combining DSC with chemometric methods for detecting adulterations in flaxseed oil and emphasizes the importance of quality assessment and authenticity verification in the food industry.

Author Contributions: Conceptualization, M.I. and J.T.-G.; methodology, M.I., A.K. and J.T.-G.; formal analysis, M.I., A.K., M.M. and J.T.-G.; investigation, M.I. and J.T.-G.; resources, J.T.-G.; data curation, M.I., A.K. and J.T.-G.; writing—original draft preparation, M.I., A.K. and J.T.-G.; writing—review and editing, M.I., A.K. and J.T.-G.; visualization, M.I., A.K. and J.T.-G.; supervision, A.K and J.T.-G.; project administration, J.T.-G.; funding acquisition, J.T.-G. All authors have read and agreed to the published version of the manuscript.

Funding: This research was funded by the NATIONAL SCIENCE CENTRE, POLAND, grant number: 2018/31/B/NZ9/02762.

Data Availability Statement: The data presented in this study are available upon reasonable request.

Conflicts of Interest: The authors declare no conflict of interest.

References

1. Jović, O.; Jović, A. FTIR-ATR adulteration study of hempseed oil of different geographic origins. *J. Chemom.* **2017**, *31*, e2938. [CrossRef]
2. Sim, S.F.; Chai, M.X.L.; Jeffrey Kimura, A.L. Prediction of lard in palm olein oil using simple linear regression (SLR), multiple linear regression (MLR), and partial least squares regression (PLSR) based on fourier-transform infrared (FTIR). *J. Chem.* **2018**, *2018*, 7182801. [CrossRef]
3. Tomaszewska-Gras, J. Rapid quantitative determination of butter adulteration with palm oil using the DSC technique. *Food Control* **2016**, *60*, 629–635. [CrossRef]
4. Carter, O.C.S. *On the Detection of Adulterations in Oils*; American Philosophical Society: Philadelphia, PA, USA, 1885; Volume 22.
5. FDA. *Economically Motivated Adulteration; Public Meeting; Request for Comment*; FDA: College Park, MD, USA, 2009; Volume 74, pp. 69–71. Available online: https://www.federalregister.gov/documents/2009/04/06/E9-7843/economically-motivated-adulteration-public-meeting-request-for-comment (accessed on 2 June 2023).
6. FAO. Food Fraud-Intention, Detection and Management. Food Safety Technical Toolkit for Asia and the Pacific No. 5. Bangkok. 2021. Available online: https://www.fao.org/3/cb2863en/cb2863en.pdf (accessed on 5 June 2023).
7. Gelpí, E.; Posada de la Paz, M.; Terracini, B.; Abaitua, I.; Gómez de la Cámara, A.; Kilbourne, E.M.; Lahoz, C.; Nemery, B.; Philen, R.M.; Soldevilla, L.; et al. The spanish toxic oil syndrome 20 years after its onset: A multidisciplinary review of scientific knowledge. *Environ. Health Perspect.* **2002**, *110*, 457–464. [CrossRef]
8. European Commission. European Commission The EU Food Fraud Network and the System for Administrative Assistance-Food Fraud. 2018. Available online: https://eur-lex.europa.eu/legal-content/EN/TXT/?uri=COM:2018:772:FIN (accessed on 27 May 2023).
9. Rocha, W.F.C.; Prado, C.B.; Niksa, B. Comparison of Chemometric Problems in Food Analysis using Non-Linear Methods. *Molecule* **2020**, *25*, 3025. [CrossRef]
10. Zhang, L.; Chen, J.; Jing, B.; Dong, Y.; Yu, X. New Method for the Discrimination of Adulterated Flaxseed Oil Using Dielectric Spectroscopy. *Food Anal. Methods* **2019**, *12*, 2623–2629. [CrossRef]
11. Rocha, W.F.C.; Vaz, B.G.; Sarmanho, G.F.; Leal, L.H.C.; Nogueira, R.; Silva, V.F.; Borges, C.N. Chemometric Techniques Applied for Classification and Quantification of Binary Biodiesel/Diesel Blends. *Anal. Lett.* **2012**, *45*, 2398–2411. [CrossRef]
12. Peng, D.; Shi, C.; Nie, Q.; Xie, S.; Bi, Y.; Li, J. Qualitative and quantitative detection of peanut oils adulteration based on fatty acid information fusion coupled with chemometrics. *Lwt* **2023**, *181*, 114785. [CrossRef]
13. Giese, E.; Rohn, S.; Fritsche, J. Chemometric tools for the authentication of cod liver oil based on nuclear magnetic resonance and infrared spectroscopy data. *Anal. Bioanal. Chem.* **2019**, *411*, 6931–6942. [CrossRef]
14. Bao, R.; Tang, F.; Rich, C.; Hatzakis, E. A comparative evaluation of low-field and high-field NMR untargeted analysis: Authentication of virgin coconut oil adulterated with refined coconut oil as a case study. *Anal. Chim. Acta* **2023**, *1273*, 341537. [CrossRef]
15. Yuan, Z.; Zhang, L.; Wang, D.; Jiang, J.; Harrington, P.d.B.; Mao, J.; Zhang, Q.; Li, P. Detection of flaxseed oil multiple adulteration by near-infrared spectroscopy and nonlinear one class partial least squares discriminant analysis. *LWT* **2020**, *125*, 109247. [CrossRef]

16. Hao, S.; Zhu, L.; Sui, R.; Zuo, M.; Luo, N.; Shi, J.; Zhang, W.; He, X.; Chen, Z. Identification and quantification of vegetable oil adulteration with waste frying oil by laser-induced fluorescence spectroscopy. *OSA Contin.* **2019**, *2*, 1148. [CrossRef]
17. Garrido-Delgado, R.; Eugenia Muñoz-Pérez, M.; Arce, L. Detection of adulteration in extra virgin olive oils by using UV-IMS and chemometric analysis. *Food Control* **2018**, *85*, 292–299. [CrossRef]
18. Vanstone, N.; Moore, A.; Martos, P.; Neethirajan, S. Detection of the adulteration of extra virgin olive oil by near-infrared spectroscopy and chemometric techniques. *Food Qual. Saf.* **2018**, *2*, 189–198. [CrossRef]
19. Huang, K.; Zhong, P.; Xu, B. Discrimination on potential adulteration of extra virgin olive oils consumed in China by differential scanning calorimeter combined with dimensionality reduction classification techniques. *Food Chem.* **2023**, *405*, 134996. [CrossRef] [PubMed]
20. De Souza, L.M.; De Santana, F.B.; Gontijo, L.C.; Mazivila, S.J.; Borges Neto, W. Quantification of adulterations in extra virgin flaxseed oil using MIR and PLS. *Food Chem.* **2015**, *182*, 35–40. [CrossRef] [PubMed]
21. Huang, Z.M.; Xin, J.X.; Sun, S.S.; Li, Y.; Wei, D.X.; Zhu, J.; Wang, X.L.; Wang, J.; Yao, Y.F. Rapid identification of adulteration in edible vegetable oils based on low-field nuclear magnetic resonance relaxation fingerprints. *Foods* **2021**, *10*, 3068. [CrossRef]
22. Sun, X.; Zhang, L.; Li, P.; Xu, B.; Ma, F.; Zhang, Q.; Zhang, W. Fatty acid profiles based adulteration detection for flaxseed oil by gas chromatography mass spectrometry. *LWT* **2015**, *63*, 430–436. [CrossRef]
23. Wang, J.; Han, Y.; Wang, X.; Li, Y.; Wang, S.; Gan, S.; Dong, G.; Chen, X.; Wang, S. Adulteration detection of Qinghai-Tibet Plateau flaxseed oil using HPLC-ELSD profiling of triacylglycerols and chemometrics. *LWT* **2022**, *160*, 113300. [CrossRef]
24. Elzey, B.; Pollard, D.; Fakayode, S.O. Determination of adulterated neem and flaxseed oil compositions by FTIR spectroscopy and multivariate regression analysis. *Food Control* **2016**, *68*, 303–309. [CrossRef]
25. Chiavaro, E.; Vittadini, E.; Rodriguez-Estrada, M.T.; Cerretani, L.; Bendini, A. Differential scanning calorimeter application to the detectionof refined hazelnut oil in extra virgin olive oil. *Food Chem.* **2008**, *110*, 248–256. [CrossRef] [PubMed]
26. Jafari, M.; Kadivar, M.; Keramat, J. Detection of adulteration in Iranian olive oils using instrumental (GC, NMR, DSC) methods. *JAOCS J. Am. Oil Chem. Soc.* **2009**, *86*, 103–110. [CrossRef]
27. Van Wetten, I.A.; Van Herwaarden, A.W.; Splinter, R.; Boerrigter-Eenling, R.; Van Ruth, S.M. Detection of sunflower oil in extra virgin olive oil by fast differential scanning calorimetry. *Thermochim. Acta* **2015**, *603*, 237–243. [CrossRef]
28. Karbasian, M.; Givianrad, M.H.; Ramezan, Y. A rapid method for detection of refined olive oil as adulterant in extra virgin olive oil by differential scanning calorimetry. *Orient. J. Chem.* **2015**, *31*, 1735–1739. [CrossRef]
29. Marikkar, J.M.N. Differential Scanning Calorimetric Analysis of Virgin Coconut Oil, Palm Olein, and their Adulterated Blends. *Cord* **2019**, *35*, 9. [CrossRef]
30. Marina, A.M.; Che Man, Y.B.; Nazimah, S.A.H.; Amin, I. Monitoring the adulteration of virgin coconut oil by selected vegetable oils using differential scanning calorimetry. *J. Food Lipids* **2009**, *16*, 50–61. [CrossRef]
31. Coni, E.; Di Pasquale, M.; Coppolelli, P.; Bocca, A. Detection of animal fats in butter by differential scanning calorimetry: A pilot study. *J. Am. Oil Chem. Soc.* **1994**, *71*, 807–810. [CrossRef]
32. Tomaszewska-Gras, J. Multivariate analysis of seasonal variation in the composition and thermal properties of butterfat with an emphasis on authenticity assessment. *Grasas y Aceites* **2016**, *67*, 4. [CrossRef]
33. Upadhyay, N.; Goyal, A.; Kumar, A.; Lal, D. Detection of adulteration by caprine body fat and mixtures of caprine body fat and groundnut oil in bovine and buffalo ghee using differential scanning calorimetry. *Int. J. Dairy Technol.* **2017**, *70*, 297–303. [CrossRef]
34. Marikkar, J.M.N.; Ghazali, H.M.; Che Man, Y.B.; Lai, O.M. The use of cooling and heating thermograms for monitoring of tallow, lard and chicken fat adulterations in canola oil. *Food Res. Int.* **2002**, *35*, 1007–1014. [CrossRef]
35. Paranthaman, R.; Moses, J.A.; Anandharamakrishnan, C. Development of a method for qualitative detection of lead chromate adulteration in turmeric powder using X-ray powder diffraction. *Food Control* **2021**, *126*, 107992. [CrossRef]
36. Clas, S.D.; Dalton, C.R.; Hancock, B.C. Differential scanning calorimetry: Applications in drug development. *Pharm. Sci. Technol. Today* **1999**, *2*, 311–320. [CrossRef] [PubMed]
37. Drzeżdżon, J.; Jacewicz, D.; Sielicka, A.; Chmurzyński, L. Characterization of polymers based on differential scanning calorimetry based techniques. *TrAC Trends Anal. Chem.* **2019**, *110*, 51–56. [CrossRef]
38. Parniakov, O.; Bals, O.; Barba, F.J.; Mykhailyk, V.; Lebovka, N.; Vorobiev, E. Application of differential scanning calorimetry to estimate quality and nutritional properties of food products. *Crit. Rev. Food Sci. Nutr.* **2018**, *58*, 362–385. [CrossRef]
39. FAO. Production/Yield Quantities of Oil of Linseed in World + (Total) [Internet]. 2020. Available online: https://www.fao.org/faostat/en/#data/QCL/visualize (accessed on 11 June 2023).
40. Tomaszewska-Gras, J.; Islam, M.; Grzeca, L.; Kaczmarek, A.; Fornal, E. Comprehensive thermal characteristics of different cultivars of flaxseed oil (*Linum usittatissimum* L.). *Molecules* **2021**, *26*, 1958. [CrossRef] [PubMed]
41. Khattab, R.Y.; Zeitoun, M.A. Quality evaluation of flaxseed oil obtained by different extraction techniques. *LWT Food Sci. Technol.* **2013**, *53*, 338–345. [CrossRef]
42. Visentainer, J.V.; De Souza, N.E.; Makoto, M.; Hayashi, C.; Franco, M.R.B. Influence of diets enriched with flaxseed oil on the α-linolenic, eicosapentaenoic and docosahexaenoic fatty acid in Nile tilapia (Oreochromis niloticus). *Food Chem.* **2005**, *90*, 557–560. [CrossRef]
43. Tuncel, N.B.; Uygur, A.; Karagül Yüceer, Y. The Effects of Infrared Roasting on HCN Content, Chemical Composition and Storage Stability of Flaxseed and Flaxseed Oil. *JAOCS J. Am. Oil Chem. Soc.* **2017**, *94*, 877–884. [CrossRef]

44. Xu, J.; Yang, W.; Deng, Q.; Huang, Q.; Yang, J.; Huang, F. Flaxseed oil and α-lipoic acid combination reduces atherosclerosis risk factors in rats fed a high-fat diet. *Lipids Health Dis.* **2012**, *11*, 148. [CrossRef]
45. Dwivedi, C.; Natarajan, K.; Matthees, D.P. Chemopreventive effects of dietary flaxseed oil on colon tumor development. *Nutr. Cancer* **2005**, *51*, 52–58. [CrossRef]
46. Popa, S.; Milea, M.S.; Boran, S.; Nițu, S.V.; Moșoarcă, G.E.; Vancea, C.; Lazău, R.I. Rapid adulteration detection of cold pressed oils with their refined versions by UV–Vis spectroscopy. *Sci. Rep.* **2020**, *10*, 16100. [CrossRef] [PubMed]
47. American Oil Chemists' Society. *DSC Melting Properties of Fats and Oils*; Cj 1-94; American Oil Chemists' Society: Urbana, IL, USA, 2000.
48. Efenberger-Szmechtyk, M.; Nowak, A.; Kregiel, D. Implementation of chemometrics in quality evaluation of food and beverages. *Crit. Rev. Food Sci. Nutr.* **2018**, *58*, 1747–1766. [CrossRef] [PubMed]
49. Indriyani, L.; Rohman, A.; Riyanto, S. Authentication of avocado oil (*Persea americana* Mill.) Using differential scanning calorimetry and multivariate regression. *Asian J. Agric. Res.* **2016**, *10*, 78–86. [CrossRef]
50. Friedman, J.H. Multivariate adaptive regression splines. *Ann. Stat.* **1991**, *19*, 1–67. [CrossRef]
51. Karami, H.; Rasekh, M.; Mirzaee–Ghaleh, E. Comparison of chemometrics and AOCS official methods for predicting the shelf life of edible oil. *Chemom. Intell. Lab. Syst.* **2020**, *206*, 104165. [CrossRef]
52. Firouz, M.S.; Omid, M.; Babaei, M.; Rashvand, M. Dielectric spectroscopy coupled with artificial neural network for classification and quantification of sesame oil adulteration. *Inf. Process. Agric.* **2022**, *9*, 233–242. [CrossRef]
53. Hai, Z.; Wang, J. Detection of adulteration in camellia seed oil and sesame oil using an electronic nose. *Eur. J. Lipid Sci. Technol.* **2006**, *108*, 116–124. [CrossRef]

Statement about the contribution of authors

Publication title A5: Islam, M.; Kaczmarek, A.; Montowska, M.; Tomaszewska-Gras, J. Comparing Different Chemometric Approaches to Detect Adulteration of Cold-Pressed Flaxseed Oil with Refined Rapeseed Oil Using Differential Scanning Calorimetry. Foods 2023, 12, 3352. https://doi.org/10.3390/foods12183352

Author	Contribution	Percentage contribution	Signature
Mahbuba Islam	Conceptualization, Methodology, Formal analysis, Investigation, Data curation, Writing- original draft preparation, Writing- review and editing, Visualization.	45	
Anna Kaczmarek	Methodology, Formal analysis, Data curation, Writing- original draft preparation, Writing- review and editing, Visualization, Supervision.	20	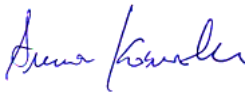
Magdalena Montowska	Formal analysis.	5	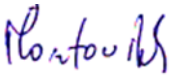
Jolanta Tomaszewska-Gras	Conceptualization, Methodology, Formal analysis, Investigation, Resources, Data curation, Writing- original draft preparation, Writing- review and editing, Visualization, Supervision, Project administration, Funding acquisition.	30	

Publication no. A6

Islam, M., Kaczmarek, A. Tomaszewska-Gras, J. Differential scanning calorimetry as a tool to assess the oxidation state of cold-pressed oils during shelf-life. Journal of Food Measurement and Characterization (2023). https://doi.org/10.1007/s11694-023-02152-8

Journal of Food Measurement and Characterization
https://doi.org/10.1007/s11694-023-02152-8

ORIGINAL PAPER

Differential scanning calorimetry as a tool to assess the oxidation state of cold-pressed oils during shelf-life

Mahbuba Islam[1] · **Anna Kaczmarek**[1] · **Jolanta Tomaszewska-Gras**[1]

Received: 24 May 2023 / Accepted: 10 September 2023

Abstract
Cold-pressed oils are highly prone to the peroxidation process, which causes a rapid decline in quality. Thus, there is a need to develop instrumental methods instead of conventional chemical analysis consuming large quantities of harmful chemicals. Differential scanning calorimetry (DSC) is a valuable analytical tool for assessing the oxidative stability of oils. Cold-pressed flaxseed, camelina and hemp seed oils from different cultivars, which had been stored for six months in room conditions under natural light exposure, were tested. Chemical methods for measuring changes in oxidative stability during storage of oils included determination of peroxide value (PV), p-Anisidine value (p-AV), total oxidation value (TOTOX) value and acid value (AV). Parameters like oxidation induction time (OIT) in isothermal mode (120, 140 °C) and onset temperature (Ton) in non-isothermal mode (heating rate 2, 5 °C/min) were established from DSC curves. Data for OIT and Ton plotted against time showed a strong, significant ($p \leq 0.05$) descending trend for all oils. However, flaxseed and hempseed oils revealed a more rapid deterioration during storage compared to camelina seed oils. All DSC results showed promising repeatability of the oxidative characteristics for three types of cold-pressed oils, regardless of their origins in different cultivars. However, the most suitable for monitoring the deteriorative changes in oils during storage was the isothermal test carried out at a temperature of 120 °C, for which the correlations with chemical indicators (PV, p-AV, TOTOX) were highly significant ($p \leq 0.0001$). Linear discriminant analysis (LDA) based on the DSC results revealed, that the first discriminating function significantly separated the fresh oils from stored oils. The study showed that, based on a starting point defined for fresh oils, the DSC technique can be used to effectively and ecologically monitor the deterioration of oils by oxidation, instead of harmful chemical analyses.

Keywords Plant oils · Oxidation induction time · Isothermal · Non-isothermal · Oxidative stability · Linear discriminant analysis · Deterioration · Flaxseed · Camelina · Hemp

Introduction

Cold-pressed oils from plant sources have recently become popular on the market due to their high nutritional value [1] and their application in different sectors e.g., the food and pharmaceutical [2], cosmetic [3] and biodiesel industries [4]. In 2021, the worldwide market for cold-pressed oils had a valuation of USD 27.05 billion, and it is anticipated to experience a compound annual growth rate (CAGR) of 5.7% from 2022 to 2028 [5]. Consumers are now becoming very diligent about new sources of foods like cold-pressed oils from plant sources to meet the requirements of essential nutrition. This approach to meeting market requirements is sometimes more based on marketing practices rather than care for product quality. Considering the importance of cold-pressed oil production, it has become extremely important to maintain the quality of products from these oils during their shelf life in the supermarkets. Primarily, the presence of unsaturated carbon bonds (C = C) makes these oils highly prone to oxidation. This oxidation while storing and processing edible oils is caused by distinct chemical

✉ Jolanta Tomaszewska-Gras
jolanta.tomaszewska-gras@up.poznan.pl

Mahbuba Islam
mahbuba.islam@up.poznan.pl

Anna Kaczmarek
anna.kaczmarek@up.poznan.pl

[1] Department of Food Safety and Quality Management, Poznań University of Life Sciences, ul. Wojska Polskiego 31/33, Poznań 60-637, Poland

mechanisms - autoxidation and photosensitized oxidation - which are dependent on the type of oxygen involved ($^3O_2$- atmospheric triplet oxygen; or $^1O_2$- singlet oxygen). While autooxidation is caused by the reaction of $^3O_2$ to lipid free radicals, photosensitized oxidation is the result of oils being exposed to light, sensitizers and atmospheric oxygens, which leads to the production of $^1O_2$ [6]. An oxidation test for oils relates to measuring the degree of oxidation in the oil, which ultimately leads to the formation of off-flavors, odors, and potentially harmful compounds [7]. Different analytical and chemical methods provide different measures of oxidative stability [8, 9]; hence, the choice of method depends on the specific application and the type of oil being analyzed. During storage time analysis, it is important to consider the shelf life condition of the oils [10] and also seeds [11, 12], as well as to consider fast and feasible methods for detecting deterioration stages of the oils. The most popular chemical methods used in the food industry for measuring oxidative stability are peroxide value determination (PV), p-Anisidine value (p-AV), total oxidation value (TOTOX) value and acid value (AV), which generally provide quantitative information about chemical changes caused by the oxidation process [13–15]. For example, these methods were used to investigate how temperature and heating time affect the deterioration of virgin olive oil, [16] and sunflower oil [17], both for food and for biodiesel production. Other studies have used these methods to explore how antioxidants increase the oxidative stability of the sunflower oil [18] or rapeseed oil [19]. However, despite of their popularity as conventional chemical measurements, these methods are subject to the technician's precision, and the quality of both the chemicals and the tools. Moreover, large amounts of harmful chemicals are used in these methods, which produces toxic chemical wastes. Following the green chemistry trend, instrumental methods should be developed and applied to assess the quality of oils. Meanwhile, thermal analysis methods e.g. DSC can generate information on both the physical and chemical changes to explain the oil samples' comprehensive character [20, 21]. Determining the phase transition [22], crystallization and melting data [23, 24], assessment for oxidation profiles [8, 25] can provide a full spectrum dataset to understand the physicochemical characteristics of fats and oils.

The DSC technique offers versatile tools for assessing the oxidative stability of oils through both isothermal and non-isothermal modes [26]. The isothermal method involves subjecting the oil to a constant temperature, allowing the determination of its oxidation induction time (OIT), making it particularly useful for measuring the oil resistance to oxidation at specific temperature [8]. On the other hand, the non-isothermal method, subjects the oil to an increasing temperature with a defined heating rate that allows the onset temperature of oxidation (Ton) to be measured. The DSC isothermal or non-isothermal oxidation tests were used to study, for instance the effect of seeds roasting [27], oils blending [28], oils extraction method [29], addition of plant extracts to fats [30] or addition of antioxidants to oils [31]. To the best of our knowledge, there are no studies on the applicability of DSC isothermal and non-isothermal oxidation tests to monitor changes in oils caused by quality deterioration during storage at conditions similar to the supermarket shelf. So far the approach taken to evaluate the oxidation state of plant oils using characteristic chemical oxidation indicators like PV or TOTOX has been proposed [32]. Since the DSC technique does not require toxic chemicals for chemical analysis, it is worth testing its usability as a method for monitoring the quality changes in oils during storage. Thus, the aim of this study was to assess the oxidative stability changes in three different cold-pressed oils during six months' storage by use of the DSC isothermal and non-isothermal tests in comparison with the conventional chemical indexes (PV, p-AV, TOTOX, AV). For this research, three popular cold-pressed oils i.e., flaxseed oil obtained from *Linum usitatissimum* (L.) crop, camelina seed oil obtained from *Camelina sativa* (L.) crop, and hemp seed oil obtained from *Cannabis sativa* (L.) crop, originated from different cultivars from Poland were studied. The most common feature of these three oils is the very high amount of polyunsaturated fatty acids (PUFA), e.g., flaxseed and hempseed oils have a PUFA level of over 70% [11, 21], while in camelina oils PUFAs account for more than 54% of their total fatty acid content [26].

Materials and methods

Chemicals

All materials utilized in this study were of the utmost quality and met analytical grade standards. Glacial acetic acid (purity of 100%) and p-Anisidine reagent (purity of 99%) were procured from Sigma Aldrich. The acquisition of potassium hydroxide, starch, and sodium thiosulfate was made from firma Chempur (Poland). Toluene (purity of 99.5%), Isopropanol (purity of 99.7%), Isooctane (pure), and phenolphthalein were acquired from POCH (Gliwice, Poland). Potassium Iodide (purity of 99%) was sourced from ALFA CHEM (Łódź, Poland). Also, distilled water used from Laboratory facility. Spectrophotometric analyses were conducted utilizing the Cary 1E spectrophotometer (Varian, Belrose, Australia). Titration analyses were executed using the Titration unit Solarus (Hirschmann Laborgeräte GmbH & Co. KG, Eberstadt, Germany.

Materials

For this study, the primary objective was to acquire 15 kg of seeds for each specific cultivar or batch of flax, camelina, and hemp from various sources. For cold-pressed flaxseed oils, seeds of three cultivars of flax (*Linum usitatissimum* L.), i.e., *Bukoz* from the Polish Institute of Natural Fibers and Medicinal Plants (Poznań, Poland), *Dolguniec* from SEMCO manufactory (Śmiłowo, Poland), *Szafir* (SEMCO manufactory (Śmiłowo, Poland) and Hodowla Roślin Strzelce Sp. z o.o. (Strzelce, Poland) were collected along with one sample of unknown cultivar from VitaCorn (Poznan, Poland). All hemp seeds were obtained from *Henola* cultivar of *Cannabis sativa* L., which were gathered from five different suppliers, and their collection was done at the Polish Institute of Natural Fibers and Medicinal Plants. Camelina seeds of three cultivars of *Camelina sativa* L. were obtained from five suppliers. Seeds of the spring *Omega* cultivar were procured from Poznań University of Life Sciences (Agriculture Research Station Dłoń, Miejska Górka), while two other camelina cultivars, *Luna* and *Śmiłowska*, were collected from SEMCO manufactory. This manufactory sourced *Luna*, a winter cultivar, from two different suppliers and *Śmiłowska*, a spring cultivar, from two different suppliers as well. All the seeds were cold-pressed under uniform conditions at the SEMCO manufactory, with the temperature maintained below 50 °C. The oils obtained through pressing were then allowed to settle for 24 h and were subsequently stored in brown glass bottles. These containers were chosen for their ability to shield the oils from light exposure as well as to replicate conditions commonly found in the market. A comprehensive storage analysis was conducted, starting from the oils' initial state and extending up to the sixth month of their shelf life. At each storage interval (0, 2nd, 4th, and 6th month), newly unsealed bottles containing samples of oil were utilized for all analytical procedures. Throughout the duration of the shelf life assessment, the samples were maintained in airtight conditions at room temperature (23–25 °C) beside a window, where they were subjected to natural sunlight exposure. The intention behind this approach was to recreate the real-life conditions that oils may encounter during processes such as transportation, distribution or household end-use.

Determination of oxidative stability by DSC

Oxidative stability was determined by following the ISO 11357-1 [33], and also implementing the ASTM D3895-14 [34]. The oil samples were subjected to analysis using a DSC 7 Perkin Elmer device, which was equipped with an Intracooler II and operated through Pyris software. Prior to testing, the instrument was calibrated using indium (with a melting point of 156.6 °C and a ΔH_f of 28.45 J/g) and n-dodecane (with a melting point of -9.65 °C and a ΔH_f of 216.73 J/g), while 99.99% pure nitrogen gas was used as the purge gas. To conduct the analysis, approximately 6–7 mg of oil samples were weighed into 50 µl open aluminium pans (Perkin Elmer, No. 02190041). An open and empty aluminium pan was used as the reference. To investigate the oxidation process, a constant oxygen flow of 20 ml/min (with a purity of 99.995%) was maintained during the analysis. Both isothermal and non-isothermal protocols were employed to determine the oxidative stability characteristics of the oils. For the isothermal program, temperatures of 120 and 140 °C were set and specific parameters such as oxidation induction time (OIT), oxidation end time (OET), length of oxidation ($\Delta t = OET - OIT$), and the rate of oxidation were determined from the DSC curves. The index of oxidation induction time (OIT) was determined based on the curves obtained after normalization of the oxidation DSC curve, by calculating the intersection of the extrapolated baseline and the tangent line to the descending exotherm. To determine the OET value at the point where the heat flow of the exotherm reached its minimum level, calculations were made to identify the end of the propagation stage and the start of the termination stage of oxidation. The oxidation rate was computed using the equation provided below

$$Oxidationrate = (Y1 - Y2)/\Delta t\,(1) \quad (1)$$

Where, Y1 stands for heat flow at OIT point (W/g), Y2 represents heat flow at OET (W/g), and Δt is the length of oxidation (minutes).

Non-isothermal analysis was conducted using a heating rate of 2 °C/min and 5 °C/min. The onset temperature (Ton) was determined from the oxidation curves by calculating the intersection of the extrapolated baseline and the tangent line to the descending curve of the recorded exotherm. On the other hand, the temperature at which the heat flow reached its minimum value was measured and recorded as Tend, signifying the transition from the propagation stage to the termination stage of the oxidation process. All DSC experiments were carried out in duplicate for each oil sample.

Chemical determination of oxidative stability

To evaluate the amount of secondary oxidative products (such as aldehydes, carbonyls, trienes, and ketones) present in the samples, the p-anisidine value (p-AV) was measured according to ISO 6885:2016 [35]. The peroxide value (PV) was determined to quantify the peroxides produced in the samples as an expression of the milliequivalents of excess active oxygen [$mEqO_2$] content as a result of the oxidation reaction by following the ISO 3960:2010 procedure

[36]. The total oxidation value (TOTOX) parameter was calculated based on the pAV and PV values by means of the following formula TOTOX = pAV + 2PV, expressing the overall rate of oil oxidation [36]. Acid value (AV), as an indicator of the degree of hydrolytic changes, expressed in milligrams of potassium hydroxide (KOH) per gram of the sample was measured according to the official AOCS method [37]. All chemical analyses were performed in three replications.

Statistics

Statistical analysis of the recorded data was conducted using Statistica 13.3 software (TIBCO Software Inc. USA), employing a robust suite of techniques to evaluate various aspects of oil storage. The significance level was set at $\alpha = 0.05$ to ensure that the results were statistically significant. Linear Regression Analysis, utilizing the method of least squares estimation was performed. Linear regression analysis was employed to evaluate the effects of oil storage on selected chemical and DSC parameters. This approach allowed modelling the relationship between the dependent and independent variables, providing information on how the storage time of oil affects these parameters. This analysis was also used to assess the significance of the relationship between DSC parameters (predictors) and chemical indicators of oil oxidation. Pearson's Linear Correlation Coefficients were calculated to express the direction and strength of the linear relationship between the variables, offering a concise summary of how the variables are correlated. Additionally, Principal Component Analysis (PCA) was conducted to identify patterns and relationships between variables and objects. By transforming the data into a new coordinate system, PCA reduced the dimensionality of the dataset while retaining most of the original variance. This allowed for the identification of the principal components that best represent the underlying structure of the data, facilitating a more nuanced understanding of the complex relationships between variables. Linear Discriminant Analysis (LDA) was used to build a classification model to categorize the oils by storage time. In this study, LDA aimed to find the linear combination of features that best separates oils into three distinct classes (0, 4- and 6-month storage time). By maximizing the between-class variance and minimizing the within-class variance, LDA created a decision boundary that effectively classified the oils based on their storage time. This method provided a powerful tool for understanding how storage time influences the characteristics of the oils, enabling precise categorization. The combination of these statistical methods provided a comprehensive analysis of the data, enabling a detailed examination of the effects of oil storage on selected chemical and DSC parameters. The simultaneous use of linear regression, correlation analysis, PCA and LDA provided a multi-faceted approach to understand the complex relationships in the dataset, contributing to the robustness and validity of the findings.

Results

Oxidative stability of cold-pressed oils during storage measured by conventional chemical methods

Conventional chemical analyses were used in food analysis to determine the changes and status of the oxidative stability of fats and oils from ages [38]. The most popular conventional methods for measuring oil quality are by determining peroxide value (PV), acid value (AV) and p-anisidine value (p-AV). The PV expresses the primary oxidation products present in the sample, whereas the p-AV value represents the secondary oxidation products. Based on the PV and p-AV, the TOTOX value (total oxidation rate) is calculated, which represents the overall oxidation status or rancidity status of the oil. The acid value, in turn, denotes the presence of free fatty acids in the oil samples.

In Fig. 1, scatterplots are shown for the aforementioned chemical indicators obtained during storage of cold-pressed flaxseed, camelina and hempseed oils of various varieties. From the results plotted for PV presented in Fig. 1 it can be seen that for all three oils the values increased until the end of the storage period. The mean values for the starting point of PV measured for fresh oils were 3.2, 3.1, 15.45 $mEqO_2/kg$ for flaxseed, camelina and hempseed oils, respectively, while at the end of storage, after six months, they were significantly higher than for fresh oils i.e. 12.4, 9.8, 32.85 $mEqO_2/kg$ ($p \leq 0.05$). Standards developed by the Food and Agriculture Organization (FAO) and the World Health Organization (WHO), known as Codex Alimentarius, can be considered as a reference for food standards and regulations. According to Codex Alimentarius, with the standard limit for the PV value established as less than 15 $mEqO_2/kg$ oil [39], cold-pressed flaxseed and camelina seed oil did not exceed the limit after six months of light exposure at room temperature, while the hempseed oils certainly did. The ascending trend in quality changes can be more precisely expressed by comparing the slope of the straight line, which was lowest for camelina oil (1.07) and highest for hemp oil (2.84), indicating the most pronounced oxidative changes in this oil. As shown in Fig. 1, correlations of PV with time were very strong and significant ($p \leq 0.05$) for all oils, as the correlation coefficients (r) were between 0.87 and 0.90.

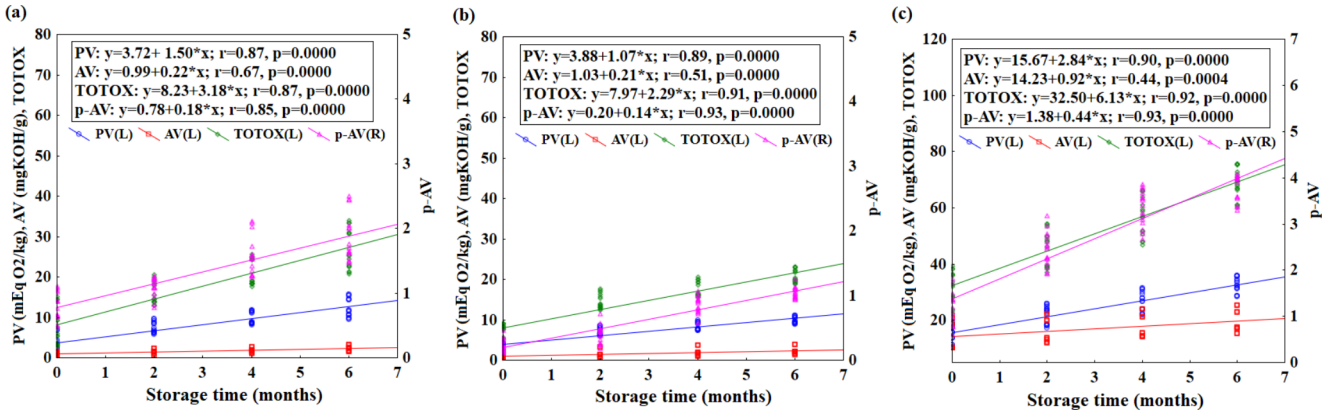

Fig. 1 Changes in oxidative stability of cold-pressed (**a**) flaxseed, (**b**) camelina, (**c**) hempseed oils during six months of storage determined by chemical indicators (PV, p-AV, TOTOX, AV)

The second indicator of the oxidative deterioration of the oils was the p-anisidine value (p-AV), for which a similar ascending trend during storage was observed (Fig. 1, scale on the right). This measure accounts for the quantification of secondary oxidation products like aldehydes, carbonyls, trienes and ketones formed in the oil. For the three oils tested, the starting point of p-AV was 0.79, 0.24, 1.21, while after six months it had increased to significantly higher values of 1.87, 1.06, 3.78 for flaxseed, camelina, and hempseed oils, respectively ($p \leq 0.05$). The slope value of the straight line plotted for the p-AV data showed that for hempseed oils it was four times higher (slope 0.44) than for flaxseed and camelina oils (slope 0.18 and 0.14, respectively). The correlation found between p-AV and storage time was significant ($p \leq 0.05$) for all three oils, for which the r values were between 0.85 and 0.93 (Fig. 1). Based on the PV and p-AV results, the TOTOX values were calculated, which cover the overall quality changes at all stages of shelf life. The slopes of straight lines plotted from TOTOX values (Fig. 1) show that the rate of total quality deterioration of oil during storage time was two times lower for flaxseed oil (slope 3.18), and three times lower for camelina oil (slope 2.29) than for hempseed oil (slope 6.13). After six months of storage, the values of TOTOX for all oils were significantly higher than for fresh oils ($p \leq 0.05$). As all TOTOX data were generated from PV and p-AV values, the correlation coefficients versus time were also high and significant, like was the case for PV and p-AV ($p \leq 0.05$).

Another important chemical indicator of oil quality is the acid value (AV), indicating a hydrolysis process occurring in the oil, which can result in the production of free fatty acids (FFA). Different factors such as high temperature [17], prolonged storage [40], or microbial contamination [41] can cause higher AV values. For flaxseed and camelina seed oil, AV values were established for the ascending trend with a slope of 0.22 and 0.21, respectively, while for hempseed oil the slope of the increase was almost four times higher (0.92) than for flaxseed and camelina oils. At the beginning of storage, the mean values of AV were 0.98, 0.99, 14.13 for flaxseed, camelina and hempseed oils, respectively, while after six months of storage, significantly higher values were observed for all oils, i.e. 2.31, 2.27 and 19.69, respectively. However, oils which exceed the limit of 4.0 mg KOH/g for AV, according to Codex Alimentarius recommendations [39], should not be considered as acceptable for consumption. In this study, flaxseed and camelina oils did not exceed the limit after storage time, but for hempseed oil the AV value was over the limit. Presumably, the quality of the seeds of hemp oil played an important role in the oxidation character of the samples [11]. Significant correlations between AV and storage time were also noted for all oils ($p \leq 0.05$), although the correlation coefficients were lower than for PV and p-AV, since the r values were between 0.44 and 0.67.

The results obtained for chemical indicators of the deterioration of three oils are in agreement with the previous studies in this area. Increasing values of PV and p-AV during storage were also reported for camelina seed oils, although the storage conditions (darkness under 8 °C for 3 weeks) were different than those used in this study [42]. There were also studies showing a significant increase in chemical indexes (i.e. AV, PV, p-AV) for stored flaxseed oil, which are comparable to this study [43, 44]. In another study on hempseed oils oxidized under accelerated test (60 °C), it was established that cold-pressed hempseed oil exceeded the Codex Alimentarius limit for PV after 18 days of storage [45].

Oxidative stability of cold-pressed oils during storage measured by DSC technique

Differential scanning calorimetry is a technique that enables resistance of oils to thermal oxidation to be measured by determining isothermally the oxidation induction time

(OIT) or non-isothermally induction temperature (Ton). Deterioration in oil quality during storage can cause a lowering of resistance to thermal oxidation. However, there are no studies showing whether these parameters change during shelf life. Resistance to thermal oxidation is a specific feature of each oil, and is influenced by the fatty acid composition, especially the content of polyunsaturated fatty acids, as well as antioxidants like tocopherols, polyphenols or prooxidants, for instance, chlorophylls and phospholipids. Determining oxidative stability by means of isothermal (OIT) or non-isothermal (Ton) process implemented using the DSC technique involves exposing the oil or fat sample to elevated temperatures in the presence of oxygen to accelerate the oxidation process.

Data acquired using these experimental methods can be used successfully to optimize processing and storage conditions to extend the shelf life of the oil. In Fig. 2, the DSC curves for one selected cold-pressed flaxseed oil (*Szafir* cultivar) are shown for both measurements i.e., isothermal at two different temperatures (120 and 140 °C) and non-isothermal at two different scanning rates (2 and 5 °C/min). To measure the changes by the isothermal mode, the oxidation induction time (OIT) parameter was calculated from the curves as a function of heating time at a constant temperature. The OIT value is equal to the time of initiation of the exothermic oxidation reaction. The oxidation profiles show the changes occurring during six months of storage. In Fig. 2a, changes in the oxidation profiles manifested by shifting the initiation time to lower values for every storage period can be seen. This suggests that storing oil samples for six months reduces the OIT, and thus resistance to thermal oxidation, as a consequence of the deterioration of the oil. Another option for measuring thermal oxidation stability is the non-isothermal analysis by DSC, where an oil sample is subjected to an increasing temperature at a constant heating rate. In this study, two different heating rates 2 and 5 °C/min were applied to observe any changes in the heat flow, manifested as exothermic phenomena during oxidation. The parameter calculated as the onset temperature (Ton) is equal to the temperature at which the oxidation process starts. As was the case with the isothermal measurement, the non-isothermal analysis showed a similar trend of decreasing oil stability during storage for all the oils tested. As shown in Fig. 2b, for a heating rate of 2 and 5 °C/min the oxidation process was initiated in fresh flaxseed oil samples at higher temperatures than after six months.

Figure 3 presents the changes in OIT values during storage of the three oils measured at 120 and 140 °C. Generally, comparing the values obtained for temperatures of 120 and 140 °C it can be seen that for a higher temperature (140 °C) lower OIT values were obtained for all oils tested. This observation is in agreement with other studies [26, 46, 47]. The points presented on each straight line for each period represent the various cultivars of flaxseed 5a, camelina 5b and hempseed oil 5c, thus the differences between the values for the same time and the same oil can be observed, which are due to differences in the composition of various cultivars.

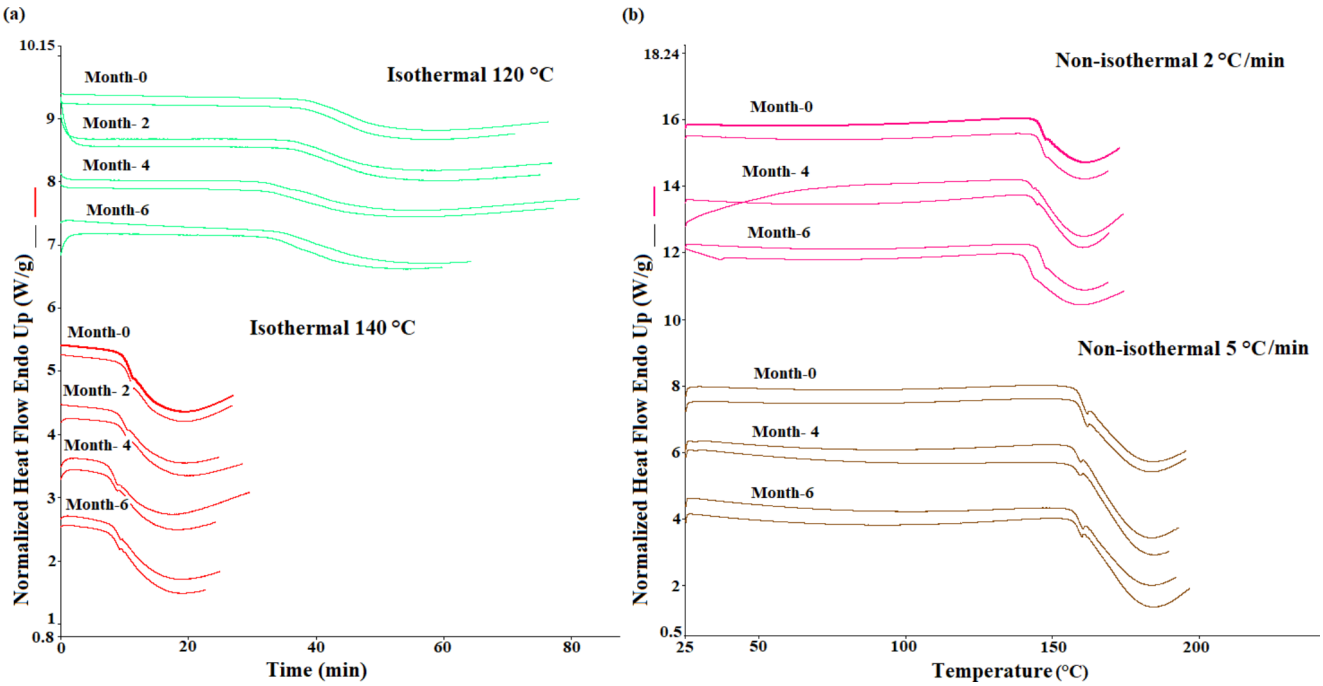

Fig. 2 DSC oxidation curves for flaxseed oil (*Szafir* cultivar) during storage, determined (**a**) isothermally (OIT at 120, 140 °C) and (**b**) non-isothermally (Ton at 2, 5 °C/min)

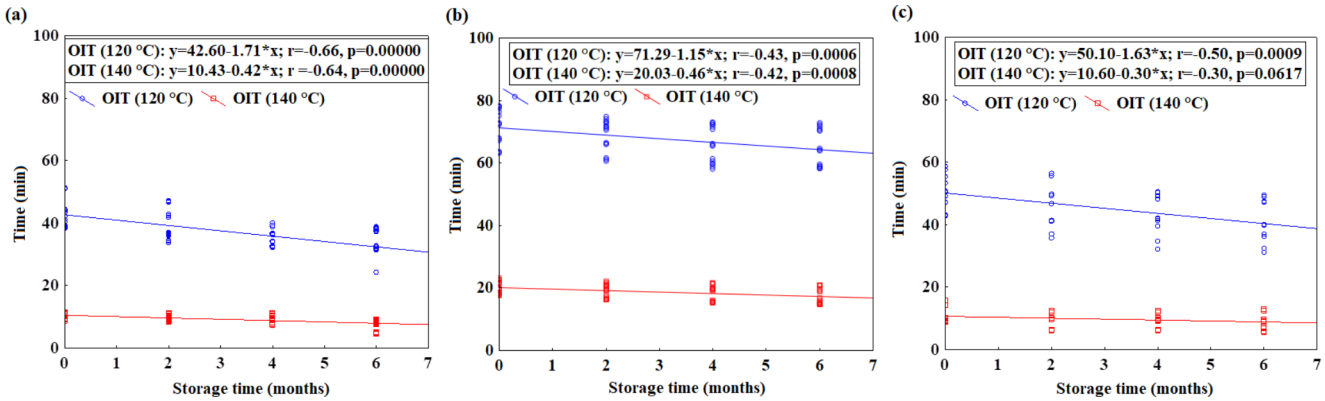

Fig. 3 Changes in oxidation induction time (OIT) of cold-pressed oils during storage (**a**) flaxseed oil, (**b**) camelina oil and (**c**) hempseed oil, determined by isothermal DSC at 120 and 140 °C

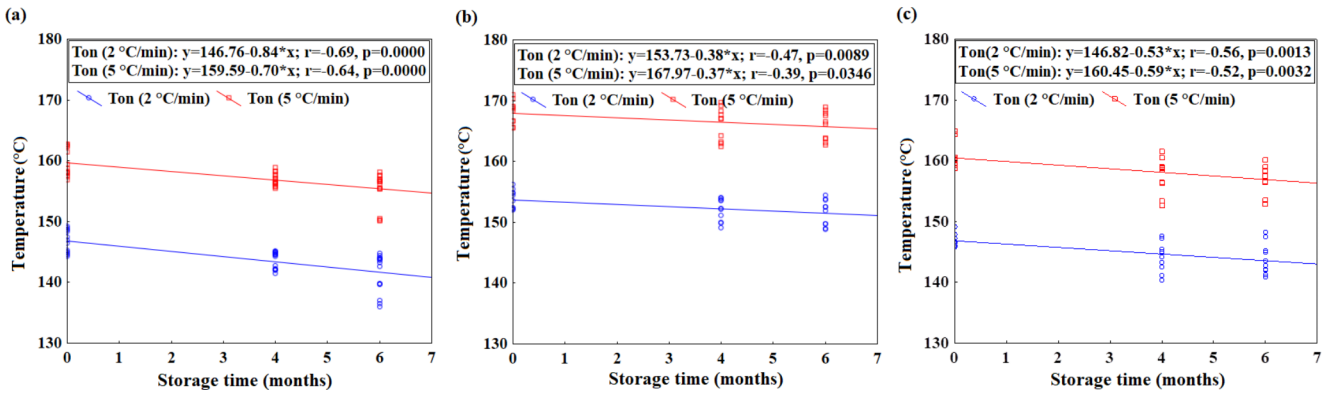

Fig. 4 Changes in onset temperature (Ton) of cold-pressed oils during storage (**a**) flaxseed, (**b**) camelina and (**c**) hempseed oil, determined by non-isothermal DSC at heating rate 2 and 5 °C/min

Generally, it can be seen that for all cultivars and all types of oils a decreasing trend was observed during the whole storage period, so for all three oils, the time required for initiation of oxidation (OIT) decreased till the end of storage. During the whole storage period of six months, OIT values determined at 120 °C were significantly reduced for flaxseed, camelina, and hempseed oils from values 43, 72, 51 min to 33, 65, 41 min, respectively. A similar trend was observed for the 140 °C program, where OIT values changed significantly for flaxseed oils from 10 to 7 min. and for camelina oil from 20 to 17 min., while for hempseed oil changes were not significant ($p > 0.05$) i.e., from 11 to 9 min. The highest OIT results for camelina oil were also observed by other authors, where among ten various oils flaxseed and hempseed oil was also analysed [48]. The rate of OIT decline can be compared for three oils by the slope of the straight line, shown in the equation in Fig. 3, which indicates how steep the line is. For the temperature program of 120 °C, the slope for camelina oil was the lowest, while for the isothermal program of 140 °C slope value was the lowest for hempseed oil. Other parameters calculated from isothermal curves i.e., oxidation end time (OET), length of oxidation ($\Delta t = OET - OIT$), and the rate of oxidation were also plotted against the storage time, as presented in Fig. S1 (Supplementary materials). Just as OIT expresses the starting point of the propagation, the parameter of OET, measured at the minimum value of the heat flow of the oxidation exotherm, indicates the end of the propagation stage and the start of the termination of oxidation. In Fig. S1, it can be seen that the values of OET decreased within the storage time for all oils, similarly to the OIT parameter. However, the changes were only significant for flaxseed oil ($p \leq 0.05$). Slope values calculated for the relationship OET vs. time shown in the equations were higher for the analysis at 120 °C for all oils than for the isothermal mode at 140 °C. On the other hand, the changes in oxidation length (Δt) and oxidation rate within the storage time were not significant ($p > 0.05$), since they did not show any trend.

Figure 4 shows changes in Ton obtained from non-isothermal measurement by DSC for the three cold-pressed oils. It can be seen that for a higher heating rate (5 °C/min), Ton values were higher than for 2 °C/min, which is the result of longer exposure to oxygen at a lower scanning rate. This is in agreement with another study conducted to describe

the flaxseed oils by means of non-isothermal DSC, where the authors reported a Ton value of 186 °C at a heating rate of 20 °C/min for fresh flaxseed oil [46]. Following the oxidation curves presented in Fig. 4 confirm that for all three cold-pressed oils, the Ton values decreased during the storage of oils for both heating rates (2 and 5 °C/min). The mean values of onset temperatures (Ton) determined at a heating rate of 2 °C/min were reduced after six months for flaxseed, camelina, and hempseed oils from values 147, 154, 147 °C to 142, 152, 144 °C, respectively.

For a heating rate of 5 °C/min, the mean value of Ton decreased after six months from 160, 168, 161 °C to 155, 166, 157 °C for flaxseed, camelina, and hempseed oils, respectively. Correspondingly, for non-isothermal measurement, the highest slope was observed for flaxseed oil for both heating rates (i.e., 0.84 for 2 °C/min and 0.70 for 5 °C/min). Implementing the DSC non-isothermal technique to show differences in the oxidative stability of various vegetable oils was presented by Qi et al. [49], using various heating rates i.e., 5, 7.5, 10, 12.5, and 15 °C/min. In addition to the Ton parameter, Tend was also determined as the parameter indicating the end of the propagation process. Fig. S2 (supplementary materials) presents the values of Tend calculated for heating rates 2 and 5 °C/min and plotted against storage time for flaxseed oil (Fig. S2a), camelina seed oil (Fig. S2b) and hempseed oil (Fig. S2c). It can be seen that a significant decrease in the Tend values within storage time were observed for all oils only for a heating rate of 5 °C/min ($p \leq 0.05$).

The data analysed for DSC parameters show promising repeatability of oxidative characteristics for three types of cold-pressed oils, regardless of their originating from different cultivars. In the supplementary material in Table S1 data concerning the repeatability of OIT and Ton measurement was shown. It can be seen that the for OIT the coefficient of variation (CV) was lower in the case of OIT measured at 120 °C (0.68–2.56) than for OIT at 140 °C (1.17 and 5.85). For the non-isothermal determination there were no differences in CV for the determination of Ton at 2 °C/min (0.20–0.38) and Ton at 5 °C/min (0.14–0.42). Thus, the stability trends presented in this research work can be considered as a basis for further statistical analysis for predicting the oxidative stability of the samples for a prolonged storage time.

The relationship between DSC parameters and chemical indicators of the oxidative stability of cold-pressed oils during storage

In order to establish the usability of DSC analysis for assessing the oxidative state of oils, the DSC parameters of OIT and Ton were compared with chemical indicators. Table 1 presents the statistical parameters (slope, correlation coefficient r, p-value) of the relationship between DSC parameters (OIT and Ton) obtained from isothermal and non-isothermal analysis and chemical indicators (PV, p-AV, AV, TOTOX). For all three oils, both OIT and Ton parameters appeared to have a descending trend within the time of storage, in contrast to the results of the chemical methods, for which all indexes increased during six months. Thus, more deteriorated oil stipulates less temperature or time for the initiation of the oxidation process by means of DSC parameters. The correlation coefficient values indicate that the highest significant ($p \leq 0.05$) correlations were observed between DSC parameters and PV, TOTOX values for flaxseed oils, while for camelina seed oils they were lowest.

For camelina seed oils, in particular, the correlations between AV values and all DSC parameters were not significant ($p > 0.05$). However, the chemical indicators for hempseed oil were significantly correlated with all the DSC parameters. For the data presented here, it can be stated that the DSC parameters can be considered to detect any oxidative degradation of the oil samples from the fresh condition to the end of shelf life, since they demonstrated parallel, and in most cases, significant correlations with chemical indicators. A similar approach to comparing analytical thermal methods with chemical indicators was presented by other authors, where flaxseed, camelina and hempseed oils were also analysed among ten various types of fresh cold-pressed oils. [48]. The isothermal pressure differential scanning calorimetry (PDSC) technique at a temperature of 120 °C was used in this study. PDSC results were also analysed for correlations with chemical methods (i.e., PV, p-AV and TOTOX), where PV and TOTOX values were reported to have significant correlations (-0.44 and 0.40, respectively), while for p-AV the correlation was not significant ($r = 0.12$) [48].

Chemometric analysis for the discrimination of fresh and stored oils based on chemical and DSC parameters

Principal component analysis (PCA) was used as an exploratory data analysis to gain insights into the underlying structure of results obtained from chemical and DSC analysis. This unsupervised technique shows the natural grouping of the samples studied, as well as the variables in a multidimensional space. First, two principal components with eigenvalues exceeding one were extracted, explaining 94% of the total variance. Figure 5a and b shows the results obtained in the space formed by the two first principal components.

The result given in Fig. 5b showed a tendency of grouping between the samples of each oil. This figure shows the separation of oil samples in two groups according to PC1. The first group consisted of camelina seed oil with the

Table 1 Relationship between DSC parameters (OIT, Ton) and chemical indicators (PV, p-AV, AV, TOTOX) for three stored cold-pressed oils (flaxseed, camelina, hempseed oil)

		PV	p-AV	AV	TOTOX
Flaxseed oil					
OIT (120 °C)	slope	-0.51	-0.04	-0.04	-1.09
	r	-0.78	-0.51	-0.34	-0.78
	p	0.0000	0.00003	0.0306	0.0000
OIT (140 °C)	slope	-1.88	-0.15	-0.14	-3.98
	r	-0.72	-0.45	-0.29	-0.72
	p	0.0000	0.0003	0.0672	0.0000
Ton (2 °C/min)	slope	-1.25	-0.10	-0.11	-2.65
	r	-0.89	-0.61	-0.44	-0.89
	p	0.0000	0.00001	0.0146	0.0000
Ton (5 °C/min)	slope	-1.11	-0.11	-0.15	-2.35
	r	-0.70	-0.56	-0.55	-0.70
	p	0.00000	0.00009	0.0015	0.0000
Camelina oil					
OIT (120 °C)	slope	-0.21	-0.03	-0.02	-0.45
	r	-0.47	-0.49	-0.14	-0.48
	p	0.0001	0.00006	0.4002	0.0001
OIT (140 °C)	slope	-0.48	-0.07	-0.05	-1.03
	r	-0.44	-0.47	-0.13	-0.45
	p	0.0005	0.0001	0.4225	0.0004
Ton (2 °C/min)	slope	-0.69	-0.09	-0.07	-1.48
	r	-0.46	-0.52	-0.14	-0.46
	p	0.0018	0.0003	0.4667	0.0015
Ton (5 °C/min)	slope	-0.46	-0.06	-0.02	-0.98
	r	-0.37	-0.43	-0.05	-0.37
	p	0.0147	0.0033	0.8005	0.0131
Hempseed oil					
OIT (120 °C)	slope	-0.48	-0.08	-0.40	-1.03
	r	-0.49	-0.54	-0.61	-0.50
	p	0.00006	0.00001	0.00003	0.00005
OIT (140 °C)	slope	-1.14	-0.16	-1.55	-2.44
	r	-0.36	-0.33	-0.74	-0.36
	p	0.0046	0.0099	0.00000	0.0045
Ton (2 °C/min)	slope	-1.85	-0.28	-1.35	-3.98
	r	-0.58	-0.58	-0.68	-0.58
	p	0.00003	0.00003	0.00003	0.00003
Ton (5 °C/min)	slope	-1.44	-0.21	-1.34	-3.10
	r	-0.53	-0.60	-0.79	-0.53
	p	0.0002	0.0004	0.00000	0.0002

highest DSC indexes and the second group of flaxseed and hempseed oil. This distribution can be interpreted from the loading plot Fig. 5a, which indicates all chemical indexes are higher for hempseed and flaxseed oil. A strong negative correlation between DSC indexes and the first component can be observed (-0.82, -0.88. -0.88, -0.88 for OIT at 120 °C, OIT at 140 °C, Ton at 2 °C/min, Ton at 5 °C/min).

In contrast, there is a strong positive correlation between chemical indexes and PC1 (0.87, 0.83, 0.73, 0.84 for PV, p-AV, AV, and TOTOX, respectively). Additionally, it can be noted that samples stored for 4 and 6 months for each oil type are located more to the right side of the two-dimensional space, which correlates with high chemical oxidation indexes. The trend supports an attempt to build a model for classifying oils in terms of storage time. For this purpose, Linear Discriminant Analysis (LDA) was used, which is one of the supervised learning pattern recognition methods. LDA is based on determining linear discriminant functions, which maximize the ratio of between-class variance and minimize the ratio of within-class variance. LDA was successfully applied to describe the freshness of olive oils using fluorescence spectroscopy, where the authors obtained 100% predictive power for the model [50]. Moreover, Kalua et al. [51] made successful use of the method for discriminating the storage conditions and freshness of virgin olive oil. Once all data had been standardized, the LDA analysis was carried out for the entire dataset i.e., for chemical oxidation indexes and DSC parameters of all types of oils and

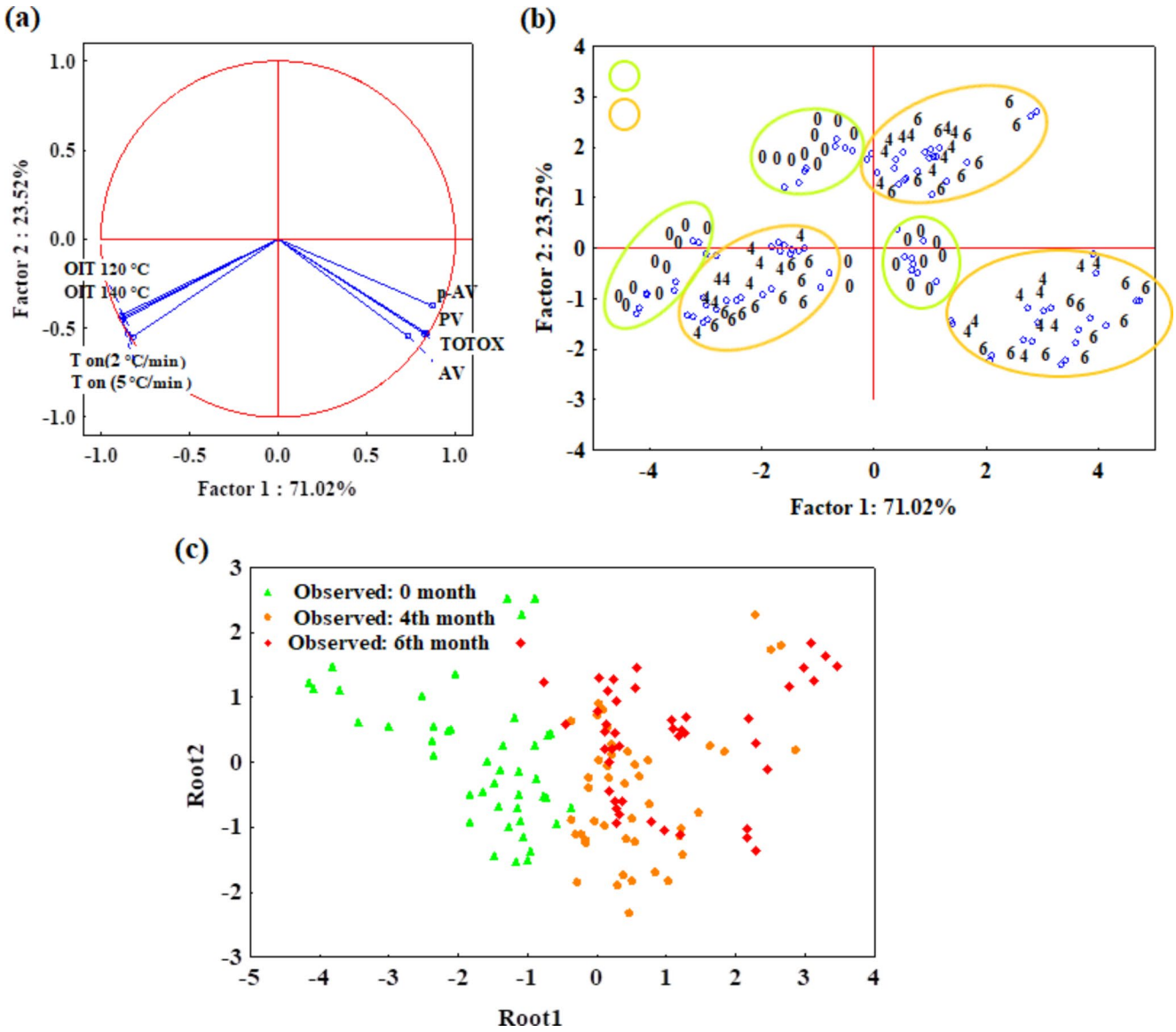

Fig. 5 PCA analysis of (**a**) loading plots PC1 and PC2 with an illustration of DSC parameters (OIT at 120 and 140 °C, Ton at 2 °C/min and 5 °C/min) and chemical indexes of oxidative stability (PV, p-AV, AV, TOTOX), (**b**) distribution of three plant oils based on a projection of cases and (**c**) discrimination analysis by LDA based on observed values (DSC and chemical) during shelf life for all three oils

three periods of storage (0, 4, 6 months). Two discriminant functions were obtained, based on Wilk's Lambda statistics, with $p < 0.05$. The first classification function explains 92% of the variance, which means that 92% of all discriminatory power is explained by this function. As Fig. 5c shows, the first discriminant function distinguishes between fresh oils and those stored for 4 and 6 months. The second classification function appears to distinguish between oils stored for 4 and 6 months, but its discriminating power is low. More than 95% of the fresh oils were correctly classified, while for those stored for 4 and 6 months, 69% and 60% correct classifications were obtained, respectively.

Considerably better classification models were obtained for individual oil types, as is shown in Fig. 6. This is probably associated with the homogeneity of the oil sample composition among one type, which allows for better detection of changes due to storage time and their use for discrimination. The discriminant analysis resulted in statistically significant functions (Wilk's Lambda statistic with $p < 0.05$) for all the oil types. In all models, the first discriminant function distinguished fresh oils from other oils, while the second discriminant function distinguished oils stored for four months from those stored for six months. This classification model shows high discrimination performance for the three classes, according to their membership. For flaxseed oil, all

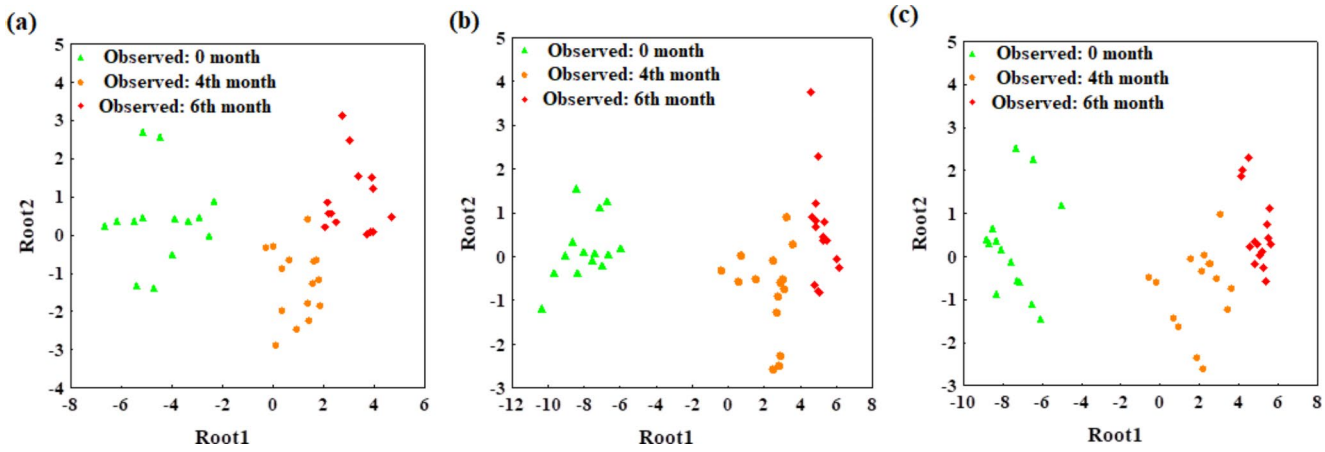

Fig. 6 Linear discriminant analysis (LDA) performed using DSC parameters (OIT at 120 and 140 °C, Ton at 2 °C/min and 5 °C/min) and chemical indicators of oxidative stability (PV, p-AV, AV, TOTOX) for cold-pressed (**a**) flaxseed, (**b**) camelina and (**c**) hempseed oils during 0, 4- and 6- month storage time

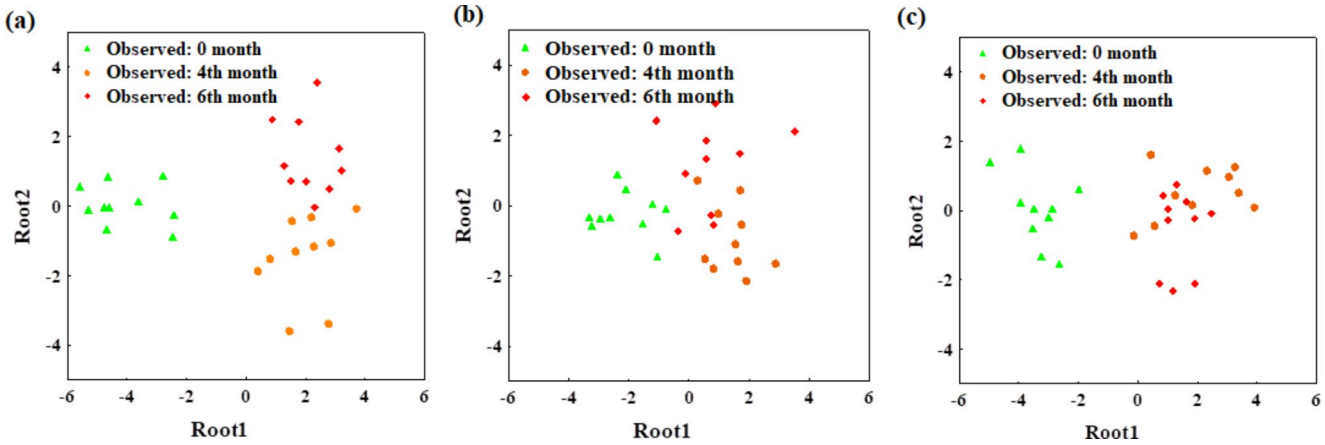

Fig. 7 Linear discriminant analysis (LDA) performed using DSC parameters (OIT, OET, Δt, oxidation rate at 120 and 140 °C; Ton and Tend at 2 °C/min and 5 °C/min) for cold-pressed (**a**) flaxseed, (**b**) camelina and (**c**) hempseed oils during 0, 4- and 6- month storage time

samples were correctly classified into the appropriate class. In the case of camelina seed and hemp seed oil, a misclassification was noted for 1 sample, which was classified as being stored for 6 months while it had been stored for 4 months. The accuracy of the models obtained indicates the potential use of DSC parameters combined with chemical indexes to build discriminant models to detect non-fresh oils within a certain type. Obviously, to build predictive models it would be required to conduct research on a significantly larger number of oil samples stored under different temperature and time conditions. As Fig. 6 shows, the LDA composed of both DSC results and chemical analysis results, the next step was to investigate whether it is possible to discriminate between fresh and stored oils based only on all DSC parameters (i.e., OIT, OET, Δt, oxidation rate, Ton, Tend).

Figure 7 shows LDA analysis conducted for three oils based on only DSC results from isothermal mode at 120 and 140 °C (OIT, OET, Δt, oxidation rate) and from non-isothermal program at 2 °C/min and 5 °C/min (Ton and Tend). The discriminant analysis resulted in statistically significant functions (Wilk's Lambda statistic with $p < 0.05$) for flaxseed and hempseed oil, while for camelina oil it was not significant. However, all "0" month camelina oils samples were properly classified as fresh oils. For flaxseed oils, all fresh and stored samples were correctly classified into the appropriate classes, and a misclassification was only observed between the 4th and 6th -month groups, for which one 6th -month sample was identified as a 4th -month sample. In the case of hempseed seed oils, two samples were classified as being stored for 4 months, while they had actually been stored for 6 months. As can be seen in Fig. 7, for flaxseed and hempseed oils the distinction between fresh and stored oils was very distinct, in contrast to camelina oils, for which the discrimination was not so clear, since these oils were the most resistant to the oxidation process.

Conclusion

In this study, deteriorative changes in three cold-pressed oils (flaxseed, camelina, hempseed) during six months' storage in conditions similar to the supermarket shelf were researched. The changes were measured by conventional chemical methods like PV, p-AV, TOTOX, and AV, as well as by means of the instrumental method of differential scanning calorimetry (DSC). The novelty of this study was its finding that DSC parameters obtained from isothermal (OIT) and non-isothermal (Ton) measurements changed corresponding to the chemical indicators during the shelf life of oils. All these parameters gradually decreased until the end of the storage period, while for chemical indicators a linear growth was observed. The oil most prone to oxidation was flaxseed oil, for which the most significant correlations between DSC parameters and PV and TOTOX were found. Of the three oils studied, the most thermally resistant to oxidation was camelina oil, for which the lowest values of the slopes of straight line plotted from DSC and chemical analysis data versus storage time were obtained. Summing up, all DSC results from the isothermal and non-isothermal experiment show promising repeatability of measuring the oxidative state for three types of cold-pressed oils, regardless of their origins in different cultivars. However, the most suitable test for monitoring the deteriorative changes in oils during storage was the isothermal test carried out at a temperature of 120 °C, since for this measurement the slope values of the straight lines plotted versus time for all three oils were the highest among all the DSC parameters tested (OIT at 120, 140 °C, Ton at 2, 5 °C/min). Moreover, for the parameters of OIT determined at 120 °C the correlation coefficients with chemical indicators were also highly significant ($p \leq 0.0001$). Thus, the approach presented here can be used to monitor oxidative deterioration of oils based on the starting point determined for fresh oils. However, these findings can also contribute to the fortification, as well as modification practices, to enhance the shelf-life stability of cold-pressed oils. One practical aspect of this study is the possibility to use this approach for predicting the shelf life for consumer safety, and also improving the stability of the oils. Linear discriminant analysis (LDA) revealed that the first discriminating function significantly separated the fresh oils from stored oils.

Supplementary Information The supplementary material is available at https://data.mendeley.com/datasets/bmcs4kwnw9/1.

Author contributions Conceptualization: [Mahbuba Islam and Jolanta Tomaszewska-Gras]; Methodology: [Mahbuba Islam and Jolanta Tomaszewska-Gras]; Formal analysis and investigation: [Mahbuba Islam, Anna Kaczmarek and Jolanta Tomaszewska-Gras]; Writing - original draft preparation: [Mahbuba Islam]; Writing - review and editing: [Mahbuba Islam, Anna Kaczmarek and Jolanta Tomaszewska-Gras]; Funding acquisition: [Jolanta Tomaszewska-Gras]; Resources: [Jolanta Tomaszewska-Gras]; Supervision: [Jolanta Tomaszewska-Gras]. All authors read and approved the final manuscript.

Funding This research was funded by the NATIONAL SCIENCE CENTRE, POLAND, grant number: 2018/31/B/NZ9/02762.

Data availability The datasets generated during and/or analyzed during the current study are available from the corresponding author upon reasonable request.

Declarations

Conflict of interest The authors declare no conflict of interest.

Ethical approval This article does not contain any studies with human participants or animals.

Informed consent Not applicable.

References

1. A. Durazzo, M. Fawzy Ramadan, M. Lucarini, Front. Nutr. **8**, 2021 (2022). https://doi.org/10.3389/fnut.2021.836651
2. M.F. Ramadan, *Introduction to Cold Pressed Oils: Green Technology, Bioactive Compounds, Functionality, and Applications* (Elsevier Inc., 2020), pp. 1–5. https://doi.org/10.1016/B978-0-12-818188-1.00001-3
3. M. Ligĕza, D. Wyglădacz, A. Tobiasz, K. Jaworecka, A. Reich, Fam Med. Prim. Care Rev. **18**, 443 (2016). https://doi.org/10.5114/fmpcr.2016.63699
4. M. Zulqarnain, M.H.M. Ayoub, M.H. Yusoff, I. Nazir, M. Zahid, F. Ameen, D. Sher, Floresyona, And E. Budi Nursanto, Sustain. **13**, 1 (2021). https://doi.org/10.3390/su13020788
5. G.V. Reasearch, *Cold Pressed Oil Market Size, Share & Trends Analysis Report By Product (Coconut Oil, Palm Oil, Ground Nut Oil, Rapeseed Oil, Soybean Oil, Sunflower Oil), By Distribution Channel, By Region, And Segment Forecasts*, 2022–*2028*. https://www.grandviewresearch.com/industry-analysis/cold-pressed-oil-market-report. (Accessed 24 April 2023)
6. E. Choe, D.B. Min, Compr. Rev. Food Sci. Food Saf. **5**, 169 (2006). https://doi.org/10.1111/j.1541-4337.2006.00009.x
7. M.H. Gordon, *The Development of Oxidative Rancidity in Foods* (Woodhead Publishing Ltd, 2001). https://doi.org/10.1016/9781855736160.1.5
8. M.D.A. Saldana, S.I. Martinez-Monteagudo, in *Appl. Calorim. a Wide Context - Differ. Scanning Calorimetry, Isothermal*

Titration Calorim. Microcalorim, edited by A. A. Elkarody (2013), pp. 445–474
9. F. Shahidi, U.N. Wanasundara, *Food Lipids* (CRC Press, 2002), pp. 484–507
10. S. Pirsa, S. Asadi, Food Addit. Contam. - part A Chem. Anal. Control Expo Risk Assess. **38**, 856 (2021). https://doi.org/10.1080/19440049.2021.1891299
11. M. Islam, Y.V. Rajagukguk, A. Siger, J. Tomaszewska-Gras, Foods 12, (2023). https://doi.org/10.3390/foods12010135
12. Y.V. Rajagukguk, M. Islam, J. Tomaszewska-Gras, Foods. **12**, 358 (2023). https://doi.org/10.3390/foods12020358
13. H. Abramovič, V. Abram, Food Technol. Biotechnol. **43**, 63 (2005)
14. A. Asdagh, S. Pirsa, Int. J. Biol. Macromol. **165**, 156 (2020). https://doi.org/10.1016/j.ijbiomac.2020.09.192
15. M. Momot, B. Stawicka, A. Szydłowska-Czerniak, Appl. Sci. **13** (2023). https://doi.org/10.3390/app13031924
16. A.M. Giuffrè, C. Zappia, M. Capocasale, JAOCS J. Am. Oil Chem. Soc. **94**, 819 (2017). https://doi.org/10.1007/s11746-017-2988-9
17. A.M. Giuffrè, M. Capocasale, C. Zappia, M. Poiana, J. Oleo Sci. **66**, 1193 (2017). https://doi.org/10.5650/jos.ess17109
18. F. Giuffrida, F. Destaillats, M.H. Egart, B. Hug, P.A. Golay, L.H. Skibsted, F. Dionisi, Food Chem. **101**, 1108 (2007). https://doi.org/10.1016/j.foodchem.2006.03.010
19. Q. Zhou, X. Jia, Q. Deng, H. Chen, H. Tang, F. Huang, Food Sci. Nutr. **7**, 3731 (2019). https://doi.org/10.1002/fsn3.1232
20. M. Islam, L. Bełkowska, P. Konieczny, E. Fornal, J. Tomaszewska-Gras, J. Food Drug Anal. **30** (2022). https://doi.org/10.38212/2224-6614.3402
21. J. Tomaszewska-Gras, M. Islam, L. Grzeca, A. Kaczmarek, E. Fornal, Molecules. **26**, 1 (2021). https://doi.org/10.3390/molecules26071958
22. J. Tomaszewska-Gras, Grasas y Aceites. **67** (2016). https://doi.org/10.3989/gya.0453161
23. J. Tomaszewska-Gras, J. Therm, Anal. Calorim. **113**, 199 (2013). https://doi.org/10.1007/s10973-013-3087-2
24. M. Islam, A. Kaczmarek, M. Rudzińska, J. Tomaszewska-gras, Appl. Sci. **13** (2023). https://doi.org/10.3390/app13063975
25. R.M. Maggio, L. Cerretani, C. Barnaba, E. Chiavaro, Food Biophys. **7**, 114 (2012). https://doi.org/10.1007/s11483-012-9248-1
26. M. Islam, M. Muzolf-Panek, E. Fornal, J. Tomaszewska-Gras, J. Therm. Anal. Calorim. (2022). https://doi.org/10.1007/s10973-022-11367-8
27. M.B. Różańska, P.Å. Kowalczewski, J. Tomaszewska-Gras, K. Dwiecki, S. Mildner-Szkudlarz, Antioxidants. **8**, 313 (2019). https://doi.org/10.3390/antiox8080313
28. J. Thurgood, R. Ward, S. Martini, Food Res. Int. **40**, 1030 (2007). https://doi.org/10.1016/j.foodres.2007.05.004
29. H.D. Belayneh, R.L. Wehling, E.B. Cahoon, O.N. Ciftci, J. Food Sci. **82**, 632 (2017). https://doi.org/10.1111/1750-3841.13652
30. M. Muzolf-Panek, A. Kaczmarek, J. Tomaszewska-Gras, R. Cegielska-Radziejewska, T. Szablewski, M. Majcher, And K. Stuper-Szablewska, Antioxidants. **9**, 1 (2020). https://doi.org/10.3390/antiox9090903
31. C.P. Tan, Y.B. Che Man, Trends Food Sci. Technol. **13**, 312 (2002). https://doi.org/10.1016/S0924-2244(02)00165-6
32. J. Cao, L. Deng, X.M. Zhu, Y. Fan, J.N. Hu, J. Li, Z.Y. Deng, J. Agric. Food Chem. **62**, 12545 (2014). https://doi.org/10.1021/jf5047656
33. ISO, *EN ISO 11357-6:2013 Plastics - Differential Scanning Calorimetry (DSC) - Part 6: Determination of Oxidation Induction Time (Isothermal OIT) and Oxidation Induction Temperature (Dynamic OIT) (ISO 11357-6:2008)* (2013)
34. A.S.T.M. International, *ASTM D3895-19. Test Method for Oxidative-Induction Time of Polyolefins by Differential Scanning Calorimetry* (ASTM Publisher, West Conshohocken, PA, USA, 2019)
35. ISO 6885, Animal and Vegetable Fats and Oils: Determination of Anisidine Value. ISO: Geneva, Switzerland 2016, (2016)
36. ISO 3960, Animal and Vegetable Fats and Oils—Determination—Iodometric (Visual) Endpoint; International Organization for Standardization: Geneva, Switzerland, 2017, (2010)
37. AOCS, AOCS Official Method Acid Value. Cd 3d-63, (Urbana, IL, USA, 2009)
38. S.S.O. Hung, S.J. Slinger, J. Am. Oil Chem. Soc. **58** (1981). https://doi.org/10.1007/BF02887323
39. Codex, Alimentarius, *Standard for Named Vegetable Oils Codex Stan 210–1999* (1999)
40. M. Islam, A. Kaczmarek, A. Grygier, J. Tomaszewska-Gras, Foods 12, 2954 (2023). https://doi.org/10.3390/foods12152954
41. R. KRAKOWSKI, Combust. Engines. **186**, 59 (2021). https://doi.org/10.19206/CE-140730
42. H. Abramovič, B. Butinar, V. Nikolič, Food Chem. **104**, 903 (2007). https://doi.org/10.1016/j.foodchem.2006.12.044
43. M. Tańska, B. Roszkowska, M. Skrajda, D. Grzegorz, J. Oleo Sci. (2016). https://doi.org/10.5650/jos.ess15243
44. K. Hasiewicz-Derkacz, A. Kulma, T. Czuj, A. Prescha, M. Zuk, M. Grajzer, M. Łukaszewicz, J. Szopa, BMC Biotechnol. **15**, 1 (2015). https://doi.org/10.1186/s12896-015-0178-0
45. M. Tura, D. Ansorena, I. Astiasarán, M. Mandrioli, T.G. Toschi, Antioxidants 11, (2022). https://doi.org/10.3390/antiox11030490
46. E. Rudnik, A. Szczucinska, H. Gwardiak, A. Szulc, A. Winiarska, Thermochim. Acta. **370**, 135 (2001). https://doi.org/10.1016/S0040-6031(00)00781-4
47. K. Ratusz, E. Popis, H. Ciemniewska-Żytkiewicz, M. Wroniak, J. Therm. Anal. Calorim. **126**, 343 (2016). https://doi.org/10.1007/s10973-016-5642-0
48. E. Symoniuk, K. Ratusz, E. Ostrowska-Ligęza, K. Krygier, Food Anal. Methods. **11**, 1095 (2018). https://doi.org/10.1007/s12161-017-1081-1
49. B. Qi, Q. Zhang, X. Sui, Z. Wang, Y. Li, L. Jiang, Food Chem. **194**, 601 (2016). https://doi.org/10.1016/j.foodchem.2015.07.148
50. A. El Orche, M. Bouatia, M. Mbarki, J. Anal. Methods Chem. 2020, 1 (2020). https://doi.org/10.1155/2020/8860161
51. C.M. Kalua, D.R. Bedgood, A.G. Bishop, P.D. Prenzler, E.H. Graham, (2006). https://doi.org/10.1021/jf061038j

Statement about the contribution of authors

Publication title A6: Islam, M., Kaczmarek, A. Tomaszewska-Gras, J. Differential scanning calorimetry as a tool to assess the oxidation state of cold-pressed oils during shelf-life. Journal of Food Measurement and Characterization (2023). https://doi.org/10.1007/s11694-023-02152-8

Author	Contribution	Percentage contribution	Signature
Mahbuba Islam	Conceptualization, Methodology, Formal analysis, Investigation, Data curation, Writing- original draft preparation, Writing—review and editing, Visualization.	51	
Anna Kaczmarek	Methodology, Formal analysis, Investigation, Writing - review and editing, Visualization, Supervision.	20	
Jolanta Tomaszewska-Gras	Conceptualization, Methodology, Formal analysis, Investigation, Resources, Data curation, Writing- original draft preparation, Writing- review and editing, Visualization, Supervision, Project administration, Funding acquisition.	29